

**Restoring Chimeric Antigen Receptor
(CAR) T Cell Function in
Chronic Lymphocytic Leukaemia (CLL)**

Dr Robin Sanderson

**A thesis submitted for the degree of Doctor of Philosophy
Queen Mary University of London**

July 2019

**Centre for Haemato-Oncology
Barts Cancer Institute**

Abstract

Differential outcomes for CD19 CAR T cells between chronic lymphocytic leukaemia, lymphoma and acute lymphoblastic leukaemia illustrate unique challenges to overcome in different patient populations. CD19 positive and negative relapses have been described for which different mechanisms of resistance have been proposed. CD19⁺ relapses could be related to the host microenvironment or T cell fitness. Therefore, there is a need for pre-clinical modelling using immunocompetent mice to explore CAR plus immunotherapy combinations to enhance efficacy. CLL is an ideal disease model to explore as it is associated with a tumour supportive microenvironment and T cells exhibit functional defects, closely recapitulated in E μ -TCL1 (TCL1) mice, and induced in healthy mice by adoptive transfer (AT) of murine CLL splenocytes.

Syngeneic donor CAR T cells were generated after rapid expansion in culture using CD3/CD28 beads and murine IL2. T cells were obtained from the spleens of wild-type mice, mice with CLL or mice with CLL pre-treated with ibrutinib or acalabrutinib. Enriched T cells were transduced with retroviral supernatant from MSGV-1D3-28Z-1.3mut (CD19-CD28) and expanded before being injected into mice with CLL. Mice received lymphodepletion with cyclophosphamide and in some experiments received a PD-L1 antibody.

Compared to wild type CAR T cells, CLL derived CAR T cells proliferate less in culture, skew towards CD8 with lower transduction efficiencies in CD8 cells and have higher expression of PD-1. All mice treated with CAR T cells can clear their CLL and normal B cells by D+7 which can reverse their exhausted T cell phenotype. Mice treated with CLL derived CAR T cells were liable to relapse with CD19⁺ disease, and the addition of PD-L1 antibody did not improve this. Pre-treatment of mice with BTK inhibitors resulted in improved T cell ex vivo expansion and a more favourable CAR T cell phenotype, with a long-term efficacy study in progress.

Statement of work undertaken

I performed all the work described in this thesis in person with all help being acknowledged. All sources of information have been properly referenced.

From July 2015-April 2019 I was responsible for the TCL1 mouse colony at Barts Cancer Institute. From July 2017 Arantxa Romero-Toledo started separate work using the colony and we shared day to day responsibilities for animal welfare, documentation and preservation of samples for the bio-bank. For Chapters 8-9 tail vein bleeds and intraperitoneal injections were performed by Arantxa Romero-Toledo and Julie Cleaver from the Animal Technician Service. All tail vein injections of TCL1 splenocytes or CAR T cells were performed by Julie Cleaver and Hagen Schmitt.

For work described in Chapter 9, I designed and coordinated this two-part experiment, and performed all the cell culture work for the manufacture of the CAR T cells. All mouse work was split between myself and Arantxa Romero-Toledo, with peripheral blood samples being shared for different flow panel analysis, looking at CAR T cells and the microenvironment. Part 2 of this experiment is ongoing, and therefore only partially included in this thesis.

Dedication

To Antonio, you literally moved continents to stand firmly by my side.

Mum and Dad, for your life-long unwavering support, love and belief in me.

Bruce, Mark, Helen, Jenny, Eleanor, Hannah and Violet.

My friends.

Acknowledgements

Supervisors

Professor John Gribben

Hamilton Fairley Chair of Medical Oncology, Centre for Haemato-Oncology, Barts Cancer Institute.

With thanks particularly for his mentorship and giving me this great opportunity to think, to read and to explore science, it has been fascinating,

Dr Jeff Davies

Reader in Haemato-Oncology, Barts Cancer Institute.

Principal Co-workers

Arantxa Romero-Toledo PhD Student, Centre for Haemato-Oncology.

For being so great with the mice, and being a good friend through this.

Dr Fabienne Lucas Postdoctoral Researcher, The Ohio State University, USA.

For teaching me the way to work in the laboratory, and all those SOPs.

Co-workers

Julie Cleaver Animal Technician Service, Barts Cancer Institute.

Dr Joe Taylor Clinical Research Fellow, Centre for Haemato-Oncology.

Hagen Schmitt Animal Technician Service, Barts Cancer Institute.

Funding

This work was supported by funds from The London Clinic Charity.

Table of Contents

Abstract	2
Statement of Work Undertaken	3
Dedication	4
Acknowledgements	5
Table of Contents	6
List of Figures	10
List of Tables	13
Abbreviations	14
Meeting Abstracts	18
1 Background	19
1.1 Chronic lymphocytic leukaemia	19
1.1.1 Definition, staging and prognosis	19
1.1.2 First-line treatment	22
1.1.3 Relapsed/refractory and unfit patients	23
1.2 Microenvironment	29
1.2.1 BCR Signalling and the Microenvironment	29
1.2.2 Modelling CLL	32
1.2.2.1 Cell lines	32
1.2.2.2 Animal models	33
1.3 Cellular immunotherapy	38
1.3.1 Chimeric antigen receptor T cells	38
1.3.2 Preclinical modelling of CAR T cells	41
1.3.3 CAR T cells in lymphoid malignancies	43
1.3.4 Novel concepts in CAR T cell therapy	52
1.3.4.1 Relapse post CAR T cells	52
1.3.4.2 Novel antigens and dual targeting	53
1.3.4.3 Predictors of response	55
1.3.4.4 Subsets	56
1.3.4.5 BTK inhibitors and immunotherapy	57

1.3.4.6	CAR T cells in other haematological diseases	59
1.3.4.6.1	Multiple Myeloma	59
1.3.4.6.2	Hodgkin Lymphoma	60
1.3.4.6.3	Acute Myeloid Leukaemia	61
1.3.4.6.4	T cell lymphoma	62
1.3.4.7	Allogeneic CAR T cells	64
1.3.4.8	Checkpoint inhibition combined with CAR T cells	66
1.3	Conclusion	67
2	Hypothesis and Aims	69
3	Materials and Methods	70
3.1	TCL1 mouse model and procedures	70
3.1.1	Background	70
3.1.2	Processing organs	71
3.1.3	Negative selection of CLL and T cells	72
3.1.4	Adoptive transfer of TCL1	73
3.1.5	Additional experimental drugs	74
3.2	CAR plasmids	74
3.2.1	MD Anderson Cancer Center	74
3.2.2	Memorial Sloan Kettering Cancer Center	75
3.2.3	National Cancer Institute	76
3.2.4	Transformation and amplification	76
3.3	Cell culture and retroviral methods	77
3.3.1	Transfection of Phoenix/Platinum-eco cells	77
3.3.2	Transduction of Mouse T-cells	78
3.3.3	Transduction HEK cells/3T3 fibroblasts	80
3.4	Flow cytometry	80
3.4.1	Surface staining	80
3.4.2	Cytotoxicity	82
3.5	Cytokines	82
3.6	Statistics	83

4	Breeding and maintenance of TCL1 and adoptive transfer CLL	84
4.1	Introduction	84
4.2	Objectives	84
4.3	Confirmation of TCL1	85
4.4	Confirmation of CLL	86
4.5	Discussion	87
5	CAR T cell manufacturing, detection and expansion	91
5.1	Introduction	91
5.2	Objectives	91
5.3	Plasmid identification	92
5.4	Fab and protein L	93
5.5	mCherry and GFP plasmids	95
5.6	Transduction of normal and transgenic mouse T cells	102
5.7	Rapid expansion protocol	103
5.8	Discussion	105
6	T cell phenotype and cytotoxicity in vitro	107
6.1	Introduction	107
6.2	Objectives	108
6.3	Materials and Methods	109
6.3.1	T cell source	109
6.3.2	Multicolour flow cytometry	110
6.4	Results	111
6.4.1	Cytotoxicity titration	111
6.4.2	T cell phenotype progression through manufacturing	112
6.5	Discussion	119
7	CAR T cell function in vivo	122
7.1	Introduction	122
7.2	Objectives	123
7.3	Materials and Methods	123
7.4	Results – in vivo optimization	124
7.4.1	CAR T cell phenotype	124
7.4.2	AT progress	126

7.5	Results	131
7.5.1	CAR T cell phenotype	131
7.5.2	AT progress	136
7.6	Discussion	143
8	In vivo modelling of CAR and checkpoint blockade	147
8.1	Introduction	147
8.2	Objectives	150
8.3	Methods and materials	151
8.4	Results	151
8.4.1	CAR production and phenotype	151
8.4.2	Treatment of AT CLL with CAR T cells	155
8.5	Cytokines	168
8.6	Discussion	169
9	In vivo modelling of CAR pretreatment with BTK inhibitors	169
9.1	Introduction	172
9.2	Objectives	174
9.3	Methods and materials	175
9.4	Results	177
9.4.1	Ibrutinib and acalabrutinib treatment of AT CLL	177
9.4.2	CAR production and phenotype	180
9.4.3	Efficacy of CAR T cells after pretreatment with BTKi	185
9.5	Discussion	189
10	Overall Discussion	192
10.2	Summary	201
11	Appendix	204
12	References	207

List of Figures

1.1	TCL1 mouse models in combination	34
1.2	Structure of a CAR	39
1.3	Clinical process of CAR production	40
1.4	Three generations of CARs	41
1.5	Ex vivo expansion of T cells in ALL, MM and CLL patients	47
1.6	Kaplan-Meier OS from ZUMA-1 of Axi-cel	50
3.1	Diagram of the laboratory process of making CAR T cells	79
3.2	Typical gating strategy	81
4.1	Genotyping TCL1 transgenic mice	86
4.2	CD5 ⁺ CD19 ⁺ in splenocytes of transgenic mice aged 9 and 12 months	86
5.1	Gel electrophoresis of MDACC CD19 CAR: Nde1 and Sap1	92
5.2	Gel electrophoresis of MSK CD19-CD28 CAR with EcoR1, Not1 and Stul ...	93
5.3	Transient transfection of CD19 CAR and GFP into HEK cells	94
5.4	Transduction of HEK using CD19 CAR retrovirus and GFP lentivirus	94
5.5	Baseline expression of protein L and fab antibodies on negatively selected mouse T cells	95
5.6	mCherry and GFP transfected into Phoenix cells	96
5.7	Highest transduction demonstrated of HER2 into murine cell lines	98
5.8	Highest transduction of CD19 CAR into PDAC cells using different supernatant obtained with differing transfection reagents	99
5.9	Comparison of transduction of 3T3 cells using concentrated (Retro-X) versus fresh viral supernatant	100
5.10	GFP ⁺ transduction of WT mouse T cells left in culture for 6 days	103
5.11	CD3 ⁺ after T cell enrichment	104
5.12	Mouse T cell concentration after proliferation with CD3/CD28 beads and varying concentrations of mIL2	105
6.1	Sources of T cells from which to make CAR T cells	109
6.2	B cell events after 72 hours co-culture with CAR T cells derived from retroviral supernatant collected at 48h and 72h	111

6.3	B cell events after 48 hours co-culture with CAR T cells	112
6.4	T cell subsets pre and post transduction with the NCI CD19-CD28 CAR	113
6.5	Phenotype of CD3 ⁺ CD8 ⁺ pre and post transduction with CD19-CD28 CAR ..	114
6.6	Flow plots of transduction efficiency in CD8 ⁺ cells by T cell source	115
6.7	Total T cell counts after activation, transduction and ex vivo proliferation .	115
6.8	B and T cell events following 48 hour co-culture with CAR T cells	116
6.9	B and T cell events following 72 hour co-culture with CAR T cells	117
6.10	T cell subsets after 72 hour co-culture with CLL splenocytes	118
6.11	Extended phenotype of T cells after co-culture with CLL splenocytes	118
6.12	GFP+ CD19-41BB T cell subsets following 72 hour co-culture with primary CLL B cells and PD-1 expression	119
7.1	In vivo experimental plan for CAR T cells using AT TCL1 mouse model	124
7.2	CD5 ⁺ CD19 ⁺ in PB obtained after AT of CLL and CAR T cell treatment	126
7.3	Individual progression of mouse weights	127
7.4	Loss of normal and CLL CD19+ cells in mice treated with CAR T cells	128
7.5	CD5+CD19+ at week 9 by organ and treatment group	129
7.6	Weights of spleen of mice culled at week 9 by treatment group	129
7.7	CD4: CD8 ratio of all T cells by organ in mice culled at week 9	130
7.8	PD-1 expression in CD3+CD8+ T cells by organ at week 9	130
7.9	Experimental groups for first in vivo comparison of CD19-CD28 and CD19-41BB derived from normal and CLL T cells	131
7.10	T cell source: PB CD5+CD19+ prior to mice being culled for T cell enrichment of their splenocytes	132
7.11	Total T cells after activation at D0 and transduction D1 and D2	133
7.12	CD4: CD8 ratio before and after activation and transduction of T cells by T cell source	135
7.13	Transduction efficiency on D4 of cell culture	135
7.14	PD-1 expression by T cell subset on D4	136
7.15	Progression of PB CD5 ⁺ CD19 ⁺ post AT and CAR T cells	137
7.16	Progression of PB CD5 ⁺ CD19 ⁺ CLL post AT of CLL T cells separating the AT CD19-CD28 treatment group by sex	138
7.17	Spleen weight at week 9	139

7.18	Splenic CD5 ⁺ CD19 ⁺ disease at week 9 by treatment group	140
7.19	CD4: CD8 in PB at week 9	141
7.20	PD-1 in CD3+CD8+ T cells in BM at week 9	142
8.1	Experimental groups	152
8.2	Transduction efficiency of CAR T cells in each subset	153
8.3	Naïve/effector/memory phenotype of CD8 ⁺ T cells	153
8.4	PD-1 expression in CD3 ⁺ CAR ⁺ T cell subsets	152
8.5	Progression of PB CD5 ⁺ CD19 ⁺ CLL post AT and CAR T cells	156
8.6	Progression of PB CD5+CD19+ CLL post AT and CAR T cells with AT CAR groups separated by sex	157
8.7	Weights of mice at their endpoints	158
8.8	Spleen weights by week 9	159
8.9	Percentage of mice in with detectable CD5 ⁺ CD19 ⁺ disease in PB	160
8.10	CD5 ⁺ CD19 ⁺ by organ when culled by treatment group	161
8.11	PD-1 expression in spleens at weeks 6 and 18	162
8.12	PD-1 expression in PB at weeks 6 and 18	163
8.13	Fab ⁺ CAR T cells of CD3 ⁺ /CD4 ⁺ /CD8 ⁺ T cells at D+7 post CAR T cell in each treatment group	164
8.14	CD3 ⁺ Fab ⁺ PD-1 ⁺ in PB at D+7	165
8.15	CD3 ⁺ Fab ⁺ % in PB after CAR injection	166
9.1	Two part sequential AT experimental plan to investigate the effect of ibrutinib and acalabrutinib pretreatment on CAR T cell function	176
9.2	CD5+CD19+ progression in PB over part 1	177
9.3	Spleen weight at week 5 after ibrutinib and acalabrutinib treatment	178
9.4	Total viable cell count of spleens at week 5 in each treatment group	178
9.5	CD5 ⁺ CD19 ⁺ in spleens at week 5 in each treatment group	179
9.6	CD3+CD8+PD-1+ expression in splenocytes by treatment group	180
9.7	Transduction efficiency (fab ⁺ %) by subset and CAR type	182
9.8	CD3+CAR+CD8+PD-1+ expression by pre-treatment group	184
9.9	Percentage CAR+ cells in the PB at D+7 by CD4/CD8 subset in each CAR T cell pre-treatment group	186
9.10	Progression of PB CD5 ⁺ CD19 ⁺ by CAR T cell treatment group	188

List of Tables

1.1	Rai and Binet CLL staging systems	20
1.2	Characteristics of autologous CAR	44
1.3	Selected early studies of autologous CAR T cells	48
5.1	Transduction of 3T3 and PDAC cells	98
5.2	Transduction HEK/mouse T cells	101
5.3	Transduction WT and Tg T cells	102
6.1	CLL and T phenotype antibodies	110
6.2	CAR characteristic post ex vivo expansion by T cell source	120
7.1	CAR cell dose corrected for T cell subset and transduction efficiency	125
7.2	CAR cell dose corrected for T cell subset and transduction efficiency	134
7.3	CAR characteristics post ex vivo expansion by T cell source	145
8.1	CAR cell dose corrected for T cell subset and transduction efficiency	154
9.1	CD4/CD8 subsets before and after CAR T manufacture	181
9.2	Shift in CD3+CD8+ subsets before and after CAR manufacture	183
9.3	Total T cells produced and CAR ⁺ T cell dose in each treatment group and by subset	184

List of Abbreviations

AITL	Angioimmunoblastic T cell lymphoma
ALCL	Anaplastic large cell lymphoma
ALL	Acute lymphoblastic leukaemia (either B or T)
AML	Acute myeloid leukaemia
APC	Allophycocyanin
ASH	American Society Hematology
AT	Adoptive transfer
ATCC	American type culture collection
B6	C57BL/6 (mouse strain)
BCL2	B-cell lymphoma 2
BCL6	B-cell lymphoma 6
BCMA	B-cell maturation antigen
BCR	B-cell receptor
BiTE	Bispecific antibodies
BM	Bone marrow
BMSC	Bone marrow stromal cell
BR	Bendamustine rituximab
BSA	Bovine serum albumin
BSU	Biological services unit
BTK	Bruton's tyrosine kinase
CAR	Chimeric antigen receptor
CD	Cluster of differentiation
CI	Confidence interval
CIT	Chemo-immunotherapy
CLL	Chronic lymphocytic leukaemia
CM	Central memory
CR	Complete remission
CRS	Cytokine release syndrome
CSF	Cerebrospinal fluid
CyTOF	Mass cytometry

DAPI	4'6-diamidino-2-phenylindole
del(17p)	Deletion 17p
DLBCL	Diffuse large B cell lymphoma
DLI	Donor lymphocyte infusions
DNA	Deoxyribonucleic acid
EDTA	Ethylenediamine tetra-acetate
EFS	Event free survival
EM	Effector memory
EMA	European Medicines Agency
FasL	Fas ligand
FCR	Fludarabine cyclophosphamide rituximab
FDA	US Food and Drug Administration
FISH	Fluorescence in situ hybridisation
FL	Follicular lymphoma
Flu/Cy	Fludarabine cyclophosphamide
FMO	Fluorescence minus one
FSC	Forward side scatter
GMP	Good Manufacturing Practice
GVHD	Graft versus host disease
GVL	Graft versus leukaemia
HEK	Human embryonic
HL	Hodgkin lymphoma
HLH	Haemophagocytic lymphohistiocytosis
HIV	Human immunodeficiency virus
HMGB1	High mobility group box 1
HSCT	Allogeneic haematopoietic stem cell transplantation
ICANS	Immune effector cell associated neurotoxicity syndrome
IEC	Immune effector cells
IFN γ	Interferon gamma
IGHV	Immunoglobulin variable region heavy chain
IGVL	Immunoglobulin variable region light chain
IHC	Immunohistochemistry

IL	Interleukin
IP	Intraperitoneal
ITAM	Immunoreceptor tyrosine-based activation motif
ITK	Interleukin-2-inducible T-cell kinase
IV	Intravenous
JULIET	Pivotal autologous CD19-41BB CAR study
LN	Lymph node
LB	Lysogeny broth
MDACC	MD Anderson Cancer Centre
MEC1	CLL cell line in prolymphocytoid transformation
M-CLL	IgHV mutated CLL
MCL	Mantle cell lymphoma
MDSC	Myeloid deprived suppressor cells
MFI	Mean fluorescence intensity
MM	Multiple myeloma
MRD	Minimal residual disease
MTA	Materials transfer agreement
NK	Natural killer cells
NCI	National Cancer Institute, Bethesda
NHL	Non Hodgkins Lymphoma
NHS	National Health Service (UK)
NLC	Nurse like cells
NS	Not significant
NSG	NON-SCID- γ mice
ORR	Overall response rate
OS	Overall survival
PB	Peripheral blood
PBMC	Peripheral blood mononuclear cells
PBS	Phosphate buffered saline
PCR	Polymerase chain reaction
PD-1	Programmed death-1
PD-L1	Programmed death ligand-1

PE	Phycoerythrin
PEI	Polyethylenimine
PerCP	Peridinin-chlorophyll-protein
PD	Progressive disease
PFS	Progression free survival
PI3K	Phosphoinositide 3-kinase
PMA	Phorbol myristate acetate
PML	Primary mediastinal B-cell lymphoma
PR	Partial remission
PTCL	Peripheral T cell lymphoma
RNA	Ribose nucleic acid
ROR1	Receptor tyrosine kinase-like orphan receptor 1
R/R	Relapse/refractory
RT	Room temperature
scFv	Single chain variable fragment
SD	Stable disease
SF3B1	Splicing factor 3b subunit 1
SLL	Small lymphocytic lymphoma
TAM	Tumour associated macrophages
TBI	Total body irradiation
TCL1	T cell leukaemia/lymphoma 1
tFL	Transformed follicular lymphoma
Tg	Transgenic (TCL1) mouse
Th1	T helper 1 cell
Th2	T helper 2 cell
T _N	Naïve T cell
TP53	Tumour protein p53
Treg	CD4 ⁺ CD25 ⁺ regulatory T cells
U-CLL	IgHV unmutated CLL
WBC	White blood cell
WT	Wild type
ZUMA-1	Pivotal autologous CD19-CD28 CAR phase 1/2 study

Meeting Abstracts

Sanderson R, Romero-Toledo A, Gribben J. CAR T Cells Derived from Healthy Mice Lead to Cytokine Release Syndrome (CRS) in TCL1 Chronic Lymphocytic Leukemia Model; Mice with CLL Treated with Acalabrutinib or Ibrutinib Have Improved CAR T Cell Function without Increasing the Cytokines of CRS. *Blood* 2019: 134; Abstract 249.

Oral presentation.

Sanderson R, Romero-Toledo A, Gribben J. CD19⁺ Relapse Post CD19 Chimeric Antigen Receptor (CAR) T cells in Chronic Lymphocytic Leukemia (CLL) is Determined by T cell Fitness. *HemaSphere* 2019; 3, 404-405. Abstract S898. *Oral presentation.*

Sanderson R, Romero-Toledo A, Gribben J. Exhausted CLL T Cells Mediated by PD-1 Expression an Important Mechanism for CD19 CAR Efficacy in CLL in the Adoptive Transfer TCL1 Mouse Model. *Blood* 2018: 132; Abstract 4537. *Poster presentation.*

Sanderson R, Romero-Toledo A, Gribben J. Exhausted CLL T Cells Mediated by PD-1 Expression an Important Mechanism for CD19 CAR Efficacy in CLL in the Adoptive Transfer TCL1 Mouse Model. UK CLL Forum, Sept 2018. *Oral presentation.*

Prize – Catovsky Prize, best oral presentation.

1. Background

1.1 Chronic Lymphocytic Leukaemia

1.1.1 Definition, staging and prognosis

B cell chronic lymphocytic leukaemia (CLL) is a clonal disorder of mature B lymphocytes (B cells), with a unique morphology and immunophenotype. It is characterized by the progressive accumulation of monoclonal B cells in the peripheral blood (PB), bone marrow (BM) and secondary lymphoid organs leading to lymphadenopathy, lymphocytosis and organomegaly. Diagnostic criteria for CLL as per WHO Classification of Tumours and Haematopoietic and Lymphoid Tissues include the sustained, persistent monoclonal lymphocytosis of greater than $5 \times 10^9/L$ with a CLL phenotype in the PB (1). The phenotype of the circulating B cells should be confirmed by flow cytometry. The leukaemia cells found in the blood smear are characteristically small, mature lymphocytes, with a narrow border of cytoplasm and a dense nucleus lacking nucleoli and have partially aggregated chromatin (2). CLL cells co-express the T cell antigen CD5 and B cell antigens CD19, CD20 and CD23. The levels of surface immunoglobulin, CD20 and CD79b are characteristically low compared to normal B cells (3).

CLL is the most common leukaemia in adults with around 3500 cases per year in the UK with 59% of patients being diagnosed in people aged 70 or over (4). There are two widely accepted staging methods for use in both patient care and clinical trials, the Rai (5) and the Binet (6) systems. Both systems describe three subgroups with discrete clinical outcomes. They rely on standard laboratory tests and clinical examination, so are both simple and inexpensive and do not require imaging (Table 1) and describe patients with a median survival ranging from <2 years to 17 years.

Rai Staging		Clinical Features	Binet Staging	Clinical Features
0	Low risk	Lymphocytosis PB/BM	A	<3 LN areas, no anaemia or thrombocytopenia
1	Intermediate risk	Lymphocytosis plus lymphadenopathy	B	≥3 LN areas no anaemia or thrombocytopenia
2		Lymphocytosis plus hepatosplenomegaly		
3	High risk	Lymphocytosis plus anaemia	C	Haemoglobin <100g/L ± platelets <100 ± lymphadenopathy or organomegaly
4		Lymphocytosis plus thrombocytopenia		

Table 1.1: Rai and Binet CLL staging systems

CLL can be divided into two groups based on the mutational status of the immunoglobulin gene. The level of somatic mutation within the variable region of the immunoglobulin heavy chain (IGHV) is important to define prognosis in CLL; patients with >98% of identity to the germline are considered as IGHV unmutated (U-CLL), and have an inferior prognosis than those with more than 2% of mutations, who are designated IGHV mutated (M-CLL) and can often survive decades without intervention (7, 8).

In the 1990s it was shown that by chromosomal banding that patients with a normal karyotype had a better prognosis than those with single or multiple karyotype abnormalities (9). This technology by using mitogen activated CLL cells allows only 50% of chromosomal changes to be detected because the harvest of the metaphases is poor. This has been overcome by fluorescence *in situ* hybridization (FISH), which has determined the most significant cytogenetic abnormality, is deletion of the chromosome region 17p13.1 (del17p) which defines a group which progresses rapidly

and tends to have a poor response to standard chemo-immunotherapy (CIT) (10). Cytogenetic abnormalities commonly observed in CLL other than 17p include deletion of 11q (del11q), trisomy of chromosome 12 and deletion of 13q (del13q) as the sole abnormality as determined by FISH (10). Median survival times for these groups were 32, 79, 114 and 133 months respectively. However, patients with combinations of abnormalities also have very poor outcomes as a complex karyotype independent from 17p and IGHV also defines a group with unfavourable survival after CIT (11) as well as novel agents ibrutinib (12) and venetoclax (13). There is also some evidence that younger people with CLL (<55 years) have slightly different biology with adverse features appearing more commonly and can have a more aggressive clinical course than in older patients (14).

Within these recurring cytogenetic abnormalities critical genes are affected including DLEU/mir15a/miR15-1 (15) for del13q, *NOTCH1* for trisomy 12 (16) and *RDX* and *ATM* for del11q (17). Common genetic mutations in CLL can be clonal or subclonal and are often heterogeneous among different patients. Different groups have identified a panel of genes found to be recurrently mutated in CLL by whole exome sequencing (most genes at frequencies <10%), with *SF3B1*, *TP53* and *NOTCH1* being among the predominantly mutated genes (18, 19). The understanding of these data was limited by the variable timing that these samples were collected in the disease course. This challenge was resolved by the direct comparison between matched pre-treatment and relapse biopsies in the phase III German CLL Study Group CLL8 study (20) demonstrating highly frequent clonal evolution (21). However, shorter progression free survival (PFS) was only associated with mutations in *TP53* and *SF3B1* and in the context of first line fludarabine based chemotherapy, the future evolutionary trajectory could be anticipated in the pretreatment sample in one third of cases. Clonal shifts also occur after treatment with ibrutinib such as mutations in *BTK* and *PLCG2* (22).

1.1.2 First-line treatment

It has been known for some time that early treatment of indolent CLL with chlorambucil does not improve survival (23), a finding which has more recently been confirmed with fludarabine (24). The new guidelines from the International Workshop on CLL (iwCLL) remain in agreement with previous guidelines that early stage disease should not be treated until their disease has progressed or become symptomatic (2, 25). Although CLL is considered incurable by standard treatment options, impressive responses have been obtained by the addition of the type 1 humanized CD20 antibody rituximab to fludarabine and cyclophosphamide which prolongs overall survival (20, 26). Prior to treatment it is important to assess comorbidities by a geriatric assessment such as the Cumulative Illness Rating Scale (CIRS) which can help define groups of patients that can tolerate CIT “go-go” patients and those who may tolerate dose reduced monotherapy “slow-go” patients (27, 28). Following these studies and others CIT with fludarabine, cyclophosphamide and rituximab (FCR) has become the standard therapy for physically fit “go-go” patients who are treatment-naïve and without del(17p). However, the regimen is associated with substantial toxicity, including prolonged neutropenia, severe infections and an elevated risk of secondary malignancy (29).

The German CLL study group performed the CLL10 study, an international phase 3, open label study to investigate the use of FCR versus the combination of the alkylating drug bendamustine and rituximab in first line CLL patients without del(17p) and confirmed the benefit in progression free survival (PFS) of FCR, but noted the reduced frequency of severe neutropenia and infections with bendamustine and rituximab (30). Treatment is only indicated if active disease criteria are met (25), and the routine upfront treatment is a combination of anti-CD20 antibody (rituximab or obinotuzumab) and chemotherapy (fludarabine/cyclophosphamide, bendamustine or chlorambucil), with the choice being determined by the physical fitness of the patient.

Although there is no cure for CLL with chemotherapy alone, it is susceptible to cell-mediated immune control associated with allogeneic stem cell transplantation (31)

(HSCT). However, it is expected that most patients that have CIT will ultimately relapse. Although novel treatments are increasingly available, it will be important to identify subgroups of patients who will likely achieve long PFS with CIT. At a median follow-up of 12.8 years, the PFS of M-CLL was 54%, and 8.7% for U-CLL. Of the 50% of M-CLL patients that achieved MRD negative complete responses (CR) after treatment, their PFS was 80% at 12.8 years with plateau of the curves (32). Similar findings were found by the German CLL study group (11), indicating a subgroup of patients with long term survival following only one treatment. This subgroup can be further defined by additional mutations, and in particular M-CLL patients with del11q, del13q and +12q have PFS>90% at 8 years (11) which will be important to consider in the era of novel therapies. Other novel factors can predict the response to FCR for example telomere length, which could be used to inform the design of future risk-adapted clinical trials (33).

1.1.3 Relapsed/refractory and unfit patients

Unfit and older patients do not tolerate chemotherapy well. When comparing single agent fludarabine and chlorambucil, whilst fludarabine is a more active drug and results in more complete responses (CR), it does not improve PFS (34). Overall survival in this study was actually improved in the chlorambucil alone arm. Obinutuzumab is a glycoengineered, type 2 anti-CD20 monoclonal humanized antibody with single agent activity (35) or in combination with standard first line chemotherapy options fludarabine/cyclophosphamide or bendamustine (36). It was initially investigated in combination with chlorambucil in untreated CLL patients with coexisting medical conditions, compared to chlorambucil with rituximab, and the novel combination demonstrated significantly longer progression free survival (PFS) and higher rates of CR although with more infusion related reactions and neutropenia (37). This combination of obinutuzumab and chlorambucil until recently represents the CIT standard of care in this patient group. Interestingly, results from the open-label phase 3 study comparing fixed duration venetoclax and obinutuzumab to chlorambucil with obinutuzumab for patients with comorbidities was presented at the European Hematology Association (EHA) Congress in Amsterdam, June 2019 and then published in the New England

Journal of Medicine (NEJM) (38). This study demonstrates venetoclax and obinutuzumab is safe in this patient population and provides superior PFS, ORR, CR and MRD- responses which importantly include IGHV unmutated and TP53 mutated patients. It remains too early to judge a survival benefit.

The options in relapsed CLL have increased hugely in recent years, with the introduction of drugs that inhibit intracellular B cell receptor signaling. The best combinations and sequences of these drugs are under intensive investigation. Ibrutinib is a first in class, oral covalent inhibitor of Bruton's tyrosine kinase (BTK), an essential enzyme in B cell receptor (BCR) signaling, homing and adhesion. Significant homology between BTK and interleukin-2-inducible kinase (ITK) support ibrutinib as an immunomodulatory inhibitor of both BTK and ITK and that ibrutinib can irreversibly bind ITK and inhibits activation of Th2 cells after T cell receptor (TCR) signaling (39). CD4+ T cell populations isolated from CLL patients on ibrutinib are skewed to a Th1 profile after exposure to ibrutinib (39). The pivotal phase 2 trial confirmed durable remissions with PFS and OS of 75% and 83% at 2 years in patients with relapsed or refractory CLL (40). Since then, it has been compared head to head with Ofatumumab (41) in relapsed patients in the RESONATE trial, and also with chlorambucil as initial therapy (42) in the RESONATE 2 trial. Both trials show ibrutinib to be a highly active and effective drug and led to approval of this agent in relapsed and treatment naïve patient populations. The long term follow-up of RESONATE was recently published, confirming the OS and PFS benefit despite this being a crossover study (43). Ibrutinib alone compared to ibrutinib or bendamustine plus rituximab was recently reported in older patients with untreated CLL demonstrating ibrutinib to be superior to the CIT combination in terms of PFS. The addition of rituximab to ibrutinib was not significantly different (44). This study confirms the findings of RESONATE 2 as ibrutinib to be the standard of care in unfit previously untreated patients.

Idelalisib, is a potent oral small molecule inhibitor which selectively inhibits the lipid kinase PI3K δ targeting the B cell receptor signaling pathway. PI3K δ inhibition in CLL induces apoptosis and suppresses AKT phosphorylation in addition to interrupting CXCR4 and CXCR5 signaling and subsequently CLL homing (45). This can lead to redistribution

of CLL cells from the lymph node microenvironment's pro-survival signals and sensitization to apoptosis (45). It has activity in relapsed/refractory patients with high-risk features including del17p (46). Other inhibitors of the PI3K δ pathway exist including umbralisib and a dual PI3K γ/δ duvelisib. These drugs have strong immunomodulatory effects on several cell types in the microenvironment, most importantly T cells, where PI3K δ is a key component of T cell receptor and CD28 signaling (47).

Proteins in the B cell CLL/lymphoma 2 (BCL2) family are key regulators of the apoptotic process. This family comprises proapoptotic and prosurvival proteins, allowing cancers to evade apoptosis. Constitutively elevated expression of BCL2 renders CLL cells resistant to apoptosis. BH-3 mimetic drugs are a new class of anti-cancer drug that are physiological antagonists of BCL2 and trigger apoptosis. ABT-199 or venetoclax is a potent and selective BCL-2 inhibitor (48). It induces apoptosis of CLL cells via a TP53 independent mechanism (49). Venetoclax has demonstrated a high overall response rate in patients with relapsed CLL of 79%, which included patients with del(17p), U-CLL and who were fludarabine refractory (50). Tumour lysis was a concern initially, but this complication can largely be avoided by dose escalation and a risk adjusted treatment approach. This pivotal phase 1 validated BCL2 as a therapeutic target in cancer. This activity has subsequently been confirmed in patients with del17p (51) although fludarabine refractoriness and complex karyotype are associated with progression on venetoclax (52). Such impressive responses have been demonstrated in UK patients, with an 88% overall response, 85% of which had previously been exposed to BTK inhibitors in recent real world data from prior to NHS commissioning (53), in this cohort 48% had *TP53* abnormalities. Whilst high rates of venetoclax responses (72%) post B cell receptor antagonists have been confirmed from real world data from the USA, after a median follow-up of 7 months, 29% of patients had discontinued venetoclax (54). Many patients may have difficulty tolerating repeated rounds of treatment, particularly in terms of cytopenias.

Combining venetoclax with rituximab results in high response rates including 51% CR and 57% MRD negative rates including heavily pretreated patients with adverse

features such as U-CLL, del17p and *TP53* mutations (55, 56). There was preliminary evidence presented at the American Society of Hematology (ASH) annual meeting in 2018 (ASH 2018) that venetoclax in combination with the anti-CD20 monoclonal antibody obinutuzumab can restore the T and NK cell compartment in lymph nodes and PB, as well as achieving high rates of MRD undetectable disease in the PB in first line unfit patients, albeit with small patient numbers reported (10/11) (57). However, despite continuous treatment it is expected patients will relapse, likely due to acquired resistance mechanisms. One such mechanism, was identified by comparing paired pre-treatment and progression samples. The novel Gly101Val mutation in *BCL2* was identified and this reduces the affinity of *BCL2* for venetoclax (58). An alternative strategy may be to use targeted therapies upfront, even in combination to aim for deep MRD- remissions. The use of venetoclax and ibrutinib together has recently been reported, is safe and after 12 cycles resulted in 88% of patients having a CR, 61% of whom were MRD- (59). The significance of this combination in the longer term for PFS and OS is unknown.

For many patients on long term ibrutinib there is eventual emergence of resistance, particularly in the most high-risk populations, including those with del17p and complex karyotype (60), or in those that develop *BTK* or *PLCG2* mutations (22). The outcome for patients with disease progression on ibrutinib is very poor. One study demonstrated the majority of such patients have very high-risk features including U-CLL (94%), del(17p) by FISH (58%) and a complex karyotype (54%) and after discontinuation had a median overall survival (OS) of 3.1 months (61). Because this represents a small number of patients a clinical trial is appropriate but at this point CIT is unlikely to provide disease control. In patients who have del(17p) venetoclax is good option, and for those without *TP53* abnormalities, venetoclax plus rituximab or idelalisib could be considered (60). Beyond this, both cellular therapies and novel agents could be considered.

HSCT remains the established cellular therapy option in younger fitter patients who are felt can tolerate the associated toxicities. HSCT takes advantage of the graft-versus-leukaemia (GvL) effect mediated by differentiated transplanted immune

effector cells (IEC), which are able to mount an anti-tumour immune response and induce long lasting clinical remission (62). Patients who relapse post HSCT respond to donor lymphocyte infusions (DLI) further demonstrating GvL in CLL (63). Long-term survival after HSCT in the largest data series of 2589 patients has been reported by the European Society of Bone Marrow Transplantation (EBMT) (64). Event-free survival, OS and non-relapse mortality at 10 years was 28%, 35% and 40% respectively. Of course, this comes with a significant risk of graft versus host disease (GVHD) and other transplant complications and the patient must have an appropriate donor.

The use of HSCT in CLL is evolving with the increased usage of the novel agents discussed above. Previous guidelines had defined patients at sufficient risk to have an HSCT as those with del17p or *TP53* mutations or those who were refractory to purine analogue combination treatment (or relapsed within two years of it) (65). In the current era of novel agents HSCT is not usually now recommended in first remission for patients with del17p (66). However, in patients with poor prognostic features in subsequent relapses it could be considered by a transplant centre with an interest in this approach after careful assessment of suitability and donor availability (66). This is supported by recent practice guidelines (67). It is at this point that a novel cellular therapy approach such as CAR T cells could be considered as an alternative but this will depend on the nature of the poor prognostic features, patient fitness and preference and of course the availability of this approach versus other novel therapies. Whilst this is currently an option for a small number of patients it could be expected that this population will grow as more patients develop ibrutinib and venetoclax resistance.

Acalabrutinib (ACP-196) is a second generation, selective, irreversible inhibitor of BTK that has improved pharmacological features, including rapid oral absorption, short half life, and the absence of irreversible targeting to alternative kinases, such as EGFR, TEC and ITK (68). Some of these alternative kinases (e.g. EGFR, TEC and ITK) of ibrutinib may account for its adverse effects such as diarrhoea, rash, atrial fibrillation and bruising (69). When the binding interaction of a comprehensive panel of kinases with both ibrutinib and acalabrutinib was determined acalabrutinib demonstrated a high degree of selectivity for BTK without significant inhibition of ITK, which is known to be

inhibited by ibrutinib at therapeutic doses (70). Further, acalabrutinib demonstrates significant and sustained inhibition of BCR signalling in the E μ -TCL1 (TCL1) adoptive transfer model and improved survival of these mice when they are treated continually via their drinking water (70). Acalabrutinib has been used in ibrutinib naïve patients with relapsed CLL safely and is effective in patients including those with del17p, in a phase 1-2 study demonstrating a 95% response rate at 14 months (68). Headache was noted to be more common but there were no cases of atrial fibrillation reported. However, its role in patients who are refractory or intolerant to ibrutinib has not been determined and a phase 3 study comparing ibrutinib with acalabrutinib in high risk patients with relapsed CLL is underway.

T-cells from patients with CLL express higher levels of checkpoint inhibitory molecules, such as PD-1 compared to normal T cells (71). Furthermore, CLL cells express ligands for PD-1 such as PD-L1 and PD-L2. Two studies combining nivolumab (anti-PD-1 monoclonal antibody) with ibrutinib in relapsed refractory CLL and Richter transformation (RT) demonstrated significant activity in these patients (72, 73). An alternative PD-1 antibody pembrolizumab also showed activity in RT patients who had previously had ibrutinib but not in patients who had relapsed CLL (74). However, a single centre published its combined experience of pembrolizumab and nivolumab in 10 patients with RT, and found 90% had treatment failure with median time treatment failure being 1.2 months and median OS after RT diagnosis being 4.2 months (75). Only one patient had a sustained response which they rapidly consolidated with an allogeneic transplant.

1.2 Microenvironment

1.2.1 BCR signalling and the microenvironment

There is a large body of evidence that suggests the interactions between CLL cells and non-malignant cells in the tumour microenvironment play a key role in the pathophysiology of the disease. When removed from the microenvironment CLL cells undergo spontaneous apoptosis under conditions that support the growth of human B cell lines *in vivo* (76), but they can be rescued by co-culture with bone marrow stromal cells (BMSC) or nurse like cells (NLC) (77). NLC can be generated *in vitro* from the monocyte fraction of CLL peripheral mononuclear cells. One mechanism by which CLL cells create their favourable microenvironment is through the secretion of the nuclear protein high mobility group box 1 (HMGB1), which can stimulate NLC differentiation *in vitro* by activating the receptor for advanced glycation end products (RAGE)-Toll Like receptor 9 (TLR9) pathway (78).

Mesenchymal stromal cells, such as BMSC contribute to normal bone marrow architecture. Such stromal cells are commonly found in the secondary lymphoid organs. CLL cells are protected from spontaneous and drug-induced apoptosis by BMSC (79), and BMSCs have been shown to down-regulate CD20 expression of CLL cells (80). Stromal cells secrete chemokines, which organize CLL cell trafficking and cell homing, such as CXCL12, which is secreted by both BMSC and NLC, and CXCL13 by NLC that bind to CXCR4 and CXCR5 respectively on the CLL cell (81, 82).

CLL is associated with a tumour supportive microenvironment and profound defects in T cell function. To engraft human CLL into immunodeficient mice, autologous T cells are required for CLL cells to survive and proliferate (83). Interactions between CD40 expressing B cells and CD154 (CD40L) on activated CD4 T cells are critical for normal antigen presentation and induction of normal B cell responses. Activated CD4 cells contribute to CLL proliferation via CD40 and IL-21 (84). In CLL, there is an absolute increase in T cell numbers primarily due to increased CD8+ cytotoxic T cells with inversion of the normal CD4: CD8 ratio. However, there is an accumulation of

terminally differentiated effector memory T cells, with a relative decrease in naïve precursors (85), which is associated with advanced disease stage (86). Both CD4 and CD8 compartments demonstrate altered gene expression compared to healthy aged matched controls, with differentially expressed genes and functional defects in cytoskeleton formation, vesicle trafficking and cytotoxicity in these cells (87). In co-culture experiments using CLL cells and healthy T cells similar defects can be induced in both CD4 and CD8 cells (87). T cells fail to form functional immune synapses (71, 88) due to impaired actin polymerization. Direct contact with CLL cells induces these defects in previously healthy T cells in vitro and in vivo. Taken together, CLL leads to significant impairment of T cell function that has been recapitulated in the TCL1 transgenic mouse model (89).

T cell exhaustion is an acquired state of dysfunction initially described in chronic viral infections (90). It is believed that T cell dysfunction in tumours is largely attributed to persistent antigenic stimulation of T cells, leading to a number of progressive phenotypic and functional changes. Exhausted T cells have low proliferative and cytokine producing capabilities and express inhibitory surface markers such as programme death-1 (PD-1 or CD279) (91, 92). PD-1 and its ligands PD-L1 and PD-L2 represent an important immune checkpoint axis in maintaining an immunosuppressive microenvironment (93). In CLL, CD8 cells exhibit defects in proliferation, cytotoxicity and have increased expression of PD-1 but not of other inhibitory receptors including CD152 (CTLA4), CD366 (TIM3) and CD223 (LAG3) and thus exhibit some of the features of exhaustion (94). However, there are other features that differ including, increased production of IFN γ and TNF α and normal IL2 (94). The authors term this 'psuedo-exhaustion' and hypothesized that this state may be due to chronic stimulation by autonomously active signalling of the B cell receptor (BCR) characteristic of CLL (95). CLL cells express higher levels of PD-L1 compared to B lymphocytes from normal donors (86). Interference with the PD-1/PD-L1 axis by PD-L1 blocking antibodies prevents CLL development and restores immune effector functions, in the TCL1 adoptive transfer model of CLL (96).

Regulatory T cells (Tregs) are a subpopulation of CD4⁺ T cells with potent immunosuppressive activity and play a role in immune homeostasis, and preventing autoimmune and chronic inflammatory diseases. Tregs often impair activation, survival and expansion of antitumour T cells through the production of immunosuppressive cytokines and metabolic changes (97). Thus, Tregs are of interest in immunotherapy. In CLL, there is an increase in absolute numbers of CD4⁺CD25⁺CD127⁻ Tregs, and higher numbers correlate with a shorter time to first treatment in treatment naïve patients (98, 99).

Myeloid derived suppressor cells (MDSC) represent a heterogeneous population that shares characteristics including an aberrant myeloid phenotype and the ability to suppress T cells. In vitro they suppress T cell activation and induce suppressive regulatory T cells and a population derived from monocytes are expanded in patients with untreated CLL (100). Both tumour associated macrophages and MDSC share common mechanisms of anti-tumour activity, for example overexpression of T cell inhibitory ligands such as PD-L1 on MDSC (100). This is also seen in the TCL1 adoptive transfer model, with CLL development leading to upregulated PD-L1 and PD-L2 expression which might contribute to T cell exhaustion in CLL (101).

The importance of the microenvironment in CLL has led to the design of immunotherapeutic strategies that either interfere with the survival signals coming from it as well as BCR signalling. Several small molecule BCR signalling inhibitors, for example targeting BTK and PI3K have excellent clinical activity. The BTK inhibitor ibrutinib is capable of overcoming pro-survival signals from the immunosuppressive CLL microenvironment for example through STAT3-mediated suppression of regulatory B cell function and inhibition of the PD-1/PD-L1 pathway. It selectively down-regulates the expression of PD-1 on both CD4 and CD8 T cells as well as PD-L1 on CLL cells (102). In T cells, three Tec kinases are expressed, ITK, RIK/TKK and TEC. ITK is expressed at highest amounts and plays a major role in regulating signalling from the T cell receptor. Ibrutinib is an irreversible inhibitor of ITK and skews T cells from a Th2-dominant to a Th1 CD8 population (39). Further, elevated T cell numbers and cytokine levels normalize, and the T cell repertoire diversity increases significantly (103).

Cytokine production by T cells is mediated by PI3K signalling, idelalisib does not show any direct cytotoxic effect on T cells, but it can inhibit several inflammatory cytokines such as IL6, IL10, TNF α and CD40L (104). It also reduces chemotaxis toward CXCL12 and CXCL13 and migration beneath stromal cells (45).

The BCR signalling pathway is central to CLL activation and is likely to be triggered by antigens in the microenvironment. However, the microenvironment provides potent pro-survival signals that are also disrupted by the new small molecule inhibitors representing new therapeutic strategies in the management of CLL.

1.2.2 Modelling CLL

1.2.2.1 Cell lines

Leukaemic cell lines are important tools for the study of disease that can be expanded *in vitro*. However, studies of CLL are impeded by the lack of continuous human cell lines. *In vivo*, CLL cells display characteristics consistent with defects in apoptosis and prolonged survival. Despite their longevity *in vivo*, primary CLL cells undergo spontaneous apoptosis in conditions that would keep human B cells alive (105). The survival and proliferation of primary cells depends on the microenvironment (106) so there is a lack of representative CLL cell lines that can proliferate alone. Systems that use multiple cell layers are inadequate to reflect the dimensions of the microenvironment. The few existing cell lines represent high-risk, IGHV U-CLL but lack primary features associated with clinical CLL (107). The expression of CD5 is obligatory but the most well characterized, MEC1, has mutated *TP53* and a complex karyotype, but is negative for CD5 and is derived from a patient with prolymphocytoid transformation (108). Because of the importance of the tumour microenvironment and the need to study the host immune response an animal model is required.

1.2.2.2 Animal models

It is already known that CLL is a two compartment disease in which CLL cells are trafficked between peripheral vasculature, bone marrow and lymphoid tissues. Gene expression profiling studies of CLL in different compartments identified the lymph nodes as the predominant site of CLL activation and proliferation (109). Such pathways include up-regulation of B cell receptor and nuclear factor- κ B activation. Further, lymph node derived CLL cells possess a distinct phenotype, and exhibit an enhanced capacity for T cell activation and superior immune synapse formation when compared with paired peripheral blood samples (110). Such findings further confirm the need for an in vivo model since in vitro systems are not able to replicate the interaction between CLL and the microenvironment in secondary lymphoid organs and the blood.

T cell leukaemia 1 (TCL1) is an oncogene activated by recurrent reciprocal translocations at chromosome segment 14q32.1 in the most common of the mature T cell malignancies, T-cell prolymphocytic leukaemia. The E μ -TCL1 (TCL1) mouse model, is a transgenic mouse in which the TCL1 gene was placed under the control of the IGHV promoter so that the TCL1 protein is expressed in immature and mature B cells (111). These mice develop a polyclonal proliferation of CD5⁺ B cells starting at 6 months, most evident in the spleen and peripheral blood but also lymph nodes and bone marrow. After 11-18 months, 100% of transgenic mice become visibly ill with hepatosplenomegaly, lymphadenopathy and high white blood cell (WBC) counts, all of which are typical of human CLL. TCL1 is highly expressed in U-CLL and this model resembles an aggressive form of human U-CLL which has wild type *p53* (112). This model has been used to investigate the autonomous signalling of the BCR in CLL (95) but is particularly useful to model a more aggressive form of CLL and the interaction between novel immunotherapeutic approaches and the microenvironment (113). Several transgenic and knockout mouse models have been crossed with TCL1 to elucidate the functional role of specific molecules in the onset and progression of CLL in vivo (figure 1) (114). For example, by crossing transgenic ROR1 and TCL1 mice their offspring rapidly develop a CLL like leukaemia at a significantly younger age than with either transgene alone (115). Further, by crossing TCL1 mice with *p53* knockout mice

they also develop leukaemia at a younger age with a more aggressive and drug resistant phenotype (116).

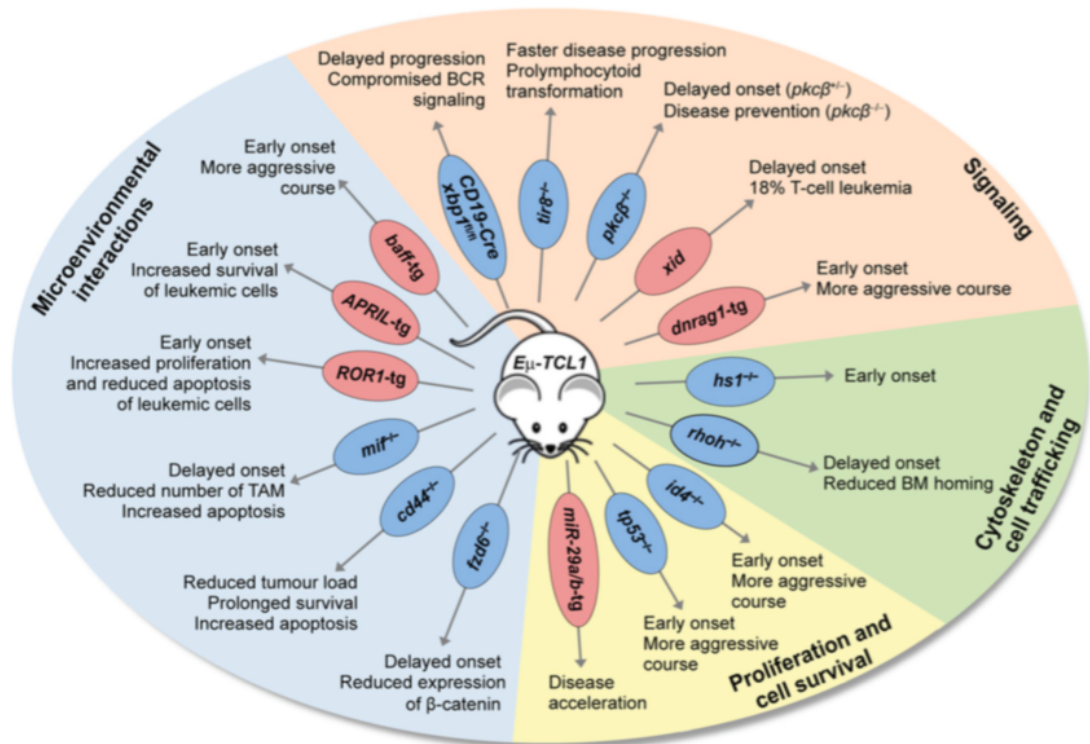


Figure 1.1: Summarised study of novel pathogenic mechanisms of CLL in the TCL1 mouse model by the crossing of the above models with TCL1 (114).

Previous studies in TCL1 mice demonstrate T cell defects and subset changes can be modelled in leukaemic mice (89, 117) and closely resemble the changes seen to represent human CLL. One limitation of the model is the delayed disease development, with variable latency from 9-14 months, albeit with 100% penetrance. Our group was the first to demonstrate that murine murine CLL is transplantable to healthy syngeneic mice by adoptive transfer of CLL by intravenous injection (hereafter referred to as AT) (89). This allows elimination of the confounding variable of aging and can shorten disease latency. Previous work from our group has demonstrated AT of TCL1 into WT mice can replicate T cell dysfunction seen in aged TCL1 leukaemia and indeed human CLL, and lead to rapid development of CLL after a median of 7 weeks with very homogenous disease among individual mice (118). Therefore, demonstrating the

suitability of this strategy to replicate T cell changes in CLL but rapid enough to conveniently investigate therapeutic interventions.

AT of TCL1 into wild type mice has been used by other groups to explore T cell function and the microenvironment. The AT of TCL1 into Rag2^{-/-} deficient mice which completely lack B and T cells have significantly shorter survival compared to WT mice indicating immune cells play a role in CLL progression (119). When CD4⁺ and CD8⁺ T cells are depleted from WT mice using antibodies, followed by AT of TCL1 only the loss of CD8⁺ T cells had a significant effect on CLL in terms of increasing WCC in the PB and spleen weight. Together this indicates CD8⁺ T cells are the main anti-tumoural T cell in CLL (119). Their anti-tumoural effects are lost by T cell exhaustion, which is further antagonized by interaction with anti-tumoural ligands such as PD-L1 overexpressed on CLL cells. In AT TCL1 a larger proportion of effector cells in the spleen express exhaustion markers such as PD-1, CD244 and Lag3 compared to the PB (119). PD-L1 is characteristic of murine CLL cells and its detection is highest in the spleen (118). PD-L1 is also highly expressed on splenic monocytes, and skew towards a Ly6C^{low} patrolling or non-classical phenotype (101). Further, blockade of the PD-1/PD-L1 immune checkpoint in this model prevents engraftment of AT CLL and restores immune effector functions (96). Taken together these data suggest that T cell activation and exhaustion is induced in secondary lymphoid organs and not the PB. Therefore, results obtained from PB derived CD8 T cells should be interpreted with caution.

Work from our group presented at ASH 2018 used the AT CLL model to investigate the effect of ibrutinib and acalabrutinib on T cell function characterized by mass cytometry (CyTOF). Ibrutinib treatment of these mice resulted in an alteration of cytokine secretion in keeping with a switch from Th2 towards Th1 polarity and increased cytotoxic T cell function (120). T cells in CLL have increased IFN- γ (94), and acalabrutinib caused its decrease in keeping with normalization. Also, CD8⁺ T cell cytotoxicity and immune synapse formation was improved (121). Given that acalabrutinib does not have an inhibitory effect on ITK, this suggests this BTKi modulates its T cell mediated immune response indirectly via their effects in the CLL B cell compartment or perhaps other immunosuppressive cells such as MDSC. As a note

a caution, mice from the same model have been treated with acalabrutinib, anti-PD-1 antibody and the combination of both (122). Acalabrutinib was the most effective therapy in reducing CD5⁺CD19⁺ disease in PB and spleen, but the combination of acalabrutinib plus PD-1 inhibitor actually reduced mouse survival, and histopathology revealed an increase in lymph node involvement with a higher mitotic rate. Such insights, are important to establish in preclinical testing. However, contradictory messages have been demonstrated in vitro and ex vivo functional assays of human T cells. They did not find Th1 skewing in ibrutinib treated patients with no change in cytokines. Ibrutinib also impaired T cell proliferation whilst other more selective BTKi zanubrutinib and acalabrutinib did not (123).

AT of TCL1 results in substantial increases in FoxP3⁺ CD25⁺ Tregs, with percentages again much higher in spleen and BM compared to PB (124). However, the depletion of Tregs using CD25 antibodies in this model after AT had no significant impact on CLL load in the spleen, BM, lymph nodes or spleen size.

More recently, the entire tumour microenvironment has been studied together in the AT TCL1 model using mass cytometry (CyTOF). This has confirmed some of the findings described above including the increased PD-L1 expression on splenic CLL cells and exhaustion markers such as PD-1 and LAG3 in CD8₊ T cells, Tregs, macrophages and natural killer (NK) cells (125). Based on their findings they treated mice using the AT TCL1 model single anti-PD1, anti-LAG3, anti-KLRG1 and dual anti-PD1/KLRG or anti-PD-1/LAG3 antibodies. Interestingly, the dual anti-PD1/LAG3 was the most efficient in terms of lowering CLL load in the spleen and PB and the only combination that resulted in disease free mice (125). Their microenvironment was also studied by mass cytometry confirming dual therapy corrected the imbalance generated by CLL and restored an immunocompetent environment with fewer Tregs and myeloid cells and more T cells (125).

The TCL1 model has also been used to gain insights into the clonal evolution of CLL. By performing whole exome sequencing of TCL1 leukaemia and leukaemia serially transplanted into WT recipients, the authors showed that similarly to CLL patients,

mutations in mice are subclonal and heterogeneous among different mice (126). This molecular heterogeneity mirrors heterogeneous disease characteristics such as organ infiltration or T cell skewing and is a further strength of this model in the future research of CLL.

1.3 Cellular Immunotherapy

1.3.1 Chimeric antigen receptor T cells

Whilst CLL patients now experience excellent responses from CIT and an exciting array of novel drugs as previously discussed, this disease remains incurable out with the context of HSCT. CLL is predominantly a disease of the elderly, many of whom would not be fit enough for HSCT and there is no standard of care for refractory patients, particularly in ibrutinib or venetoclax refractory CLL. For all these reasons there is still a need for new treatments, and given the outstanding success of immunotherapy in other CD19 malignancies to provide genuine long-term remissions and perhaps a hope for a cure this as an active area of investigation in CLL.

CAR T cells are genetically engineered T cells containing CAR receptors, which are a class of synthetic receptors that reprogramme lymphocyte specificity and function. They are derived from a CAR construct which consists of an extracellular tumour antigen targeting binding domain (ectodomain), a hinge region, a trans-membrane domain that anchors the CAR to the cell membrane, and an intracellular domain (endodomain) which leads to cell signalling (figure 1.2). The extracellular tumour antigen target is typically derived from the light and heavy chain portions of a single chain variable fragment (scFv), which are commonly derived from monoclonal antibodies, which are often murine (127). This enables the T cell to recognize the target in a non MHC restricted way. The main disadvantages being the tumour antigen needs to be extracellular and since the scFv are often murine derived they may be more immunogenic.

From a clinical perspective, autologous cells are used, so first the patients peripheral blood mononuclear cells must be collected by a leukapheresis procedure. This is generally well tolerated, with the main concerns being intravenous access and reactions to the citrate anticoagulant used. Following collection of lymphocytes, in the commercial setting the cells are then sent to an appropriate clinical good manufacturing practice (GMP) cell manufacturing facility, where the cells are

genetically modified and expanded ex vivo. Processed and harvested T cells can be used either used directly or cryopreserved for future use. There are pros and cons of both approaches but the licensed autologous CD19 products are cryopreserved at the manufacturing facility. The overall process is summarized in figure 3. Automated GMP compliant platforms now exist which can generate genetically modified T cells like CAR T cells on a smaller scale, which can feasibly be done in cellular therapy centres currently in the context of clinical trials. Instruments such as CliniMACS Plus and Prodigy systems allow the enrichment of specific subsets of T cells, such as CD4⁺, CD8⁺ or CD62L⁺. Multiple centres presented early phase 1 data at ASH 2018 of their experience using such automated platforms, predominantly testing novel CAR with dual targets, which will be discussed in more detail later.

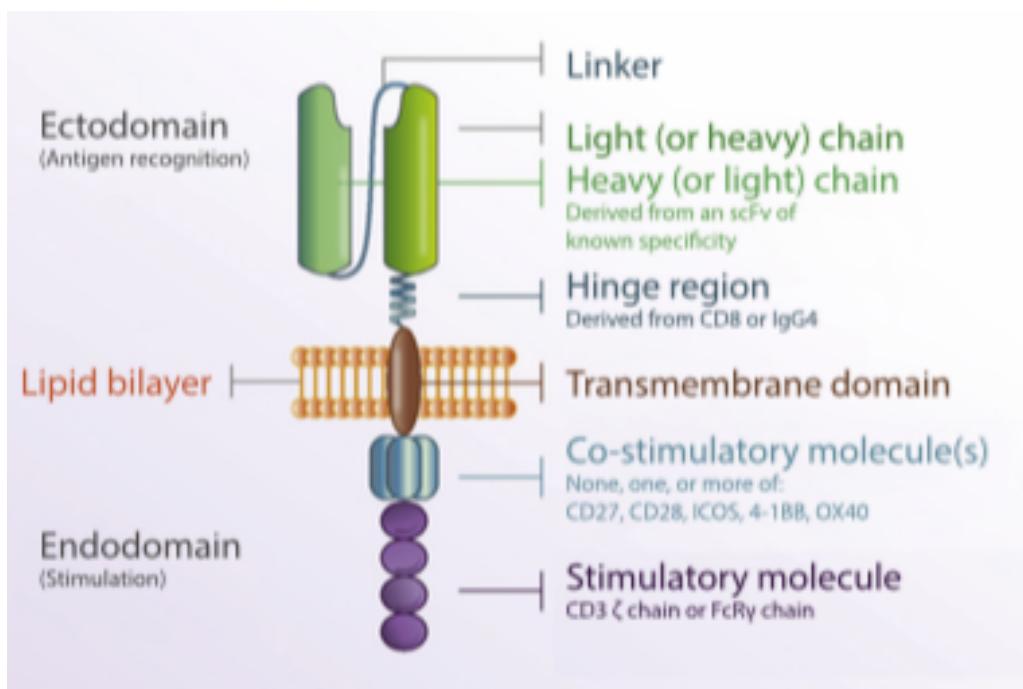


Figure 1.2: Structure of a second generation CAR (128).

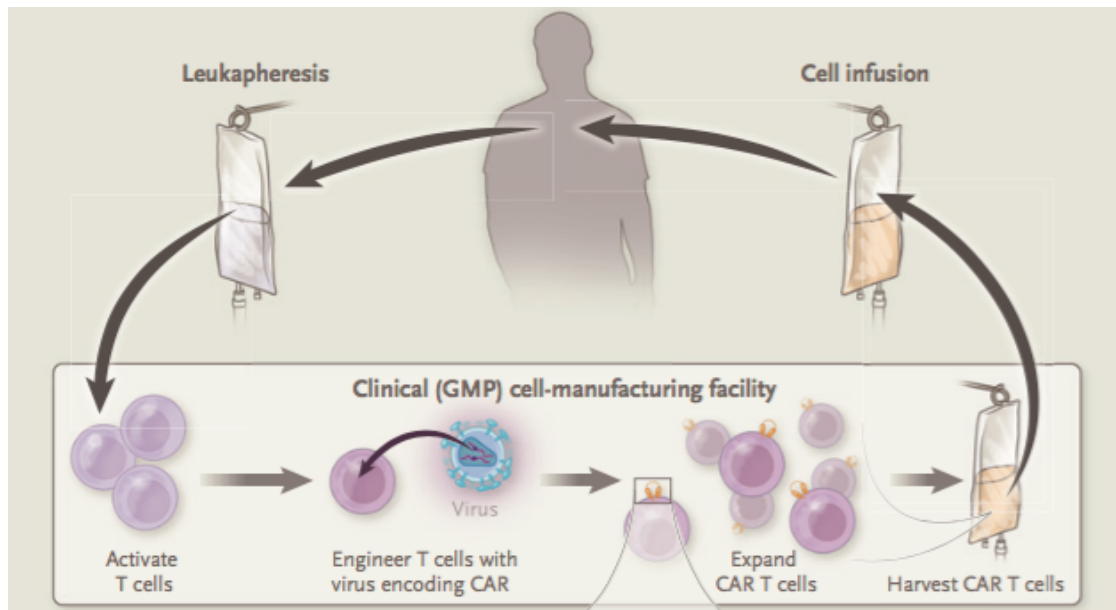


Figure 1.3: Clinical process of CAR production - Tran et al NEJM 2017 (129)

First generation CAR linked the engagement of the CAR signal to the intracellular machinery, typically via CD3 ζ . The incorporation of co-stimulatory domains such as CD28 and CD137 (41BB) can augment this signalling and enhance T cell proliferation and persistence (130, 131). CAR constructs with one additional co-stimulatory domain are referred to as second generation, which are to be the focus of my PhD thesis, but third generation constructs exist with additional co-stimulatory domains. The optimal design of a CAR is the subject of active clinical investigation, and there is evidence that the 41BB co-stimulatory domains are better at preventing T cell exhaustion than those based on CD28 (132). Third generation CARs have been used in limited phase I studies targeting CD20, HER-2 and CD19. For the third generation CD19 CAR combining a CD28 and 41BB co-stimulatory domain a comparable response to second generation CAR T cells was seen with modest toxicity but the overall survival data was poor (133). The structural differences between the generations of CAR T cells is summarized in figure 1.4.

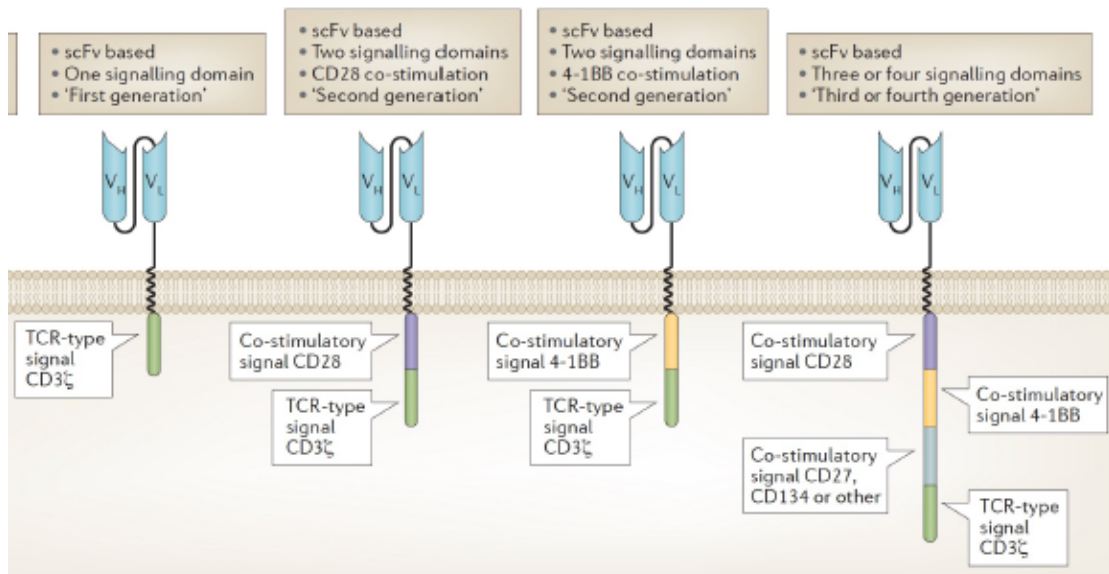


Figure 1.4: Three generations of CARs (134)

Gammaretroviral and lentiviral vectors have been commonly used to integrate the CAR construct in the T cell and provide stable CD19 expression (135). However, non-viral approaches such as the transposon/transposase Sleeping Beauty system have also been used (136), but not widely in the CARs currently being used in clinical practice or trials. Different centres employ variable expansion protocols and it remains unclear how differences in manufacturing processes between units will affect outcomes. CAR T cells generated from CD3⁺ population are widely used in clinical trials. T cells of a specific phenotype or subset could be selected prior to starting the manufacturing process rather than simply enriching for CD3⁺. Studies from different laboratories have demonstrated that naïve (T_N) (137), central memory (T_{CM}) (138) or memory T cells T_M (139) have functional advantages, but the effect this has on CAR efficacy is an active subject of both preclinical and clinical investigation.

1.3.2 Preclinical modelling of CAR T cells

Whilst some CAR constructs are based on existing monoclonal antibodies, it is important to recognize that the safety of an antibody may underestimate the toxicity of CAR T cells, as their sometimes dramatic in-vivo expansion can amplify their activity. Therefore, studies of potential antigen expression on normal tissues must be performed, and constructs tested in clinically relevant models (140). The efficacy of

CD19 CAR T cells was originally investigated in vitro by the cytotoxicity of CLL cells and cell lines with transduced autologous or allogeneic human T cells. Following this, in vivo models used immunodeficient mice injected with CD19⁺ cell lines and treated with xenografted transduced human T cells (135, 141, 142). Whilst the use of such mice that lack their own B, T cells and NK cells ensures any therapeutic effect is due to the CAR T cells, they do not have their own immune system the response of which can be studied. Humanized CD19 specific scFv is superior to the most commonly CD19 scFv used FMC63 which is murine derived in treating human lymphoma xenografts in immunodeficient mice (143). It is also unclear from the evidence in clinical trials in humans if retrovirally or lentivirally transduced T cells are more effective, it is challenging to transduce mouse T-cells using lentiviral infection systems (144), therefore a retroviral system in a mouse model better allows for the rapid testing of multiple biological parameters.

An alternative physiological pre-clinical model to test CAR T cells is in immunocompetent mice, using validated in vivo models of CLL such as TCL1. This concept has been applied to other lymphoid disorders both using syngeneic CAR T cell models. Sadelain et al. adoptively transferred E μ -myc B-ALL into WT mice to produce a phenotype that resembles B-ALL. Normal syngeneic T cells were then retrovirally transduced with a CD19-CD28 CAR and used to treat these WT mice with ALL, in this way not only survival, but also the host immune response can be studied (145). Further, an alternative CD19-CD28 CAR used retrovirally transduced normal syngeneic T cells to treat WT mice injected with 38c13 lymphoma of murine origin from the same strain of mice. However, they were first conditioned with total body irradiation (5 Gy) and given subcutaneous IL2 after CAR T cell injections to promote engraftment and expansion. Of note the efficacy of this CAR was dependent on the irradiation of the mice first but they demonstrated significant antilymphoma activity and profound B cell aplasia (146). No such immunocompetent models have been reported in CLL and of note both models used normal syngeneic T cells to produce their CAR T cells. As previously discussed, the T cell dysfunction characteristic of CLL could impact CAR function and this has not been explored in an immunocompetent model of CLL. Given the significantly reduced response rates in CLL compared to ALL this represents a good

opportunity to understand the reasons for loss of CAR persistence through the host immune system in more detail.

1.3.3 CAR T cells in lymphoid malignancies

There has been outstanding success using CD19 directed CAR T cells in relapsed and refractory B cell malignancies, in patients who essentially had palliative diagnoses and therefore limited life expectancies. Such malignancies are particularly amenable, due to the conservation of the CD19 antigen on B cell malignancies from the most immature B-ALL to the most mature lymphomas (147).

In 2010, Kochenderfer et al. at the National Cancer Institute (NCI), Bethesda, MD published a pivotal report in *Blood* demonstrating engraftment of their CD19-CD28 retrovirally transduced CAR, B cell aplasia and a dramatic regression of lymphoma in a patient with advanced follicular lymphoma (148). Design and the construction of this CAR had been recently described (149). This was one of the first descriptions of successful CD19 CAR engraftment and efficacy in a lymphoid disease.

Following this, the first successful use of CD19 CARs in B cell leukaemias were reported. In 2011, the group from the University of Pennsylvania published their pivotal paper in the *NEJM* demonstrating CAR T cell expansion of a lentiviral CD19-41BB CAR in a patient with refractory *TP53* deleted CLL resulting in tumour lysis syndrome and a CR (150), and then in two further patients (151). This was followed by the use of the same CAR in two children with relapsed B-acute lymphoblastic leukaemia (ALL) resulting in a CR (152) having initially been announced on the front cover of the *New York Times* in December 2012. At the same time Brentjens et al. from Memorial Sloan Kettering Cancer Center (MSKCC) published their series of 10 patients with ALL and CLL treated with a retrovirally transduced CD19-CD28 CAR, albeit without such a marked clinical response (153). In 2010 in a letter Brentjens had described some of the patients from this series, providing one of the earliest descriptions of cytokine release syndrome (154). Since then CD19 CAR T cells have been shown to be active in CLL, but particularly in NHL and ALL. In the early years, the majority of the CAR T cells

that had made it to human studies were manufactured and infused in the USA. Three pharmaceutical companies have second generation autologous CD19 CAR T cell products in advanced development, each of which has collaborated with an academic centre due to the massive investment and expertise required to produce a cellular product that complies with GMP. These leading partnerships include Kite Pharma with the NCI, Novartis with the University of Pennsylvania and Juno with MSKCC and Fred Hutchinson Cancer Research Center (FHRC).

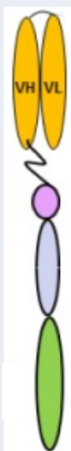
Name	Axicabtagene-ciloleucel	Tisagenlecleucel	Lisocabtagene-maraleucel
Product Name	Yescarta®	Kymriah®	
Trial	Zuma	Juliet	Transcend
	FMC63 (murine)	FMC63 (murine)	FMC63 (murine)
	CD28	41BB	41BB
	CD3z	CD3z	CD3z
Gene transfer	Retroviral	Lentivirus	Lentivirus
Cell source	PBMC	PBMC	CD4: CD8 = 1:1
Company	Kite/Gilead	Novartis	Juno/Celgene
Approval	FDA/EMA	FDA/EMA	Investigational

Table 1.2: Characteristics of three autologous second-generation CAR T cell products.

Table 1.3 highlights significant results for the early clinical trials of CD19 CAR T cells. The updates of the JULIET study from Novartis and ZUMA-1 from the Kite CAR at ASH 2016 represented the first reported multi-centre studies with centralized manufacturing of cryopreserved leukapheresis collections with national or international supply chains. This represented a significant advance in the technology to produce economies of scale to make it more feasible and affordable.

Early clinical trials of CD19 CAR T cells quickly revealed greater toxicities than those seen in other cellular therapies. Recent consensus guidelines from the American Society for Transplantation and Cellular Therapy (ASTCT) brings together the definition and grading of the main complications of CAR T cell therapy (155). Cytokine release syndrome (CRS) is defined as a supraphysiologic response following any immune therapy that results in the activation or engagement of endogenous or infused T cells. Symptoms can be progressive, must include fever at the onset, and may include hypotension, capillary leak (hypoxia) and end organ dysfunction. It is characterized by elevated serum concentration of various cytokines but particularly IFN γ , TNF α and IL6 (151). The anti-IL6 receptor monoclonal antibody tocilizumab is approved for the treatment of CRS and indeed to access CAR T cell therapy in the National Health Service (NHS) tocilizumab must be kept on site with 24-hour availability. Haemophagocytic lymphohistiocytosis (HLH) is a rare complication of CAR T cell therapy which overlaps with CRS but is considered distinct. Many patients with CRS have laboratory results that fulfil HLH criteria without hepatosplenomegaly, lymphadenopathy or overt haemophagocytosis.

Neurotoxicity is considered a separate entity to CRS due to its distinct timing and response to intervention. It is now referred to as the Immune Effector Cell Associated Neurotoxicity Syndrome (ICANS) and is defined as a pathological process of the central nervous system following IEC. Symptoms or signs can be progressive and may include aphasia, altered level of consciousness, impairment of cognitive skills, motor weakness, seizures and cerebral oedema. Headache is not included in this definition although it is common. Preliminary clinical experience suggests tocilizumab fails to prevent delayed ICANS when given for CRS (156), presumably because it does not generate significant levels of drug in the cerebrospinal fluid (CSF), as is the case in rhesus monkeys (157). Further, tocilizumab when given as prophylaxis prevents CRS but not ICANS (158). Some early CAR trials were stopped because of cerebral oedema, and this remains one of the most alarming potential complications of this therapy. Neurotoxicity is more common in patients with ALL and proinflammatory cytokines

were enriched in the CSF during severe neurotoxicity with high levels of IL6, IL8, MCP1 and IP10 (159).

Still one of the largest and most important CLL CAR specific studies remains that by Porter et al. at the University of Pennsylvania (160). Their mature data, including the initial three patients that comprised their pivotal early publication reported 14 patients. The overall response rate (ORR) in these heavily pre-treated patients was 8 out of 14 (57%), with 4 CR and 4 PR (both 29%). No patient that obtained a CR has relapsed and all responding patients developed CRS and B cell aplasia. In vivo expansion correlated with clinical response and long term persistent and functional CAR T cells have been found four years after infusion. Turtle presented impressive results in CLL at ASH in 2016 and subsequently published his series of an exceptionally high-risk CLL cohort (161). They reported on 24 patients with a median of 5 previous therapies, 3 post HSCT, 23 patients had del17p or a complex karyotype and most had already received ibrutinib and some also venetoclax. The ORR four weeks post CAR infusion was 71%, with 83% developing CRS and 33% neurotoxicity with one fatal outcome. Of the 24 patients who received the preferred Flu/Cy conditioning and $<2 \times 10^6$ CAR T-cells, 19 patients were restaged at four weeks with a CR rate 21% and PR 53%. Interestingly, 15/17 patients (88%) with marrow disease had no detectable disease post CAR T cells. Note the comparable relatively low overall CR rate in these studies.

Superior results have been presented in abstract form. At ASH 2018, data using the CD19-41BB CAR from Juno/Celgene lisocabtogene maraleucel (liso-cel) was presented (162). Of note this product has a defined composition of CD8: CD4 CAR⁺ cells which are transduced separately. The patients presented were equally high risk with either at least three previous treatments or two treatments and high-risk genetic features. Of the 10 patients studied 9 had received ibrutinib and 6 venetoclax. Of the 8 patients evaluable at 30 days 6 of the 8 had responded with 4 CR (50%). Of the patients evaluable for MRD 6 of the 7 were MRD negative. 8 out of 10 patients experience CRS but all were mild (grade 1 or 2).

The ability of T cells to proliferate in response to stimulation, differs between diseases as T cells from CLL patients are often difficult to expand and demonstrate functional deficits when compared to patients with ALL and healthy donors (163). Figure 5 shows the inferior proliferative burst of CLL T cells when stimulated with CD3/CD28 beads compared to age matched patients with relapsed/refractory myeloma or ALL. This also results in a significantly lower yield of T cells from patients with CLL at the end of the expansion.

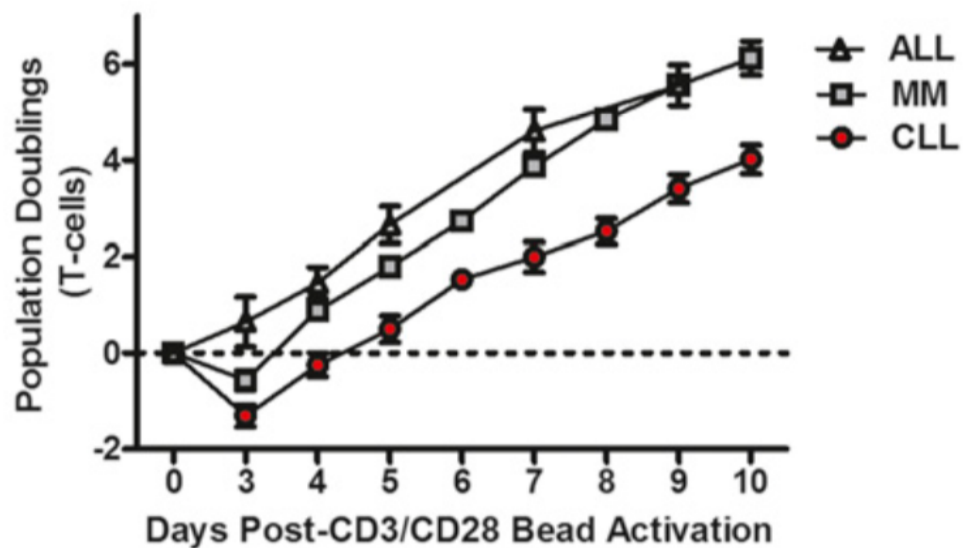


Figure 1.5: Ex vivo expansion of T cells post stimulation with CD3/CD28 beads (163).

T cells in CLL patients have been shown to be pseudo-exhausted due to exposure to high antigen loads and immunosuppressive cytokines (94) as previously discussed. Table 3 demonstrates response rates in ALL are clearly better than in CLL (~80-90% vs ~25-30%), particularly in relapsed/refractory (R/R) paediatric ALL, is this because of the impaired T cell function in CLL? Responses in relapsed DLBCL appear to be mixed, albeit in small subgroups it does appear transformed FL and PMBCL respond well. The difficulty in comparing these studies, and in indeed optimizing this technology, is the huge array of variables in terms of method of gene transfer (lentivirus vs retrovirus), the scFv affinity, co-stimulatory domains, manufacturing conditions, the starting T cell population and cell dose used and chemotherapy conditioning that could be applied.

Table 1.3: Selected early studies looking at autologous CD19 CAR T cells

Ref	Patients	Disease & Status	Ages	LV/ RV	Co- stim	Response & notes
<i>University of Pennsylvania (Porter 2011)</i>						
(151)	3	R/R CLL	64-77	LV	41BB	2 CR, 1 PR
<i>MSKCC (Brentjens 2011)</i>						
(153)	10	R/R CLL (8), ALL (2)	48-73	RV	CD28	1 PR
<i>NCI (Kochenderfer 2012)</i>						
(164)	8	R/R FL (3), CLL (4), SMZL	47-63	RV	CD28	1 CR, 5 PR
<i>University of Pennsylvania (Maude 2014)</i>						
(165)	30	R/R ALL	5-60	LV	41BB	CR 90%, all had CRS
<i>MSKCC (Davila 2014)</i>						
(166)	16	R/R ALL	23-74	RV	CD28	CR 88%
<i>NCI (Kochenderfer 2015)</i>						
(167)	15	R/R DLBCL (5), CLL (4), iNHL (2), PMBCL (4)	30-68	RV	CD28	8 CR, 4 PR (CR in 3 CLL, 2 PMBCL, 1 DLBCL)
<i>NCI (Lee 2015)</i>						
(168)	21	R/R ALL, DLBCL	1-30	RV	CD28	CR 70%
<i>University of Pennsylvania (Porter 2015)</i>						
(160)	14	R/R CLL	51-78	LV	41BB	4 CR (29%)
<i>CTL019 - ELIANA, Novartis (Grupp 2016)</i>						
(169)	50	R/R ALL	<25	LV	41BB	41 CR (82%)
<i>CTL019 – JULIET, Novartis (Schuster 2016)</i>						
(170)	15	R/R DLBCL	25-77	LV	41BB	6 CR (40%), 1 PR
<i>ZUMA-1 (cohort 1), Kite Pharma (Neelapu 2016)</i>						
(171)	101	R/R DLBCL	25-76	RV	CD28	47% CR, 29% PR
<i>ZUMA-1 (cohort 2), Kite Pharma (Locke 2016)</i>						
(172)	6	R/R PMBCL, tFL	28-60	RV	CD28	100% CR
<i>FHCRC & Juno (Turtle 2016)</i>						
(173)	18	R/R CLL	40-73	LV	41BB	5 CR (27%), 8 PR
<i>FHCRC & Juno (Turtle 2016)</i>						
(174)	29	R/R ALL	20-73	LV	41BB	93% CR
<i>FHCRC & Juno (Turtle 2016)</i>						
(175)	32	R/R DLBCL (11), tFL (10) FL (5), MCL (4)	22-70	LV	41BB	DLBCL 18% CR, tFL 60% CR, FL 40% CR, MCL 0% CR

Abbreviations: ALL: Acute lymphoblastic leukaemia. CLL: Chronic lymphocytic leukaemia. CR: Complete remission. CRS: Cytokine release syndrome. DLBCL: Diffuse large B cell lymphoma. FL: Follicular lymphoma. iNHL: Indolent non Hodgkin lymphoma. LV: Lentiviral. MCL: Mantle cell lymphoma. PMBCL: Primary mediastinal B cell lymphoma. PR: Partial response. R/R: Relapsed or refractory. RV: Retroviral. SMZL: Splenic marginal zone lymphoma. tFL: Transformed follicular lymphoma.

Second generation CAR T cells require a CD28 or 41BB co-stimulatory signalling domain (176), which influences the metabolic characteristics of CAR T cells, which may explain the differences seen in their persistence in humans (177). Second generation CAR T cells based on CD28 and 41BB co-stimulation, are associated with approximately 3 logs-folds expansion and persistence for months to years. In some patients, B cell aplasia continues well beyond the last point CD19 CAR T cells were detected by flow while the transgene is still detectable by PCR, suggesting B cell aplasia is a suitable surrogate for CD19 CAR T cell persistence (165). In CLL, the efficacy of CAR T-cells with 41BB co-stimulatory domains (160) appears superior to that of CD28 domains (153) with sustained expression and effector functions of 41BB CAR T-cells has been reported to exceed 4-5 years (178, 179).

At ASH 2017, data using the two main autologous CD19 CAR in commercial development were first presented in larger patient numbers in high grade lymphoma. This led to back to back papers in the NEJM papers updating the results for these two pivotal CAR products in lymphoma. The use of CTL019 (CD19-41BB) in 28 patients resulted in CR in 6/14 (43%) patients with DLBCL and 10/14 (71%) in FL. CTL019 proliferated and was present in the PB and BM in patients who and did not have a response. In the majority of patients that had responded it was sustained and there was one death due to neurotoxicity. Severe CRS occurred in 18% and in a proportion of patients there was improvement in immunoglobulins after 6-18 months (180). The now phase 2 ZUMA-1 study was updated with 101 patients infused who had DLBCL, PMBCL or tFL. It demonstrated an ORR of 82% and CR rate of 54%, the OS at 18 months was 52% (181). Whilst CRS occurred in 93% of patients, severe CRS occurred in 13% with 2 deaths, one due to HLH and the other due to a cardiac arrest. Neurologic toxicity occurred in 64% of patients and in 28% it was severe with two associated deaths. Rates of CRS and neurotoxicity decreased over the study and the use of tocilizumab and steroids did not affect apparent response rates. This latter study led to Yescarta® or axicabtagene ciloleucel (axi-cel) to be the first US Food and Drug Administration (FDA) and European Medicines Agency (EMA) approved CAR in lymphoma in 2017 and 2018 respectively. Their long term data of 108 infused patients was updated at ASH 2018 which represents the longest follow-up of any CD19 CAR T

cell study (182). The median duration of response was 11.1 months and median OS not reached, figure 6 demonstrating the Kaplan-Meier estimate of OS with levelling of the curve. This finding represents a major improvement in clinical outcomes for these patients, for whom the expected median OS with conventional therapies is approximately 6 months, with a two year OS of around 20% (183). No new deaths were reported related to the CAR T cells and there were only 6 additional deaths due to progressive disease since the last report. This emphasizes the risks from both toxicity and progressive disease remain immediately after CAR T cell treatment. Despite B cell aplasia significant long-term problems with infections have not occurred and 75% of patients with an ongoing response show evidence of B cell recovery by 24 months which in some patients initiated at 9 months. This suggests that durable responses in patients with lymphoma do not require long term persistence of functional CAR T cells, which is perhaps contrary to what has been seen in ALL. Less than 20% of patients had ongoing grade 3 cytopenias, the pathophysiology of which is unclear.

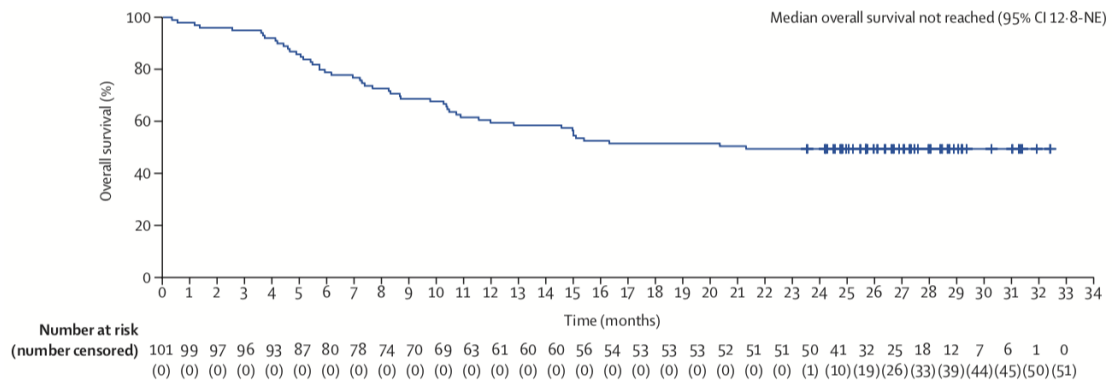


Figure 1.6: Kaplan-Meier estimate of overall survival of 108 patients infused with CD19-CD28 CAR Axi-Cel on the pivotal Zuma-1 study (182).

The results of the pivotal paediatric ELIANA study were updated in 2018 for ALL, using tisagenlecleucel (formerly CTL019) in a 25 centre international study with 75 patients with relapsed/refractory ALL infused demonstrating an overall remission rate of 81% at 3 months (184). All patients found to have responded were also found to be MRD- by flow cytometry. OS was 90 and 76% at 6 and 12 months respectively. 77% of patients experienced CRS and 40% neurotoxicity. Up to 50% of patients received some care on

intensive care and 25% received high dose vasopressors. Earlier reports of this study had led to FDA and EMA approvals for the use of tisagenlecleucel or Kymriah® in r/r ALL in children and young adults up to the age of 25. Many patients have received a stem cell allograft after CD19 CAR T cells for ALL, so the morbidity associated with long term survival is more complicated than that data presented in lymphoma.

Tisagenlecleucel/Kymriah has also been approved for DLBCL in 2018 based on data from the JULIET study which has recently been updated (185). They reported a best ORR 52% (40% CR and 12% PR) in 111 infused patients. Grade 3 or 4 CRS was 22% and neurotoxicity 12% with no deaths attributable to tisagenlecleucel, CRS or cerebral oedema. One important difference between JULIET and ZUMA-1 was bridging chemotherapy was allowed after leukapheresis in JULIET and 92% of patients did receive combinations of rituximab (54%), gemcitabine (40%), etoposide (26%), dexamethasone (25%), cisplatin (19%) and cytarabine (19%), as well as newer agents such as ibrutinib (9%) and lenalidomide (7%).

Both tisagenlecleucel and axi-cel are approved by the National Institute for Health and Care Excellence (NICE) and are available via the Cancer Drugs Fund in a limited number of specified CAR centres in the UK, for the indications discussed above in relapsed ALL (<26 years), DLBCL, tFL and PML. There is currently no licensed product by either the FDA or EMA for use in CLL. In lymphoma, for these licensed products the scFv is the same, but with clear differences in the CAR co-stimulatory domain and method of gene transfer. Also, the dosing of both products and its lymphodepletion is slightly different. Axi-cel requires lymphodepletion with fludarabine (30mg/m²) and cyclophosphamide (500mg/m²) on D-5, -4 and -3 before infusion at a target cell dose of 2 x 10⁶ CAR T cells/kg of bodyweight (target 1-2 x 10⁶). Tisagenlecleucel requires the same lymphodepletion schedule but with different doses of fludarabine (25mg/m²) and cyclophosphamide (250mg/m²), with a target cell dose 0.6-6 x 10⁸ (non-weight based dosing). The significance of these differences is as yet unclear.

The author is now delivering the lymphoma CD19 CAR T cells in the NHS at King's College Hospital, which was the first UK centre to infuse lymphoma patients with both licensed products.

1.3.4 Novel concepts in CAR T cell therapy

1.3.4.1 Relapse post CAR T cells

Despite robust expansion and subsequent achievement of CR, relapses do frequently occur. When relapse is with disease that still expresses CD19⁺, it is suggestive of CAR failure, perhaps due to lack of persistence due to the hostile immune microenvironment or specifically in CLL due to impaired or exhausted CAR T cell function. Significant differences between the CD19-CD28 and CD19-41BB trials make direct comparison difficult, but certainly persistence of the CD19-41BB CAR has been demonstrated for many years in ALL and CLL (160, 184). However, in ZUMA-1 many patients with NHL with durable long-term responses showed evidence of B cell recovery without relapse, so further study of the importance of long term persistence in different diseases is warranted (182). Specifically, at 2 years 66% of patients had detectable CAR T cells by PCR, and 75% of patients with an ongoing response had detectable CAR T cells by flow (186).

Many relapses are associated with loss of the CD19 antigen, for which different mechanisms leading to antigen escape have been reported. In the largest paediatric ALL study reported, in the characterization of CD19 status at the time of relapse only one patient had a CD19⁺ recurrence and 15 patients had CD19⁻ disease (3 with concomitant CD19⁺ blasts) (184). In patients with persistent CAR T cells, in B-ALL a mechanism for this has been found to be due to splice mutations in CD19 (187). Other mechanisms may be important, for example, a case report of a patient with CLL and Richter transformation treated with a CD19 CAR relapsed with a clonally related CD19⁻ plasmablastic lymphoma highlights the ability of mature lymphomas to evade immunotherapy by differentiating along pathways comparable to counterparts (188). In lymphoma, preliminary abstract data from the ZUMA-1 study indicated of those

patients which had relapse biopsies 67% were CD19+ and 33% CD19- (189, 190). The high occurrence of CD19+ relapses could be related to T cell fitness or perhaps a reflection of the hostile immune microenvironment the CAR faces. Also, in the same abstract data was presented indicating the high expression of PD-L1 in both CD19- and CD19+ progression biopsies.

In adult ALL, in an analysis of 22 patients who had initially responded to a CD19-41BB CAR, 14/22 had a CD19+ relapse although in 5 of these patients the leukaemic blasts had diminished CD19 expression. 6/22 had a CD19- relapse including one patient with an MLL-rearranged B-ALL who relapsed with AML. This patient along with a second from another series were reported as having an AML relapse which was demonstrated to be clonally related to their ALL, indicating a novel mechanism of CD19- antigen escape (191). In this series CD19+ relapse was associated with loss of CAR persistence and CD19- relapse despite persistent cells and B cell aplasia (192). Finally, a fascinating case report details how one patient with ALL who relapsed 9 months after tisagenlecleucel, was due to the CAR gene being unintentionally transduced into a single leukaemic B cell during T cell manufacturing, and its product binding to the CD19 epitope on the surface of leukaemic blasts, masking it from recognition by and conferring resistance to tisagenlecleucel (193).

1.3.4.2 Novel antigens and dual targeting

An obvious strategy to prevent antigen negative relapses is the targeting of alternative or additional B cell specific antigens. CD22 is highly expressed on mature lymphoid malignancies and as such was one of the first alternative CAR to be developed to overcome the selection of antigen loss variants (194). Initially, the CD22 CAR was used after the CD19 CAR, with demonstrated efficacy leading to MRD- CR in CD22+ ALL in 4/9 children and young adults after using a lentiviral CD22-41BB CAR (195). A rapidly evolving area of CAR research is the use of bispecific CAR T cells, typically using the combination of CD19 and CD22 CAR T cells. Multiple groups presented early phase 1 data at ASH 2018 of dual antigen CAR targeting in relapsed B cell malignancies. Of interest, is the methods by which you get to dual targeting. Tandem transduction

starts with one selected T cell population which can be transduced twice with two completely different CAR constructs, for example the FHCRC group using CD19 and CD22 CARs leading to 83% CR in R/R paediatric ALL in 7 patients (196). Alternatively, the Stanford group used a bivalent CAR, in which one CAR incorporates both the FMC63 CD19 scFv with M971 CD22 scFv and a 41BB co-stimulatory domain. 4/4 paediatric ALL patients infused achieved a CR, 3 of which were MRD- by flow cytometry (197). The group at Great Ormond Street lead a study using a CD19/CD22 CAR with novel CD19 and CD22 components, which was bicistronic i.e. two independent CAR were transduced within one retroviral vector. 9/10 patients evaluable in this study achieved a flow MRD- CR with 4 patients having ongoing responses at the data cut off with MRD- remissions (198). In R/R NHL a dual CD19/CD20 CAR was reported in 6 patients with 2/6 achieving CR and 2/6 PR (199). The latter two groups used the automated platform CliniMACS Prodigy system which allows for close to point of care manufacturing complying with GMP practices.

There are alternative and novel targets in B cell malignancies. Combining CD19 with CD123 CAR T cells prevented antigen negative relapses in xenograft models of ALL (200). In CLL, CD23 CAR T cells show activity against CLL cell lines, primary CLL cells and in a xenograft mouse model, and could preserve normal B cell function (141). ROR1 is detected on malignant B cells in CLL and MCL (201), and at lower levels in adipose cells and some B cell precursors and so targeting of this antigen could spare normal B cells (202). In a retrospective review of 1500 patients, ROR1 expression was divided into ROR1 low and high expression, those patients with higher expression had significantly shorter treatment free survival and overall survival (203). The MD Anderson Cancer Center has a ROR1 CAR currently being tested in phase 1 in CLL patients (204), but there is also broader interest as ROR1 is expressed on a number of solid tumours including non small cell lung, pancreatic and triple negative breast cancers. CD37 is expressed in NHL and CLL, and in some cases of peripheral T cell lymphoma. CD37 CAR T cells show antigen driven activity, cytokine production and cytotoxicity in in vitro B and T cell lymphoma models, including patient derived xenografts (205). CAR T cells targeting such novel antigens remain an area of active investigation in lymphoid malignancies.

Despite the outstanding success of CD19 CAR T cells the main licensed products are obtained from murine antibodies. T cell mediated immune responses specific for peptides from the murine FMC63 scFv could result in premature elimination of CAR T cells and relapse. Groups have created a humanised scFV equivalent to FMC63 (143). CARs with several scFvs were used to transduce human T cells and eliminated lymphoma xenograft models in immunodeficient mice. Imaging of cell surface distribution of human CARs revealed no clustering without T cell engagement. The same group also altered the fusion sites between different CAR components to reduce immunogenicity (143). Many groups now use humanized CD19 scFv which are being used in larger scale clinical trials.

1.3.4.3 Predictors of response

Little is known about predictive indicators of response to CAR T cell therapy. Particularly in CLL, where response rates do not match those seen in ALL, this is an important area of research. In an analysis of 41 patients who received a lentivirally transduced CD19-41BB CAR, in vivo expansion was required to be effective but also ex vivo expansion during manufacture was a simple predictor of response and correlated with proliferation in vivo. They carried out a thorough evaluation of the apheresed T cells and CAR T cell product from non-responding (NR) and responding (CR) patients and found the transcriptomic profile from NR were enriched with genes belonging to terminal differentiation and exhaustion and CAR T cells from CR patients were enriched in memory related genes (206). Flow cytometry also demonstrated significantly lower percentages of CAR T cells with the CD8⁺PD-1⁺ phenotype from CR patients and elevated levels of other exhaustion markers such as LAG-3 and TIM-3 co-expressing PD-1 predicting a negative response to treatment whilst a sustained remission was associated with elevated CD27⁺CD45RO⁻ CD8⁺ T cells at the time of leucopheresis which are memory-like characteristics (206). They then used CAR T cells from NR and CR patients in an immunodeficient murine xenograft model (NSG mice engrafted with the CD19⁺ NALM-cell line). This led to prolonged survival of mice compared to those mice treated with CR derived CAR T cells. In this model, CAR T cells

derived from healthy donors were used as a control and performed the best in terms of mouse survival and tumour regression (206). They also treated these mice with CR patient T cells that were enriched or depleted of CD27+PD-1-CD8+ T cells. Removal of this population resulted in loss of tumour control. Taken together, this indicates the intrinsic T cell fitness dictates both response and resistance to these CAR T cell. Drugs with the potential to reverse the exhausted phenotype represent an opportunity to modulate CAR function or the subsets used to manufacture CAR T cells may also be important. However, efficacy was not related to patient age, prior therapy, peripheral tumour burden or p53 status.

In lymphoma, a recent clinical paper looked at factors associated with a durable remission after CD19 CAR T cells. Multivariate analysis of clinical and treatment characteristics, serum biomarkers, manufacturing and pharmacokinetic data show that lower pre-lymphodepletion serum LDH and a favourable cytokine profile, defined as serum monocyte chemoattractant protein-1 (MCP-1) and peak IL-7 above the median, were associated with better PFS (207). Even in high-risk patients with pre-lymphodepletion serum LDH levels above normal, a favourable cytokine profile after lymphodepletion was associated with a low risk of a PFS event. They conclude strategies to augment the cytokine response to lymphodepletion could be used to alter outcome.

1.3.4.4 Subsets

The absolute number of CD4+/CD8+ T cells, their phenotypes (naïve (T_N), central memory (T_{CM}), or effector ($T_{EM/EMRA}$)), the detrimental effects of previous treatment regimens and the intrinsic functional capabilities of T cells varies between patients which are in turn is influenced by their diseases, significantly affect the ability to produce effective CAR T cells. There is not the same body of evidence in lymphoma to suggest T cell dysfunction as there is in CLL. In most reported trials, including the large registration studies of the two licensed CD19 autologous CAR T cells, patients have received products containing random compositions of CD4⁺ and CD8⁺ naïve and memory T cells. This could explain some of the differences seen in efficacy and toxicity

in clinical trials. There is preclinical evidence that CAR T cells enriched for naïve and memory phenotypes as starting material and using defined CD4+/CD8+ subset compositions have a better performance in mice xenograft models (208). On this basis of this preclinical evidence the same group performed trials of autologous CD19-41BB CAR T cells with defined subset compositions in ALL (174), NHL (175) and CLL (161) with impressive outcomes and led to the ongoing TRANSCEND clinical trials in lymphoma and CLL. Of course, this may be limited in some patients who have skewed starting material. Single cell analysis of the preinfusion CD19 CAR product in patients with NHL demonstrate that these CAR products contain polyfunctional T cell subsets. When using a prespecified T cell polyfunctional strength index applied to the preinfusion product, associations with clinical outcomes were greater with polyfunctional CD4+ compared to CD8+ T cells (209). It has been shown that antigen experienced subsets promote the differentiation of T_N into T_{EM} via a non-apoptotic Fas signal (210). Altering the culture conditions may enable specific T cell populations from which to manufacture CAR T cells. Alternative methods of using combinations of interleukin-7 (IL-7) and interleukin 15 (IL-15) in culture after preselecting naïve precursors may allow to generate CAR T cells with a T stem cell memory (T_{SCM}) phenotype (211).

1.3.4.5 BTK inhibitors and immunotherapy

Whilst there has been extensive investigation of the effect of ibrutinib on the B cell receptor, there is growing evidence to suggest it may have a positive effect on T cell function including absolute numbers, repertoire and immune reconstitution (39, 103). In a phase II study ibrutinib reduced expression of activation markers and PD-1 on T cells (212). Further, it is an inhibitor of ITK, an essential enzyme in Th2 T cells which can enhance antitumour responses (39). Combining ibrutinib with PD-1 blockade can improve T cell responses against solid tumours that do not express BTK (213). In a small cohort of patients with CLL treated with CAR T cells and ibrutinib, 3 patients treated with ibrutinib for >1 year at the time of apheresis had improved T cell ex vivo and in vivo expansion and subsequent clinical response (163). They also demonstrated that patients who had received more than 5 cycles of ibrutinib, produced more

interferon- γ after stimulation with CD3/CD28 beads or phorbol myristate acetate (PMA)/ionomycin and their CAR T cells had better ex vivo expansion. Interestingly, patients with CLL who were ibrutinib naïve had poorer ex vivo expansion. They propose that ex vivo proliferation appears to be consistent with the ability of CAR T cells to expand when infused. In this study ibrutinib was not continued concurrently after CAR T cells, but they did evaluate the effect of this in a xenograft mouse model. Ex vivo exposure of ibrutinib to CAR T cells does not alter their function. NOD-SCID- γ (NSG) mice were engrafted with Nalm-6 (human ALL cell line) or OSU-CLL (human CLL cell line). CAR T cells were derived from healthy donors and injected 7 days after tumour engraftment. In both the Nalm-6 model, which would be expected to be ibrutinib resistant, and in OSU-CLL injected mice, ibrutinib improved engraftment and expansion of CAR T cells and the overall survival of the mice. Although this effect could be because of ibrutinib mediated changes in lymphocyte chemotaxis and adhesion, the improvement in mouse survival argues for an increase in CAR T cell function (163).

Preliminary evidence of the success of this synergy was presented at ASH 2018. In an ongoing prospective trial of a humanized CD19-41BB CAR ibrutinib was used both pre and as a concurrent treatment in patients who were not in CR despite 6 months of ibrutinib (214). Lymphodepletion was with the standard Flu/Cy and this was a dose escalation study. This was again a high-risk population as 11 of the 19 patients infused had del17p or p53. 18/19 patients had CRS which was mostly grade 1-2 and 5 patients had neurotoxicity. One patient died of a cardiac arrhythmia during severe neurotoxicity after resolution of CRS. Median follow-up for 18 surviving patients is 18.5 months. The 3-month bone marrow demonstrates morphological remission in 17 and 15 by flow cytometry MRD. By iwCLL criteria at 3 months for 14 patients evaluable 6 were CR (43%), 4 in PR. 6 patients discontinued ibrutinib at a median of 8 months and overall at last follow-up 16/18 remain in morphologic remission. A second group also reported a cohort treated with a CD19-41BB, with a higher ORR but their CR rates by iwCLL criteria alone were not presented (215). They did have one death due to arrhythmia in the context of CRS, but overall they saw much less severe CRS in the CAR plus ibrutinib group. Of note ibrutinib was only administered from 2 weeks prior to leucopheresis until 3 months after CAR infusion.

The concept that ibrutinib can optimise T cell function has been explored in other types of immunotherapy. In a small study of ibrutinib given to 27 patients with relapsed CLL post ASCT, 87% of patients had a response, with no GVHD and multiple patients with CLL relapse associated mixed chimerism converting to full donor chimerism post instigation of ibrutinib, they concluded ibrutinib enhances graft versus leukaemia through a T cell mediated effect (216). CD19/CD3 bispecific antibodies (BiTE) recruit T cells to form cytolytic synapses with CD19⁺ tumour cells. Blinatumomab is licensed and improves survival in R/R B-ALL (217) and has demonstrated activity in R/R DLBCL (218). In CLL there is demonstrated activity in vitro and only recently activity has been demonstrated in patient derived xenograft models using a novel CD19/CD3 BiTE (219). Interestingly, in these xenograft models their novel CD19/CD3 BiTE induced more rapid killing of CLL cells from ibrutinib treated patients than those from treatment naïve patients. However, potent activity was also demonstrated against CLL cells from patients with acquired ibrutinib resistance. It is not clear if the effect of ibrutinib was on T cells or simply a reflection of taking samples from patients with a lower CLL burden (220), but it still supports the concept.

1.3.4.6 CAR T cells in other haematological diseases

1.3.4.6.1 Multiple Myeloma (MM)

There are case reports of the use and efficacy of the autologous CD19-41BB in myeloma leading to a CR for 12 months (221). In this case the CAR was used following a second high dose melphalan autologous stem cell transplant. Four years earlier the patient had received the same treatment without CAR and only had a transient PR. MM is a B cell malignancy which is usually CD19⁺, and in the case of this patient the myeloma cells were CD19⁺ in 99.9% of the patients' neoplastic cells. It has been suggested a minor component of the MM clone with drug-resistant, disease propagating properties has a B cell phenotype i.e. CD19⁺ (222) which would explain this activity. None the less novel myeloma specific CAR T cells are in development. B-cell maturation antigen (BCMA) is a cell surface receptor expressed primarily and

during plasma cell differentiation and is expressed consistently on MM cell lines and primary patient samples (223). A phase 1 study using a BCMA-41BB autologous lentivirally transduced CAR T cell in myeloma has recently been published (224). There was an ORR of 12/25 although CRS was seen in 22 patients and a range of responses including 2 CR of 25 patients in a dose escalation study. Three patients had ongoing responses and responses as well as in-vivo expansion were associated with a higher CD4: CD8 ratio and higher frequency of CD45RO-CD27+CD8+ T cells in the premanufacturing product. This phenotype primarily identifies naïve but also T_{SCM} populations. CAR T cells in myeloma is a very promising therapeutic approach and the subject of many ongoing clinical trials. Interestingly, they looked at the differences in these populations when comparing leucopheresis samples obtained at completion of induction therapy and those in relapse/refractory status. They found this early memory phenotype significantly higher in patients collected after induction therapy, as was CD4: CD8 ratio and the measured ex vivo expansion. They suggested that timed and earlier lymphocyte collection before exposure to multiple lines of therapy may yield better clinical responses (224). At ASH 2018, initial results from the phase I/II EVOLVE study using a fully humanized lentivirally transduced BCMA-41BB CAR, for patients who have received 3 or more therapies were presented. Of the 13 patients treated, eight were evaluable for safety who had all been heavily pretreated. Grade 3 or above CRS did not occur, and there was one self limited transient episode of grade 3 neurotoxicity, suggesting an acceptable safety profile for this type of CAR (225).

1.3.4.6.2 Hodgkin lymphoma

Immunotherapy has already been shown to be effective for relapsed Hodgkin lymphoma (HL) in the form of checkpoint inhibition (226). Preliminary data has been published on the use of the CD30-CD28 CAR in 9 patients with CD30+ malignancies HL but also anaplastic large cell lymphoma (ALCL). It demonstrated a CAR T cell that expanded and persisted, which was safe with no unexpected on target off tumour toxicity. Of the 7 patients with relapsed HL two had a CR for over two years (227). A Chinese group has also published a series of 18 patients with relapsed HL but the best response was a PR in 7 patients. Again, they could demonstrate CAR T cell expansion

and no new safety signal was found (228). Both groups updated their data at ASH 2018, with the former group presenting data this time using lymphodepletion prior to their CD30-CD28 CAR. 6/8 patients assessed 6 weeks after infusion were in CR which lasted from 6 weeks to 6 months (229). The Chinese group this time presenting 4 HL and 2 ALCL patients, 5 patients obtaining a CR and for 3 of these patients lasted over a year. However, one patient died of CRS and pulmonary haemorrhage 20 days after CAR T cells (230). Finally, a group from North Carolina presented their CD30-CD28 CAR in 14 patients using bendamustine and fludarabine conditioning resulting in 6 CR and 1 PR, 2 of which patients remain in CR at 1 year (231).

1.3.4.6.3 Acute Myeloid Leukaemia (AML)

The great success of CAR T cells in ALL obviously makes their use in AML an area of active investigation, especially in poor risk cytogenetic AML or indeed relapsed AML. However, the biggest challenge in comparison to lymphoid disorders is identifying an appropriate surface antigen target, as those known to be present on AML cells are also present on healthy haematopoietic stem cells (HSC) predicting for BM aplasia. CD33 has heterogeneous expression on leukaemia blasts but there are many splice variants that impact protein structure, which may not be recognized by current CD33 directed therapeutics (232). Also, CD33 is present on healthy myeloid cells in the BM but also macrophages in the liver. Therefore, on target, off-tumour toxicity is anticipated. Preclinical testing of a humanized CD33 based on the scFv used in gemtuzumab demonstrated eradication of leukaemia and prolonged survival in AML xenografts. It also resulted in significant cytopenias and loss of myeloid progenitors in xenografts of haematopoietic toxicity. Unlike CD33, which is expressed at high levels on both leukaemic and normal HSC, CD123 expression on HSC is low to negligible (233). Pre-clinical testing of a CD123-CD28 CAR demonstrates anti-leukaemic activity in vitro and in vivo in a xenograft mouse model of AML. Further, when expressed in T cells from AML patients, these CD123 CARs could redirect patient derived T cell cytolytic activity against their autologous leukemic blasts (234). However, work from Gill et al. have raised safety concerns of targeting CD123 for AML patients. Testing a CD123-41BB CAR they reported rapid elimination of AML in a xenograft model but also eradication of

normal myelopoiesis (140). They suggest CD123 CAR T cells are a viable AML therapy but raise concerns for its use without the option of HSCT rescue (140). Separately, the FDA has approved the clinical trial use of the allogeneic CD123 CAR in AML in January 2017.

Other more novel AML antigens include human C-type lectin-like molecule-1 (CLL-1), which is restricted in myeloid cells as well as the majority of AML blasts. Importantly, it is also present on leukaemic stem cells but not HSC cells (235). CLL-1 CAR T cells lyse CLL-1⁺ cell lines and primary AML patient samples in vitro. Myeloid progenitor and mature myeloid cells are eliminated, but not normal HSC cells (236). Preliminary clinical data was presented by a Chinese group using a CLL1-CD33 CAR at ASH 2018. They reported a single paediatric patient with complex karyotype post multiple lines of therapy experiencing ablation of myeloid cells by D+19 post the CAR and lymphodepletion, to MRD- which they consolidated with an ASCT (237). Finally, CAR T cells have the ability to recognize non-protein antigens, an example being the Lewis Y antigen (LeY), an oligosaccharide structurally related to the Lewis blood group antigens. Is found on tumour associated antigens on multiple cancers including AML. A retrovirally transduced LeY-CD28 CAR was given to 4 patients after lymphodepletion, 1 patient had a cytogenetic remission and another a reduction in PB blasts. They demonstrated persistence by PCR and flow but all patients progressed with LeY⁺ disease.

1.3.4.6.4 T cell lymphoma

There are currently limited options for targeting T cell malignancies with CAR T cells. There is shared expression of most targetable surface antigens between malignant and normal T cells, potentially leading to profound immunodeficiency or CAR T cells targeting themselves. CD5 is present on approximately 80% of T-cell acute lymphoblastic leukaemia (T-ALL) (238) and T cell lymphoma and it is sometimes expressed on B cell lymphoma. When T cells are transduced with a CD5 CAR, they undergo only limited self targeting and expand ex vivo. They can eliminate T-ALL and T cell lymphoma cell lines and inhibit disease progression in xenograft models (239). NK

cells are both CD3- and CD5- and are an important part of the innate immune system. NK cells have a short lifespan in comparison to T cells but the lack of shared antigens would preclude self-targeting. Exploratory work has been performed transducing a CD5 CAR into a human NK cell line with stable expansion. The NK CD5 CAR had significant activity against T-ALL and T cell lymphoma cell lines and control of T-ALL in xenograft mouse models (240).

A novel approach has been recently reported. The $\alpha\beta$ TCR is a pan-T cell antigen that is expressed on normal T cells and highly expressed on mature peripheral T cell lymphomas (PTCL) >95% and most angioimmunoblastic T cell lymphoma (AITL) (241). These mature T cell lymphomas are aggressive and their treatment is a clear area of need given their outcomes and much worse than B cell lymphomas. TCR α and β chains comprise N-terminal variable and C-terminal constant regions and both must be present for it to be expressed. TCR diversity is generated by somatic recombination, when each TCR chain selects a variable (V), diversity (D), joining (J) and constant (C) region. In a clonal T cell population they all possess the same unique TCR. A single gene codes for the α chain of the TCR, whilst a feature of TCR β -chain (TCRBC) recombination is the presence of only two genes associated with the β -chain constant region, either TCRBC1 or TCRBC2 (242). University College London have confirmed TCRBC monoclonality in many types of T cell malignancies and demonstrated the efficiency of targeting TRBC1 in cell lines and a disseminated model of T-ALL (243). This represents the first T cell malignancy targeted treatment with the potential to eradicate the T cell clone while preserving sufficient normal T cells to maintain cellular immunity.

1.3.4.7 Allogeneic CAR T cells

In heavily pre-treated patients, it is not always possible to manufacture a therapeutic product (152), often because of a failure to mobilise sufficient T cells or for failure of the expansion process fails. In CLL, as previously discussed the disease itself impairs T cell function and ex vivo expansion. Further, as currently licensed CD19 CAR T cell products are autologous and bespoke, there is a significant delay after apheresis and some patients may not receive the product due to disease progression. The point at which enrolment occurs into the two major studies ZUMA-1 and JULIET were different, so the drop-out rates shouldn't be compared directly before the cells are available for infusion, but the JULIET study gives more detail on the patients enrolled but not infused. Of the 50/165 patients enrolled but not infused, 12 had manufacturing failure (7%) and 38 (23%) had reasons that related to disease progression including death in 16 and the primary physician deciding against further participation in 16 patients (185). Since the NHS England/Cancer Drugs Fund process started in late 2018 for tisagenlecleucel and axi-cel there have been limited numbers of manufacturing slots available to CAR T cell centres in the UK, as well as local limits due to access to apheresis slots in the NHS. Whilst tisagenlecleucel is made in Europe, to make axi-cel the cells are still shipped via the manufacturers production facility in Amsterdam to Los Angeles, USA. This leads to much longer delays in production time and acquisition of cells than those reported in ZUMA-1, the authors clinical experience determining for axi-cel this to be 26 days. Taken together, whilst there are solutions to these challenges as CAR services expand in the UK (and Kite/Gilead starts to produce axi-cel in their manufacturing facility in Amsterdam), there is still a clinical need for off the shelf, immediately available CAR T cells, for patients who are rapidly progressing using donor or allogeneic T cells.

The production of universal CD19 CAR T cells from non HLA matched donor cells uses transcription activator-like effector nuclease (TALEN) mediated gene editing of the T cell receptor and CD52 gene loci (244). The first reported successful use of the of an allogeneic CAR T cell was in an infant with refractory B-ALL who had relapsed post unrelated donor ASCT and progressed post blinatumumab, along with a second infant

(245). The first TALEN was used to disrupt the CD52 gene, the target of alemtuzumab, in T cells transduced to express a CD19 CAR. This was designed to enhance survival in the presence of the anti-CD52 lymphodepleting antibody. At the same time a second TALEN was used to target the constant region of the T cell receptor α chain (TRAC), thereby disrupting cell surface expression of the TCR $\alpha\beta$. Manipulations were performed by electroporation of TALENs into lentiviral transduced CD19 CAR T cells. Residual TCR $\alpha\beta$ T cells were removed by magnetic beads although small numbers theoretically could remain which could cause GVHD. A suicide gene was also incorporated. Two clinical trials are currently evaluating this allogeneic CD19 CAR UCART19 in adult B-ALL (CALM, NCT02746952) and paediatric B-ALL (PALL, NCT02808442). Pooled data from these studies was presented at ASH 2018 (246). 20 patients have been infused, with 13 CALM and 7 PALL patients. At D28, of 16 patients evaluable (1 death, 2 not having reached D28, 1 data not collected) 14/16 achieved CR or Cri and 12/14 were MRD- by flow or PCR. 2/16 patients showed no CAR expansion and refractory disease. CSR was reported in 17/18 patients which was mostly mild, although one patient had severe CRS and died of neutropenic sepsis. Mild neurotoxicity was less common with 6/18 patients and two patients had mild skin GVHD which resolved with steroids. These cells are not expected to persist for long periods, but of the 5 patients in which no expansion was detected, 3 of these had not received alemtuzumab indicating that it is necessary to use the anti-CD52 antibody to promote CAR expansion. These trials are ongoing.

Gene editing allogeneic cells is a fast-moving field, and more precise techniques of encoding the CAR construct are being developed. Using a viral vector, the genes encoding the construct are integrated in a semi random fashion. Techniques which link the CAR with the TRAC may be more precise and allow TRAC disruption to occur only in cells successfully transduced with the CAR. These cells show superior anti-tumour efficacy in a murine xenograft model compared to unedited CAR cells and less PD-1 expression (247).

An alternative type of allogeneic CAR, is the manipulation of donor lymphocyte infusions post ASCT in B cell malignancies (248). The ability to harvest cells for

manufacture directly from the donor in patients who have relapsed post ASCT would probably yield cells with less exposure to cytotoxic substances and an abnormal tumour microenvironment. It also reduces the need for TCR knockout and GVHD. Using this strategy, the NCI demonstrated feasibility as 4/5 patients with ALL and 1/5 patients with CLL achieved CR despite no lymphodepletion, and importantly no evidence of GVHD. However, this approach can only be used after an ASCT, and given this treatment strategy is rare in the management of NHL and CLL it is not a practice approach in lymphoid disorders except ALL.

There is preliminary data suggesting the benefit of a radically different approach. The Rezvani laboratory at the MD Anderson are investigating the use of CD19 CAR NK cells. The source of NK cells is from their large umbilical cord blood bank in Houston, USA. Whilst no data has yet been published, preliminary data from their phase 1 dose escalation cohort has been presented in small meetings. In eight patients (5/8 had CLL or Richters) discussed, there was no CRS like toxicity, and 6 patients had a CR (Rezvani, personal communication).

1.3.4.8 Checkpoint inhibition combined with CAR T cells

The evidence for exhausted T cells in CLL which could be predictive of CAR T cell efficacy, the use of such checkpoint inhibitors to improve CAR T cell function is alluring. There is very preliminary clinical evidence of the feasibility of this, in a case report of a patient with relapsed DLBCL which describes the use of pembrolizumab (anti-PD1 monoclonal antibody), 26 days after receiving CAR T cells, he showed significant clinical improvement ultimately with an increase in CD4 and CD8+ CAR T cells and an initial IL6 response (249). This indicates the powerful potential of combining immunotherapy agents but the difficulty in the very small number of patients being treated so far.

As previously discussed abstract data from ZUMA-1 had indicated the high prevalence and upregulation of PD-L1 in progression biopsies in both CD19+ and CD19- relapses (190). It is likely that CAR T cells, like regular T cells, are inhibited by PD-L1 expression,

and that administration of PD-1 blockade may interrupt this interaction leading to increased CAR T cytotoxicity (250). Based on the ZUMA-1 subgroup analysis ZUMA-6 was launched, the phase 1 data of which was reported at ASH 2018. This analysis looks at the safety and preliminary efficacy of axi-cel in combination with the anti-PD-L1 antibody atezolizumab for four doses post CAR infusion in patients with refractory DLBCL. No new safety signal was identified and there were no deaths. Of the 12 patients who were evaluable 10 had received all 4 doses of atezolizumab, the best overall response was 7/12 CR (58%), 4/12 PR (33%) and 1 PD. 2 patients that had initially had a PR converted to CR at 6 and 9 months (251). There are other studies open but with no reported results of combinations including the Juno CD19-41BB CAR with durvalumab (NCT02706405) in Seattle, the CD19-41BB CAR with pembrolizumab in patients with DLBCL, FL and MCL (NCT02650999) at the University of Pennsylvania and finally the CD19/CD22 CAR in combination with pembrolizumab at University College Hospital. There are no studies of such combinations in CLL. In myeloma, some patients enrolled on a BCMA CAR study who had at best a PR from this therapy, have been given pembrolizumab in combination with other novel agents afterwards. The University of Pennsylvania immunotherapy group have described one patient who received pembrolizumab in a combination the patient had previously been refractory to, resulting in transient CAR T cell expansion and temporary response, indicating the promise of this approach across disease areas (252).

Rather than relying on antibody blockade it is perfectly feasible to disrupt the PD-1/PD-L1 using the CAR construct. This is feasible in the testing of allogeneic CD19 CAR T cells in xenograft mouse models with CRISPR mediated gene editing of PD-1 in the CAR T cells to render them nonresponse to PD-1 signalling (253).

1.4 Conclusion

CLL remains incurable with conventional CIT but improved molecular and genetic characterization of the disease has identified a subpopulation with long term survival following standard of care FCR. There have been exciting developments in targeted therapies which are better tolerated oral medications suitable for patients unfit for

intensive therapy. CLL is amenable to cellular therapies as indicated by the long-term survival seen in a cohort of younger fit patients with CLL who have had HSCT. Patients who progress on the new targeted therapies should be considered for novel cellular therapy approach such as CAR T cells. Whilst this is currently a small number of patients it could be expected that this population will grow as more patients develop ibrutinib and venetoclax resistance.

The first two autologous CD19 CAR T cells targeting CD19 have now been approved for the treatment of ALL and refractory lymphomas. Despite impressive responses in these diseases, results remain consistent in CLL. It is unknown if this reflects the CAR design or an effect of the underlying function of CLL T cells. These second-generation CAR T cells require CD28 or 41BB co-stimulatory signalling domains, but they have not been compared directly in humans in CLL. Pre-clinical models afford the opportunity to do so. However, modelling of CAR T cells has mostly been performed in vitro or using immunodeficient mice, which limits the ability to study more complex immune biology. CLL is associated with a tumour supportive microenvironment and T cells exhibit multiple defects including decreased proliferation, aberrant subsets, impaired effector function and irregular expression of exhaustion like surface markers such as PD-1. These T cell defects in CLL are recapitulated in TCL1 (TCL1) mice, and such defects can be induced in healthy mice by adoptive transfer (AT) of murine CLL cells. We aimed to demonstrate the effect of CLL T cell dysfunction on CAR T cell efficacy and compare CD28 and 41BB directly.

2. Hypothesis and Aims

2.1 Hypothesis

The inefficiency of CAR T cells in CLL are contributed to by the defects in T cell function. Using the AT mouse model for CLL I will investigate and repair the T cell defect to improve CAR efficacy.

2.2 Aims

- 1) To investigate T cell function *in vitro* following transduction of CD19 CAR into normal WT T cells versus CLL T cells.
- 2) Establish the AT TCL1 mouse model as an *in vivo* model of CAR T cell function in an immunocompetent murine host following *ex vivo* transduction and expansion of T cells from a syngeneic donor.
- 3) To model CAR function using the TCL1 mouse comparing different CD19 CAR plasmids transduced into both normal and CLL T cells. Compare CAR and T cell phenotype before and following CAR infusion.
- 4) Combining CAR T cells with checkpoint inhibitors to enhance T cell function by reversing T cell exhaustion.
- 5) Investigate the pretreatment of mice post AT TCL1 with ibrutinib and acalabrutinib to optimize CAR phenotype and improve efficacy.

3. Materials and Methods

3.1 TCL1 Mouse Model and procedures

3.1.1 Background

All animal work was carried out under Project Licence PPL 70/7530 and later P68650650, which has been updated to include all the procedures being used in this PhD. The original TCL1 colony was established by Dr Fabienne McClanahan from breeding pairs provided to Professor John Gribben by Dr Carlo Croce at The Ohio State University, Columbus, Ohio, USA. My personal license was awarded in June 2015 and I was primarily responsible for the colony kept in the Biological Services Unit (BSU) at Charterhouse Square at Barts Cancer Institute (BCI) from July 2015- March 2019. The principles of the Three Rs, replacement, reduction and refinement were applied throughout the performed work. Because to study the interaction of a novel immunotherapeutic strategy such as CAR T cells in the treatment of CLL requires the interaction of both CLL and the microenvironment no suitable cell line would replace this animal work. Reduction of animal usage is a constant consideration as the minimum numbers of animals were used for in experiments. Refinement refers to the vigorous procedures in place to ensure mice are culled at defined endpoints below which minimize suffering of the animals.

The founder TCL1 mice were backcrossed into the wild type mice C57BL/6 and the colony is maintained by breeding cages with one heterozygote transgenic male in a harem with two wild type (WT) females. Male transgenic breeders are paired at 6-8 weeks of age with WT females purchased from Charles River laboratories, UK. Mice born from these harems can be WT or heterozygote for TCL1. Litters in breeding cages are weaned at 3-4 weeks, ear-marked and genotyped with wild type mice either culled or used for optimization experiments. Depending on the need for aged mice, heterozygote mice (TCL1 mice) were aged routinely till 11 months to maintain a supply of leukaemia for adoptive transfer and in vitro experiments. As per the project license,

beyond 11 months the mice need to be weighed regularly with weight loss of >15% deemed as ill health and these mice were euthanized. However, there is often weight gain in these animals due to hepatosplenomegaly and the mice are observed regularly for signs of ill health or stress such as hunched posture, ruffled fur or lack of activity. Disease status was assessed primarily by immunophenotyping of PB but also by physical examination of splenomegaly. Mice were euthanized as stated if they showed signs of ill health or if >70-80% lymphocytes CD19⁺CD5⁺ CLL cells. Endpoints in some experiments varied as time specific or disease progression.

3.1.2 Processing organs

When mice were culled, I harvested organs in the BSU immediately after death of the mouse by cervical dislocation. Splenectomy was performed first and afterwards a femor was removed, both being kept on ice in PBS with 10-20% FCS. Cell suspensions of spleens were prepared using an automated tissue dissociator (Miltneyi Biotec, UK), erythrocytes were lysed using lysis buffer containing 154.9 nM NH₄Cl, 10mM KHCO₃ and 0.1mM ethylenedi-aminetetraacetic acid (EDTA) at pH 7.2. The suspension was filtered through a 70µm strainer twice. After the spleens had been processed, the fat and tissue was removed from the femor and ends of the bones removed leaving only the femoral long bone and bone marrow. Bones were crushed with a mortar and pestle and then filtered through a 70µm strainer. Bone marrow erythrocytes were then lysed. All centrifugation steps for mouse organs were performed at 1200rpm for 5-7 minutes at 4°C. Cells were used fresh or cryopreservation was performed by concentrating cells to a maximum density of 200 x10⁶ cells/ml in media plus 10% DMSO and freezing in 1ml ampules in a Mr Frosty container at -80°C and subsequent transfer into liquid nitrogen. Cell counting was determined by an automated dual fluorescence (acridine orange/propidium iodide stain) or brightfield haemocytometer (Logos Biosystems, South Korea).

As transgenic mice age and after AT experiments the primary determinant of disease status monitoring is the CD5⁺CD19⁺% in their PB which correlates most closely with splenomegaly and general assessment of health. It also allows for early identification

of the small but significant percentage of TCL1 transgenic mice which develop non CD5⁺CD19⁺ causes of splenomegaly so they can be culled. To obtain PB mice were pre-warmed in a heating chamber in LG08 procedure room in BSU. A technician from the Animal Tech Service (ATS) assisted with all procedures. After warming the mice were removed from the chamber and placed in a restrainer. Their tail vein is punctured using a 25G needle and the other assistant uses a 200µl pipette set to 50µl to transfer blood to a 1.5ml Eppendorf containing 5µl of EDTA. A second venepuncture was permitted if insufficient blood was obtained after the first attempt. The sample was placed on ice and transferred to the lab for processing. For a limited number of experiments 20µl was taken off at this point and placed in a second Eppendorf for centrifugation to obtain plasma. Red cell lysis was then added at room temperature and left for 5-10 minutes. This was then transferred to 5ml polypropylene round bottom tubes (flow tubes), cells were washed with PBS to stop the reaction then red cell lysis was repeated. At this point the PB single cell suspension was analysed for CD5⁺CD19⁺ or for more detailed T cell and CAR phenotyping panels.

3.1.3 Negative selection of CLL and T cells

Negative selection of both CLL/B cells and T cells were required for AT of CLL and production of CAR T cells. Such cells must be enriched and not left with antibodies or beads attached as they are injected into mice. For T cells the eBioscience Magnisort negative selection kit was used as per the manufacturers instructions. Briefly, cell suspensions were resuspended in PBS at 10×10^6 cells/100µl in 5ml flow tubes. First 20µl/100µl cells of antibody cocktail was added, the cells were vortexed 5 times and incubated at RT for 10 minutes. Cells were washed and resuspended in the same volume of PBS, after which 20µl/100µl negative selection beads were added and incubated for 5 minutes. The volume was brought up to 2.5ml and resuspended and the tube placed in a MPC-50 magnet. After 5 minutes, the supernatant from the tube was poured into a new 5ml tube to leave negatively selected cells.

For CLL/B cells the Miltenyi mouse Pan-B cell isolation kit was used as per the manufacturers instructions. Briefly, cell number was determined and resuspended in 40µl MACS buffer per 10^7 cells. First 10µl of biotin-antibody cocktail was added per 10^7 cells. After incubation for 5 minutes 30µl buffer per 10^7 cells was added. Then 20µl of anti-biotin beads were added, mixed and incubated for 10 minutes at 5°C. LS columns with a maximum capacity of 2×10^9 cell were placed in a magnetic field in a MACS separator. The column was first washed with buffer, then the labelled cell suspension was applied to the column and collected into a 15ml falcon tube. As much as possible cell suspensions and reagents were kept on ice. The kit used selects for CD19⁺ so does not distinguish between normal B cells and malignant CLL cells and so both populations would be enriched.

3.1.4 Adoptive Transfer (AT) of TCL1 cells

To establish TCL1 leukaemic mice by AT young WT litter mates from the TCL1 colony or C57BL/6 mice (males and females) aged 10-12 weeks were obtained from Charles River. They received $10\text{-}40 \times 10^6$ frozen and thawed syngeneic splenocytes by intravenous tail vein injection from pooled leukaemic TCL1 donors to ensure an identical composition of donor cells. Mice were injected after pre-warming in a heating chamber in LG08 in BSU using U-100 insulin needles (BD Micro-Fine). Mice were typically injected with 125µl of cell suspension (5ml/kg). Prior to AT splenocytes were purified using a Pan-B cell Isolation Kit (Miltenyi) to ensure CD19⁺ cells are >95%. Mice were given lymphocyte depleting chemotherapy conditioning for CAR T cells with intraperitoneal cyclophosphamide one day before intravenous tail vein injection of CAR T cells. Conditioning was commenced 2-3 weeks after AT of TCL1 after confirmed engraftment of CLL in the PB. After AT mice were monitored for signs of ill health, with tail vein bleeds every 1-2 weeks (or longer if disease was in a steady state of remission). Again, they were culled if they showed signs of illness or distress, or their PB CD5⁺CD19⁺ was rapidly rising >70-80%.

3.1.4 Additional experimental drugs

Additional drugs were given to experimental mice by intraperitoneal injection, the maximum volume is as per defined in the project license at 10mg/kg and usually 200 μ l. Drugs were made in batches by dissolving in sterile PBS so all mice received the same batch of a drug within the same experiment date. Cyclophosphamide was given at 100mg/kg as a stat dose D-1 prior to CAR T cells in all mice receiving CAR T cells or untransduced control T cells. PD-L1 blocking antibody (α PD-L1), the murine equivalent to durvalumab (AstroZeneca) was obtained directly from the drug company and was given at 10mg/kg by intraperitoneal injection every 72 hours starting D-1 prior to CAR T cells in the mice given this combination. Two oral BTKi were given continuously via drinking water with the drug dissolved using a vehicle, 2-hydroxypropyl- β -cyclodextrin (HPBD) with both ibrutinib and acalabrutinib (Acerta) given at the same concentration (0.15mg/l).

3.2 CAR plasmids

3.2.1 MD Anderson Cancer Center (MDACC)

The retroviral murine pRV2011G CD19 1D3-28Z 1-3 plasmid (MDA) with the first and third immunoreceptor tyrosine-based activation motifs (ITAM) of the CD3 ζ molecule inactivated, and the gp75 control plasmid were designed and constructed by Professor Laurence Cooper from the University of Texas MD Anderson Cancer Center and were a kind gift to our centre. The CD19 antibody sequence is derived from the 1D3 hybridoma from American Type Culture Collection (ATCC) that secretes a rat anti-mouse CD19 antibody that specifically recognizes murine CD19 and the construct contains the CD28 co-stimulatory domain. The original plasmids were received in June 2013 as the MDACC has an ongoing Materials Transfer Agreement (MTA) with BCI. The TA99 CAR plasmid is targeted at TYRP-1 (gp75), a melanoma-associated-antigen that is physiologically associated with processes in melanocytes such as melanin synthesis and melanosomal maturation (254). This CAR was intended to be used as an inactive CAR control in in vitro and in vivo experiments. Plasmid maps are shown in Appendix 1.

To facilitate easy identification of gene transfer and downstream experiments both the original MDA plasmids CD19-CD28 and TA99 had the fluorescent protein mCherry inserted at an appropriate point in their sequence (herein called the mCherry plasmids). The original unmodified FASTA sequences were obtained from the MDA and restriction enzymes identified. After consultation with Dr Tanya Klymenko we decided to insert the red fluorescent protein (RFP) mCherry with a CMV promoter into both plasmids. mCherry is photostable and much smaller in terms of molecular weight than the alternate RFP (255). For the MDA-CD19 plasmid mCherry was inserted at SapI (position 5597), and into both MDA-CD19 (position 7777) and TA99 (position 8636) at NdeI. As mCherry+CMV contains NdeI already we altered the mCherry sequence to contain a degenerate NdeI changing CA↓TATG to GA↓TATG. This work was sent to Genscript (New Jersey, USA) and I received them on 15th September 2016 (mCherry plasmids),

3.2.2 Memorial Sloan Kettering Cancer Center (MSKCC)

The retroviral murine plasmids SFG-m19BBmZ-GFP (41BB-GFP), SFG-m1928z-GFP (CD28-GFP) and SFG-137L-2A-m1928z (CD137L-GFP) were received as a kind gift from Dr Michel Sadelain's laboratory at the Memorial Sloan Kettering Cancer Center on 30th October 2016. The FASTA sequences were also received by email. The m1928z plasmid is the CD19-CD28 CAR used in an immunocompetent mouse model of B-ALL by the same laboratory (145), along with two variants of the co-stimulatory domains combined with CD19. The CD8 transmembrane region, CD28 co-stimulatory domain, and mouse CD3ζ were cloned from C57BL/6 mouse splenocytes. These plasmids use the high-titre, Moloney murine leukaemia virus-derived SFG, a variant of the MFG gamma-retroviral vector and CD19 component is derived from the 1D3 hybridoma. Each of the plasmids contain green fluorescent protein (GFP) to simplify the assessment of gene transfer and in downstream experiments (Appendix 2).

3.2.3 National Cancer Institute (NCI)

The retroviral murine plasmid MSGV-1D3-28Z-1.3mut was designed by Dr James Korchenderfer at the NCI, Bethesda and the CD19 antibody is also derived from the 1D3 hybridoma. Its construction and design was first described in 2009 (149). It also contains the CD28 co-stimulatory domain and the cytoplasmic region of CD3 ζ both from mouse. The 1D3-28Z sequence was inserted into the mouse stem cell virus-based splice –gag vector (MSGV) retroviral backbone. The current construct, 1D3-28Z-1.3mut has the first and third ITAM of the CD3 ζ inactivated, which has been shown to decrease the apoptosis of T cells (256). It doesn't contain a fluorescent marker. The plasmid was received from CALIBR (San Diego, USA) on 27th February 2017 after a MTA was kindly signed by Dr Kochenderfer at the NCI. This plasmid has been reported in a murine model of CD19⁺ lymphoma (146). Plasmid map is shown in appendix 3.

3.2.4 Transformation and amplification

GFP, mCherry and NCI plasmids were received at room temperature and centrifuged at 5000g for 1 minute at 4°C. The vial was then opened and 20 μ l of sterilized water added. The lid was closed and the vial vortexed, followed by 15 minutes at 50°C to dissolve the DNA. Subcloning efficiency DH5 α e-coli or STbl3 competent cells were taken out of -80°C (previously aliquoted 50 μ L into eppendorfs) and thawed on ice. Plasmid DNA (200ng) was mixed into 50 μ l aliquot of E-coli for 10 minutes. Heat shock transformation by placing the lower 1-2 thirds of the tube into a 42°C water bath for 30-60 seconds followed by 3 minutes on ice. Add in 500 μ l of warmed lysogeny broth (LB) and grow in 37°C shaking incubator for 45 minutes. All plasmids carry the ampicillin antibiotic resistance gene. Single colonies were selected and inoculated into LB broth containing ampicillin in an Erlenmyer flask (100 μ g ampicillin/ml medium) and left overnight at 37°C in a shaking incubator. After confirming visually bacteria has grown and repeatedly pour cell suspension into a 50ml falcon tube and centrifuge at 2500rpm for 30 minutes per tube to pellet cells. To recover plasmid DNA the Plasmid Midi Kit (Qiagen, UK) was used following the manufacturers instructions. The pellet was resuspended in buffer and LyseBlue reagent applied, after added precipitation

buffer the lysate was transferred to the QIAfilter cartridge which was filtered into the HiSpeed Tip. DNA was eluted and precipitated with isopropanol and the QIAprecipitator. The eluate was concentrated using the SpeedVac set on low heat. The concentration and purity of the plasmids was measured on the NanoDropTM spectrophotometer (Thermo Scientific).

Confirmatory restriction enzyme digestion was performed on MDA and GFP plasmids to verify the purified plasmids. NdeI and Sall were used to cleave the MD Anderson plasmid DNA prior to insertion of mCherry and SapI was used to confirm it as a cutting site for mCherry. EcoRI, NotI, Stul and PmlI were used to cleave the plasmid DNA of the GFP plasmids and confirm their identity (all enzymes from New England Biolabs, UK). For a total of 11µl, 1µl of plasmid DNA, 1µl enzyme, 8µl of nuclease free water and 1µl of buffer were mixed in PCR tubes and left in the thermocycler overnight at the appropriate temperature and time for each enzyme (generally 37°C for 12 hours then 4°C). DNA was separated by gel electrophoresis and samples were ran on agarose gel with a 1kB ladder.

3.3 Cell culture and retroviral methods

3.3.1 Transfection of phoenix/platinum-eco cells

Transfection experiments were originally carried out with Phoenix-amphotropic cells (gift from Dr Sergey Krysov, February 2016) having obtained these cells from Southampton University. Platinum-ecotropic cells were received on 16th March 2017 (Generon, UK). Phoenix or platinum-eco cell lines are packaging cells used to produce a retroviral supernatant after transient transfection by plasmids encoding gammaretroviral vectors. These lines are derived from 293T cells (a human embryonic kidney line transformed with adenovirus). Retroviral packaging systems offer the main advantage that their integration into the host genome allows for stable transmission through cell division. This ensures the retroviral construct will remain resident and continue to express.

The original transfection/transduction protocol is derived from the Sadelain laboratory (MSKCC) used in an immunocompetent mouse model of ALL (145) but also published in full here (257), which I have optimized. Phoenix/platinum cells were plated in 10cm tissue culture plates or 75cm² cell culture flasks, after previously coating with poly-L-lysine. The day before transfection, I seeded 2-5 x 10⁶ cells. After 16-24 hours, transfection was started when the cultures became 70-80% confluent. I aspirated the culture medium and rinsed with PBS, then added back 7ml of culture medium. In a 500µl eppendorf, dilute 10-40µg of plasmid DNA into jetPRIME buffer, mix by vortexing. Add 20-40µl jetPRIME, vortex and incubate at room temperature (RT) for 10 minutes. Add the transfection mix drop wise onto the cells. If needed, replace transfection medium after 4-8 hours with fresh medium. Plates/flasks are cultured in DMEM, 10% FCS, and 100U/ml penicillin and 100µg/ml streptomycin and are incubated at 37°C in 5% CO₂. At 48, 72 and 96 hours, viral supernatant was collected, either filtered through a 0.45µm filter or centrifuged at 300g for 5 minutes and either used fresh supernatant for transduction or snap freeze at -80°C in cryovials for later use. In later experiments, retroviral supernatant was pooled and concentrated using Retro-X (Clontech) as per manufacturers instructions and resuspended in enough RPMI for the required experiment and then used fresh.

The above transfections were also scaled down into 6 well plates, in experiments using plasmids with fluorescent markers, with visual fluorescence confirmed at 48 hours using a fluorescent microscope in those transfections using a fluorescent marked plasmid.

3.3.2 Transduction of mouse T-cells

Single cell suspensions of mouse splenocytes were prepared as previously described. The T cell population was negatively selected using a magnetic antibody cocktail kit (eBioscience Magnisort Mouse T cell enrichment kit) according to the manufacturers instructions. Enriched mouse T cells are activated for 24 hours using either CD3/CD28 Dynabeads (Invitrogen) or antibodies and recombinant human (hIL2) or mouse IL2 (mIL2). Prior to use Dynabeads were washed by diluting the required number of beads

($25\mu\text{l}/1 \times 10^6$ T cells or 10×10^6 cells) in PBS with 0.5% FCS in a FACS tube, placing the suspended beads in a MPC-50 magnet, aspirating the PBS/FCS solution and repeating for three washes. Activated mouse T cells were transduced at various concentrations as part of optimization experiments, using fresh or thawed viral supernatant in 6 or 24 well plates coated with RetroNectin ($15\mu\text{g}/\text{ml}$ in PBS). Typically, T cells were activated at 1×10^6 cells/ml with 20 units of mIL2 for 24 hours, and then resuspended at 3×10^6 cells/ml with 80 units of mIL2 for transduction. In 6 well plates 1ml of cell suspension was added to 1ml fresh or thawed viral supernatant and spun at 2000g for 1 hour at 30°C . After 24 hours at 37°C , 1ml of medium was aspirated, replaced with 1ml viral supernatant and again spinoculated under the same conditions. From day 3 cells were maintained at a concentration of $1\text{-}2 \times 10^6$ cells/ml for expansion and on alternate days fresh RPMI with 20 units of mIL2 was supplemented. Transduction efficiency was analyzed from day 3-5 onwards depending on the experiment.

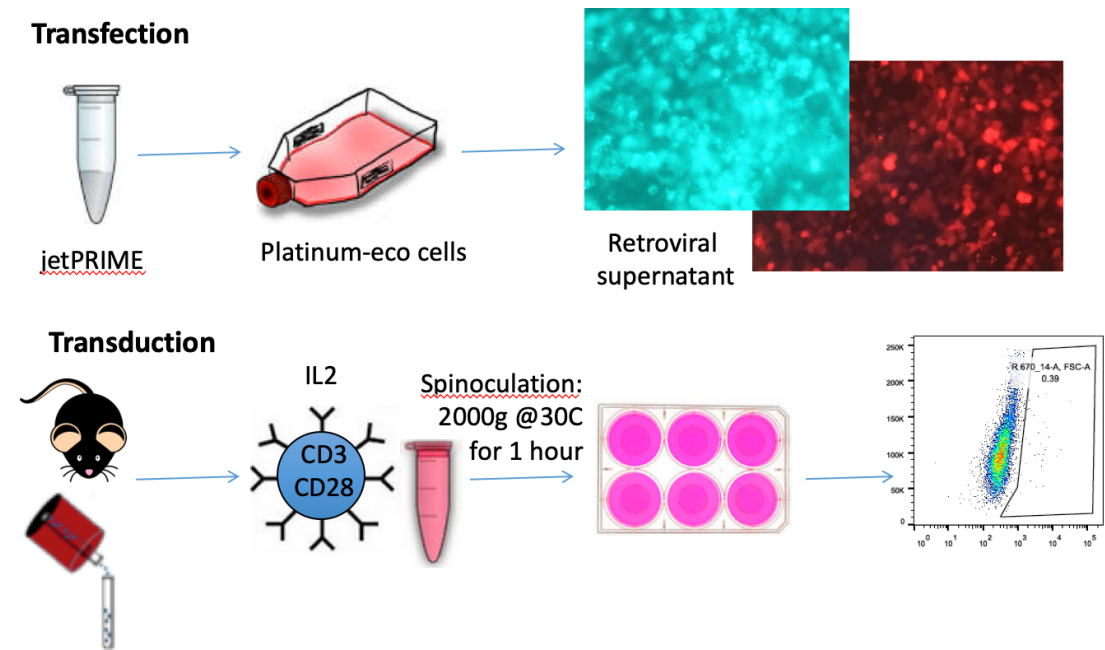


Figure 3.1: Transfection of packaging cells with CAR plasmid to make retroviral supernatant used to transduce enriched and activated mouse T cells.

Following the original Sadelain protocol recommended the use of mIL2 from Roche. However, there is no WHO standard unit for mIL2 (unlike hIL2), and I experimented with different mIL2 from R&D Systems (Minneapolis, USA) when trying to optimize my T cell rapid expansion protocol which required titration.

3.3.3 Transduction of HEK/3T3 fibroblasts

To attempt to determine the multiplicity of infection (MOI), supernatant from the plasmid transfections were harvested and serial dilutions used to culture 293T human embryonic kidney (HEK) cells seeded in 6 well plates 18 hours previously. Polybrene was also added at 8-16 μ g/ml to increased transduction efficiency. After 48 hours the supernatant was removed, cells were trypsinised from the plates and resuspended in Fluorescence Analyser and Cells Sorter (FACS) buffer and the proportion of cells that were GFP or mCherry positive were assessed by flow cytometry (see section 3.4). Because of low transduction efficiencies HEK as well as and mouse 3T3 fibroblasts (3T3) and pancreatic adenocarcinoma (PDAC) cells were used to test various viral supernatants as these cells are easier to transduce than mouse T cells.

3.4 Flow cytometry

3.4.1 Surface staining

Immunophenotyping was performed by multicolour flow cytometry with surface staining using anti-CD5, CD19, CD3, CD4, CD8, CD44, CD62L, PD-L1 and PD-1 antibodies available from eBioscience, BD Bioscience or BioLegend (all San Diego, USA). After modification the MDA plasmid contains mCherry, and the MSK plasmid came with GFP already, which is an important feature to assess gene transfer and monitor transduced T cells in downstream experiments as it allows direct detection by flow cytometry. Surface staining was performed in FACS buffer (PBS/2% FCS) for 30 minutes at 4°C. After washing twice, samples were analysed on a four laser BD LSR Fortessa Analyzer after resuspension in FACS buffer containing 4'6-diamidino-2-phenylindole (DAPI) to allow live/dead cell discrimination. Cells transduced with a GFP or mCherry plasmid

required washing and then were resuspended in FACS buffer to determine transduction efficiency. DAPI-, viable, single mononuclear cells were used for analysis, and fluorescence-min-one (FMO) and untransduced T cell negative controls were used as required. Compensation beads coated with an antibody for each fluorochrome used in a specific panel were used. The compensation matrix was then applied to all samples in that experiment. Specific populations were generally expressed as a percentage of a defined parent population. Stopping gates and recorded events varied in different experiments but were usually determined on viable or T cell events if possible recording 10,000 events or to complete aspiration of the flow tube. Recorded data was exported as .FCS files and analysed with FlowJo software.

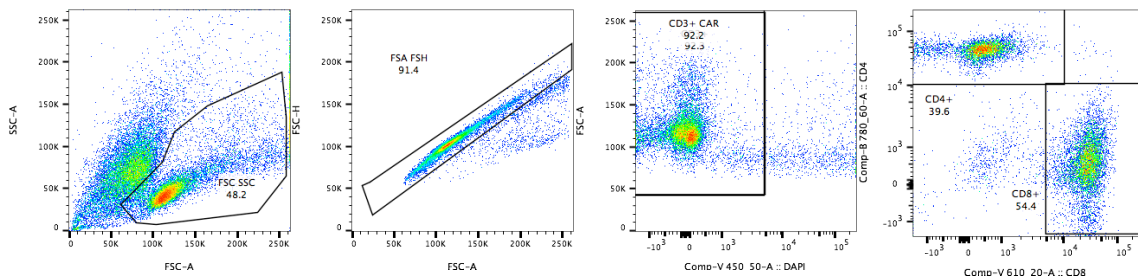


Figure 3.2: Typical initial gating strategy adopted prior to selection of cells of interest. If possible, 10,000 viable (DAPI) mononuclear cells of interest were collected, usually either CD5⁺CD19⁺ CLL cells or CD3⁺/CD4⁺/CD8⁺ cells, alternatively the flow tube was run until near completely aspirated. For rare T cell populations particularly CAR⁺ cells an additional CD19⁻ gate was used prior to selection of T cells.

Protein L is a bacterial surface protein isolated from *Peptostreptococcus magnus* that selectively binds to variable light chains (kappa chain) of immunoglobulin without interfering with antigen binding properties of the antibodies. It binds to light chain of all classes of immunoglobulin and it also binds single-chain antibody fragments scFv. This has been validated in human and murine derived scFvs and in different CARs (258). Other groups have used anti-rat-F(ab)₂ antibodies (herein fab antibodies - Jackson ImmunoResearch Laboratories) to detect the 1D3 scFv (146). The fab antibody is a biotin conjugated antibody so must be used with a secondary streptavidin fluorochrome such as phycoerythrin (PE).

3.4.2 Cytotoxicity

Flow cytometry based assays will be used to determine CAR T cell cytotoxicity to primary CLL cells. CellTrace Yellow/Red Cell Proliferation Kit (Thermo Fisher Scientific) was used to label enriched and negatively selected CLL cells, taken from from a spleen single cell suspension from an aged TCL1 mouse with confirmed high CD5⁺CD19⁺ disease. To label cells up to 5×10^7 cells were resuspended in warmed PBS /5% FCS and transferred to a 15ml Falcon tube wrapped in aluminium foil. CellTrace Yellow/Red staining solution was added (1:500 dilution) and the falcon tube was incubated at 37°C for 20 minutes. Complete culture medium was added to end the reaction, cells pelleted to remove the supernatant and then between 1×10^5 - 10^6 cells were incubated in a 96 well plate for up to 72 hours with transduced CAR T cells at different T cell effector: target cell ratios; 5:1, 1:1, 0.3:1 and 0.1:1. Samples were taken at 24, 48 and 72 hour time points for analysis by flow cytometry to look at CD3, CD4, CD8 and CAR⁺ (Fab⁺ and GFP⁺) and determine loss of B cells and T cell proliferation. T cells were also phenotyped at the end of the cytotoxicity experiment as per the surface staining panel previously described. When samples were being prepared to flow cytometry samples were resuspended in FACS buffer with counting beads to ensure equal numbers of events were counted for each condition.

Intracellular cytokine staining assays on permeabilized cells staining for interferon- γ (IFN γ) and interleukin-2 (IL2) after incubation with primary CLL cells for 5 hours to determine the percentages of transduced T cells that produce these cytokines in a CD19 specific manner will be calculated.

3.5 Cytokines

For the final experiment, for each of the tail vein bleeds post CAR T cell injection plasma was obtained first. After tail vein blood was obtained as described previously, 20 μ l of blood anticoagulated with EDTA was spun in a fresh 500 μ l eppendorf at 1200g for 10 minutes. Carefully, 10 μ l of plasma was transferred to a new 500 μ l eppendorf and stored at -22°C for later analysis. The Mouse Th Cytokine Panel (BioLegend, San

Diego CA) is a bead-based multiplex assay panel, using fluorescence-encoded beads. The panel selected detects IFN- γ , TNF- α , IL2, IL6 and IL10. The assay was performed as per manufacturers instructions, but briefly standards were set up using the cytokine standard cocktail. Plasma samples were diluted 1:1 in assay buffer and suspended with beads and detection antibodies in a 96 well plate, covered with aluminium foil and put on a plate shaker at 600rpm for 2 hours at room temperature. The streptavidin-PE antibody was subsequently added and then placed on a plate shaker again at 600rpm for 30 minutes. After washing with wash buffer samples were read on a flow cytometer. Data (FCS files) were analysed using the LEGENDplex Data Analysis Software as provided by the manufacturers.

3.6 Statistics

Differences between the phenotypes by flow cytometry of CAR T cells were frequently only described as there was no biological replicate in such experiments in that only one batch of CAR T cell product of each type was produced due to the technical challenges in producing these cells. Datasets were subjected to normality testing using the Shapiro-Wilk and D'Augustino and Pearson normality tests. To compare the phenotype of groups of mice if parametric I used one-way ANOVA (with Tukey's multiple comparison) to compare all means of percentage expression against each other between experimental groups. For non-parametric data Kruskal-Wallis with Dunn's multiple comparisons was performed. In all figures in this thesis and where stated, $P < 0.5$ was considered statistically significant, with different significance levels defined as follows (* $P < 0.05$, ** $P < 0.01$, *** $P < 0.001$, **** $P < 0.0001$). Analyses were performed using Prism Version 8 for Mac.

4. Breeding and maintenance of transgenic TCL1 mice and AT CLL

4.1 Introduction

I took over the responsibility for the colony in July 2015, which includes maintaining the breeding strategy and keeping proper records after completion of appropriate training and the award of a personal Home Office license. Transgenic (Tg) mice develop leukaemia from 6 months of age, but initially this is low level and is unlikely to make the animals sick. The project license specifies that they must be most intensively monitored from 11 months of age as it is from this time point when most mice develop significant levels of CLL in the PB. We were the first group to demonstrate that TCL1 CLL is transplantable into healthy WT mice by AT (89), which is a convenient model to study novel immunotherapeutic strategies in CLL, which has been confirmed by others (70, 117). The biological course of CLL after AT into healthy mice has been fully characterized and published by our group, particularly with regard to PD-1 and PD-L1 expression (118). However, to perform large studies of mice using this platform, a constant and consistent supply of CLL from aged transgenic mice must be maintained. The methods by which this is done were discussed in Chapter 3, but an important part of my PhD has been the ability to produce CLL for AT which is fully traceable to an individual mouse, with corresponding breeding records to ensure appropriate material has been transplanted into WT mice to study their resulting CLL.

4.2 Objectives

My first objective was to obtain a Home Office personal license and take responsibility for a large established TCL1 colony. Beyond this the main use of the colony was to supply a consistent supply of TCL1 CLL for use in AT experiments. To do this the following objectives were set:

- Maintain 2-3 breeding harems in the transgenic colony, identifying WT and heterozygous TCL1 mice using ear clip genotyping with full traceable records kept for the duration of my PhD.

- WT mice identified from genotyping can be used for optimization experiments as a source of normal T cell splenocytes for transduction to make CAR T cells and as AT recipients if required, reducing the total number of animals needed as much as possible.
- Tg mice were aged and from 11 months of age are more closely monitored so they can be culled when they become fully leukaemic. Spleens are processed as previously described and single cell suspensions stored in liquid nitrogen for use in AT experiments. Prior to storing spleens for AT, CLL must be confirmed by flow and full records kept.

4.3 Confirmation of TCL1

All TCL1 mice produced under this project license were genotyped to confirm the presence of the transgene. Genotyping of mice was done using ear punches, which was also performed on WT mice who had received AT CLL as identification for experiments. DNA was extracted using alcohol precipitation after digestion at 55°C overnight with buffer consisting of 50mM TRIS pH 8.0, 25mM EDTA pH 8.0 (both Sigma), 100mM NaCl (Fisher Scientific), 1% SDS and Proteinase K 20mg/ml (Roche). DNA content was determined using NanoDrop. TCL1 primer sequences are: (TCL1 Forward) 5'-GCCGAGTGCCCGACTC-3'; (TCL1 Reverse) 5'-CATCTGGCAGCAGCTCGA-3'. The endogenous mouse globin gene was used as an internal positive control. PCR conditions for TCL1 are activation at 95°C (5 min), then denaturation at 95°C (30 sec), annealing at 58°C (30 sec) and extension at 72°C (30 sec) for 35 cycles, and final extension at 72°C (5 min). PCR products, controls and a 100bp DNA ladder (Life Technologies) were separated on a 2% agarose gel containing 20µl GelRed nucleic acid gel stain and visualized in a Transilluminator (Figure 4.1). Agarose gel is made from 6g agarose plus 200ml TBE buffer heated in a microwave until dissolved and clear. After re-establishing the procedure in the laboratory it was largely performed by the BSU ATS under my supervision of results.

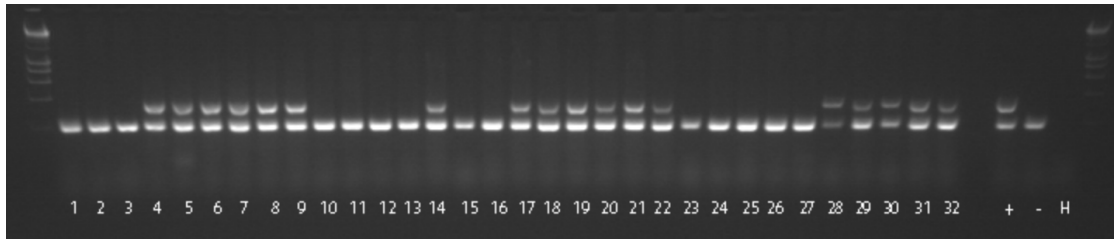


Figure 4.1: Example of genotyping results of TCL1 transgenic mice. DNA was extracted from ear clips and TCL1 primer sequences are as described in chapter 4.3. PCR was cycled as above and gels run. Above we see the results of 32 colony mice to determine their TCL1 status from ear clips. As mice were bred in harems for a transgenic male with two WT females, the results above are expected as around 50% of offspring are TCL1 heterozygotes.

4.4 Confirmation of CLL

To ensure ageing mice were developing CLL as expected I have checked CD5⁺CD19⁺ disease (CLL load) on mice of various ages. Here we see CLL in a mouse of 9 months vs 12 months with expected levels of CLL (Figure 4.2). Mice were routinely culled at 11 months or more intensively monitored if >11 months old and had their CLL routinely checked prior to cryopreservation.

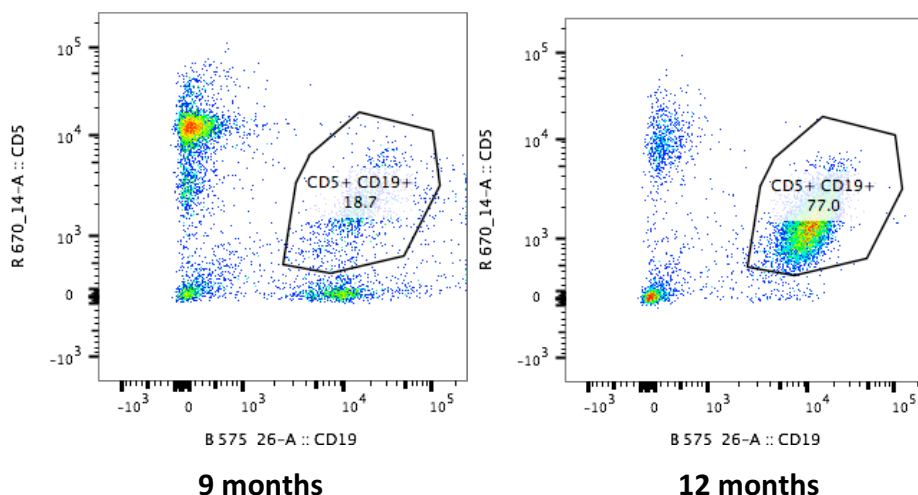


Figure 4.2: DAPI-, viable, single mononuclear splenocytes were gated for CD5⁺CD19⁺ CLL from transgenic mice culled at 9 and 12 months demonstrating increase in load of disease with age. 10,000 events were recorded as per chapter 3.4.1.

4.5 Discussion

The TCL1 colony and its standard operating procedures (SOP) were set up prior to my starting this work, but I took responsibility for the colony throughout my PhD. Whilst the transgenic model does have 100% penetrance of a lymphoproliferative disorder, there was a small but significant number of mice that developed hepatosplenomegaly and became sick much earlier than the usual time frames described. These mice appeared to have a T cell proliferation looking at their basic flow phenotype and were pre-emptively culled if identified in the PB prior to them becoming sick. Typically, such mice became sick from around 6 months of age and had unusually large palpable spleens, which is atypical for mice heterozygote for the transgene.

During my PhD I always used a harem of one transgenic male and two WT female mice. The harem was used to increase the quantity of offspring, and the combination of using Tg and WT mice in combination results in two outcomes, 50% heterozygote TCL1 mice and 50% WT mice. This setup had been defined by SOP from the Carlo Croce laboratory and optimised in the Gribben laboratory, so further optimisation of this breeding strategy was not the focus of my PhD. It is felt that mice with homozygous TCL1 the CLL is too aggressive (Fabienne McClanahan, person communication) and alternative breeding strategies were not explored. Ensuring this breeding strategy was maintained, supervising animal welfare, documenting all offspring, ear clipping and at first performing and then supervising the PCR to check for the transgene were all essential work that I performed all the way through my PhD. Once WT mice were identified by PCR they may have been culled, but many were kept as a source of WT T cells and by keeping mice from the same litter I had a convenient source of age matched controlled normal T cells and source of tissue for optimisation experiments. Although in the BSU there are staff responsible for feeding mice and cleaning cages, a regular part of my work was checking on animal welfare, particularly if there were sick mice. Indeed, I was primarily responsible for the colony so any health alerts would be directed to me to immediately check on animal welfare and make a decision on how to manage sick mice. In later experiments in chapters 6-9 I used both male and female mice equally as a source of CLL and T cells, male mice from this background are liable

to fight and would need to be separated in this instance. As part of the breeding strategy I had 2-3 breeding cages producing offspring at a time, so the requirement for cells for AT could be scaled up easily, although the amount of work required to do so was very time consuming. Forward planning in terms of in vivo experiments was essential, because of the time lag of at least 9 months after setting up a breeding cage before regularly being able to harvest CLL splenocytes for AT. The methods used to process mouse organs are described in chapter 3.1. BSU staff would help wean offspring from breeding cages, at which time we would separate offspring into male and female cages and ear clip them so PCR could be performed for the transgene. Mice remained in the same single sex same litter cages for the rest of their lives unless further separated due to animal welfare reasons or to be separated into different experimental groups. Female mice particularly have a tendency to over groom sometimes resulting in alopecia and need to be separated if it is severe.

The transgenic model is reassuringly heterogeneous in its clinical phenotype in terms of its CLL. In a similar way to patients, some mice seem to tolerate massive splenomegaly whilst others less so, and lymphadenopathy can sometimes be obvious but other times difficult to find, although lymph nodes were not routinely kept. Previous work from my group has demonstrated T cell changes in this model to be more consistent in the spleen (118), which is much more technically easy to obtain, compared to lymph nodes in these mice. Also in terms of storing the required number of cells for the AT model, only the spleen can produce enough CLL cells to be a reliable source, as lymphadenopathy in mice although clinically evident is very low volume relative to splenomegaly. Of mice that have serial blood tests some mice rapidly progress after 11 months whilst others do not, but generally most transgenic mice being kept to harvest cells were culled between 11-13 months of age. Part of the regular check of animal welfare in mice particularly aged over 11 months, was palpation of their abdomen to assess splenomegaly. As I monitored all mice aged over 11 months more regularly, I used the combination of monitoring PB CLL load, weighing mice and clinical examination for splenomegaly to determine the optimum time to call mice so the maximum amount of CLL splenocytes would be able to be stored in our

tissue bank for further AT experiments, whilst of course maintaining humane clinical endpoints in accordance with our Home Office project licence.

Previous work from my group, had defined 40×10^6 enriched splenocytes as the optimum dose for AT experiments (118). Recent studies have injected less cells for AT (70) using 10×10^6 splenocytes. In my experiments described in chapters 7-9, varying this cell dose between $10\text{-}30 \times 10^6$ cells does vary the disease latency but not the penetrance, as this model does reliably induce CLL in 100% of mice. This may be important for determining CAR engraftment, efficacy and persistence. Whilst the transgenic form of CLL is heterogenous, the AT form of CLL is relatively homogenous in its clinical behaviour. In all experiments after AT of CLL, mice will have low level CLL in the PB at week 1, with typically $>10\%$ of all nucleated cells in the PB being $CD5^+CD19^+$ by week 2. On this basis, I made week 3 the time for injection of CAR T cells, because I wanted this model to treat confirmed engrafted CLL in all mice, as this model is meant to reflect treatment of florid CLL with CAR T cells not MRD levels of CLL.

In chapters 7-9 I state for each experiment the number of enriched CLL splenocytes used for AT of CLL for the in vivo experiment. These large in vivo experiments are challenging to prepare for, to try and remove the confounding variable of different leukaemia phenotype, mice in these experiments were injected with pooled CLL. In general, it was my preference to only use pooled CLL which had come directly from transgenic mice, as this produced a CLL with the expected latency and phenotype. An alternative method is to do AT into a group of mice, pool this CLL and then use it for a further AT. Whilst this method is very effective at rapidly increasing the number of splenocytes available for the next pool in a short time period, it results in a tendency for the next AT to exhibit a much more aggressive phenotype. Putting the same pool through mice multiple times rapidly increases the aggressiveness of the CLL (personal communication, Arantxa Romero-Toledo). This may be desirable in other experiments, a colleague in my group had done such experiments with very different experimental goals, but on reflection this is not appropriate for experiments with the objectives described in this thesis. My first attempt at the experimental plan described in chapter 9, used a significant number of CLL pools from mice that had AT CLL rather than

primary transgenic CLL. In this attempted experiment many mice needed to be culled by week 2 due to obvious ill health and very high PB CLL so the experiment had to be aborted. I had used pools of AT CLL for further AT in this experiment really only due to a lack of available CLL in the tissue bank from transgenic mice. In subsequent attempts at the two part experiments described in chapter 9 I only used pools of CLL derived from transgenic mice. I had to wait for further pools from transgenic mice before being able to proceed with this experiment so I had enough cells for AT. I make this point to illustrate that a critical part of my experimental work depended on the maintenance of a colony, with a strict breeding strategy and good documentation of records, to ensure a large enough supply of CLL for AT experiments that could produce a consistent phenotype. Without such an attempt to produce a consistent phenotype of AT CLL, it is challenging to interpret the conclusions in the subsequent experiments.

In conclusion, although the TCL CLL mouse model is well established in the investigation of the CLL microenvironment, its use as a source of syngeneic T cells to model CAR T cell function is novel. The prerequisite to establish differences between CAR T function derived from normal and CLL T cells requires a consistent mouse model, following established SOP with good records to ensure traceability of stored pools of CLL for AT, this was an essential part of the work towards my thesis.

5. CAR T cell manufacturing, detection and expansion

5.1 Introduction

Retroviral gene transfer and subsequent expansion of primary murine T cells is challenging to achieve. I initially set out to use Phoenix-amphotropic cells for transfection but these were replaced with platinum-ecotropic packaging cells to produce retroviral supernatant after transient transfection by plasmids encoding gammaretroviral vectors. I describe the optimization of a protocol to transduce primary murine T cells activated with magnetic beads coated with CD3 and CD28 antibodies (Dynabeads). Activated enriched T cells are subsequently transduced by centrifugation (spinoculation) on retronectin (Takara) coated tissue coated plates with retroviral supernatant. These cells were then expanded by culture with the same beads and using interleukin-2 (IL2).

5.2 Objectives

- Confirm the identity of the CAR plasmids received from collaborators.
- Transfect HEK cells using the selection of CD19 plasmids received from our collaborators and establish an antibody that reliably detects the plasmid or confirm fluorescence if the plasmid contains a fluorescent marker.
- Transduce HEK cells and murine cell lines 3T3 and PDAC using retroviral supernatant from CAR plasmids to optimize transduction conditions.
- Produce CD19-CD28 and CD19-41BB-GFP CAR T cells from normal and CLL T cells from WT and transgenic TCL1 mice and demonstrate stable transduction using the same antibody or by detection of GFP.
- Optimize the ex vivo expansion of normal T cell derived CAR T cells using CD3/CD28 beads and cytokines.

5.3 Plasmid identification

On receiving the various plasmids which all originated in the USA, their identities were confirmed using restriction enzyme digestion which was performed to verify the purified plasmids as described in chapter 3. Enzymes were identified after reviewing FASTA sequences sent by email from the original institutions. DNA was separated by gel electrophoresis and samples were run on agarose gel with a 1kb ladder (Figures 5.1 and 5.2).

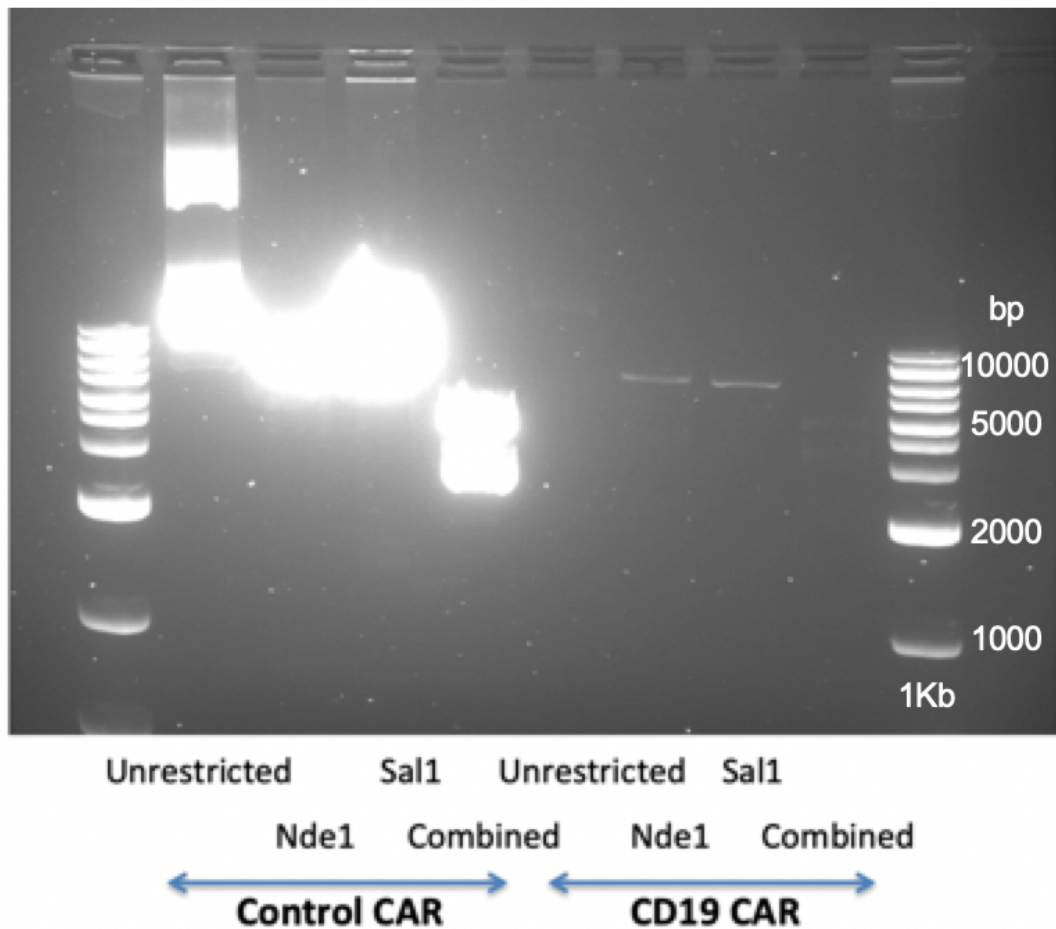


Figure 5.1: Confirmatory restriction enzyme digestion was performed on MDA CD19 to verify the purified plasmids. Nde1 and Sal1 were used to cleave plasmid DNA. For a total of 11 μ l, 1 μ l of plasmid DNA, 1 μ l of enzyme, 8 μ l of nuclease free water and 1 μ l of buffer were mixed in PCR tubes and left in the thermocycler overnight at the appropriate time (generally 37°C for 12 hours then 4°C. DNA was separated by gel electrophoresis and samples were run on agarose gel with a 1kb ladder (far left and right).

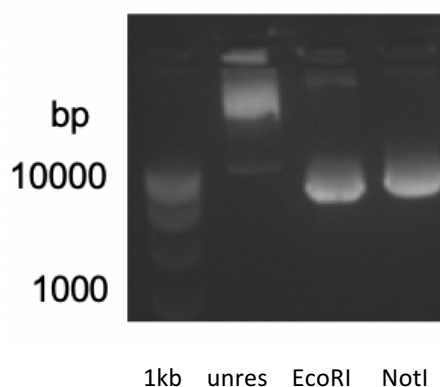


Figure 5.2: Confirmatory restriction enzyme digestion was performed on MSK CD19-CD28, CD137L and 41BB with EcoRI and NotI to verify the purified plasmids. Enzymes were used to cleave plasmid DNA. For a total of 11 μ l, 1 μ l of plasmid DNA, 1 μ l of enzyme, 8 μ l of nuclease free water and 1 μ l of buffer were mixed in PCR tubes and left in the thermocycler overnight at the appropriate time (generally 37°C for 12 hours then 4°C. DNA was separated by gel electrophoresis and samples were ran on agarose gel with a 1kB ladder marked on the left.

5.4 Fab and protein L

When I first started to optimize my transfection/transduction protocols I only had the MDA plasmid before the insertion of the fluorescent protein mCherry. I therefore needed an indirect antibody to detect the transfection or transduction of the plasmid. I therefore started by investigating the use of protein L and fab antibodies to detect expression of the CAR. Initially, to check the plasmid I performed transient transfection into HEK cells using the transfection reagent jetPRIME (Polyplus), using a GFP plasmid as a positive control and detected the CAR on 58% cells with a fab antibody (figure 5.3). The TA99 plasmid could not be detected after transfection into HEK cells but the CD19 plasmid transfected well confirming my transfection conditions work.

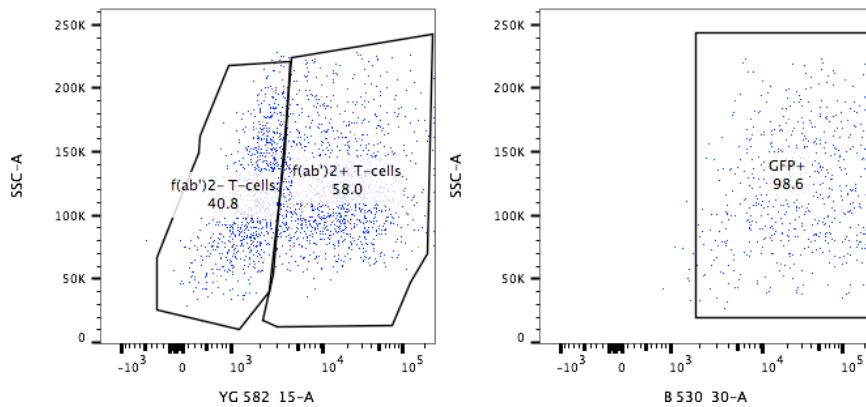


Figure 5.3: Fab+ (CD19 CAR+) GFP

Transient transfection of CD19 CAR and GFP into HEK cells as described in chapter 3.3.1. DAPI-, viable, single mononuclear cells with fab-biotin PE or HEK cells transfected with GFP. Gates were established using non-transfected HEK cells.

Then after multiple attempts to optimize my transduction conditions I demonstrated transduction of HEK cells using viral supernatant. I used a GFP lentiviral supernatant as my positive control, the TA99 viral supernatant did not transduce, presumably because the transfection had not worked so the supernatant didn't contain virus. Alternatively, the Fab antibody may not recognize the extracellular sequence for the TA99 CAR. In figure 5.4, we see Fab antibodies can be used to detect the CD19⁺ CAR transduction into HEK cells, with a transduction efficiency of 43.1%.

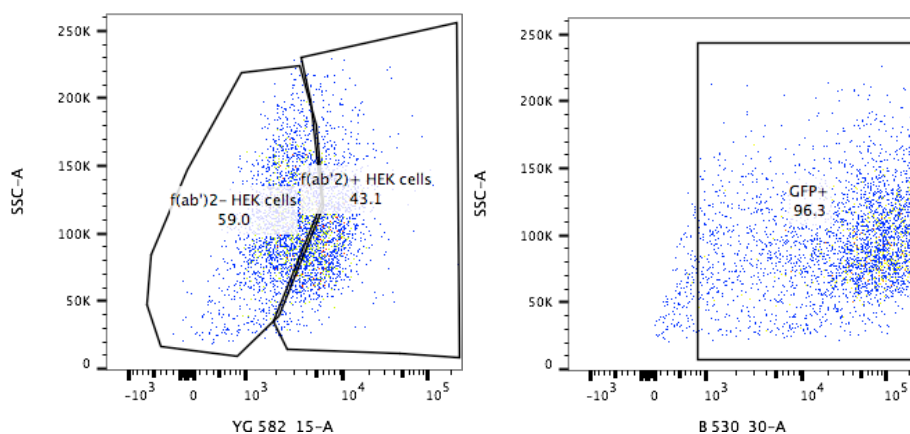


Figure 5.4: Fab+ (CD19 CAR+) GFP

Transduction of HEK using CD19 CAR retroviral and GFP lentiviral supernatant as described in chapter 3.3.3. DAPI-, viable, single mononuclear cells with fab-biotin PE or HEK cells transduced with GFP. Gates were established using non-transduced HEK cells.

I then checked the baseline expression of my CAR detection antibodies on enriched mouse T cells. I found protein L binds to negatively selected mouse T cells prior to transduction so is not a useful antibody (figure 5.5). Even though other groups have used these antibodies in murine cells for this purpose (258). The Fab antibody did not bind to untransduced mouse cells (figure 5.5), so I went on to use this for mouse transduction experiments.

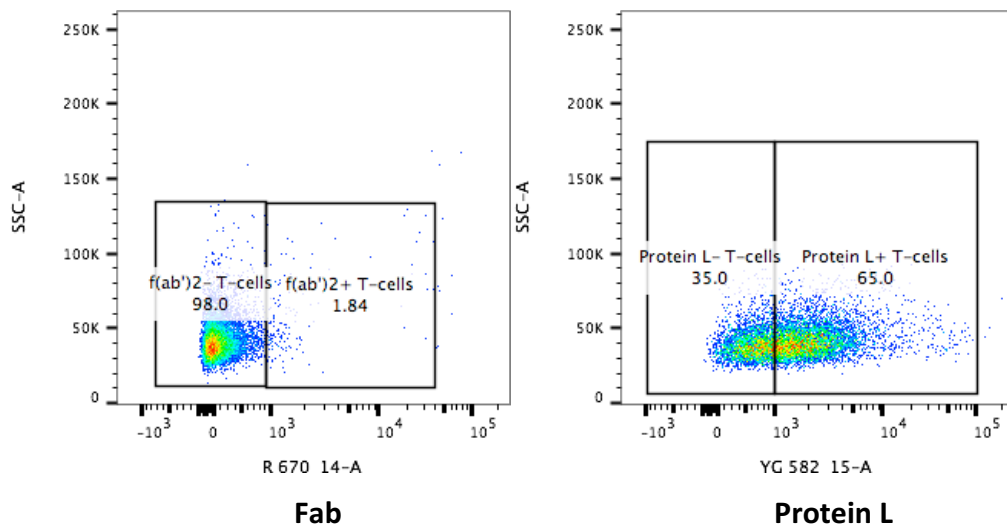


Figure 5.5: Baseline expression of protein L and Fab antibodies on negatively selected mouse T cells. DAPI-, viable, single mononuclear cells were gated, and negative gate was determined using FMO controls.

5.5 mCherry and GFP plasmids

As previously stated mCherry was inserted into the MDA CD19-CD28 and TA99 plasmids. To confirm their identity, I amplified them as previously described (chapter 3.3) and transfected them into Phoenix cells in a 6 well plate to confirm fluorescence (figure 5.6 left). Fluorescence appearances were similar for both MDA-CD19 and TA99 mCherry.

Because of the challenges associated with achieving transduction of mouse T cells we sought a new collaboration with Dr Michel Sadelain's laboratory (Memorial Sloan

Kettering Cancer Center, New York, USA) who have expertise in murine CD19 CAR T cell models. They kindly gifted their murine second generation CD19 CAR (MSK-CD19) with various co-stimulatory domains (41BB, CD28 and CD137) which importantly also contains green fluorescent protein (GFP) (herein the GFP plasmids). These plasmids were amplified as previous described and transfected into Phoenix cells in a 6 well plate to confirm fluorescence (figure 5.6 right). Appearances were representative for both the MSK-CD19-41BB and MSK-CD19-CD28 plasmids.

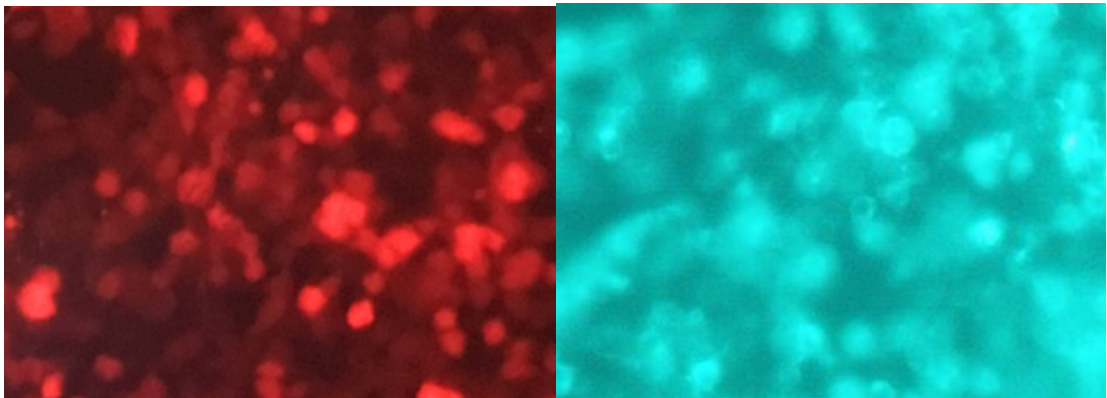


Figure 5.6: Visual appearance of mCherry (left) and GFP (right) after transfection of plasmids containing these fluorescent markers into Phoenix cells in a 6 well plate using using 10-40g of plasmid DNA and jetPRIME buffer with visual fluorescence confirmed at 48 hours using a fluorescent microscope (chapter 3.3.1).

My first attempt at transducing activated mouse T cells with viral supernatant produced using the mCherry and GFP plasmids failed, and therefore again I attempted to optimize transduction conditions with HEK cells. After multiple attempts the mCherry plasmids did not transduce HEK cells and the best positive results for GFP plasmids just showed low level transduction of only the MSK-CD19-41BB plasmid.

Despite the time taken to insert mCherry into the MDA plasmid, after a long series of experiments to make transfection and transduction work, I moved onto other plasmids which had more positive results. Experiments involving the mCherry and GFP plasmids are summarized in table 5.2 which list the multiple optimizations of experimental conditions. In many of these experiments I first confirmed visual fluorescence in phoenix cells after transfection (HEK 1-5, Table 5.2) as a visual check of transfection. It

was possible to demonstrate low level transduction of the GFP plasmid CD19-41BB but not CD19-CD28 with some titration of virus but this was insufficient to determine MOI presumably due to low viral titres.

To explore why this system was not working, in HEK transduction (5) (table 5.2), I transduced a HER2 plasmid as my positive control as this had worked well for colleagues at BCI. This did not work using the same retroviral system indicating a problem with virus production in the transfection step. I therefore investigated my transfection step by comparing two different methods of plasmid transfection using jetPRIME and polyethylenimine (PEI) in HEK transduction (6), and then comparing fresh supernatant collected at 48 vs 72 hours. This again showed low level transduction in the CD19-41BB GFP plasmid, at best 4.4% in with viral supernatant made with jetPRIME collected at 72 hours.

I investigated transducing alternative murine cells that should be more easily transducible to try and determine which transfection conditions would improve viral titre. For this I transduced both murine 3T3 fibroblasts and pancreatic ductal adenocarcinoma cells in experiments run side by side using thawed supernatants but comparing those made with PEI vs jetPRIME, and collected at 48 vs 72 hours. Again, I used HER2 as a positive control, the expression of which was not associated with a fluorescent protein so required a primary and secondary antibody. This represented a crucial series of experiments summarized in table 5.1.

Table 5.1: Transduction efficiency of various plasmids in 3T3 and PDAC cells with viral supernatant collected after 48 and 72 hours post transfection.

Cell	Supernatant	Transfection	48h	72h
PDAC	<i>Untransduced</i>		0.5%	
PDAC	CD19-CD28-GFP	jetPRIME	3.0%	5.7%
PDAC	CD19-CD28-GFP	PEI	4.4%	8.7%
PDAC	CD19-41BB-GFP	jetPRIME	/	11.6%
PDAC	CD19-41BB-GFP	PEI	2.7%	10.7%
PDAC	<i>Untransduced HER2</i>		4.6%	
PDAC	HER2	PEI fresh	11.4%	14.9%
3T3	<i>Untransduced</i>		0.8%	
3T3	CD19-CD28-GFP	jetPRIME	2.3%	2.9%
3T3	CD19-41BB-GFP	jetPRIME	3.1%	5.0%
3T3	<i>Untransduced HER2</i>		1.4%	
3T3	HER2	PEI fresh	4.9%	2.2%

This time I saw transduction in the positive control HER2 did work, and was greater in PDAC than 3T3 cells indicating they are more easily transducible (14.9 vs 5%) (figure 5.7) when comparing the highest transduction achieved.

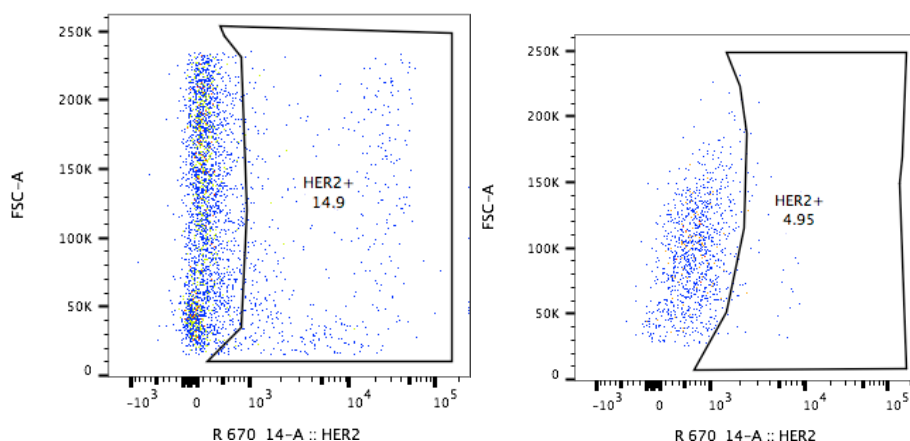


Figure 5.7: DAPI-, viable, single mononuclear PDAC (left) or 3T3 (right) cells transduced (see chapter 3.3.3) with HER2, with highest transduction demonstrated. Gate was determined compared to same cell type untransduced controls (not shown).

Further, the transduction efficiency of HER2 in 3T3 and PDAC cells could be replicated using the CD19-41BB-GFP plasmid, and in general 72h viral supernatant was more effective than 48h supernatant, and jetPRIME transfection reagent better than PEI (figure 5.8).

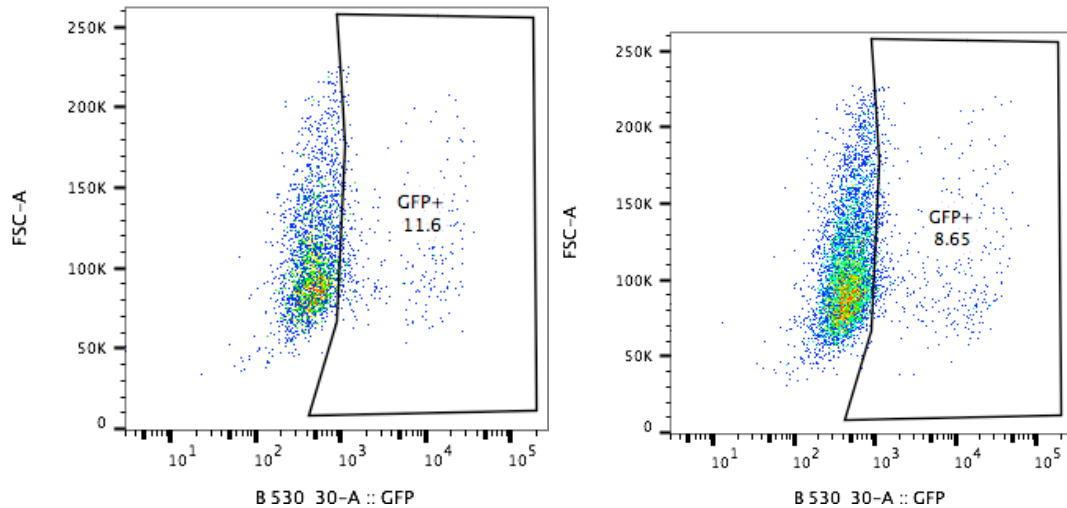


Figure 5.8: DAPI-, viable, single mononuclear PDAC cells transduced using retroviral supernatant (see chapter 3.3.3) derived from CD19-41BB plasmid with jetPRIME (left) and CD19-CD28 plasmid using PEI (right). Highest transduction efficiency in this experiment demonstrated with positive gate determined by comparison with untransduced PDAC control cells cultured in the same conditions (not shown).

All together this does indicate this system is producing virus, but the major problem lies with either viral titre or the viral particles that are produced because of the type of packaging cell line. After further investigation, I discovered I had been using Phoenix-amphotropic cells, which produce viral particles which should infect all mammalian cells. The protocols I have followed recommend ecotropic packaging cells as these are specific for rat and mouse cells. Further, the phoenix cells I had been using were now at a very high passage. I therefore employed multiple strategies to improve viral production including buying new packaging cells, changing to ecotropic cells which are more specific to transduce murine cells, using fresh supernatant and concentrating the viral supernatant e.g. using the Retro-X concentrator. Having received a new plasmid

through a new MTA with the NCI I have also started to investigate the feasibility of using this plasmid in this model.

Below we see transduction of 3T3 cells using fresh viral supernatant collected at 72 hours or 48 hour supernatant concentrated with Retro-X for the NCI CD19-CD28 plasmid. The fresh 72 hour supernatant has a transduction efficiency of 19.7% and concentrated 48 hour supernatant 42.8% (figure 5.9). The CD19-41BB-GFP plasmid had a very similar transduction using the concentrated 48 hour supernatant. This clearly demonstrates that concentrating the viral supernatant improves transduction efficiency.

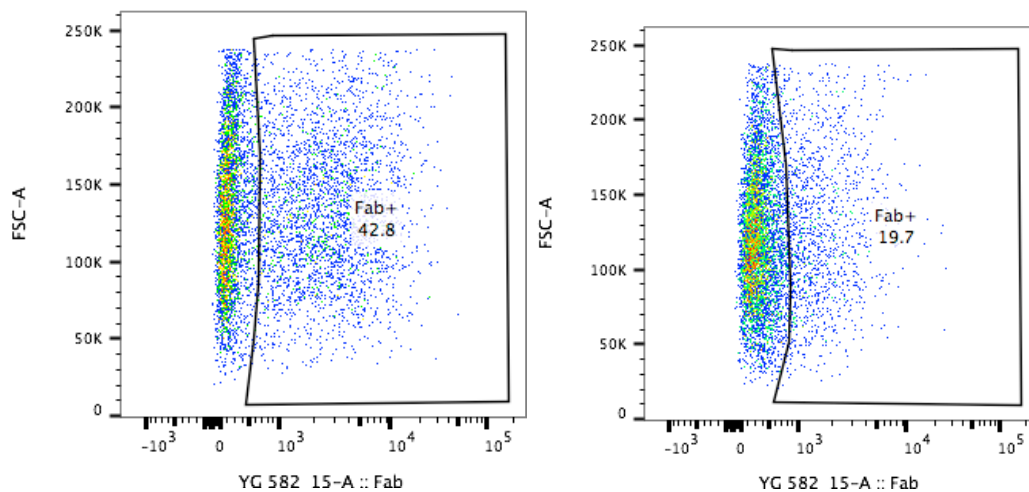


Figure 5.9: DAPI-, viable, single mononuclear 3T3 cells transduced using retroviral supernatant from NCI CD19-CD28 plasmid (see chapter 3.3.3) collected at 48 hours concentrated with Retro X (left) or collected at 72 hours (right) and used fresh. CAR⁺ cells determined using fab antibody. Highest transduction efficiency this this experiment demonstrated with positive gate determined by comparison with untransduced 3T3 control cells cultured in the same conditions (not shown).

Finally, table 5.2 shows the transduction efficiencies of 3T3 cells using concentrated virus. Having adopted various strategies for improving the viral particles and concentration I have now demonstrated high transduction efficiency using murine cell lines using both my NCI CD19-CD28 plasmid detected using a fab antibody and MSK CD19-41BB-GFP plasmid detected by GFP directly by flow cytometry.

Table 5.2: Transduction efficiency of various primary cells and cell lines with experimental optimizations and outcomes.

Cell	No.	CAR	Efficiency	Notes	Optimizations
Mouse	1	GFP/mCherry		Failed	
HEK	1	GFP/mCherry	GFP-41BB 7%	mCherry failed	Double transduction
HEK	2	GFP/mCherry	GFP-41BB 3%	mCherry failed	
Mouse	2	GFP/mCherry		Failed	R+D rmlL2
HEK	3	GFP/mCherry		Failed viral titre	↑polybrene
HEK	4	GFP/mCherry	GFP-41BB 7%	Viral titre	Perform side by side with fresh 72h supernatant Compare T cell concentration $1/3 \times 10^6$
Mouse	3		GFP-41BB 1.7%	Remove CD3/CD28 beads at D5	
<i>Conclusion – Problem with virus production. 3 better than 1×10^6 mouse T cells in 6WP. mCherry plasmid transduction repeatedly fails.</i>					
HEK	5	GFP/HER2	GFP-41BB 6% HER2 Failed	Viral titre HER2 +ive control failed	Compare 48h vs 72h thawed supernatant ↑plasmid DNA in transfection
<i>Conclusion – Demonstration of 41BB virus titration but positive control failed</i>					
HEK	6	GFP/HER2	GFP 41BB 72h jetPRIME 4.4%, PEI 1.5%		PEI vs jetPRIME 48h vs 72h supernatant
<i>Conclusion – GFP seen at transfection, therefore problem with virus production</i>					
PDAC	1	GFP/HER2	GFP-41BB 11.6% HER2 14.9%	Side by side	Frozen supernatant PEI vs jetPRIME 72h better than 48h
3T3	1	GFP/HER2	41BB 5% HER2 4.9%		
<i>Conclusion – Virus present but must be low titre. 72h better than 48h, jetPRIME and PEI similar</i>					
3T3	2	GFP/NCI	41BB 40.1% NCI 42.8%	Retro-X concentrated 48h vs fresh 72h	Platinum-Eco passage 1 cells for transfection Fresh viral supernatant Retro-X 48h supernatant
<i>Conclusion – Concentrated 48h supernatant better than fresh 72 hour supernatant Good transduction efficiency, change of cells and concentrating improves viral titre</i>					
3T3	3	GFP/NCI	41BB 21.2% NCI 42.8%	Retro-X concentrated 48h vs 72h	Platinum-eco transfection Retro-X supernatant
<i>Conclusion – Using Retro-X concentrated viral supernatant produces the highest transduction efficiency of murine 3T3 cells.</i>					

5.6 Transduction of normal and transgenic mouse T cells

Having optimized transfection and transduction conditions using human and murine cell lines I then performed a series of experiments to optimize transduction of normal (WT) and transgenic (Tg) mouse T cells. Table 5.3 summarizes some of the key experiments and notes important learning points.

Table 5.3: Transduction and optimization of normal and transgenic mouse T cells.

Cell	Exp No.	CAR	Highest Efficiency	Notes
WT	2	NCI CD19-CD28	20.5% 48h Retro-X	Compare Retro-X 48h vs 72h supernatant
		MSK CD19-41BB-GFP	15.1% 48h Retro-X	
<i>Conclusion – Retro-X concentrated 48h supernatant gives highest transduction efficiency.</i>				
WT	5	NCI CD19-CD28	WT 67.8% Tg 41.1%	Fresh Tg cells used (CLL load 62%)
Tg		MSK CD19-41BB-GFP	WT 31.8% Tg 21.9%	
<i>Conclusion – Better transduction using fresh Tg cells (rather than thawed).</i>				
WT	6	NCI CD19-CD28	For CD19-41BB:	Change in T cell phenotype through manufacturing noted.
Tg		MSK CD19-41BB-GFP	WT: CD4 43%, CD8 23% Tg: CD4 21%, CD8 8%	
<i>Conclusion – Differential transduction efficiency of CD4 and CD8 T cells.</i>				
Aged WT	8	NCI CD19-CD28	Aged WT 24.3%	Compare transducing Tg and aged WT T cell
Tg			Tg 5.9%	
<i>Conclusion – Excludes normal aging as cause of lower transduction seen in Tg T cells.</i>				

Following mouse WT transduction (experiment 2) I kept the CAR T cells in culture to confirm stable transduction after six days. Figure 5.10 shows a transduction efficiency of 14.2% six days after the transduction efficiency of 15.1% noted in Table 5.3 of mouse CD19-41BB-GFP CAR T cells kept in culture. Further experiments in table 4 confirm that concentrated retroviral supernatant produces highest transduction efficiency and the differential transduction of different T cell subsets. Finally, experiment 8 comparing transduction of aged WT mice versus age matched Tg controls demonstrates the lower transduction efficiency seen in Tg mouse T cells is due to the CLL and not age alone.

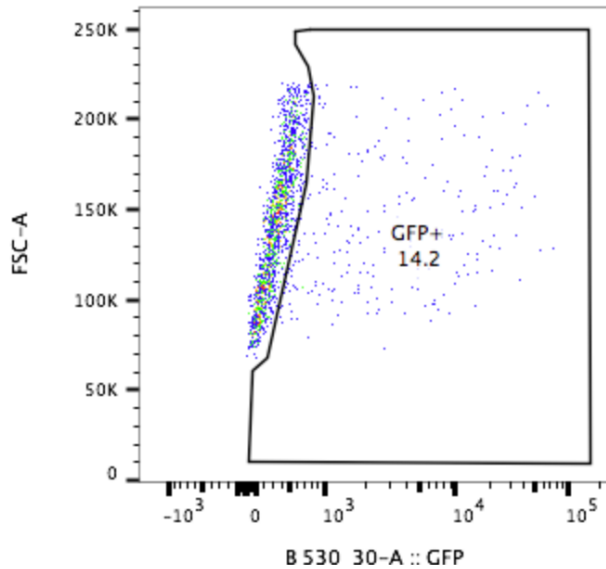


Figure 5.10: DAPI-, viable, single mononuclear WT mouse T cells transduced with donated lentiviral supernatant (gift from Dr Deepak Raj, Barts Cancer Institute) showing stable transduction after cells being kept in culture for 6 days. GFP⁺ gate determined by comparison to untransduced control WT T cells cultured in the same 6 well plate (not shown).

5.7 Rapid expansion protocol

As the Sadelain protocol enriches mouse single cell suspensions for a pure T cell population to improve transduction, I first ensured that the enrichment kit worked in these mouse T cells and then validated my detection antibodies in mouse T cells. Following enrichment 95.3% of cells were CD3⁺ and on average I was left with 20% of the original splenocyte single cell suspension cell count if derived from WT T cells.

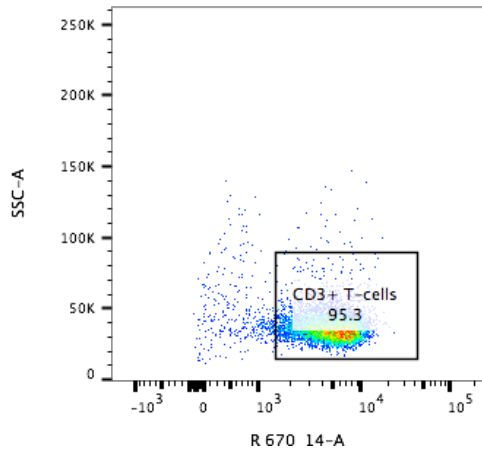


Figure 5.11: DAPI-, viable, single mononuclear murine CD3⁺ cells after T cell enrichment using eBioscience Magnisort Mouse T cell enrichment kit demonstrating 95.3% purity of T cells. Gate is determined compared to non-enriched PBMC following red cell lysis.

Activated mouse T cells double from 48 to 72 hours after 24 hours in culture using my rapid expansion protocol with anti-CD3/CD28 beads and murine IL2 (mIL2). Initially I had trouble proliferating T cells using Roche IL2 but I think this may have been due to an issue with reconstitution. In a titration experiment to determine the best dose of mIL2 from R&D Systems 3000U/ml medium provided the best cell count (figure 5.12) and viability although the cell counts obtained were similar. However, there were very minor differences in T cell expansion which different IL2 doses in this experiment (n=1) and because of previous issues with IL2 reconstitution this result may not be valid. This is contrary to what would be expected in terms of increasing the IL2 dose on T cell proliferation. Most importantly for future experiments, it demonstrated that after 72 hours the T cells are most rapidly multiplying, which is when it is best to harvest the cells so proliferating cells can be injected into the mice for best effect.

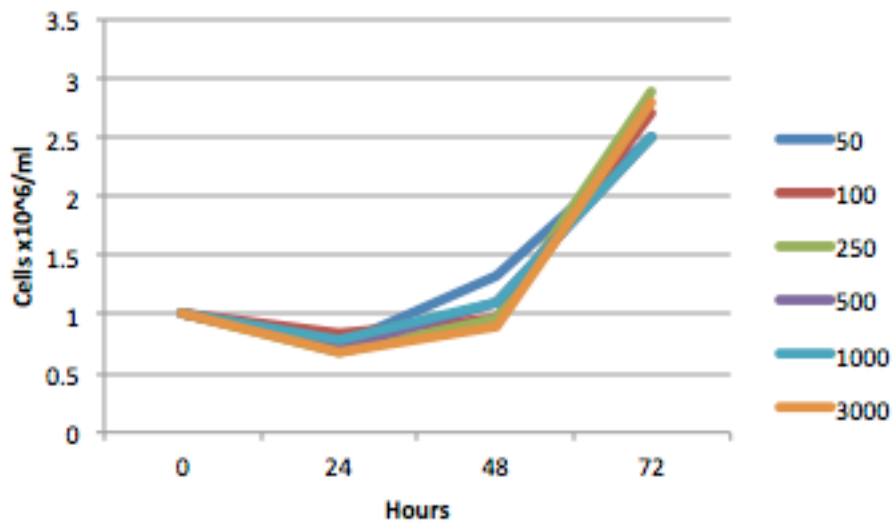


Figure 5.12: Mouse T cell concentration counted by an automated brightfield haemocytometer (Logos Biosystems, South Korea) after proliferation with CD3/CD28 beads and varying concentrations of mIL2 (units) (n=1) at various time point in culture (0-72 hours).

5.8 Discussion

To achieve stable transduction of murine T cells is challenging and the initial part of my PhD was spent optimizing every step of this complex method. Although this was at times frustrating, troubleshooting the experiments actually allowed me to identify the optimal steps to take for the future experiments. Further, because of the underlying characteristics of CLL T cells from the TCL1 model, transgenic CLL T cells do not rapidly proliferate in culture which made this process all the more difficult. Some plasmids work better than others in this model, and the issue of CAR detection complicates matters. Whilst direct visualization with a fluorescent tag has huge advantages for downstream assays and indeed in vivo experiments, manipulation of the construct directly had an effect on transduction efficiency, therefore, the manipulated MD Anderson plasmid with mCherry never made it past cell culture experiments. It was both the MSK CD19-41BB-GFP and NCI CD19-CD28 plasmids that I could demonstrate stable transduction in mouse T cells, after resolving issues with packaging cells and the crucial determination that low viral titre was the main cause of low transduction efficiencies. In my experiments, concentration of retroviral supernatant using Retro-X

was an essential step. For cell culture experiments the GFP tagged CD19-41BB is very useful to identify CAR transduced T cells, whilst for CD19-CD28 I needed to use a primary/secondary Fab antibody for CAR detection. My preliminary optimization experiments here demonstrate that WT T cells transduce more readily than CLL T cells, and even if age as a confounding factor is removed, as aged WT T cells transduce more readily than transgenic CLL T cells. In summary, I describe an optimized method for making retrovirally transduced murine CAR T cells, which can be expanded ex vivo for downstream experiments.

6. CAR T cell phenotype and cytotoxicity in vitro

6.1 Introduction

Having optimised the CAR T cell manufacturing process as described in Chapter 5, I had an established method for producing CAR T cells so the phenotype of CAR T cells derived from normal/WT and CLL mice (AT and transgenic) can be compared. Our group has previously explored the differences in T cell function between Tg TCL1 mice and AT CLL in general (89), particularly with reference to the exhaustion phenotype (118). The differences between CAR T cells derived from normal and CLL T cells has not been described in the TCL1 model or AT CLL, but recently it has been in studies of untreated CLL patients compared to healthy donors (259). In a small number of patients (n=3), there was a greater expansion in naïve CAR T cells (CD45RA⁺CCR7⁺) from healthy donors compared to untreated CLL patients, who had greater expansion in effector CAR T cells (CD45RA⁺CCR7⁻). PD-1 expression was higher on naïve and central memory CAR T cells from untreated CLL patients compared to healthy donors (259). Similarly, differences in cytokine profiles have been demonstrated. The frequency of CAR T cells producing IFN- γ in-vitro was significantly higher in CLL CAR T cells compared to those derived from healthy donors (260).

Defining the optimum phenotype from which to make CAR T cells may be an important determinant of CAR T cell function, and the prospective determination of a set T cell phenotype for manufacturing is not done for either of the two licenced CAR T cell products. CD19-41BB CAR T cells of defined CD4⁺:CD8⁺ composition has been done using the investigational lisocaptogene maraleucel (liso-cel) but prior to its commercialisation Turtle et al. had reported its use in ALL (174), NHL (175) and CLL (161). Again, the CR rate reported in CLL (21%) for the same product was much lower than that reported in ALL (93%) and NHL (50%). At ASH 2018 the early phase 1 dose escalation data from TRANSCEND CLL-04 from the same group was updated (162), revealing higher response rates in patients who had previously received ibrutinib but still with small numbers of patients reported. 6/8 evaluable responded including 4 CR

at day 30 so this study needs more time to accrue more patients to fully understand the impact of set CD4: CD8 ratio in CLL. The rationale for this approach was based on pre-clinical data, which demonstrated synergistic enhancement of anti-tumour activity by administering defined ratios of human CD19 CAR T cells subsets to treat immunodeficient mice (208) engrafted with Raji cells as compared to giving these subsets alone or from unselected T cells. Using this approach CD4⁺ and CD8⁺ T cell subsets must be separately enriched from apheresis products, transduced and proliferated ex-vivo separately and then recombined.

A comprehensive retrospective review of genomic, phenotypic and functional evaluations to identify determinants of response in CLL has been recently performed (206). Transcriptomic profiling revealed that CAR T cells from patients with CLL who achieved complete responses were enriched in memory related genes, whereas T cells from non-responders upregulated genes involved in effector differentiation, glycolysis, exhaustion and apoptosis. Sustained remission was associated with an elevated frequency of CD27⁺CD45RO⁻CD8⁺ T cells before CAR T cell generation, and these lymphocytes possessed memory like characteristics (206). Finally, a population of CD27⁺PD-1⁻CD8⁺ CAR T cells expressing high levels of IL6 receptor predicts therapeutic response and is responsible for tumour control (206). These findings suggest the potential for pretreatment CAR phenotype as a biomarker and the manufacturing of CAR T cells from specific subsets of T cells to improve CAR response. Here I investigate the difference between deriving CAR T cells from normal or CLL T cells and its effect on CAR T cell phenotype and cytoxicity in vitro.

6.2 Objectives

- Produce CAR T cells using the same optimised protocol from pooled WT spleens, or make CAR T cells from mice with both sources of CLL, either aged transgenic mice (Tg) or mice with AT CLL.
- Phenotype each set of CAR T cells, before, during and after the manufacturing process to understand the differences in CAR phenotype when using these different cell sources.

- Compare the in vitro cytotoxicity of CAR T cells derived from each cell source.
- Phenotype CAR T cells derived from each cell source after co-culture experiments with CLL B cells.

6.3 Materials and methods

6.3.1 T cell source

In this chapter I used the transfection and transduction protocol to make murine CAR T cells as defined in Chapter 3 and optimised in Chapter 6.5. I had three sources of cells to compare, normal or WT T cells from pooled WT spleens from the TCL1 colony, in which there were two groups of CLL T cells; either aged transgenic mice with confirmed $CD5^+CD19^+$ disease (Tg) or fully leukaemic WT mice who had previously received AT TCL1 CLL. All had $CD5^+CD19^+$ cells confirmed by PB flow from a tail vein bleed. These AT mice were allowed to develop leukaemia and were culled prior to reaching humane endpoints. These T cell sources are summarised in figure 6.1.

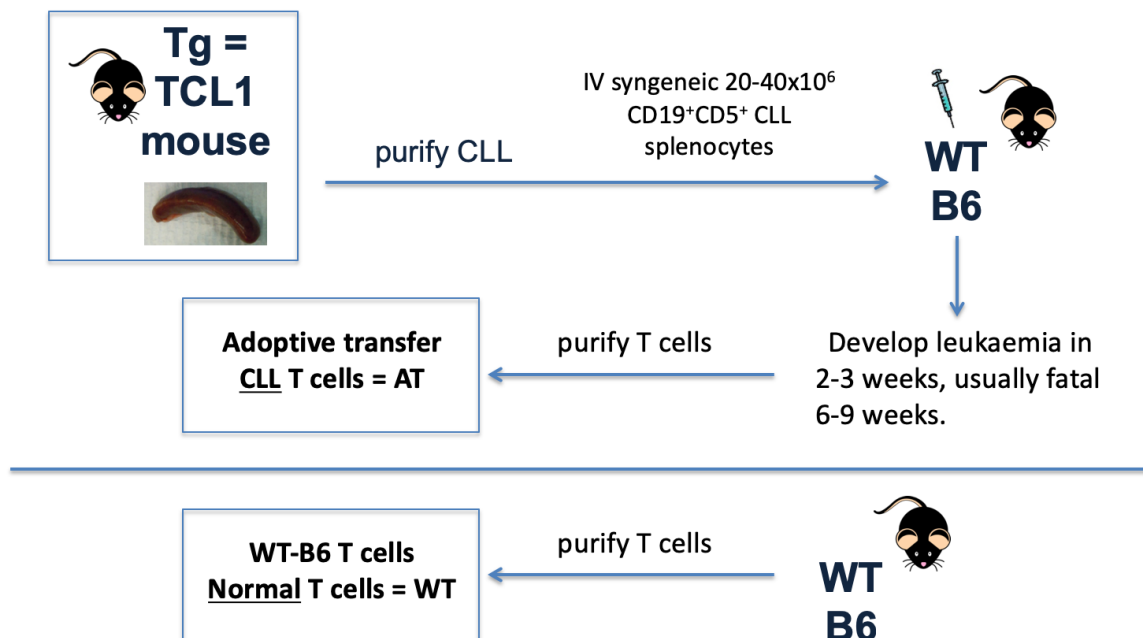


Figure 6.1: CAR T cells were either derived from transgenic mice (Tg), normal or WT T cells, or from mice that had AT of CLL when they were confirmed to be leukaemic by PB flow cytometry looking for $CD5^+CD19^+$ CLL.

6.3.2 Multicolour flow cytometry

T cells are identified by CD3, with CD4 and CD8 being used to identify helper and cytotoxic T cells. CD62L (L-selectin) is a peripheral lymph node homing receptor and marker of T cell development, it is expressed on naïve and memory T cells, whilst effector T cells downregulate CD62L (261, 262). CD44 corresponds to human CD45RO as a marker of antigen-experienced T cells, and are highly expressed on memory and effector T cells (263). In these experiments, T cells were characterised based on surface expression of CD3, CD4, CD8, CD62L, CD44 and PD-1. CLL was identified using CD5 and CD19. The antigens and corresponding fluorochromes, clones and suppliers are listed in table 6.1.

Mouse Antigen	Fluorochrome	Clone	Supplier
CD3	PerCP-eFluor710	17A2	eBioscience
CD3	APC-eFluor780	17A2	eBioscience
CD4	PE Cyanine7	GK1.5	eBioscience
CD8a	BV605	53-6.7	BioLegend
CD44	PE	IM7	eBioscience
CD62L	FITC	MEL-14	eBioscience
PD-1	Allophycocyanin (APC)	J43	eBioscience
PD-1	PerCP-eFluor710	RMP1-30	eBioscience
CD19-41BB CAR	GFP	Transduced T cell only	
CD19-CD28 CAR	Streptavidin PE/FITC	f(ab') ₂	eBioscience
CD5	APC	53-7.3	eBioscience
CD19	PE	1D3	eBioscience/BD

Table 6.1: CLL and T cell antibodies used for phenotyping.

6.4 Results

6.4.1 Cytotoxicity titration

To initially demonstrate the cytotoxicity of CAR T cells in vitro, I performed an experiment using different effector: target ratio of WT CAR T cells to CLL cells. I also compared different sets of CAR T cells produced with the retroviral supernatant collected after both 48 and 72 hours transfection of packaging cells. The transduction efficiency of the NCI CD19-CD28 CAR versus MSK CD19-41BB CAR is as per table 5.3 in chapter 5, the highest was 20.5% and 15.1% respectively using the concentrated supernatant collected after 48 hours of transfection. The CAR T cells and CLL B cells were co-cultured for 72 hours.

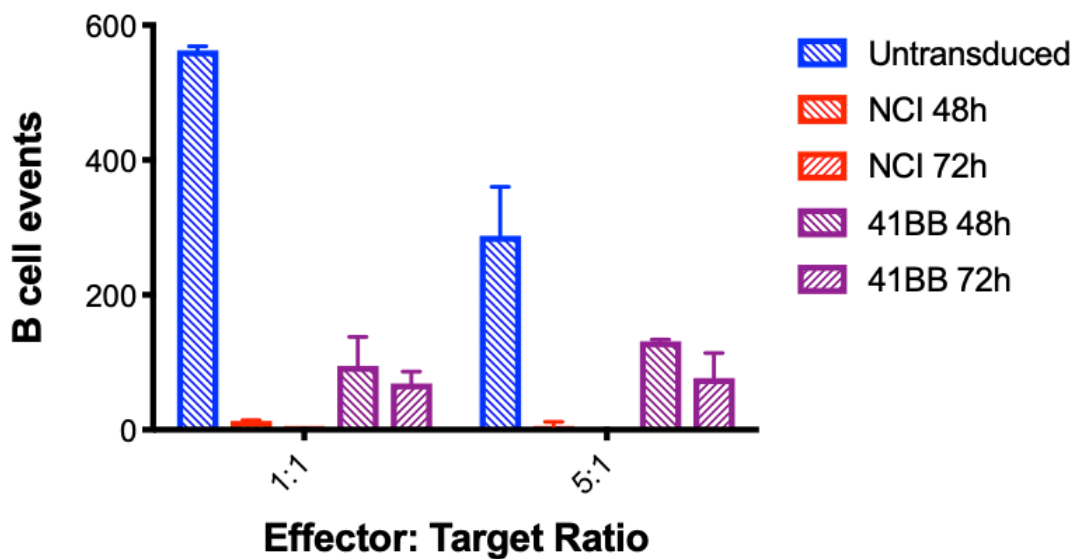


Figure 6.2: Remaining B cell events (CellTrace Yellow) after 72 hours co-culture of CAR T cells transduced with CD19-CD28 (NCI) and CD19-41BB-GFP (41BB) using retroviral supernatant collected at 48h and 72h with primary murine enriched CLL B cells at different effector (total T cells including CAR T cells) to target (B cell) ratios. Samples were re-suspended in FACS buffer with counting beads to ensure an equal number of total events were collected.

Following this, the same CAR T cells were using at lower effector: target ratios to determine the ratio required to demonstrate cytotoxicity in subsequent cytotoxicity experiments. Figure 6.2 demonstrates that lower effector: target ratios than 1:1 are less effective at killing B cells. The data together suggests improved cell killing by the NCI CD19-CD28 CAR then the MSK CD19-41BB in vitro in CAR T cells derived from WT cells with an optimum target: effector ratio of 1:1 for future experiments.

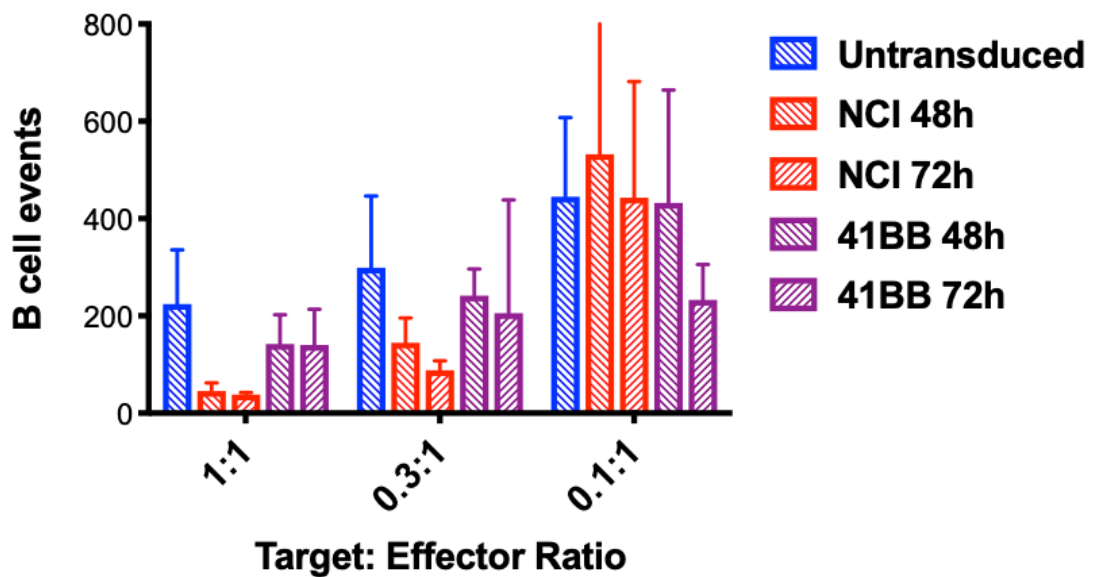


Figure 6.3: Remaining B cell events (CellTrace Yellow) after 48 hours co-culture of CAR T cells transduced with CD19-CD28 (NCI) and CD19-41BB-GFP (41BB) using retroviral supernatant collected at 48h and 72h with primary murine enriched CLL B cells at different effector (total T cells including CAR T cells) to target (B cell) ratios. Samples were re-suspended in FACS buffer with counting beads to ensure an equal number of total events were collected.

6.4.2 T cell phenotype progression through manufacturing

During CAR manufacturing, flow was performed to phenotype the CAR T cells from each T cell source (and untransduced controls) at various points to compare the evolution in phenotype through the manufacturing process. This included, after T cell enrichment pre manipulation, immediately following transduction, and after 72 hours 1:1 co-culture with CLL cells stained with CellTrace yellow. As previously described, CLL

development in Tg and AT mice results in the relative expansion of CD3⁺CD8⁺ cells in the spleen and within this population, CD44⁻CD62L⁺ naïve cells are lost with a shift to CD44⁺ antigen experienced, and more CD44⁺CD62L⁺ effector cells in the spleen (118). This was reflected in my starting pre-manipulation T cell suspensions, and post transduction, an increase in CD8⁺ cells with a reduction in naïve CD8⁺ T cells in WT CAR T cells and complete disappearance of this population in AT/Tg CAR T cells (figure 6.4 and 6.5).

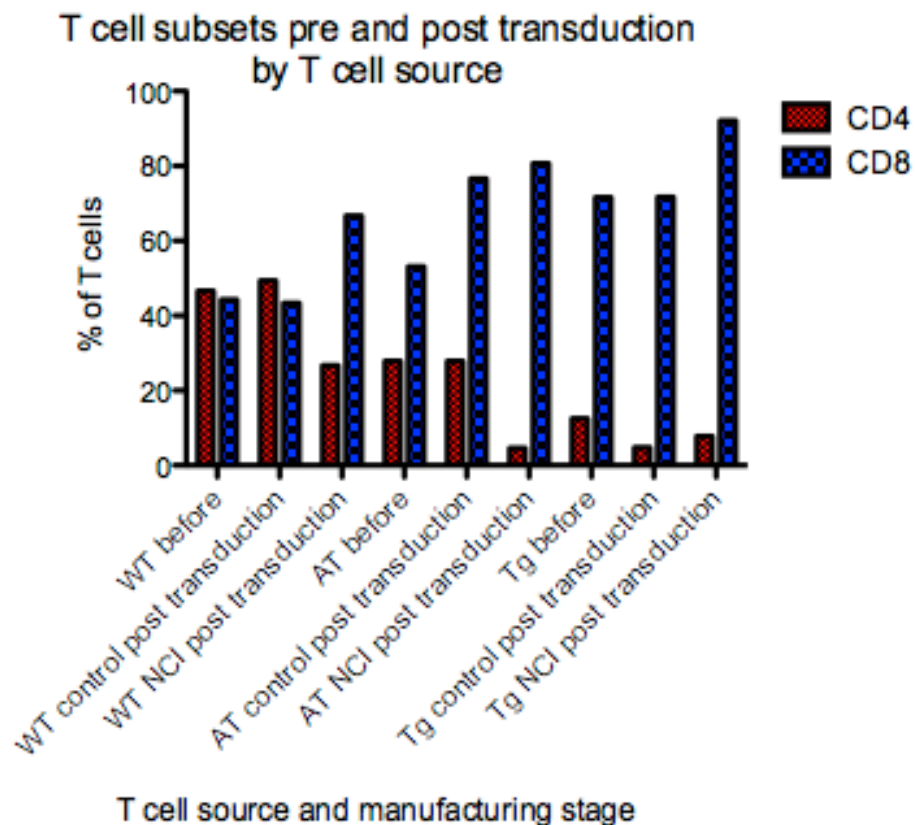
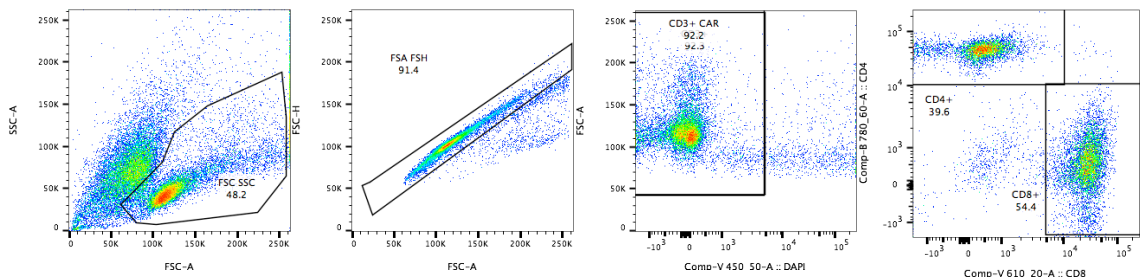
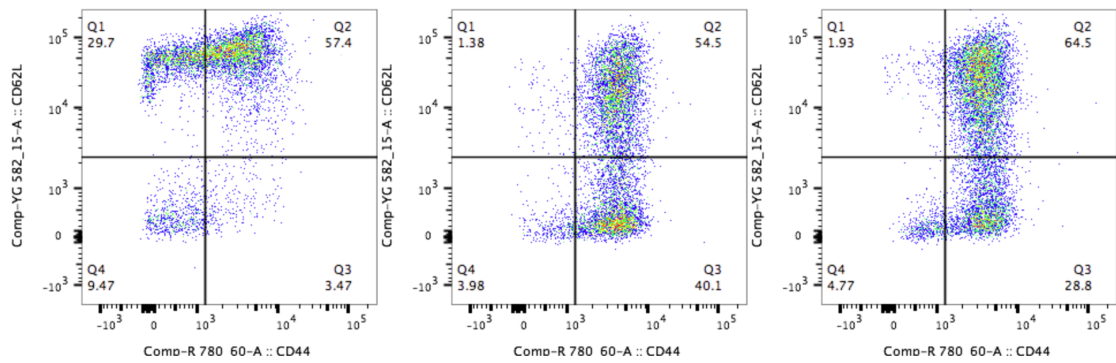


Figure 6.4: DAPI-, viable, single mononuclear murine T cells which are CD4⁺ and CD8⁺ pre and post transduction with the CD19-CD28 CAR. T cells were derived from WT or Tg mice, or WT mice that had received AT of CLL. Gating strategy for determination of CD4⁺CD8⁺ is above.



Phenotype of CD3+CD8+ cells pre and post transduction by T cell source

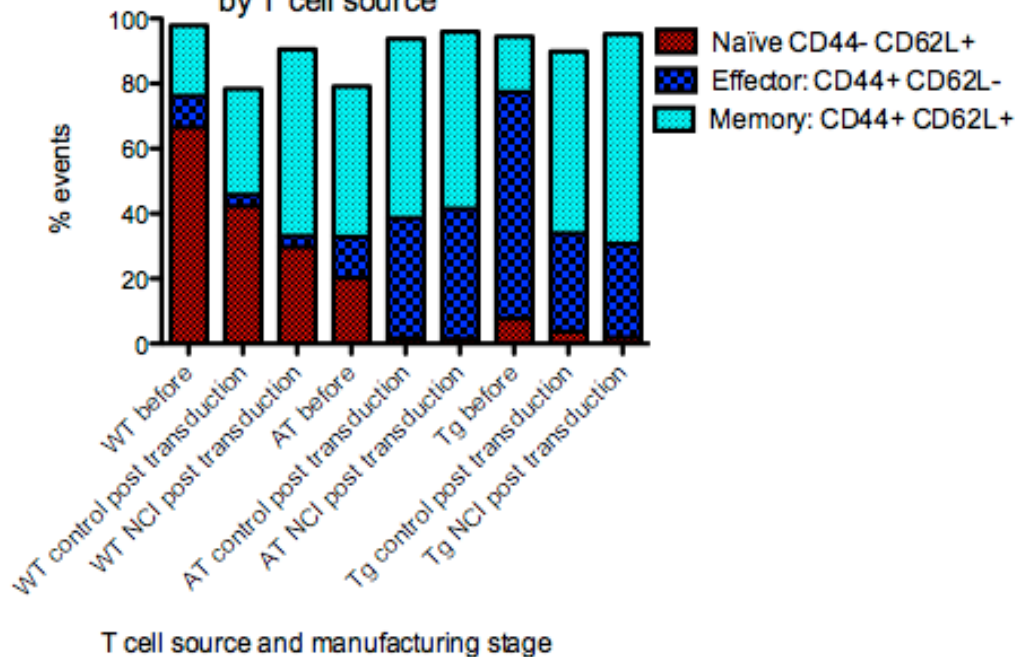


Figure 6.5: Gating strategy of DAPI⁻, viable, single mononuclear murine T cells which had naïve (CD44⁻CD62L⁺), effector (CD44⁺CD62L⁻), and memory (CD44⁺CD62L⁺) phenotypes of the CD8⁺ cells identified in figure 6.4. T cells were derived from WT or Tg mice, or WT mice that had received AT of CLL, phenotype pre and post transduction by source of T cells transduced with retroviral supernatant from the NCI CD19-CD28 CAR plasmid.

I have previously seen big differences in transduction efficiency between WT and Tg T cells, and again in this experiment when comparing WT to AT and Tg transduction, it is WT cells which are most readily transduced using identical retroviral supernatant and culture conditions (figure 6.6).

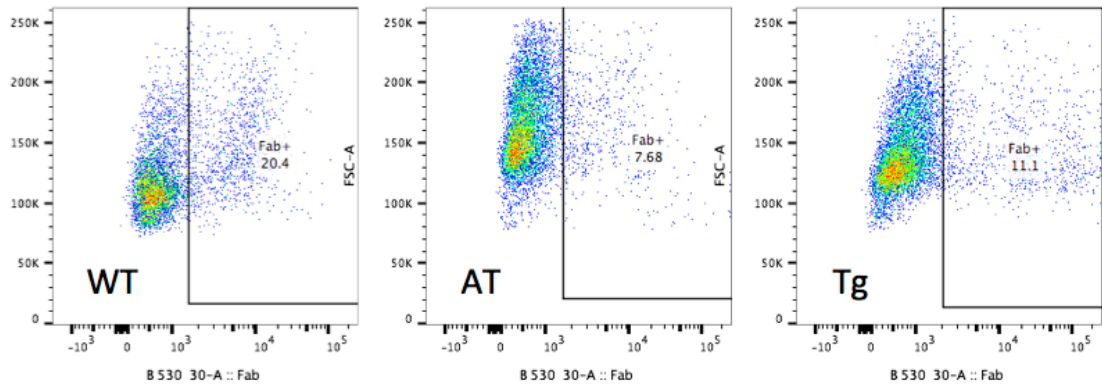


Figure 6.6: Flow plots of transduction efficiency (Fab) by FSC determined in DAPI-, viable, single mononuclear T cells with fab-biotin with negative gate established comparing transduced to untransduced T cells, by T cell source.

In previous experiments I have seen that WT CAR T cells proliferate in culture much more readily than CLL T cells. Figure 6.7 shows the proliferation of CAR T cells during the manufacturing process, which demonstrates that CAR T cells derived from Tg T cells do not proliferate as well as WT or AT T cells.

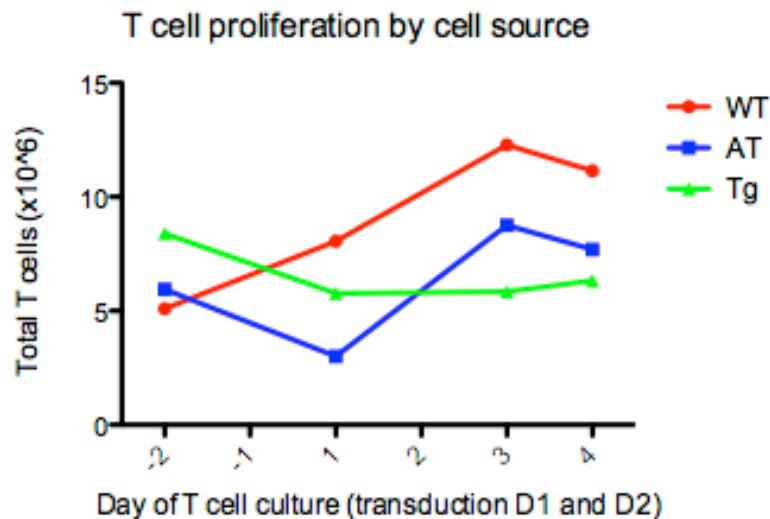


Figure 6.7: Total T cell count ($\times 10^6$ cells) in culture from activation of T cells on D-2 to -1, transduction on D1 and D2 and expansion from D3 onwards determined by an automated dual fluorescence (acridine orange/propidium iodide stain) haemocytometer (Logos Biosystems, South Korea) by source of T cells, WT or Tg mice or WT mice after AT of CLL.

On day 4 of CAR T cell culture, the cytotoxic CD19 specific killing was evaluated by setting up co-culture with CLL cells at 1:1 effector to target ratio. The effector count was taken as the total T cell count and not selected for CAR⁺ cells and the targets were CD19 enriched (negative selection) splenocytes from other aged TCL1 mice from the colony. The CLL cells were labelled with CellTrace yellow. CAR⁺ T cells were not selected as the optimal dose at this stage was not known and in planned murine experiments I was not going to enrich for CAR T cells. Cytotoxicity was assessed at 24, then 48 and 72 hours using counting beads. No significant cytotoxicity was demonstrated after 24 hours.

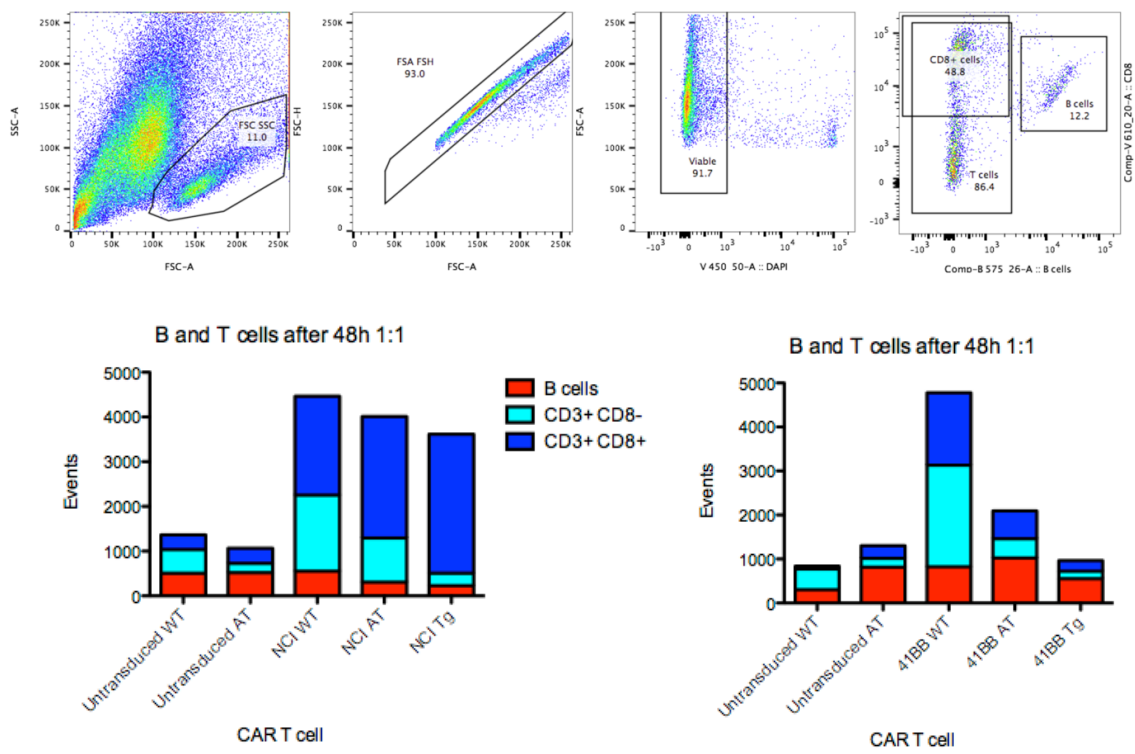


Figure 6.8: CLL B cell (labelled with CellTrace Cell Proliferation Kit) and T cell events (CD3/CD8) following 48 hours co-culture of non-enriched T cells containing CAR T cells derived from WT, Tg and AT T cells at 1:1 ratio separated by the NCI CD19-CD28 CAR (left) and CD19-41BB CAR (right) showing T cell expansion, or with untransduced T cell controls. Samples were prepared in FACS buffer with counting beads and 1000 events were recorded for each condition.

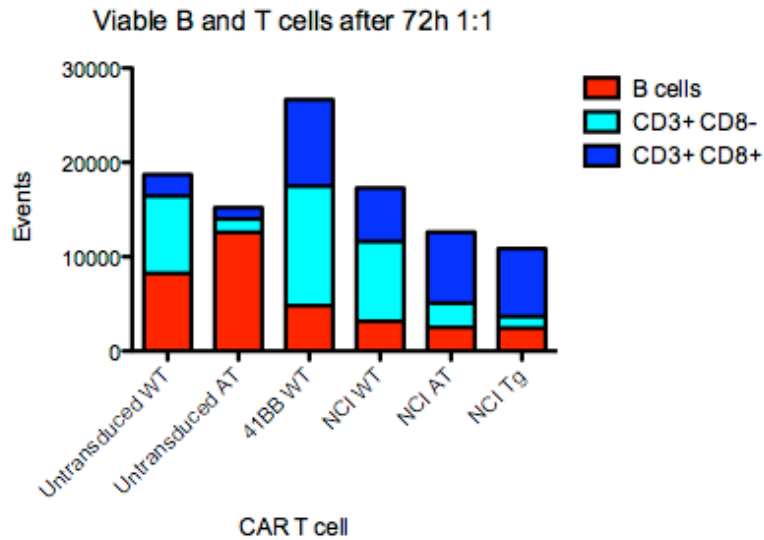


Figure 6.9: CLL B cell (labelled with CellTrace Cell Proliferation Kit) and T cell events (CD3/CD8) following 72 hours co-culture of non-enriched T cells containing CAR T cells derived from WT, Tg and AT T cells at 1:1 ratio separated by the NCI CD19-CD28 CAR (and CD19-41BB CAR showing T cell expansion, or with untransduced T cell controls. Samples were prepared in FACS buffer with counting beads and 1000 events were recorded for each condition. For gating strategy see figure 6.8.

In figures 6.8 and 6.9, we see that following 48-72h of co-culture there was expansion of T cells in the NCI CD19-CD28 CAR in WT/AT and Tg groups. In the CLL with CD19-41BB CAR co-culture experiment it was only the CAR derived from WT T cells where there was significant T cell expansion at 48 and 72 hours. Following the cytotoxicity co-culture the remaining T cells were phenotyped and demonstrate again an expansion of CD8 T cells, markedly in AT and Tg T cells. Further these CD8⁺ T cells become almost entirely antigen experienced i.e. CD44⁺, and mostly effector T cells in AT and Tg CAR T cells (figures 6.10 and 6.11). There is a complete loss of naïve T cells in the co-culture using WT, AT or Tg derived CAR T cells, but in the WT derived CAR T cell co-culture there is still a healthy mixture of memory and effector T cells.

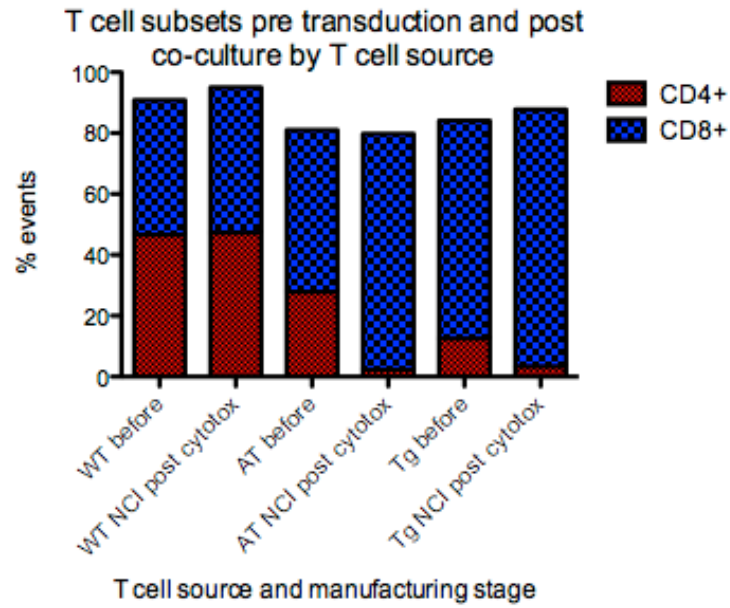


Figure 6.10: T cell subsets, post 72h co-culture with CellTrace yellow stained CD19⁺ enriched CLL mouse splenocytes, in comparison to their phenotype pre-manipulation. For gating strategy see figure 6.8.

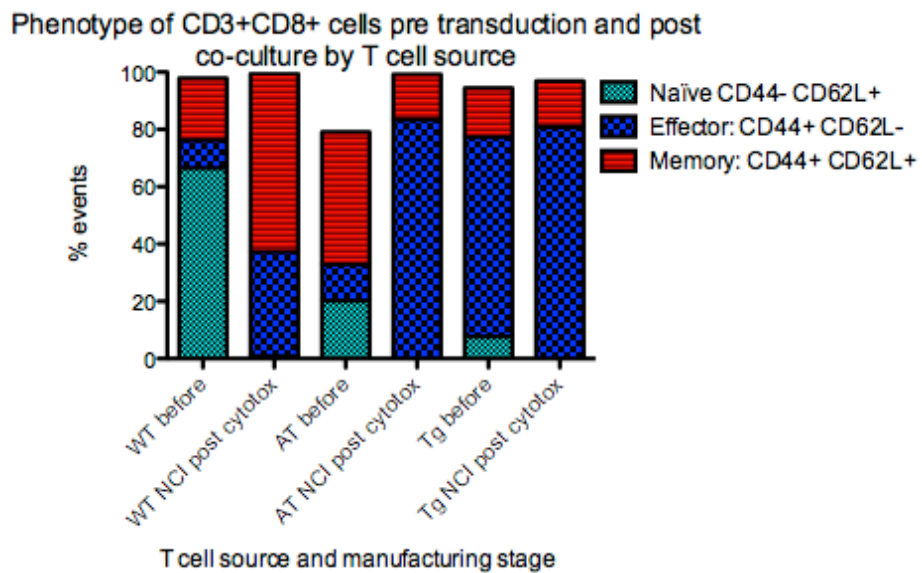
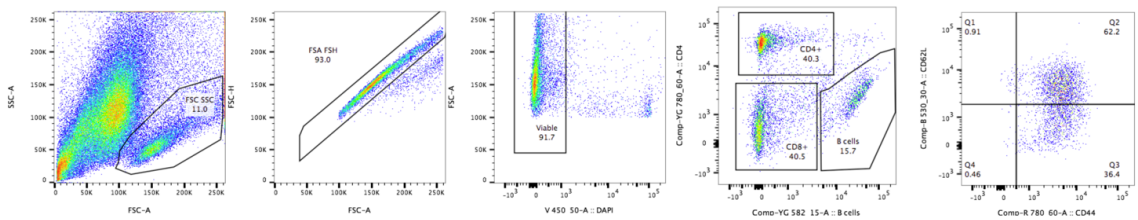


Figure 6.11: Extended naïve/effector/memory phenotype of T cells, post 72h co-culture with CellTrace yellow stained CD19⁺ enriched CLL mouse splenocytes, in CD8⁺ cells only CD44/CD62L.

The NCI CAR does not have a fluorescent tag so it is more challenging to monitor the progression of the expanding CAR T cell population in culture. However, for the 41BB WT CAR this population can easily be tracked by GFP. Figure 6.10 demonstrates that after co-culture the expanded T cell population are varying mixtures of CD4⁺ and CD8⁺, but the CAR⁺GFP⁺ cells are all CD8⁺ and these CD8⁺GFP⁺ cells are almost entirely PD-1⁺ (figure 6.12).

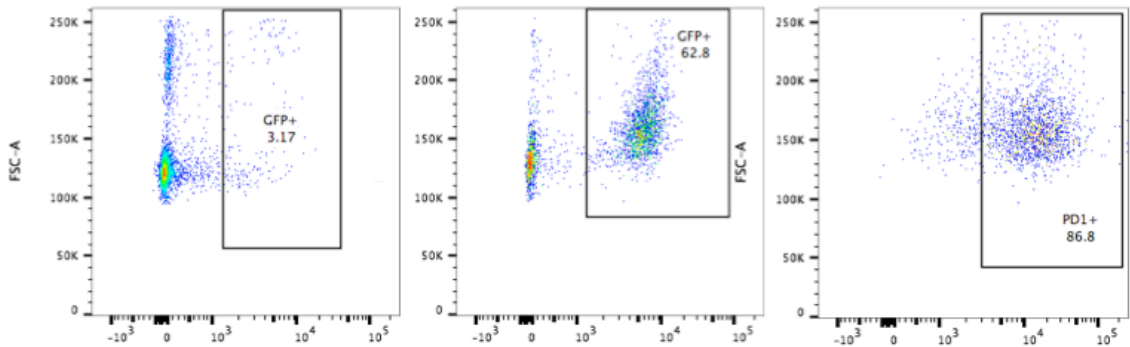


Figure 6.12: Demonstration of GFP⁺ cells in CD4⁺ (left) and CD8⁺ (centre) T cells following 72h 1:1 co-culture with CellTrace yellow stained CD19⁺ enriched CLL mouse splenocytes and WT CD19-41BB CAR T cells. PD-1 expression in CD8⁺GFP⁺ CAR T cells in the same experiment (right).

6.5 Discussion

When CAR T cells are made from WT or CLL T cells, the CAR T cells display markedly different phenotypes at the end of applying an identical optimised manufacturing process. Some of the phenotypic differences are evident prior to transduction, as they reflect the well described phenotypic differences between normal and CLL T cells, illustrated in previous publications by our group (89, 118). However, activation and transduction of T cells as required to make CAR T cells, accentuates the phenotypic differences, but the effect is differential when considering WT and CLL T cells, summarised in table 6.2. It is not clear the reason for this but it is an observation that I observed in subsequent experiments. Activation of T cells required for transduction, results in skew to CD8 in both WT and CLL T cells, but this effect is heightened for both types of CLL T cells. Further, for both cell types, there is loss of naïve CD8 T cells during

CAR manufacture, but this is almost entirely complete for AT and Tg T cells. For AT and Tg T cells, after both manufacture and then co-culture with CLL cells, there are mostly terminally differentiated effector T cells left, compared to a majority of memory balanced with some effector T cells for WT CAR T cells. There is significant preclinical evidence in xenograft mouse models CAR T cells enriched in naïve and memory T cells and using defined CD4: CD8 ratios can improve CAR efficacy (208), although the disease being treated is CD19⁺ engrafted Raji cells. Interestingly, in the pivotal CLL CAR study (160), of the products infused the median CD4% was 81% with a median of 20% CD8 T cells. There is no detailed analysis of extended T cell phenotype in this study but it does state phenotype did not predict response (160).

In these experiments there is not a comprehensive analysis of changes in PD-1 expression due to technical issues. Following the co-culture experiment, it was much easier to identify CAR⁺ T cells of CD19-41BB due to the GFP in that plasmid, so only in the CD19-41BB CAR T cell co-culture experiment it was possible to establish that of the CAR⁺ T cells, the vast majority (87%) are PD-1⁺, which in this context can of course reflect both activation and exhaustion.

WT/normal CAR T cells	CLL (AT/Tg) CAR T cells
CD4 ⁺ :CD8 ⁺ = 1 manufacture and co-culture	CD4 ⁺ ↓, CD8 ⁺ ↑ manufacture and co-culture
CD4 ⁺ =CD8 ⁺ transduction efficiency	CD8 ⁺ transduction ↓ CD4 ⁺ transduction preserved
PD-1 ⁺ low	PD-1 ⁺ high (41BB)
CD44 ⁺ high	CD44 ⁺ high
CD3 ⁺ CD8 ⁺ memory	CD3 ⁺ CD8 ⁺ effector (loss of naïve)

Table 6.2: Key phenotypic differences between CAR T cells derived from WT and CLL T cells (AT and Tg) after expansion and in co-culture experiments.

In vitro cytotoxicity experiments demonstrate that murine CAR T cells derived from both WT and CLL T cells can exhibit cytotoxicity of CD19⁺ enriched CLL cells after 48-72 hours in co-culture. When comparing of the efficacy of CD19 CAR T cells with different co-stimulatory domains in this model, the cytotoxicity of WT CD19 CAR T cells is greater at all effector: target ratios using the CD19-CD28 CAR. In these co-culture experiments, after 48-72 hours there is both loss of B cells but marked apparent expansion of T cells, for the CD19-CD28 regardless of the T cell source but when using CD19-41BB CAR T cells only when they were derived from WT T cells was a significant T cell expansion seen. Interestingly, of the co-culture CAR T cell in vitro expansion, when the T cell source was normal T cells these T cells are 1:1 CD4: CD8, but like in the ex vivo expansion phase of manufacturing, when the T cell source was CLL T cells, the in vitro expansion is predominantly CD8⁺ T cells. This was true for both AT and Tg T cells, although the skew to CD8 T cell expansion in co-culture is more marked for Tg CAR T cells.

In summary this series of experiments demonstrate a specific phenotype of CAR T cells when an identical manufacturing process is applied to both groups of cells. The resulting CAR T cells demonstrate in vitro cytotoxicity, although the CD19-CD28 CAR T cells to a greater extend and in all cell types. Because of ongoing issues with ex vivo expansion of Tg T cells in culture and poor viability, for future experiments I decided to use AT CLL T cells as my main T cell source to model CLL T cells. Some of the phenotypic changes induced by CAR manufacture are actually due to the method of T cell activation, and as control WT and CLL T cells not transduced but activated under identical conditions exhibited the same phenotypic changes. It is worth noting, there are other less established methods for activation and transduction of a murine T cell, and therefore opportunities to optimise CAR T phenotype for efficacy by manipulation of these methods.

7. CAR T cell function in vivo

7.1 Introduction

The majority of published data regarding pre-clinical investigation of CAR T cells in murine models uses human CAR T cells in immunodeficient mice engrafted with either human primary tissue or human derived cell lines. Such models clearly indicate CAR efficacy, but they do not allow for more complex study of the interactions between CAR T cells and the host immune response. Whilst the transgenic and AT TCL1 mouse models were already setup in the Gribben laboratory, no CAR work was established prior to starting my PhD. The broad schematic for the in vivo experiments was taken from the development of a syngeneic and immunocompetent mouse model of B-ALL (145) from the Sadelain laboratory at MSKCC. They isolated malignant progenitor B cells from a lymph node from an E μ -myc C57BL/6 transgenic mouse with progressive disease. The isolated cells were cultured until transformation and have an immunophenotype and gene expression profile that resembles B-ALL. These transformed cells are then injected intravenously into WT C57BL/6 mice and they die 2-4 weeks after AT of BM failure due to ALL infiltration. In mice treated with their CD19-CD28 CAR, they received lymphodepleting conditioning chemotherapy with IP cyclophosphamide, the dose of which they modelled as they also did for the cell dose. The CD19-CD28 CAR I obtained from the NCI has been tested on WT immunocompetent mice with lymphoma but these mice received an immunosuppressive 5 Gy of total body irradiation (TBI) prior to the injection of lymphoma. They then received retrovirally transduced syngeneic CD19-CD28 CAR T cells and demonstrated efficacy that was dependent on the TBI for CAR T cell activity (146). There is no published data in CLL defining how to test CAR function using an immunocompetent mouse model such as TCL1 in CLL. Therefore, in this chapter, I describe the setup of an in vivo model of syngeneic CD19 CAR T cells in an immunocompetent mouse model of CLL.

7.2 Objectives

- To establish the AT TCL1 mouse model as an immunocompetent mouse model in which to study CAR T cell function in CLL.
- To study the efficacy of CAR T cells derived from WT T cells in a limited number of mice, comparing the NCI CD19-CD28 and MSK CD19-41BB-GFP CAR plasmids to optimize experimental conditions.
- Confirm the phenotype of CAR T cells derived from normal/WT and CLL/AT T cells prior to using in vivo.
- Compare CD19-CD28 and CD19-41BB CAR efficacy when those CARs are derived from WT or AT T cells in AT TCL1 CLL.
- Compare the CLL load and T cell phenotype of the PB, spleen and BM of mice treated with CAR T cells derived from WT and AT T cells, to see if CAR T cells can reverse the expected CLL T cell phenotype and treat CLL.

7.3 Materials and methods

To establish the in vivo conditions an exploratory experiment was first carried out using CAR T cells derived from WT T cells transduced only with either the CD19-CD28 and CD19-41BB-GFP CAR. Initially, nine mice received 13×10^6 CLL B cells by AT and one aged matched male control from the same litter had no AT so as to be able to compare phenotype of processed organs. By week 2 the mice had low level CD5⁺CD19⁺ engraftment and were injected with CAR T cells at week 3. I determined the cyclophosphamide and cell doses from the mid range as to that modelled by the Sadelain group in an immunocompetent model of ALL (145). All mice tolerated cyclophosphamide dosing without signs of ill health. Mice had regular bleeds until week 9 when they were culled and their PB, spleen and BM processed and analysed. The regular bleeds identified CD5⁺CD19⁺ CLL, normal B cells, T cell subsets and post CAR T injection looked for CAR⁺ T cells.

Following this optimization experiment, it was then repeated with CAR T cells derived from both normal/WT and CLL/AT T cells in much larger numbers of mice. For the second experiment 48 mice were injected with 14×10^6 CLL B cells by AT and again after confirming CLL engraftment at week 2, CAR T cells were injected at week 3. Cyclophosphamide dosing remained unchanged. Mice again had regular tail vein bleeds until week 9 when they were culled and PB, spleen and BM processed. The regular bleeds identified $CD5^+CD19^+$ CLL, normal B cells, T cell subsets and post CAR T injection looked for CAR^+ T cells. Mice were weighed throughout the experiment and the spleen weight was measured when mice were culled.

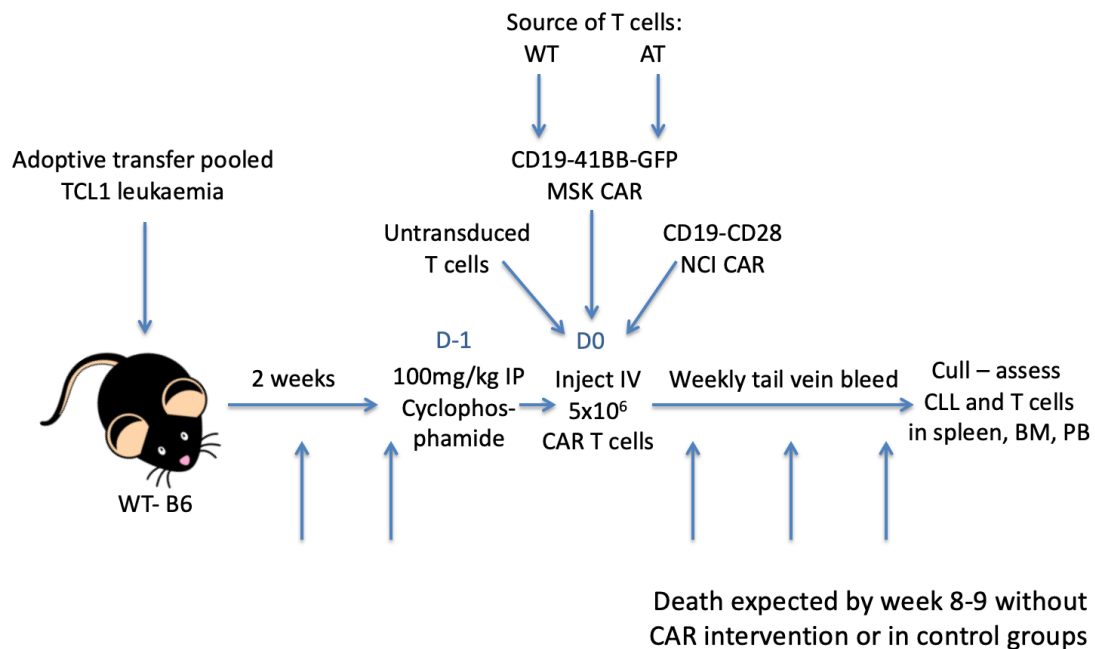


Figure 7.1: In vivo experimental plan to deliver CAR T cells from different T cell sources to the AT TCL1 mouse model. PB bleeds prior to CAR T cell infusion determined $CD5^+CD19^+$ load but PB bleeds afterwards looked for CAR^+ T cells.

7.4 Results – In vivo optimization

7.4.1 CAR T cell phenotype

For the first optimization experiment, I prepared 18×10^6 WT T cells as a single cell suspension obtained from genotype confirmed WT colony mice. These were activated

for 24h prior to being transduced by spinoculation on two consecutive days as previously described. CAR T cells were cultured for four days then harvested and debudded and mice which had received D-1 IP cyclophosphamide were injected between 4.7-5.1 x10⁶ total T cell each. There were three groups, mice treated with CD19-CD28, CD19-41BB both derived from WT T cells and a control group injected with untransduced T cells. Cell dose was determined as a total T cell dose, the CAR⁺ T cell dose corrected for transduction efficiency and subset is shown in table 1. Basic CAR phenotype demonstrated that CD19-CD28 and CD19-41BB CAR T cells were approximately 1:1 CD4: CD8 by flow immediately before being injected. CD4 and CD8 transduction efficiency was determined separately as per Table 7.1.

Subset	CD19-41BB-GFP		CD19-CD28	
	GFP ⁺ %	Cell dose (x10 ⁶)	Fab ⁺ %	Cell dose (x10 ⁶)
CD4 ⁺	40.3	1.0	47.1	1.29
CD8 ⁺	29.7	0.76	41.7	1.15

Table 7.1: Cell dose by T cell subset corrected by transduction efficiency.

It is unclear when determining cell dose if it is best to give an equal number of total T cells across groups, or correct for transduction efficiency or the number of transduced T cells in a specific T cell subset. However, as this was an exploratory optimization experiment I gave a similar total T cell dose and looked for trends in the other factors. Of note, whilst these cell dose numbers are similar to described in published data in animal models, these cell doses would be equivalent to at least 40 x10⁶ CAR⁺ T cells/kg if you compare the cell dose per kilogram used in the ZUMA-1 study, which is much higher than those doses given in the licensed product. For example, axi-cel cell dose is 1-2 x10⁶ CAR⁺ T cells/kg for lymphoma.

7.4.2 AT progress

At the first tail vein bleed post CAR T cell injection at week 4.4 or D+10 all the mice treated with the CD19-CD28 CAR had no detectable CLL or normal B cells by PB flow cytometry. For the mice treated with CD19-41BB 1/3 had no B cells and the other two had low level detectable disease. Subsequently, the mice were bled regularly and the progression of their PB CLL is shown in figure 7.2. The CD19-CD28 treated mice all remained in remission until week 9 when one mouse relapsed which was also evident in the spleen and bone marrow. The one initially responding mouse that received CD19-41BB remained in remission but the other two mice rapidly progressed and like the control mice that received untransduced T cells needed to be pre-emptively culled at week 9. All mice were therefore culled at week 9 for phenotypic comparison of T cells and assessment of CLL load in all organs.

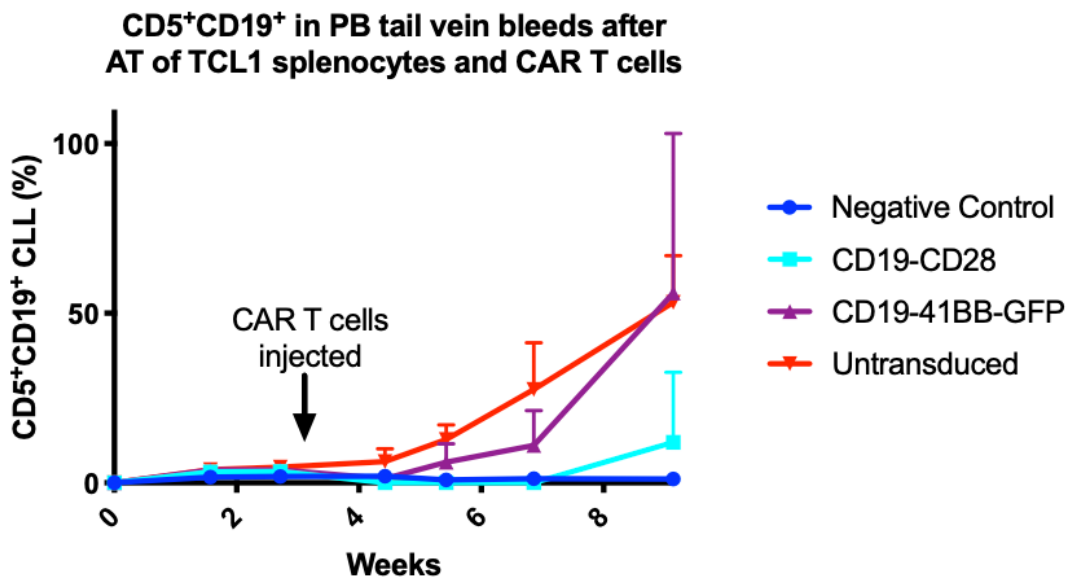


Figure 7.2: CD5⁺CD19⁺% in the peripheral blood of DAPI-, viable mononuclear cells following red cell lysis obtained by tail vein bleed by week after each mouse received AT of 13×10^6 CLL splenocytes and were treated with $\sim 5 \times 10^6$ T cells of which $\sim 2 \times 10^6$ were different CAR T cells or were untransduced T cells. Within groups mice (x3 mice in each CAR group, x1 mouse negative control) receiving CD19-CD28 and CD19-41BB-GFP were injected with split pooled cell doses of subsets defined in table 7.1.

The mice were weighed regularly and observed to establish signs of ill health post AT or CAR T cell injection. As per the project license significant weight loss would require animals to be pre-emptively culled. One control mouse that received untransduced T cells was culled at week 7 due to showing signs of ill health but overall all the mice put on weight through the experiment. This mouse had a very large spleen and undoubtedly was sick due to progressive disease. All mice that received active CAR T cells were intensely monitored for the first week post CAR T cell injection but none showed obvious acute signs of ill health immediately after CAR T cells as CRS would be theoretically possible in this model. All mice who progressed or relapsed did so with CD19⁺ disease. Figure 7.3 shows progression of weight for individual mice through this experiment. Mice that responded all demonstrated loss of both normal and malignant CD19⁺ B cells (figure 7.4) whilst mice treated with untransduced T cells have CD5⁺CD19⁺ disease.

Weight of mice following adoptive transfer of TCL1 leukaemia and CAR T cells

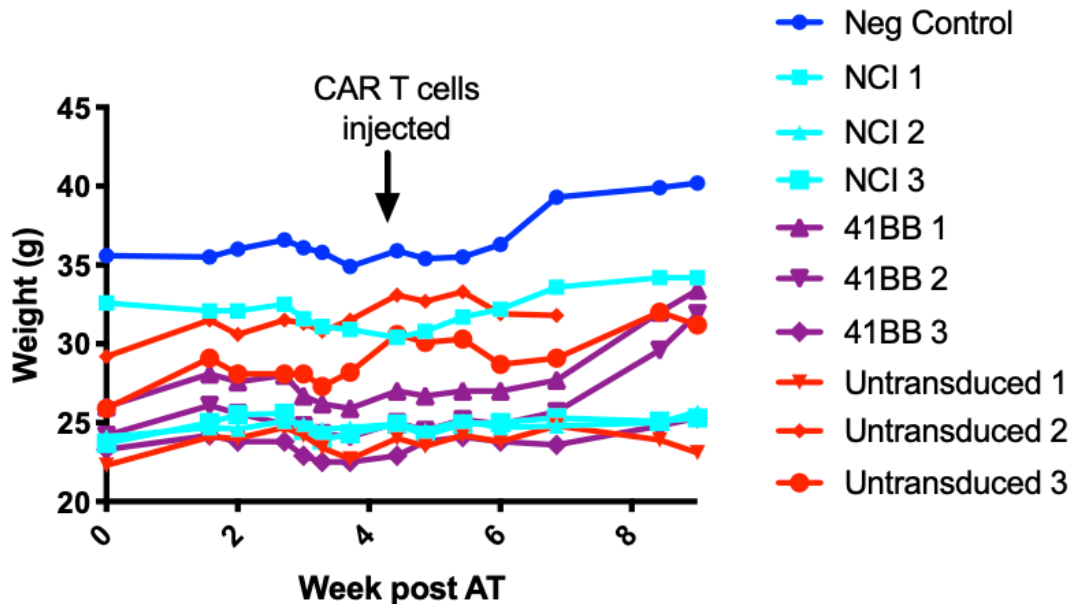


Figure 7.3: Individual progression of mouse weights (grams) after first AT of 13×10^6 CLL splenocytes and then treatment with $\sim 5 \times 10^6$ T cells of which $\sim 2 \times 10^6$ were different CAR T cells or were untransduced T cells (note mixture of sexes used).

Peripheral blood, mononuclear, lymphocyte gate, exclude doublets, DAPI negative viable:

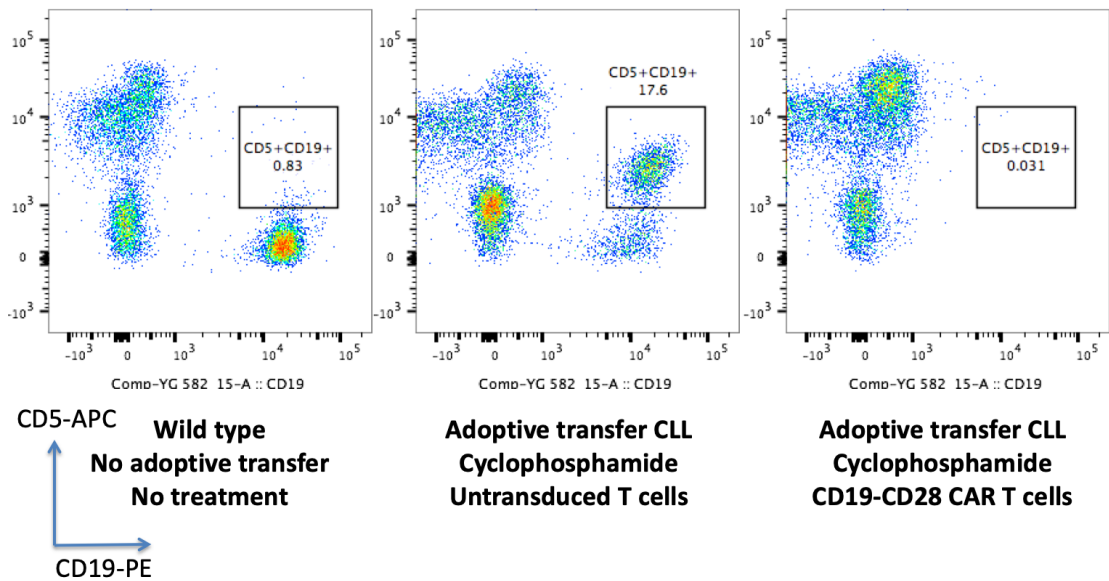


Figure 7.4: Flow plots demonstrating loss of both normal ($CD5^-CD19^+$) and malignant B cells ($CD5^+CD19^+$) in mice responding to CD19-CD28 CAR T cells and progressive $CD5^+CD19^+$ with normal $CD19^+$ B cells in mice treated with untransduced T cells. DAPI-, viable, mononuclear cells gated with 10,000 events recorded.

At week 9, all mice were culled and their spleens and BM harvested. For purposes of analysis the CD19-41BB group was split into mice 1-2 which did not respond and mouse 3 which did respond. Figure 7.5-8 demonstrates their $CD5^+CD19^+$ disease by organ, spleen weight, CD4: CD8 ratio and PD-1+ expression in specific organs and T cell subsets all at week 9. It shows the CD19-CD28 CAR can clear detectable disease in the PB, spleen and BM by W9 (figure 7.5), with equivalent spleen weights of mice responding to CAR T cells to age matched controls (figure 7.6). Further, in the spleen and PB, responding mice normalize CD4: CD8 ratios (figure 7.7) and PD-1⁺ expression (figure 7.8) compared to aged match controls. All relapsing mice relapsed with $CD5^+CD19^+$ disease and all mice with an ongoing response had loss of normal $CD19^+$ B cells in all organs.

CD5⁺CD19⁺ disease by organ at W9

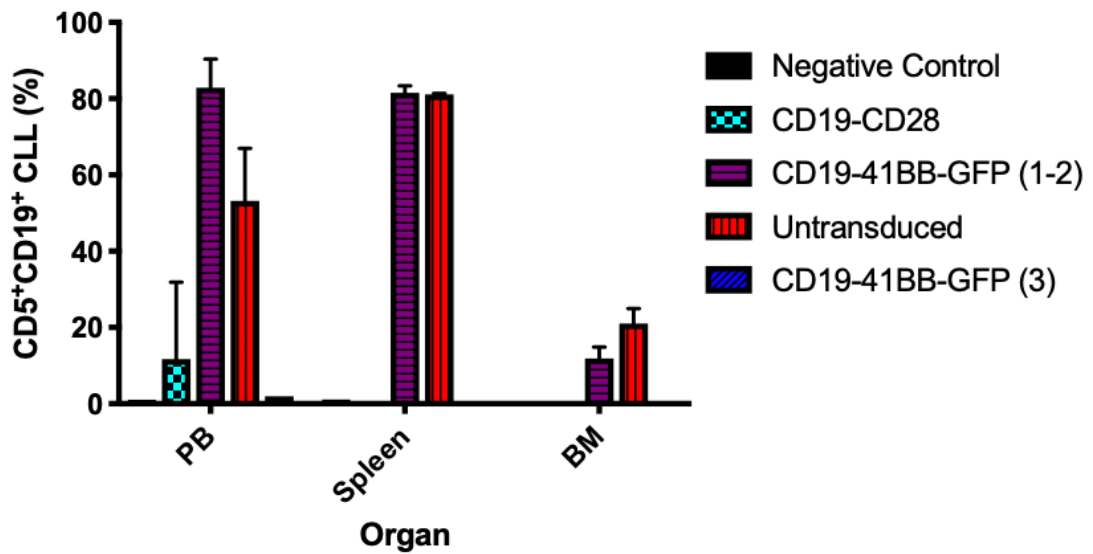


Figure 7.5: CD5⁺CD19⁺% of DAPI⁻, viable mononuclear cells by organ at week 9 in 10 mice treated with different CAR T cells showing clearance of disease with CD19-CD28 (3 mice) and CD19-41BB (mouse 1 or 3) CAR or no response to untransduced T cells (3 mice). Negative control mouse did not receive AT of CLL (1 mouse).

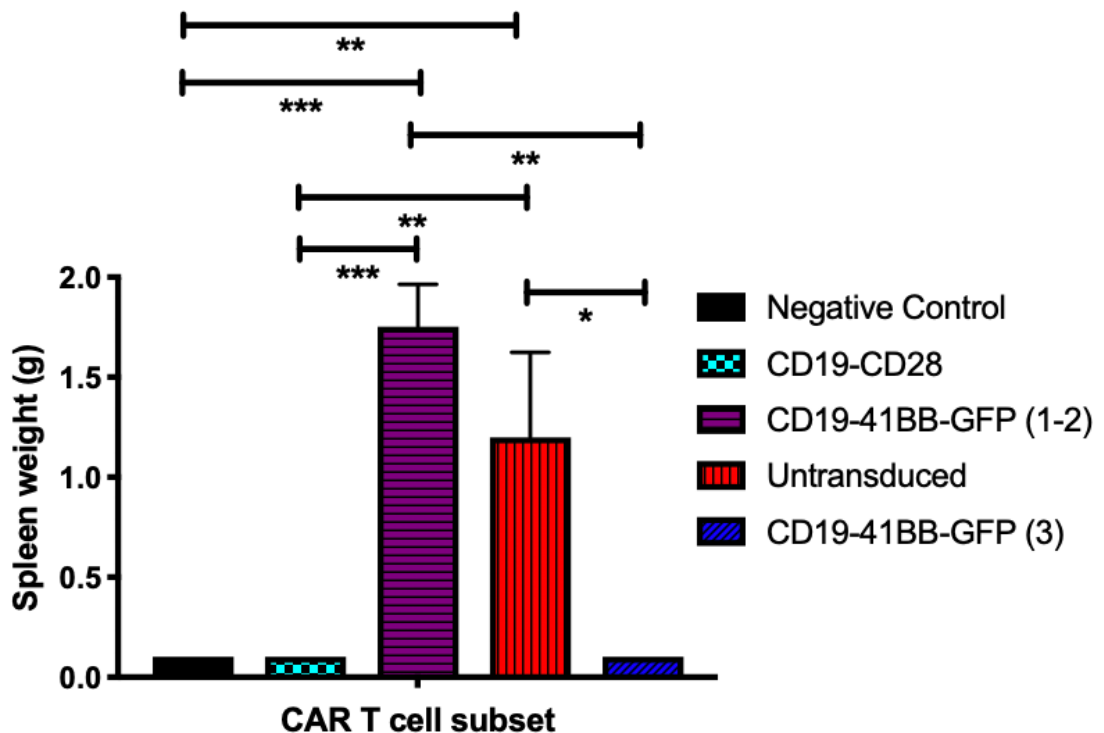


Figure 7.6: Weights of spleen of 10 mice culled at week 9 treated with different CAR T cells with significant differences (* $P < 0.05$, ** $P < 0.01$, *** $P < 0.001$). CD19-41BB CAR group split into non-responding (mouse 1-2) and responding (mouse 3).

CD4: CD8 ratio by organ at W9

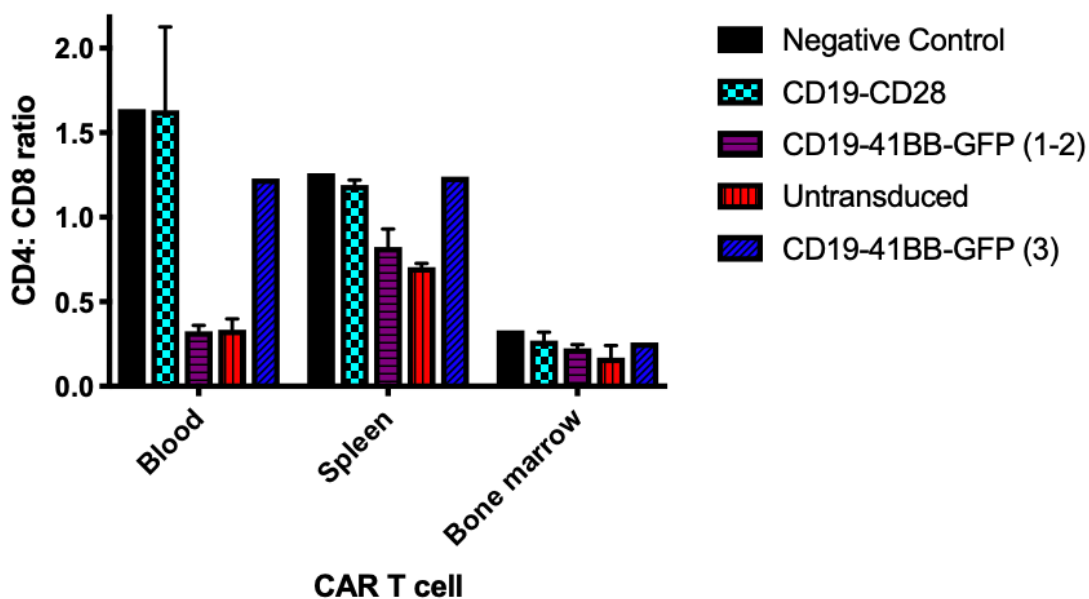


Figure 7.7: CD4: CD8 ratio of all T cells by organ in 10 mice culled at week 9 treated with different CAR T cells. CD19-41BB CAR group split into non-responding (mouse 1-2) and responding (mouse 3), CD19-CD28 and untransduced T cells treated 3 mice each.

PD-1⁺ in T cell subsets by organ at W9

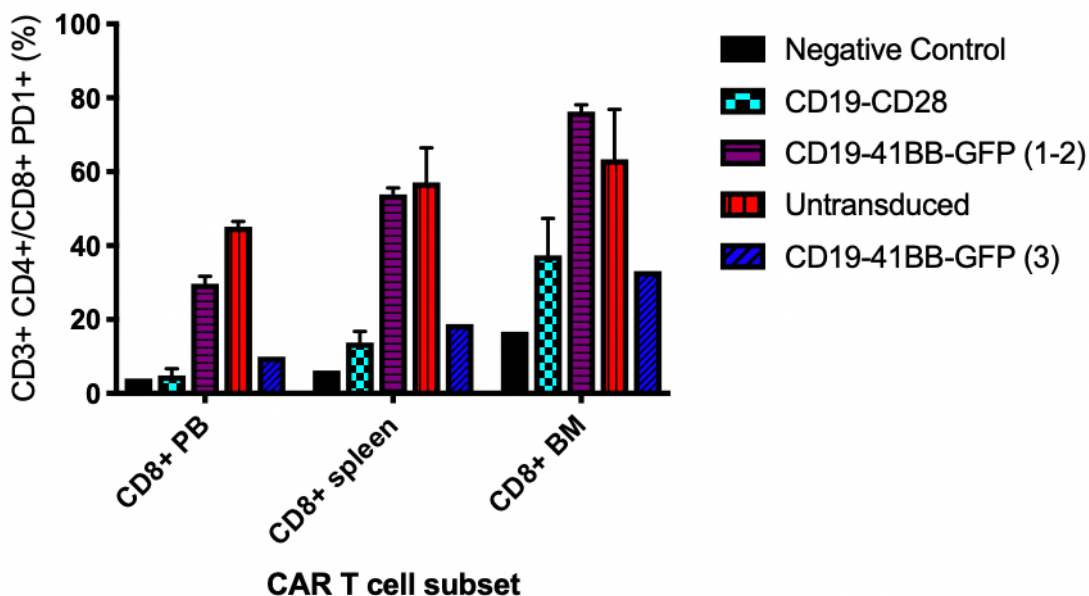


Figure 7.8: PD-1⁺ expression of CD3⁺CD8⁺ T cells by organ when culled at week 9 after treatment with different CAR T cells. CD19-41BB CAR group split into non-responding (mouse 1-2) and responding (mouse 3), CD19-CD28 and untransduced T cells treated 3 mice each.

7.5 Results

7.5.1 CAR T cell phenotype

My first optimization in vivo experiment had demonstrated the efficacy of the CD19-CD28 CAR and partial efficacy of CD19-41BB CAR derived from WT/normal T cells, so the same experimental plan and methods were used to repeat this experiment in a larger number of mice, but this time deriving CAR T cells from both WT/normal and AT/CLL T cells. The groups to be studied in this experiment are as below (figure 7.9).

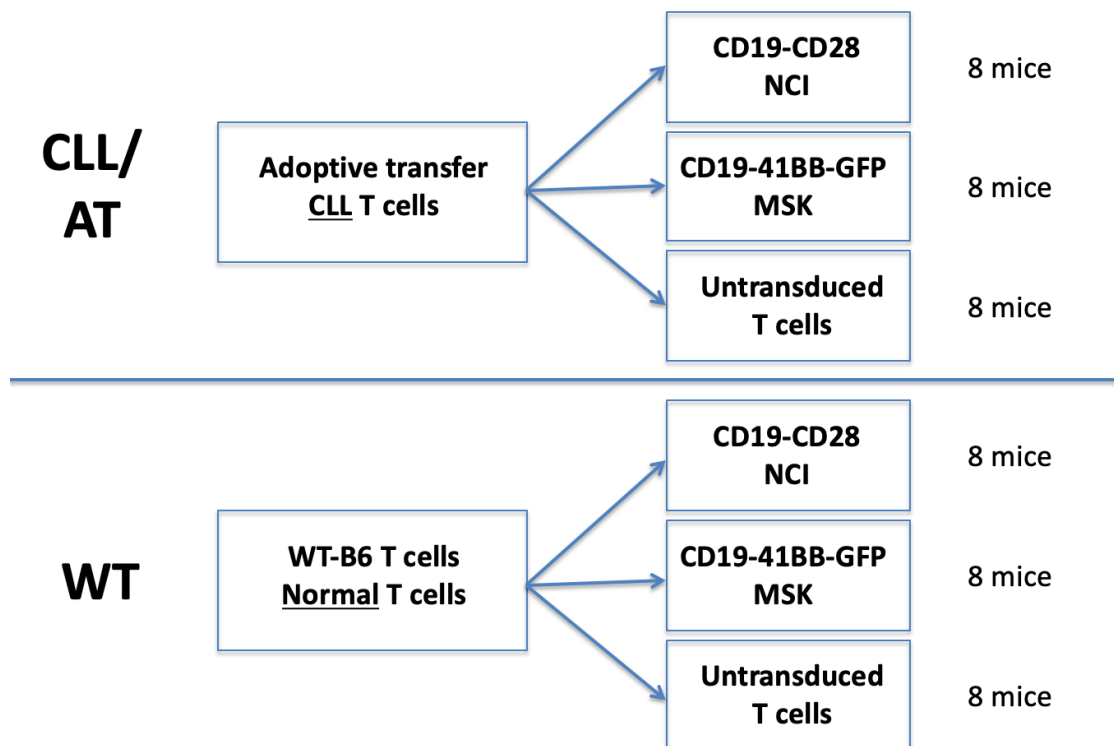


Figure 7.9: Experimental groups for first in vivo comparison of CD19-CD28 and CD19-41BB CAR derived from normal/WT and CLL/AT T cells.

Prior to commencing the main part of the experiment, I took transgenic mouse CLL splenocytes from our tissue bank and injected five male mice with 40×10^6 enriched CLL/B cells by AT. These mice were the source of AT/CLL T cells, and were monitored as

previously described with PB $CD5^+CD19^+$ load. They were culled at week 6, when they had high CLL and one spleen was used from which to enrich T cells to make CAR T cells. For the WT T cells six aged matched littermates were used to pool their spleens to get sufficient T cells. The last PB CLL load prior to these mice being culled to compare the extent of CLL WT and AT T cells were exposed to is shown in figure 7.10.

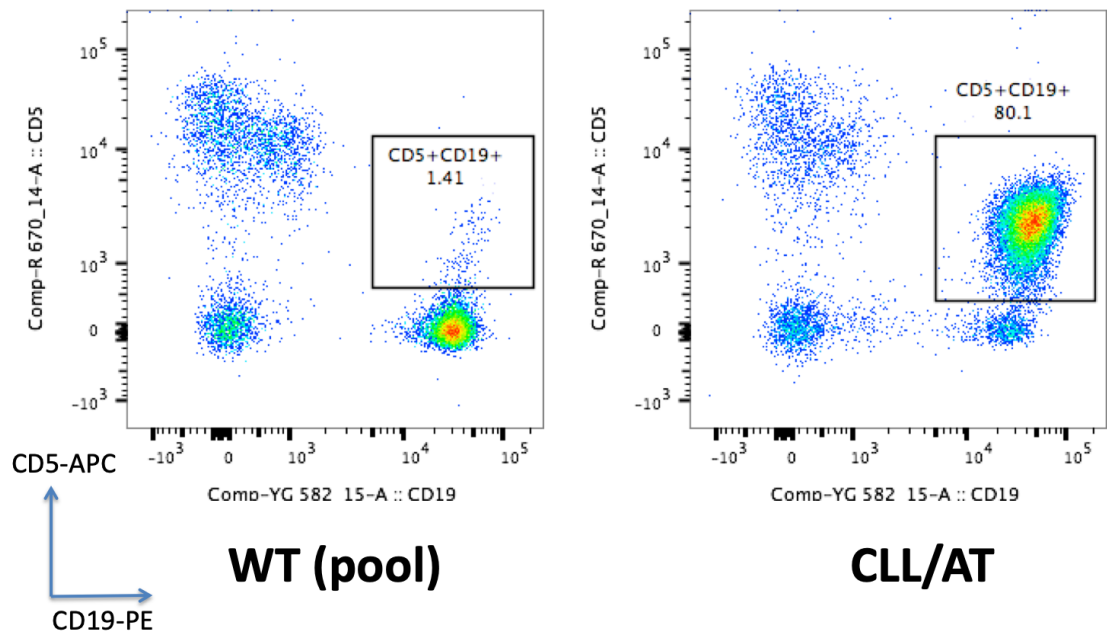


Figure 7.10: $CD5^+CD19^+$ or CLL load in PB (post red cell lysis) prior to mice being culled and the T cell enrichment of their spleens to make CAR T cells. DAPI-, viable mononuclear, 10,000 events recorded.

For each experimental group 18×10^6 enriched T splenocytes were activated for 24 hours prior to being transduced with retroviral supernatant from either SFGm19BBmZGFP (CD19-41BB-GFP) or MSGV1D328Z1.3mut (CD19-CD28) by spinoculation on two consecutive days as previously described. CAR T cells were cultured for four days in total then harvested and debeaded. Cell counts were taken daily except on day 2 as this was prior to the second transduction. Proliferation of T cells by group is compared in figure 7.11, showing that WT T cells proliferate after transduction more readily than T cells derived from AT mice. There seemed to be no difference in this proliferation within groups when comparing T cells transduced with

the two different CARs. As per previous experiments day 4 seemed the optimum day to harvest T cells from culture to prepare for in vivo experiments and mouse injections.

Total T cell proliferation during CAR T cell production

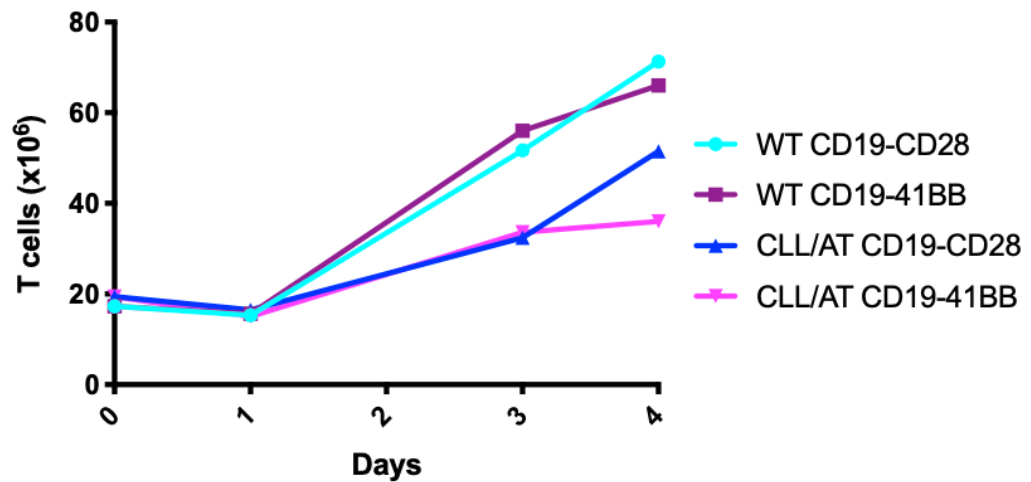


Figure 7.11: Total T cell count ($\times 10^6$ cells) in culture from activation of T cells on day 0 using CD3/CD28 beads and IL2, transduction on day 1-2 and expansion from day 3 onwards determined by an automated dual fluorescence (acridine orange/propidium iodide stain) haemocytometer (Logos Biosystems, South Korea) by source of T cells splenocytes, WT or WT mice after AT of CLL transduced with either the retroviral supernatant using the CD19-CD28 or CD19-41BB plasmid.

After harvesting the CAR T cells from cell culture they were phenotyped prior to injecting into the mice. Cell dose was broadly matched across experimental groups in terms of total T cells, with 6-8 $\times 10^6$ /mouse total T cells (or untransduced T cells) being injected. However, this approach resulted in different cell doses of CAR⁺ T cells in terms of different T cell subsets as the phenotype and transduction efficiency of normal and AT T cells is different. Table 7.2 further characterizes the CAR T cell doses in terms of subsets corrected for transduction efficiency.

CAR	T cell dose x10 ⁶ /mouse	Transduction efficiency (%)		CAR ⁺ cell dose/mouse x10 ⁶	
		CD4	CD8	CD4	CD8
WT CD19-CD28	8.9	27%	27.5%	1.0	1.3
AT CD19-CD28	8.6	52%	5.4%	0.2	0.4
WT CD19-41BB	8.3	20.9%	19.7%	0.7	0.9
AT CD19-41BB	6.1	46.8%	6.4%	0.9	0.3

Table 7.2: CAR cell dose by T cell subset at the end of the 4 day expansion correcting total T cell dose given to each group by transduction efficiency in CD4⁺ and CD8⁺ subsets.

CAR T cells derived from WT and AT T cells exhibit different phenotypes. WT CAR T cells proliferate more readily in culture and exhibit higher transduction efficiencies in the CD8 subset although CD4 transduction is preserved. Following activation and transduction WT CAR T cells have a CD4: CD8 ratio of 1:1 whilst those from AT are heavily skewed to CD8. In both groups >90% T cells are CD44⁺ indicating antigen experience. PD-1⁺ expression in both CD4 and CD8 subsets is significantly higher in AT compared to WT CAR T cells. Figures 7.12-7.14 demonstrate the key phenotypic differences on the fourth day of cell culture comparing CAR T cells derived from WT or AT T cells using both the CD19-CD28 and CD19-41BB plasmids.

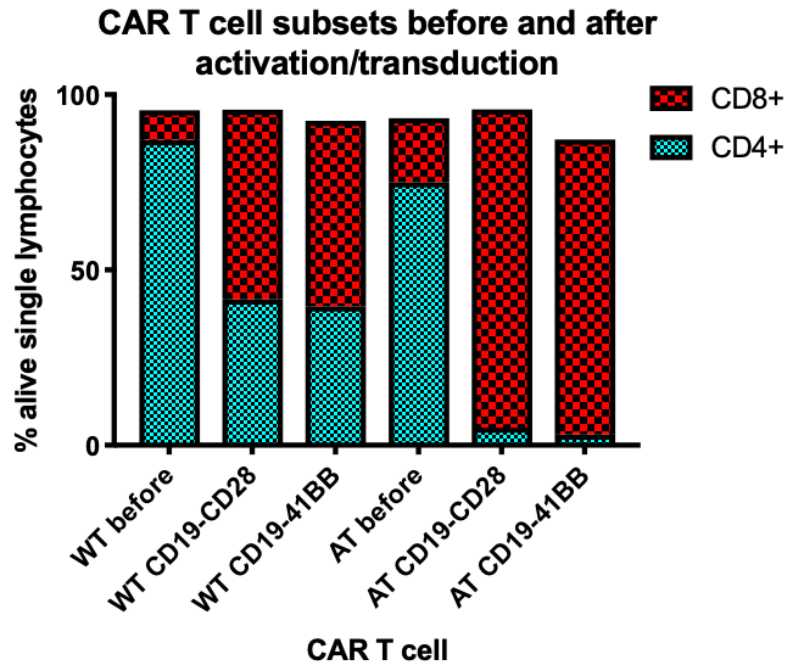


Figure 7.12: CD4: CD8 ratio as a proportion of DAPI-, viable single lymphocytes before and after activation and transduction of T cells by T cell source and using the different plasmids CD19-CD28 and CD19-41BB.

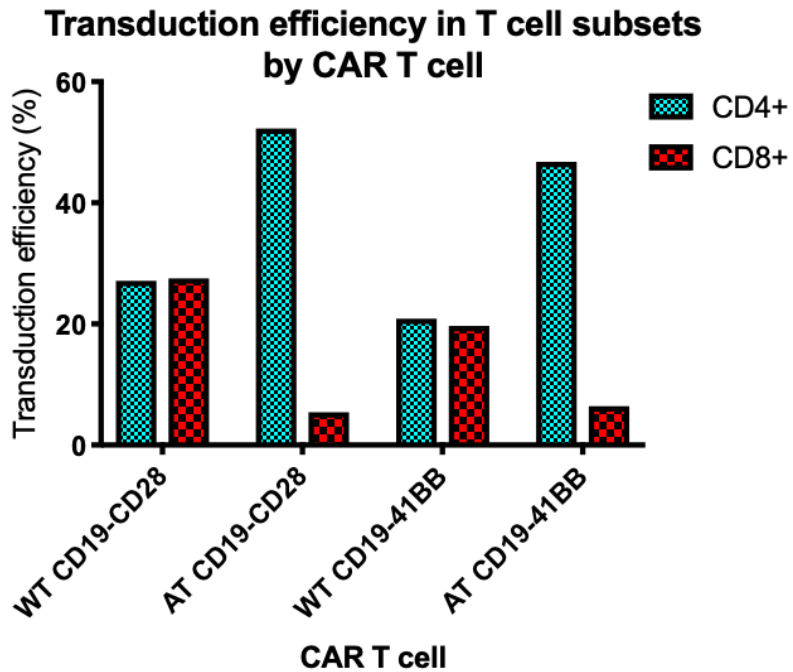


Figure 7.13: Transduction efficiency (GFP⁺% or Fab⁺%) as a proportion of DAPI-, viable single lymphocytes in CD4⁺ and CD8⁺ T cells after four days of cell culture following transduction with CD19-CD28 or CD19-41BB retroviral supernatant.

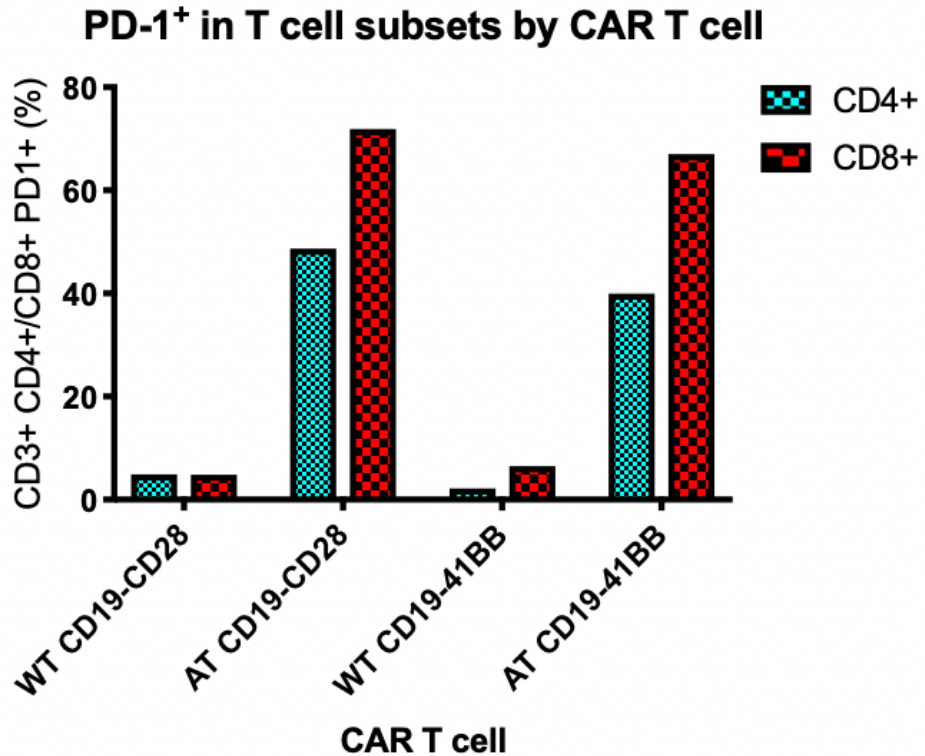


Figure 7.14: PD-1⁺ expression of DAPI⁻, viable mononuclear CD3⁺CD4⁺ or CD8⁺ T cells after 4 days of culture including activation and transduction with CD19-CD28 or CD19-41BB retroviral supernatant.

7.5.2 AT progress

Forty-eight immunocompetent WT mice each received AT of pooled 14×10^6 CLL cells from fully leukemic TCL1 mice from the same background from our tissue bank. All treatment groups were composed of half male and half female mice. CLL engraftment was confirmed at week 2 and CAR T cells injected at week 3. At the first tail vein bleed at week 4 post AT or D+7 post CAR T cells mice treated with the CD19-41BB CAR derived from WT and AT T cells or untransduced T cells did not respond. There was no evidence of CAR expansion i.e. CD3⁺GFP⁺ expression in the PB of the mice given the CD19-41BB CAR. 100% of mice treated with CD19-CD28 CAR derived from WT T cells had a complete response with loss of CLL and normal B cells compared to 50% of mice treated with CD19-CD28 derived from AT T cells. Mice were bled weekly to every two weeks to assess CLL load and T cell subsets and were culled when they appeared sick or peripheral blood (PB) CLL > 70%. Progression of PB CLL from weeks 0-9 is shown in

figure 7.15. All mice that progressed did so with CD19⁺ disease and all mice with an ongoing CD5⁺CD19⁺ response had no detectable normal CD19⁺ B cells indicative of ongoing CAR activity. Normal B cell aplasia is expected as a response to a persistent CAR T response as of course CD19 CAR T cells do not distinguish between normal and malignant B cells.

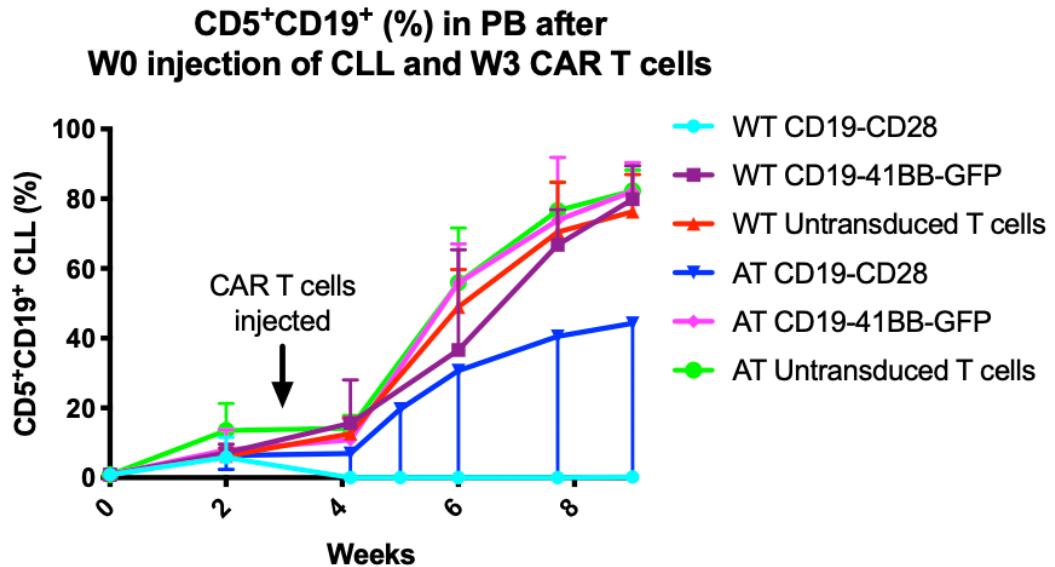


Figure 7.15: Percentage of DAPI-, viable mononuclear cells in PB that are CD5⁺CD19⁺ CLL post AT of CLL at week 0 and injection of IP cyclophosphamide and IV CAR T cells at week 3 separated by CAR treatment group.

In a subgroup analysis, of the 6 mice given the AT CD19-CD28 CAR, the 3 male mice all had an ongoing response and the three female mice relapsed in a similar fashion to the other non-responding groups (figure 7.16). This observation was not consistent in previous and subsequent experiments so could just be chance, but it would be an interesting observation if different CAR responses could be demonstrated according to the sex of mice.

**CD5⁺CD19⁺ (%) in PB after
W0 injection of CLL and W3 CAR T cells**

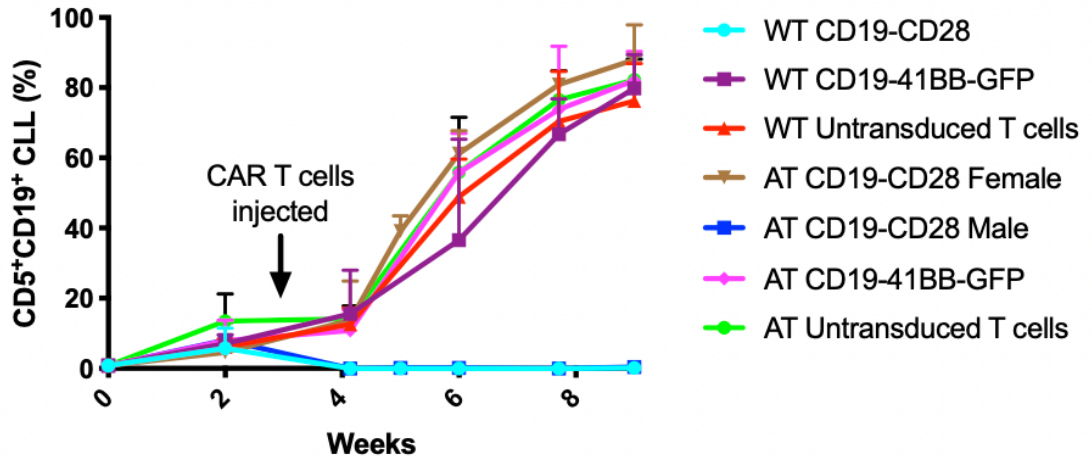


Figure 7.16: Percentage of DAPI-, viable mononuclear cells in PB that are CD5⁺CD19⁺ CLL post AT of CLL at week 0 and injection of IP cyclophosphamide and IV CAR T cells at week 3 by treatment group separating the AT CD19-CD28 treatment group by sex.

All non-responding mice were culled at week 9 due to progressive leukaemia as were control mice treated with untransduced T cells. Half of the responding mice were culled for phenotypic comparison at week 9 and the other half observed for survival analysis. All mice with an established response had a continued complete response for 31 weeks following CAR T cell injection when they were culled. Those mice that responded and culled at week 9 had equivalent spleen size (0.1g) to age matched WT mice controls whilst non-responding mice had significantly larger spleens (0.53-3g), shown in figure 7.17.

Spleen weight (grams) at week 9

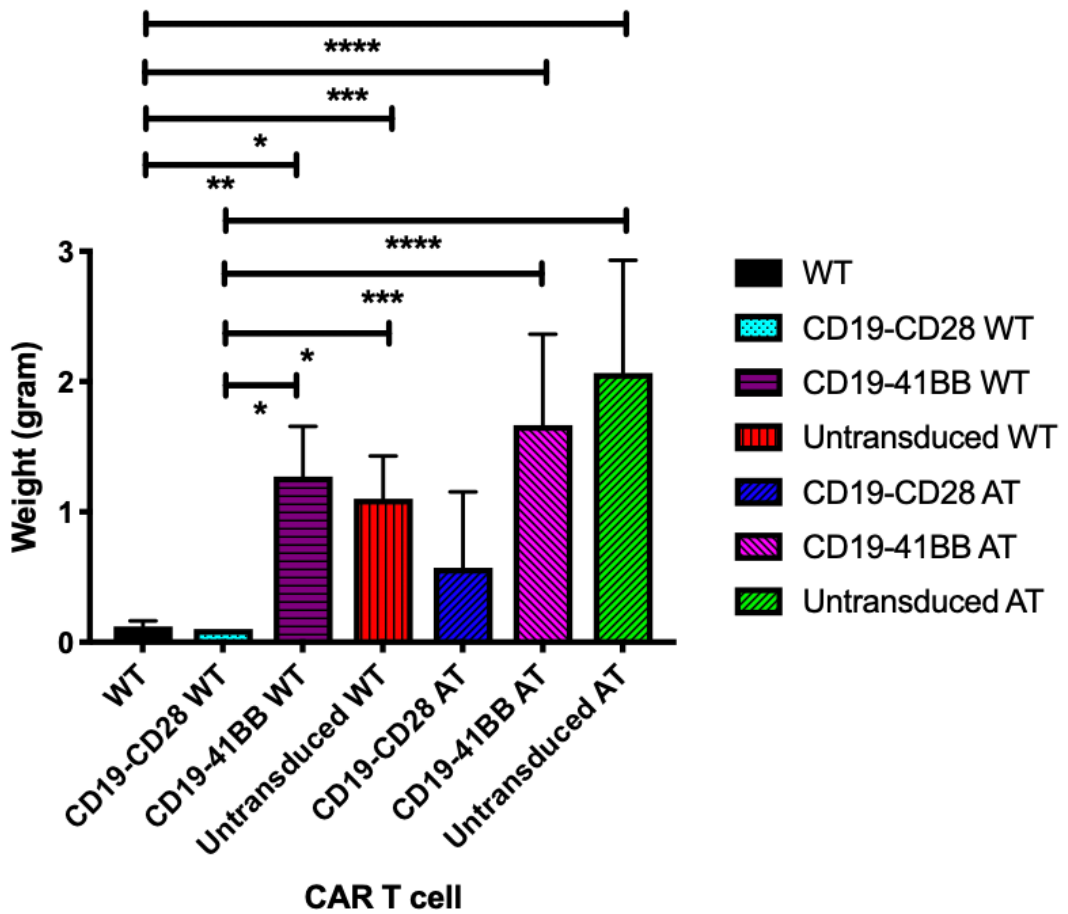


Figure 7.17: Spleen weight (grams) when mice are culled at week 9 after AT of CLL and treatment with CAR T cells derived from different sources of T cells and transduced with CD19-CD28 or CD19-41BB retroviral supernatant showing significant differences ($*P<0.05$, $**P<0.01$, $***P<0.001$, $****P<0.0001$).

What is less clearly illustrated by simply looking at the median or mean spleen weight is in the mice treated with CD19-CD28 CAR from AT T cells the response was dichotomous, in that these mice had either a complete and ongoing response or their disease accelerated at the same pace as for mice who received untransduced T cells. These explains the large error bars seen in this group in figure 7.15. The subgroup analysis reveals that it is the male mice that have responded and the female mice which relapse. This polar response is seen more clearly in figure 7.18, showing the level of CLL in the spleen at week 9, but a trend clearly demonstrated in PB and BM as well. Importantly, there is no difference between CLL in the spleen comparing mice

treated with CD19-CD28 derived from WT T cells but very significant differences between this group and all other groups which all had very high levels of CLL.

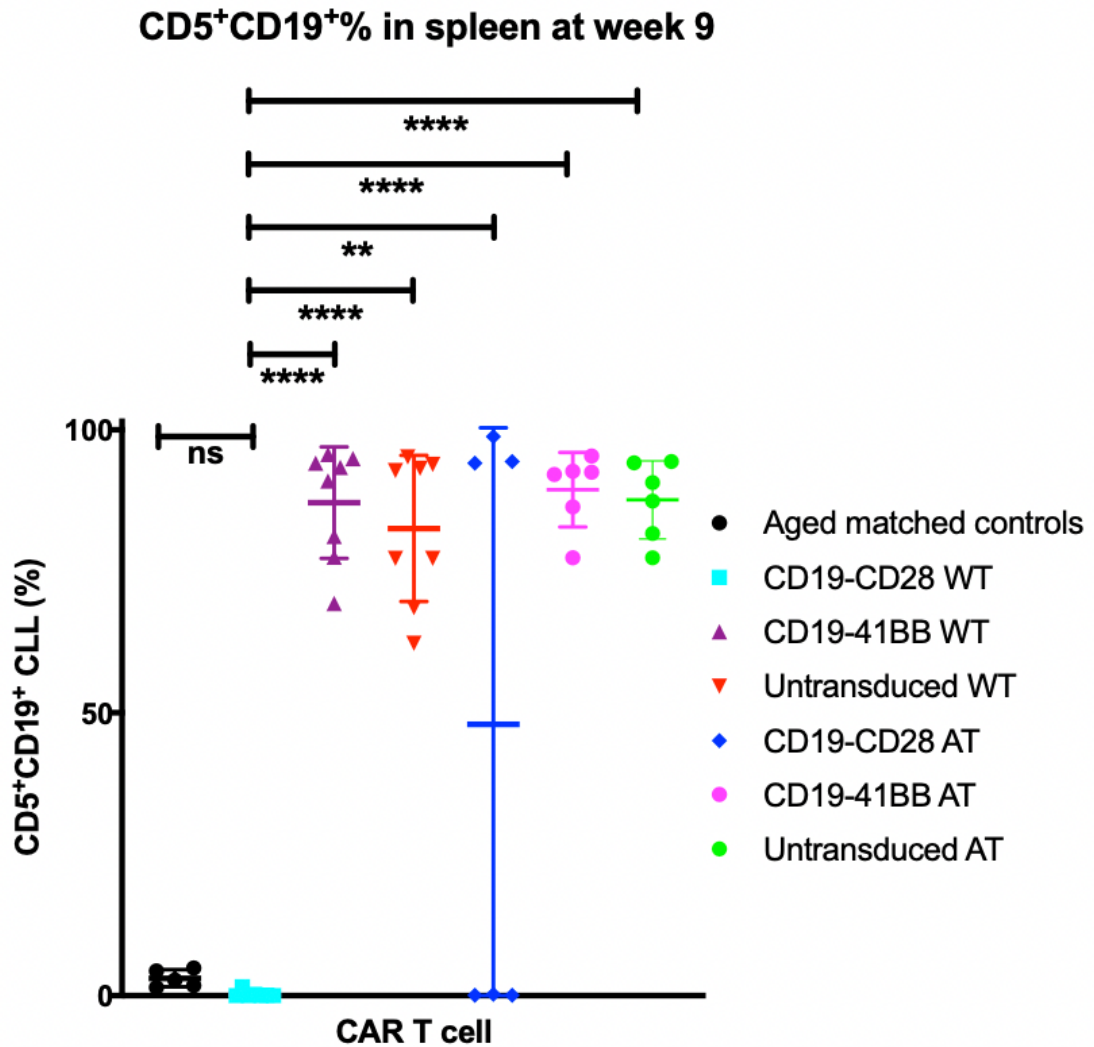


Figure 7.18: Percentage of DAPI⁻ viable, mononuclear splenocytes that are CD5⁺CD19⁺ when mice are culled at week 9 after AT of CLL and treatment with CAR T cells derived from different sources of T cells and transduced with CD19-CD28 or CD19-41BB retroviral supernatant also compared to aged matched controls showing significant differences (* $P < 0.05$, ** $P < 0.01$, *** $P < 0.001$, **** $P < 0.0001$).

CAR T cells were only detectable in significant numbers in the PB at D+7 post injection. Interestingly, for the responding mice from the WT and AT CD19-CD28 treated mice, the CAR⁺% of CD3⁺CD8⁺ T cells was much higher for those mice treated with an AT CAR (18.8-32.1%) than a WT CAR (1.6-6.7%). Of the mice that had a detectable expansion of

CAR⁺ T cells in the PB, for those treated with AT CD19-CD28 the CAR⁺ cells were mostly CD8⁺ T cells (all >67%), but the mice treated with WT CD19-CD28 had a range of CAR⁺ cell CD4: CD8 ratios (0.08-2.1). This may purely be a reflection of the starting population with skewing of CAR T cells derived from CLL T cells to CD8⁺, but it does seem that from the above results CAR T cells which expand from CLL T cells expand in greater numbers with a skew to CD8⁺ CAR T cells compared to WT CAR T cells in vivo. In the PB there was restoration of CD4: CD8 ratios in responding mice compared to leukaemic mice at week 9 (figure 7.19), but not in the spleen or BM.

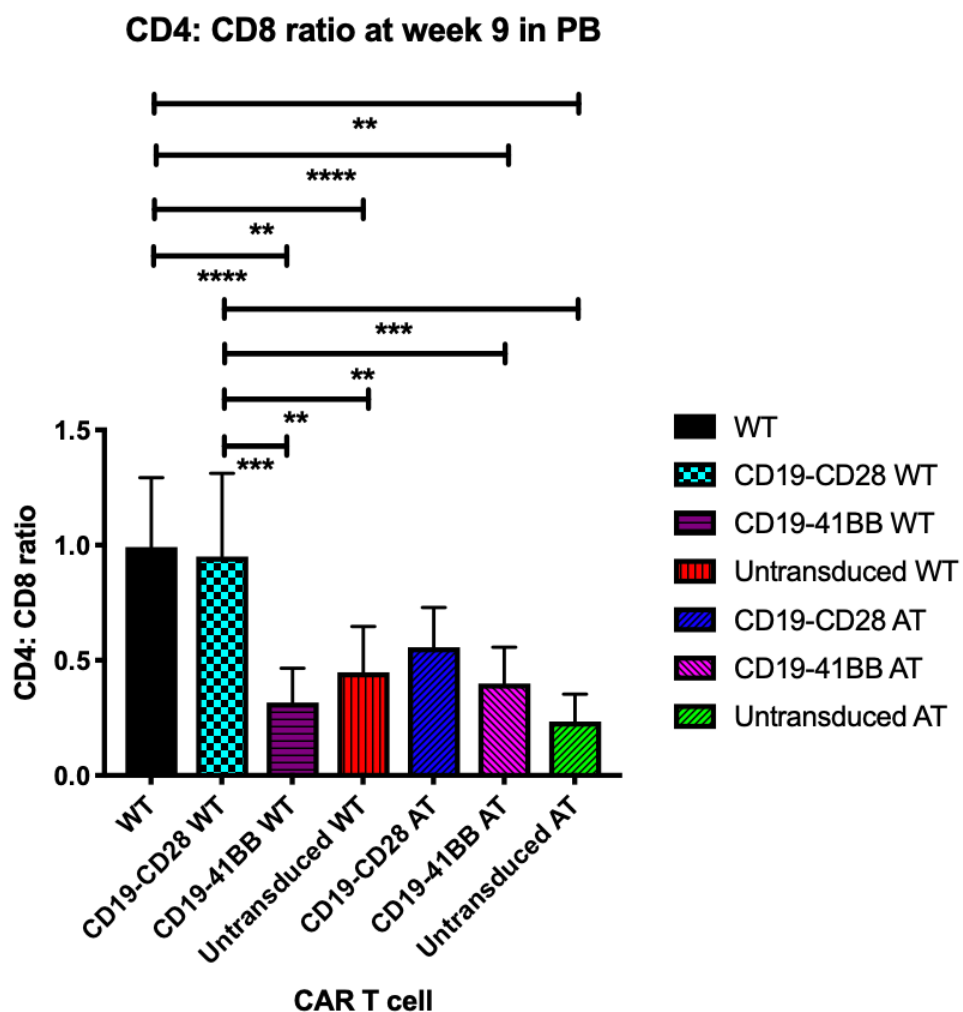


Figure 7.19: Ratio of DAPI⁻ viable, mononuclear splenocytes that are CD4⁺ and CD8⁺ when mice are culled at week 9 after AT of CLL and treatment with CAR T cells derived from different sources of T cells and transduced with CD19-CD28 or CD19-41BB retroviral supernatant also compared to aged matched controls showing significant differences (* $P < 0.05$, ** $P < 0.01$, *** $P < 0.001$, **** $P < 0.0001$).

PD-1 expression in the spleen and BM in CD3⁺CD8⁺ and CD4⁺ T cells normalised in responding mice compared to non-responding mice but not in the PB. Figure 7.20 shows PD-1⁺ expression in CD3⁺CD8⁺ T cells in the BM.

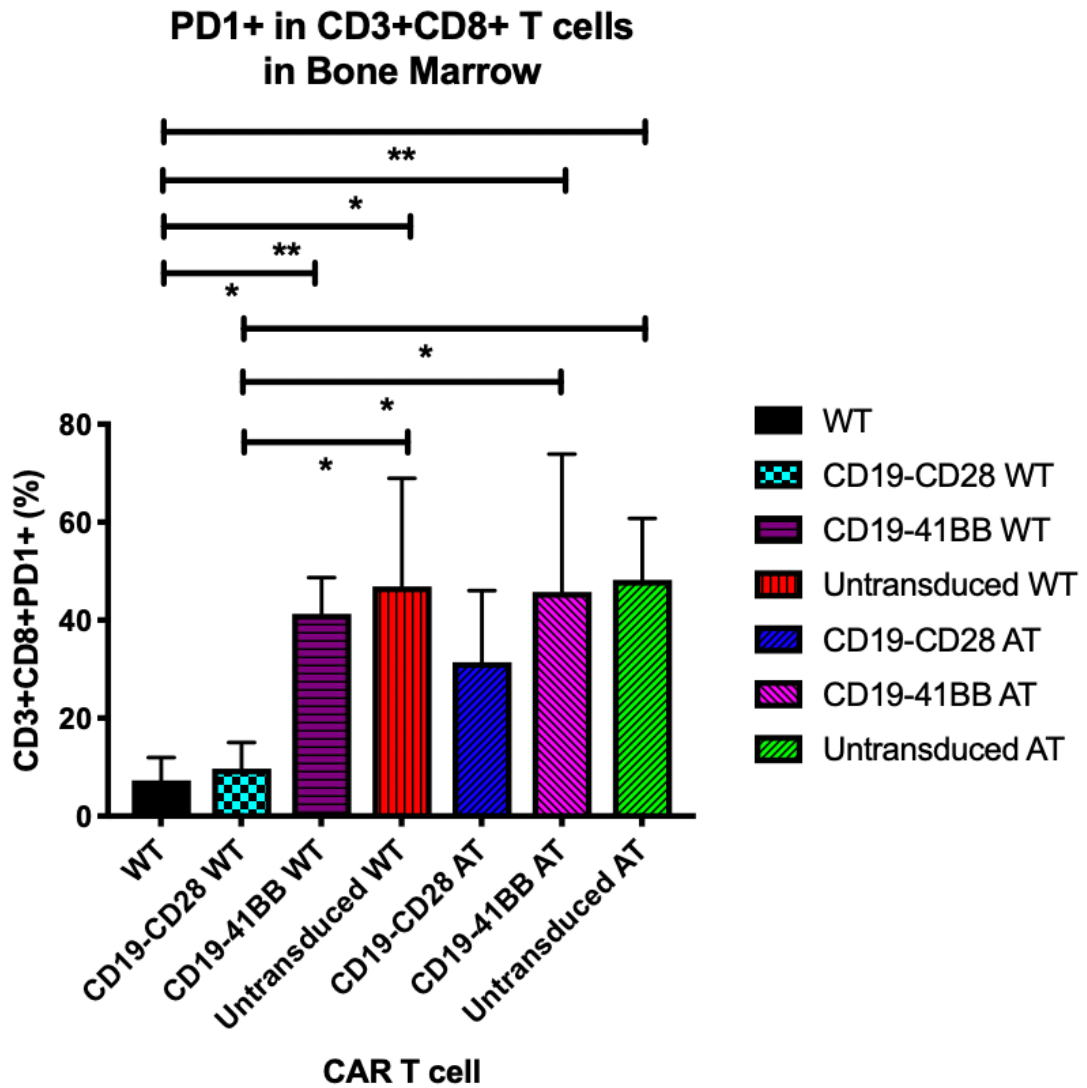


Figure 7.20: PD-1⁺% expression of DAPI⁻ viable, mononuclear CD3⁺CD8⁺ T cells in the bone marrow when mice are culled at week 9 after AT of CLL and treatment with CAR T cells derived from different sources of T cells and transduced with CD19-CD28 or CD19-41BB retroviral supernatant also compared to aged matched controls showing significant differences (**P*<0.05, ***P*<0.01, ****P*<0.001, *****P*<0.0001).

7.6 Discussion

These data demonstrate that the AT of TCL1 CLL into immunocompetent mice is a viable model in which to study in vivo CAR T cell function and the host immune response. This is itself a novel finding, most published CAR preclinical data using xenograft models in SCID or other types of immunosuppressed mice. Syngeneic CD19-CD28 CAR T cells engraft in this model when derived from both WT and AT T cells with maximum in vivo expansion of these CAR T cells occurring one week post their tail vein injection. There was no clinical evidence of CRS in these mice in this series of experiments. I did not measure cytokine levels in this experiment but I did attempt to do so in subsequent experiments. CD19-CD28 CAR T cells derived from WT T cells lead to a complete response in all of the mice but this response is markedly reduced if T cells exposed to CLL are used. The source of CLL T cells is a separate group of syngeneic mice which also had AT CLL for 6 weeks prior to being culled with high levels of CLL confirmed in the PB. It is interesting that T cells need to be exposed to CLL for such a short period before they establish functional differences which can lead to marked differences in CAR efficacy. Although our group has been reported widely on the functional defects in T cells in both humans (88, 94) and mice (89, 118) with CLL this is our first effort to extrapolate the effects of these functional defects to CAR T cells in terms of preclinical investigation. For those mice that did respond to either the AT or WT CAR T cells they achieved long term disease control in this model for up to 31 weeks. In mice that have an ongoing response I detected ongoing B cell aplasia, in terms of no normal CD19⁺ population in the PB so in this model an ongoing functional effect of CAR T cells seems to be important to maintain remission. However, ongoing B cell aplasia does not require a high percentage of CAR⁺ in the PB. After maximum CAR expansion at 1 week post injection of CAR T cells they are rapidly lost from the PB by D+21. This is whilst acknowledging that the primary secondary Fab⁺ antibody used to detect the CD19-CD28 CAR I would not consider accurate CAR⁺<1% in the PB because even when using the isotype control antibody I always found there is a degree of background staining <1% of DAPI⁻CD19⁻CD3⁺ cells.

In the first optimisation experiment there was one mouse that responded to the CD19-41BB CAR from WT T cells, but in the larger experiment no mice responded to this CAR, and I postulate that failure of the CD19-41BB CAR in vivo relates to rejection of the GFP construct. From this observation I do not imply that CD19-CD28 CAR would be better than CD19-41BB in humans, as there was clearly an issue with the CD19-41BB CAR T cell engrafting in this model.

The central hypothesis of my PhD is that the activity of CAR T cells in this model is related to the underlying T cell function, which is perhaps reflected in the differing phenotypes when deriving CAR T cells from WT or AT T cells. When you look at the CAR⁺ adjusted cell doses given to each group of mice, I do acknowledge that the CAR⁺ cell dose given to mice if derived from AT T cells in both CD4 and CD8⁺ subsets is much lower. However, given I started with the same number of WT or AT T cells to make each group of CAR T cells, and applied the same optimised manufacturing process to both groups of cells and an identical amount of virus, the resulting differing cell doses are a reflection of the poor proliferative capacity of AT T cells and also a reflection that they are much harder to transduce in the CD8⁺ subset.

Experiments described in chapter 6 also showed that AT CAR T cells are mostly of an effector T cell phenotype with complete loss of naïve T cells, whilst WT CAR T cells are a mixture of memory and effector T cells, which may be a further explanation for the differences in performance. These results, combined with further experiments in this chapter demonstrate the key phenotypic characteristics when CAR T cells are derived from normal or CLL T cells in table 7.3.

WT/normal CAR T cells	AT/CLL CAR T cells
Proliferation in culture ↑	Proliferation in culture ↓
CD4 ⁺ :CD8 ⁺ = 1	CD4 ⁺ ↓, CD8 ⁺ ↑
CD4 ⁺ =CD8 ⁺ transduction efficiency	CD8 ⁺ transduction ↓ CD4 ⁺ transduction preserved
PD-1 ⁺ low	PD-1 ⁺ high
CD44 ⁺ high	CD44 ⁺ high
CD3 ⁺ CD8 ⁺ memory	CD3 ⁺ CD8 ⁺ effector (loss of naïve)

Table 7.3: CAR characteristics post ex-vivo expansion by T cell source.

Beyond clearing CLL from all organs in this model, successful CAR treatment restores normal T cell subset ratios in the PB and normalises PD-1 expression of T cells in all organs. Mouse models afford the opportunity to model interventions which could improve CAR efficacy by altering the phenotype of cells to which the manufacturing process is applied. There are significant differences in PD-1 expression between WT and AT derived CAR T cells, which suggest strategies to repair exhausted T cells may improve the clinical response to CAR T cells in CLL. However, to do so will require the treatment of the mouse or indeed a patient after infusion of the CAR T cells to support the CAR T cell function. More simply, there are major differences in the basic phenotypes of CAR T cells when you derive them from different sources and apply the same manufacturing process to them. After the total cell dose has been corrected for CD4: CD8 ratio and transduction efficiency, it became clear it is difficult to expand CD8⁺CAR⁺ and CD4⁺CAR⁺ when the cell source is CLL T cells. However, when CAR T cells derived from CLL T cells do engraft, the initial expansion is mostly CD8⁺CAR⁺ cells, in comparison to the cell source being normal T cells when the initial CAR⁺ expansion is more balanced in CD4/CD8⁺ T cells. Most importantly, CLL T cells expand less well ex vivo, which has now been determined to be an important biomarker from in vivo

expansion after infusion in patients (206). The underlying explanations for why CLL T cells are not as readily transduced and proliferate in culture, most likely are the answers to how CAR T cell function can be improved in this disease, but are not answered by this series of experiments. Prior to understanding this more, simply requiring that CAR T cells are manufactured from specific T cell subsets and the optimisation of what combination of initial components produces the best outcomes, would be a worthwhile use of further preclinical testing using this model.

The observation that female mice do not respond to CD19-CD28 CAR T cells derived from CLL T cells whilst male mice do respond is interesting. Both sexes respond to CAR T cells from WT T cells, so this is not an absolute rule. If there is a genuine difference between how the sexes respond to CAR T cells in mice, and this could be extrapolated to humans, it certainly contradicts what was reported in the largest series of real world data of lymphoma patients treated with the CD19-CD28 CAR in humans (264). By univariate analysis females respond significantly better than males in terms of response at 3 months. However, this finding warrants further investigation.

8. In vivo modelling of CAR T cells with checkpoint blockade

8.1 Introduction

Having established a difference in efficacy of the CD19-CD28 CAR T cells when they are derived from normal/WT versus CLL/AT T cells, and confirmed the ability of CAR T cells to reverse an exhausted phenotype in the AT TCL1 CLL model in a time limited experiment, the next step was to test the model as a reflection of relapse risk. For this a much greater length of experiment would be required. A major objective of this PhD was to identify potential routes to improve CAR T cell function in CLL, given the lower response rates when CD19 CARs have been used in this disease in comparison to other lymphoid disorders. The use of combinations of CAR T cells with drug therapy is very much a research question, given no additional chemotherapy or small molecule inhibitors were permitted following CAR infusion in the major reported clinical trials (182, 185).

An immunocompetent mouse model is ideally placed to answer research questions about whether CAR T cell function can be improved in combination with immunomodulatory drugs as well as looking for new safety or toxicity signals. In solid tumours where PD-L1 is upregulated, PD-1⁺ cells undergoing exhaustion which is characterized by reduction of functional capacity, proliferation and cytotoxic activity (265). CAR T cells are also subject to inhibition of their cytotoxic and cytokine secretion upon repeated antigen encounter in vivo, for example by PD-L1 expression on tumour/leukaemia cells and therefore the administration of antibodies that block the PD-1/PD-L1 axis may lead to increased CAR T cell cytotoxicity (266). Preclinical data has supported this in animal models of other malignancies, for example a murine model of mesothelioma in which PD-1 blockade restored effector function of CAR T cells with a CD28 co-stimulatory domain (266). In a model testing CAR T cells directed at Her-2+ tumours, the addition of PD-1 antibodies reduced the growth of the Her-2+ tumours which correlated with an increase function of the CAR T cells (267). Interestingly, the combination led to a significant decrease in the number of MDSC in the

microenvironment. Myeloid cells that overexpress PD-L1 converted TBET⁺ T_H1 cells into FOXP3⁺ Treg in a xenograft model of GVHD (268), suggesting another mechanism by which this axis impairs immune responses.

Formal studies of combinations of checkpoint inhibitors are underway in clinical trials but an early case report in a patient was promising. A letter in 2017 described the use of the PD-1 antibody pembrolizumab with the CD19-41BB CAR in a patient with refractory DLBCL and progressive lymphoma post CAR T cells (249). Following pembrolizumab at day 26 after CAR T cell infusion the patient had a proliferation of CAR⁺ cells, with corresponding increase in cytokines particularly IL-6 and a reduction in CAR⁺ cells expressing PD-1. Most importantly, he had a significant and ongoing clinical response. Further, Fraietta et al. reported the varied frequencies of preinfusion CD8⁺CAR⁺ expressing PD-1, TIM-3 and LAG-3. Patients who subsequently had a CR, had a lower percentage of CAR⁺ cells with a PD-1⁺ phenotype, but this did not correlate with the percentages of CD8⁺ T cells expressing inhibitory receptors at the time of apheresis. To investigate further, all phenotypes associated with PD-1 expression were correlated with clinical outcome, and the infusion of high doses of CD27⁺PD-1⁻CD8⁺ was significantly associated with response, suggesting CAR T cells should be enriched for this population (206). If enriching preinfusion CAR T cells for a PD-1 negative population has a significant effect, then post infusion manipulation of this axis may also be important.

Work has previously been presented in abstract form on the high occurrence of PD-L1 on progression/relapse post CAR biopsies in the ZUMA-1 study in both CD19⁺ and CD19⁻ negative relapses (189) and the up-regulation of T cell activation, effector, chemokine and immune checkpoint genes (190). This led to ZUMA-6 which is currently active and investigating the combination of CD19-CD28 CAR T cells with the PD-L1 inhibitor atezolizumab, preliminary safety results of which have been reported in abstract form at ASH 2018 (251). Such an approach has demonstrated the BCMA CAR re-expansion using pembrolizumab in myeloma (252). Combinations of CAR T cells and checkpoint inhibition have not been reported in CLL, nor are there any active studies, so would represent a novel approach.

There is now a large body of evidence for the efficacy of checkpoint inhibition in haematological malignancies. In classical Hodgkin lymphoma, alterations in chromosome 9p24.1 increase the abundance of PD-L1, and promote their induction through Janus kinase (JAK)-signal transducer and activation of transcription signalling (269). Epstein-Barr virus (EBV) infection also increases the expression of PD-L1 in EBV+ HL (270). In a pivotal study Ansell et al. demonstrated an ORR 87% in patients with R/R HL (226), updated results reveal these responses to be robust. Pembrolizumab, has now also been used in a similar patient population with an ORR 69% and acceptable safety profile (271) and recently this PD-1 antibody has been used to increase PFS as consolidation post autologous stem cell transplant (272). Post HSCT both antibodies have been used, again with high ORR 77%, but in a retrospective study of 31 lymphoma patients 17 developed GVHD, indicating both the efficacy and the risk of this approach (273).

The expression of PD-1 on infiltrating T cells and PD-L1 on lymphoma cells has been demonstrated in DLBCL (274) but is more heterogeneous. In a more detailed analysis, the prevalence of PD-L1 on the lymphoma cell versus non-malignant cells in the microenvironment (mPD-L1) by immunohistochemistry was performed on 1253 DLBCL samples (275). Of the 273 patients for whom clinical information was available, the prevalence of PD-L1+ and mPD-L1+ was 11% and 15.3% respectively. Both types were associated with non-germinal centre B-cell (GCB) type. They demonstrated that patients with PD-L1+ DLBCL has an inferior survival compared to PD-L1- DLBCL. A previous study, had linked PD-L1 expression to activated B-cell (ABC)/non-GCB DLBCL, which has an inferior survival compared to the GCB subtype, so it is possible PD-L1 contributes to the more aggressive behavior of ABC DLBCL (276). Therefore, there is a distinct subgroup of DLBCL that may benefit from checkpoint blockade single therapy.

The largest reported study of the use of checkpoint inhibitors in haematological malignancies including NHL and T cell lymphomas is a phase 1b study of nivolumab (277). 81 patients in total, but 10 patients with FL and 11 with DLBCL were treated. ORR were 40%, 30% and 40% in FL, DLBCL and PTCL respectively. In a phase 2 study an

alternative PD-1 antibody pidilizumab, was given as consolidation between 1-3 months post autologous stem cell transplant to patients with DLBCL, demonstrated an overall response rate of 51% (278) and a significant increase in CD4+ T cells.

From the early stages of CLL, disease progression in patients results in a loss of naïve CD4 and CD8 T cells, inversion of the CD4: CD8 ratio and the emergence of a CD8+PD-1+ phenotype which is associated with a more aggressive disease course (85), findings which are demonstrated by the TCL1 mouse model both aged and via AT (118). Given the demonstrated difference in chapter 7 between CAR T cells derived from normal and CLL T cells in terms of PD-1 expression, this affords an excellent opportunity to trial novel combinations in preclinical testing. The safety and dosing of a PD-L1 antibody had already been set up using this model in our laboratory and has reported that it can prevent the engraftment of CLL after AT into WT mice, indicating the importance of this axis in CLL development in this model (96). The use of this antibody alone as a treatment for AT CLL has not been established. I therefore describe the use of the same antibody with and without CD19-CD28 CAR T cells derived from CLL T cells as a therapy to restore CAR T cell function.

8.2 Objectives

- Study the efficacy of CD19-CD28 CAR T cells derived from normal and CLL T cells, the latter in combination with a PD-L1 antibody (α PD-L1) prior to and after the injection of CAR T cells to enhance its function.
- Use the α PD-L1 alone post engraftment of CLL to establish its individual activity as a treatment in this preclinical model.
- For treatment groups with a response, to continue the experiment post CAR therapy to determine the rate of relapse and survival.
- Investigate if ongoing B cell aplasia is necessary for an ongoing CAR response to prevent CD19⁺ relapse.

8.3 Materials and methods

Immunocompetent WT received AT of pooled 32-33 $\times 10^6$ TCL1 cells from fully leukaemic TCL1 mice from the same background thawed from our tissue bank. Such cells were B cell enriched and $CD19^+ > 95\%$ was confirmed prior to injecting into mice. Syngeneic donor CAR T cells were derived from either pooled spleens from aged matched WT mice or WT mice given AT CLL with CLL load $> 80\%$ (AT CAR). Single cell suspensions from spleens were obtained and splenocytes were enriched for $CD3^+$ with magnetic beads then activated with CD3/CD28 Dynabeads (Thermofisher) and mouse r-IL2 (Roche). They were transduced with retroviral supernatant from the transfection of platinum-eco cells with the MSGV-1D3-28Z-1.3mut plasmid (CD19-CD28) and cultured and expanded for 4 days before injection. Two groups of mice received intraperitoneal (IP) α PD-L1 10mg/kg from the day before CAR injection (D-1) every 72 hours (with and without AT CAR T cells) until week 12. All groups (except α PD-L1 alone) were given 100mg/kg IP cyclophosphamide on D-1 as lymphocyte depleting conditioning for CAR T cells. On D0 the CAR groups received between $4-6 \times 10^6$ CAR T cells with α PD-L1 continuing until W12. Mice were bled every two weeks starting D+7 from CAR T cells to assess CLL load, CAR/T cell subsets and groups were culled together when they got sick or PB CLL $> 70\%$ leading to two overall end points, week 6 (α PD-L1 alone and untransduced T cells) or week 18 for all other mice.

8.4 Results

8.4.1 CAR production and phenotype

CAR T cells were derived from pooled spleens from five aged matched WT colony mice or WT mice which had received AT CLL as previously described. Prior to harvesting the spleens to make CAR T cells derived from AT/CLL T cells, the AT mice were bled to confirm their PB CLL load. The two mice whose spleens were used to enrich their T cells from had PB CLL 84.0 and 80.4% prior to being culled. The experimental groups in this experiment are shown below in figure 8.1, with one group using WT derived CAR T cells and two groups using AT/CLL derived CAR T cells, with and without α PD-L1.

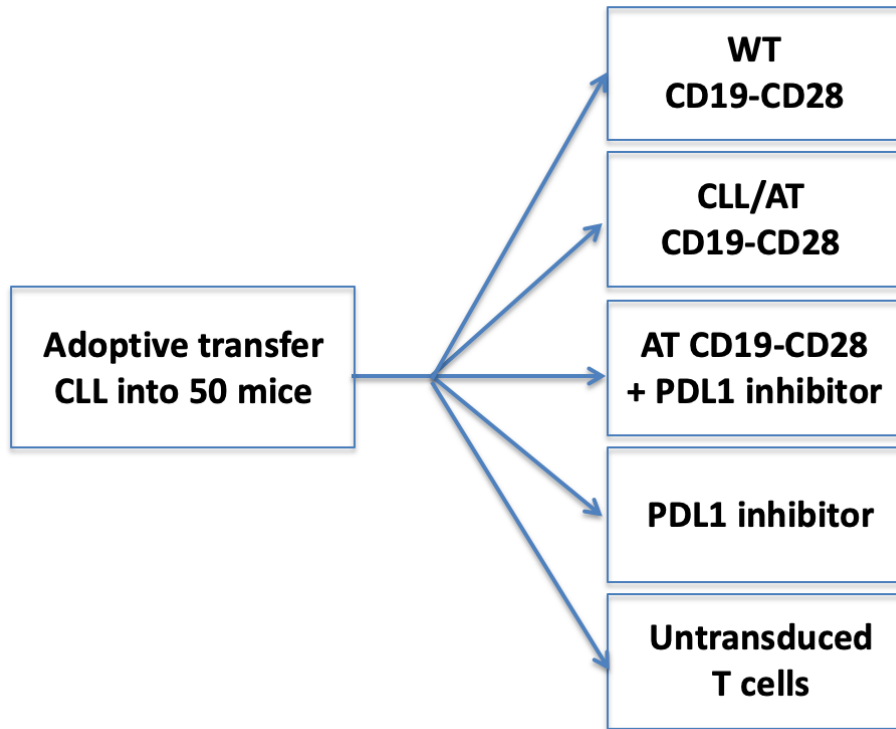


Figure 8.1: Treatment groups post engraftment of AT CLL.

T cells were activated and transduced as previously described. I transduced 18×10^6 cell WT enriched T cells and two 6WP of 18×10^6 AT/CLL enriched T cells for each of the AT treatment groups. After harvesting CAR T cells from culture they were counted and phenotyped. Again, WT CAR T cells proliferate more in culture and exhibit higher transduction efficiencies in the CD8 subset although CD4 transduction is preserved (figure 8.2). As previously described, in the CLL/AT derived CAR T cells there was relative expansion of CD8⁺ T cells with lower transduction efficiency, compared to CD4⁺ CAR T cells. Again there was a shift in CD3+CD8+ phenotypes which is exaggerated by the T cell activation. WT CAR T cells are predominantly of a memory phenotype CD44⁺CD62L⁺, with the rest a mixture of naïve and effector T cells. AT CAR T cells are shifted to an effector phenotype and memory, but with complete loss of CD8+ cells of a naïve phenotype (figure 8.3). Our group has described the shift to terminally differentiated effector T cells that CLL causes in both humans (94) and mice (118), and this effect is exaggerated by the CAR production process using anti-CD3/CD28 beads and mIL2.

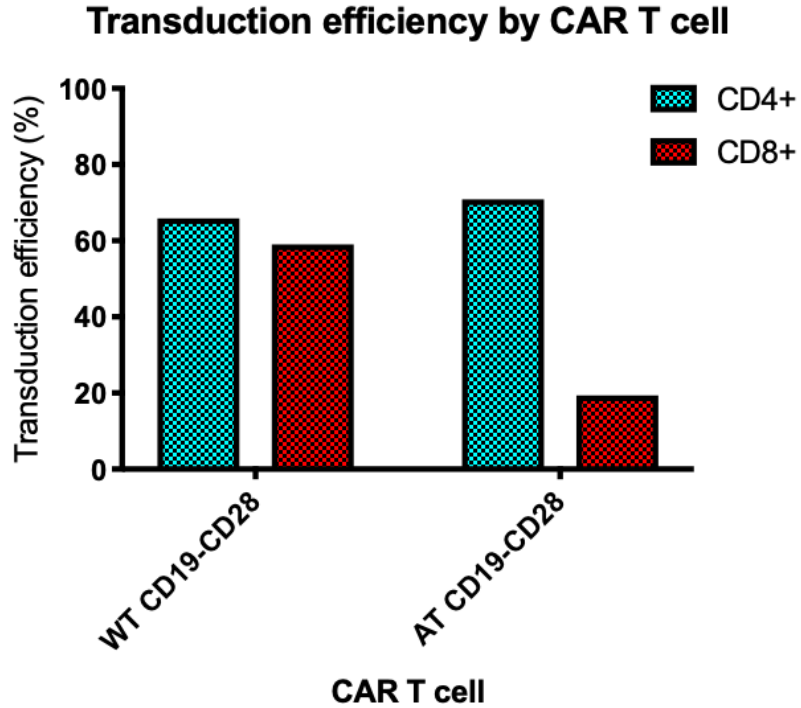


Figure 8.2: Transduction efficiency (Fab⁺%) as a proportion of DAPI-, viable single lymphocytes in CD4⁺ and CD8⁺ T cells after four days of cell culture following transduction with CD19-CD28 retroviral supernatant.

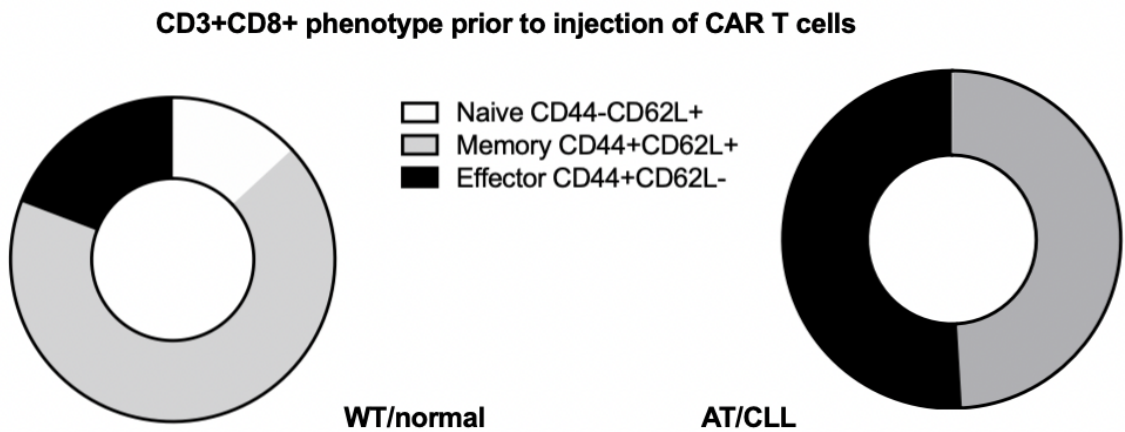


Figure 8.3: Pie charts of the naïve (CD44⁻CD62L⁺)/effector (CD44⁺CD62L⁻)/memory (CD44⁺CD62L⁺) phenotype as a proportion of DAPI-, viable single CD8⁺ lymphocytes after four days of cell culture following activation then transduction with CD19-CD28 retroviral supernatant prior to injection of CAR T cells.

In terms of cell dose injected the total T cell dose was differed between WT and AT CAR groups in this experiment to attempt to broadly match the CAR⁺ T cell dose whilst maintaining the same mouse group sizes. Mice were injected with between 4.5-6.5 x10⁶ T cells and table 8.1 shows the CAR⁺ T cell dose by treatment group when corrected for transduction efficiency and subset ratio. As this shows the CAR⁺ dose was maintained around 1 million CAR⁺ cells in each subset and group except for the CD4⁺ AT CAR T cells. This group is low in number because after manufacturing CAR T cells from CLL/AT T cells there are very few CD4⁺ T cells left, although they are highly transduced. This is mostly a reflection of the skew to CD8⁺ cause by a high CLL burden in the mouse, which is well described in this model and in humans.

CAR	T cell dose x10 ⁶ /mouse	Transduction efficiency (%)		CAR ⁺ cell dose/mouse x10 ⁶	
		CD4	CD8	CD4	CD8
WT CD19-CD28	4.5	65.9%	59%	1.45	1.19
AT CD19-CD28	6.5	75.3%	19.4%	0.20	0.92

Table 8.1: CAR⁺ cell dose by T cell subset corrected by transduction efficiency.

PD-1⁺ expression is higher in both Fab⁺ T cells and T cells in general from both CD4 and CD8 subsets in AT compared to WT CAR T cells (figure 8.4). This is a reflection of the acquisition of T cell PD-1⁺ expression whilst exposed to CLL and not due to activation by CD3/CD28 beads/IL2 activation then transduction.

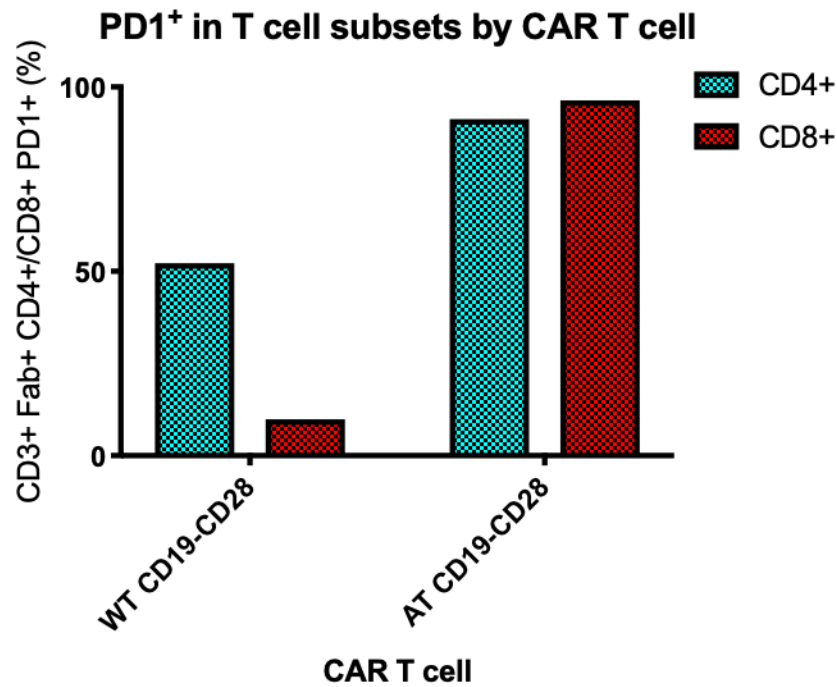


Figure 8.4: PD-1 expression as a proportion of DAPI-, viable single lymphocytes in CAR⁺ (Fab⁺) CD4⁺ and CD8⁺ T cells after four days of cell culture following activation then transduction with CD19-CD28 retroviral supernatant.

8.4.2 Treatment of AT CLL with CAR T cells

Fifty WT mice each received AT of pooled 32-33 x10⁶ CLL cells from fully leukaemic TCL1 mice from the same background from our tissue bank. Good CLL engraftment was confirmed at week 2 (all groups over 50% in the PB) and CAR T cells were injected at week 3 as previously described and with the cell doses states in table 1. At week 4, or CAR D+7, all mice treated with all types of CAR T cells cleared their CLL and normal B cells, and those mice treated with WT CAR T cells all remained in remission until week 18. Mice treated with AT CAR T cells, after initially all responding at D+7, had either an ongoing complete response or slowly relapsed from D+21 onwards with CD19⁺ CLL. All CAR treated mice were culled at week 18 as some mice in the AT CAR groups had reached their endpoint. Mice that had received untransduced T cells or αPD-L1 alone were all culled at week 6 due to rapid CLL progression as these were both essentially control groups. Figure 8.5 shows the progression of PB CLL in each group of treated mice over the 18 week experiment.

In chapter 7, I describe that mice treated with an AT CD19-CD28 CAR have a mixed response over a 9 week experiment. In that cohort all of the male treated mice fully responded and all of the female treated mice did not respond. To investigate if this important difference holds in this experiment, I again balanced the CAR treatment groups with equal numbers of male and female mice. In this experiment again all mice treated with a WT CD19-CD28 CAR responded for the duration of the experiment but again in comparison there was a very different relapse rate of mice treated with the AT CD19-CD28 CAR, with or without α PD-L1. Because the response of both these groups seemed remarkably similar (figure 8.5), in another subgroup analysis I combined both the male and female response from each of the AT CD19-CD28 CAR \pm α PD-L1 groups to see if this sex difference holds in this experiment. Figure 8.6 shows the similar progression of CLL in all AT CAR treated mice regardless of sex with very wide error bars indicative of the polar responses obtained with AT CARs.

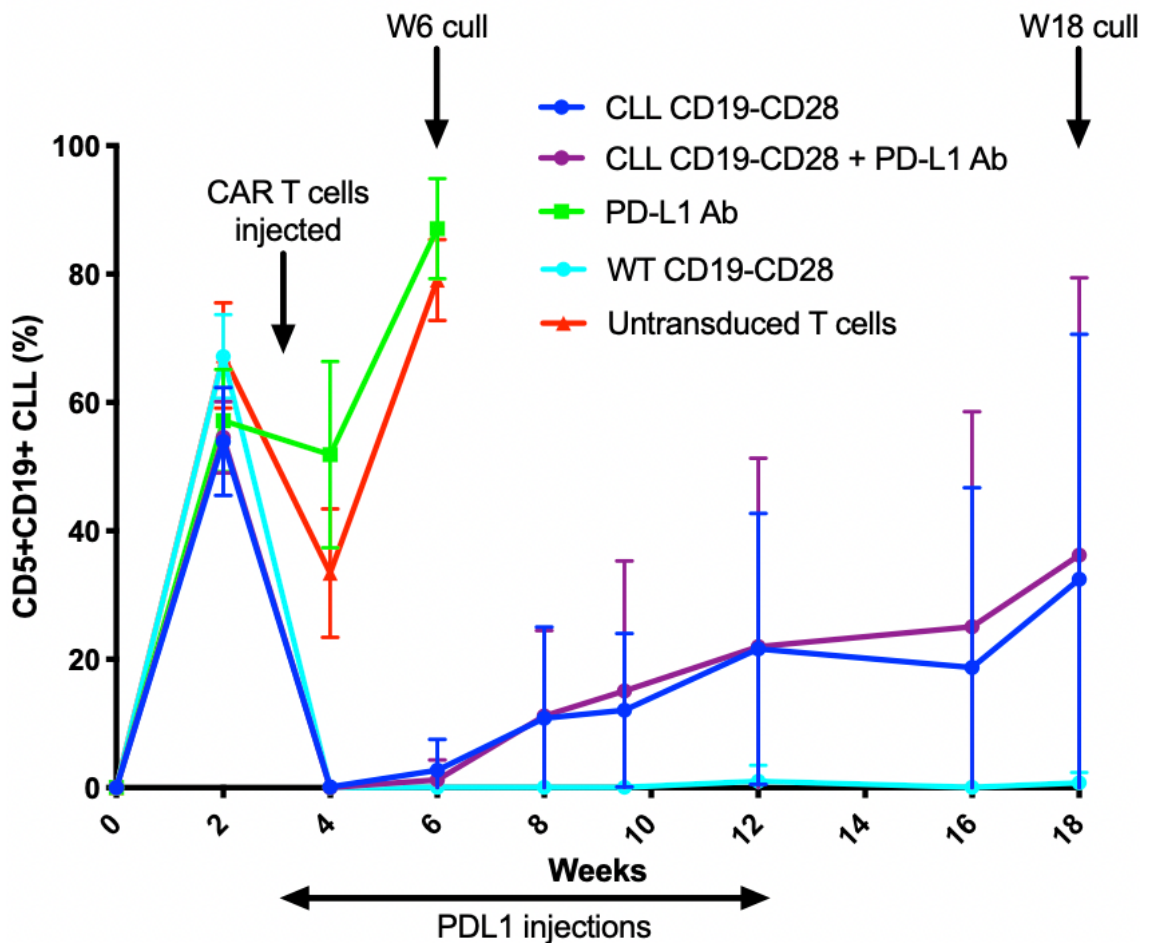


Figure 8.5: Progression of PB CD5⁺CD19⁺ CLL by treatment group post AT at week 0 and CAR T cell injection at week 3 over the whole 18 week experiment.

This shows this time the response of male versus female mice to an AT CD19-CD28 CAR does not differ. Mice with an ongoing CAR response also had no normal CD5⁻CD19⁺ B cells. When mice relapsed with CD19⁺ disease they also had recurrence of their normal B cells. Mice tolerated both CAR T cell and α PD-L1 well with no signs of ill health or distress after commencing these therapies, specifically CRS was not clinically evidence after CAR injection. There were no significant differences between the weights of the mice between treatment groups or compared to aged matched controls when they were culled at their end points at week 6 or week 18 (figure 8.7), but as previously described, sick mice do not tend to lose weight in this model due to their pronounced hepatosplenomegaly.

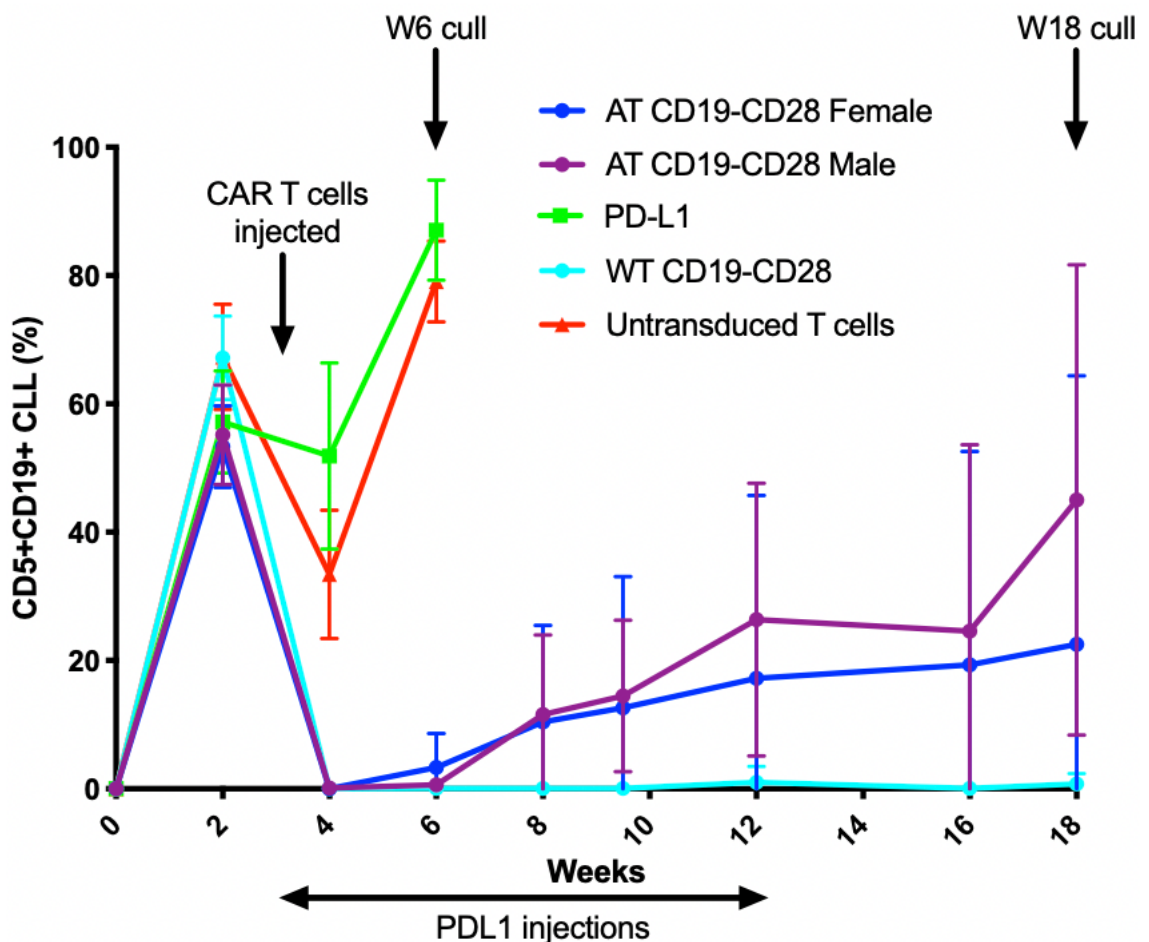


Figure 8.6: Progression of PB CD5⁺CD19⁺ CLL by treatment group post AT at week 0 and CAR T cell injection at week 3 over the whole 18 week experiment. AT CD19-CD28 CAR \pm PD-L1 were combined and separated into male and female groups.

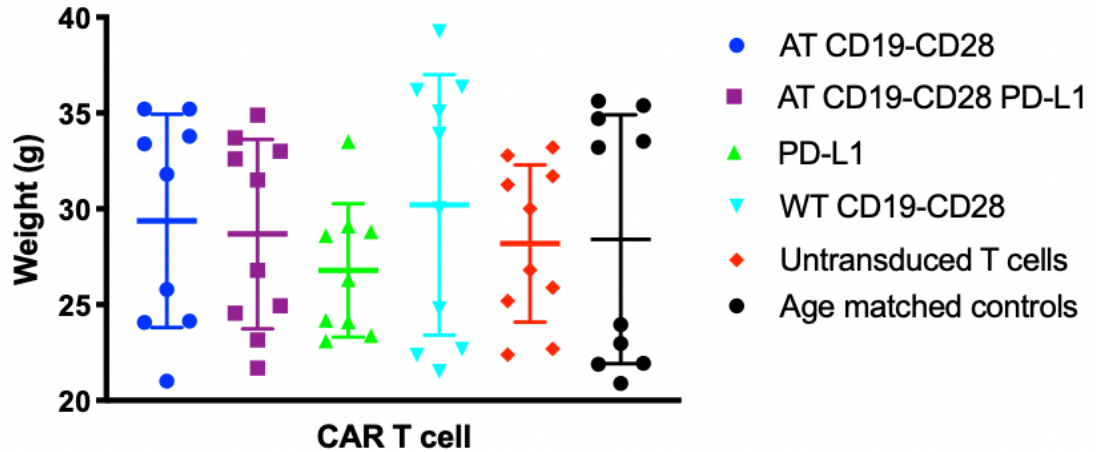


Figure 8.7: Weights of mice (grams) separated by treatment groups at their endpoints at week 6 or 18 following AT of CLL and treatment with CAR T cells, PD-L1 antibody, untransduced T cells or age matched controls. No significant differences.

Spleen weights in the responding WT CAR treated mice were equal to age matched controls (0.1g) whilst AT CAR treated again showed a polar response again with mice either in complete remission or with significant amounts of disease, i.e. with normal sized spleens or very large spleens (figure 8.8). As expected, mice treated with untransduced T cells had very large spleens, as did mice treated with α PD-L1 alone. Although α PD-L1 alone can prevent CLL engraftment in this model when used as a treatment it appears to have limited activity as these mice also needed to be culled at week 6 like the control mice treated with untransduced T cells.

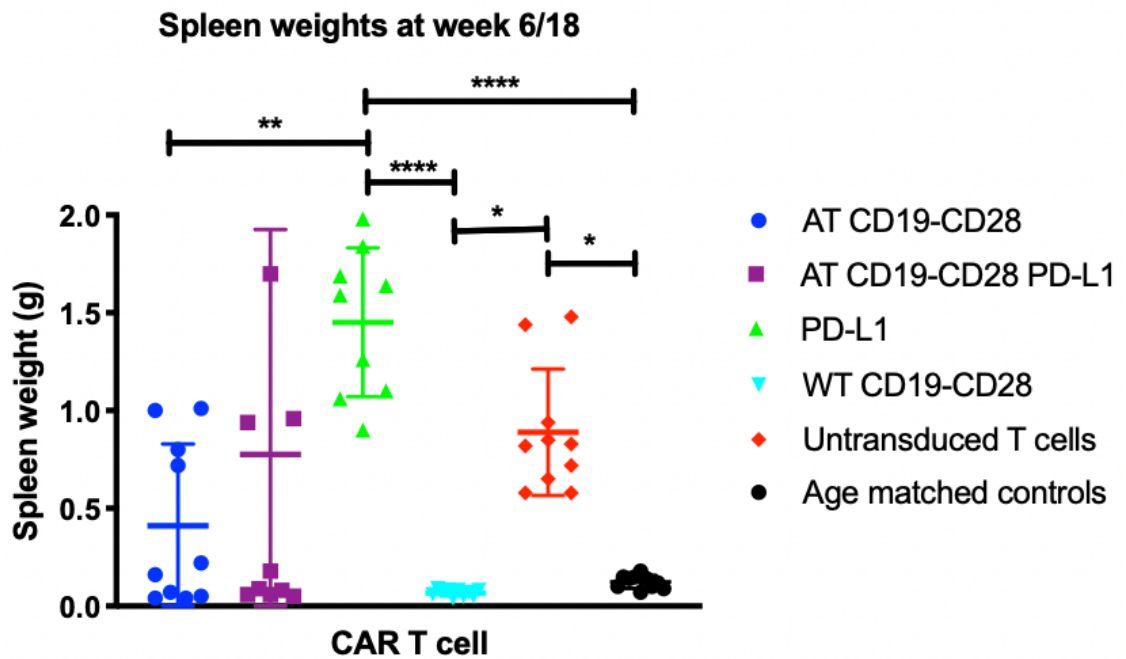


Figure 8.8: Spleen weight (grams) when mice are culled at week 6 or 18 after AT of CLL at week 0 and treatment with CAR T cells at week 3 derived from different sources of T cells transduced with CD19-CD28 retroviral supernatant showing significant differences ($*P < 0.05$, $**P < 0.01$, $***P < 0.001$, $****P < 0.0001$).

To demonstrate the relapse rate of mice treated with different groups, figure 8.9 shows the percentage of mice in each group, that have significant disease in the PB by week after AT of CLL at week 0 and CAR T cell injection at week 3. This more clearly demonstrates that whilst all mice who received a CAR initially completely responded as the CARs engraft at week 4, what differs about the mice that receive CAR T cells derived from AT T cells is that up to 50-60% of these mice slowly relapse with CD19+ disease. This model very much reflects what is reported in the CLL CAR trials, albeit only very small numbers have been reported in those studies. Those studies also reflect that long term persistence is important in CLL (160), which can be indicated by B cell aplasia. Likewise, in this model mice with long term responses maintained a loss of normal B cells.

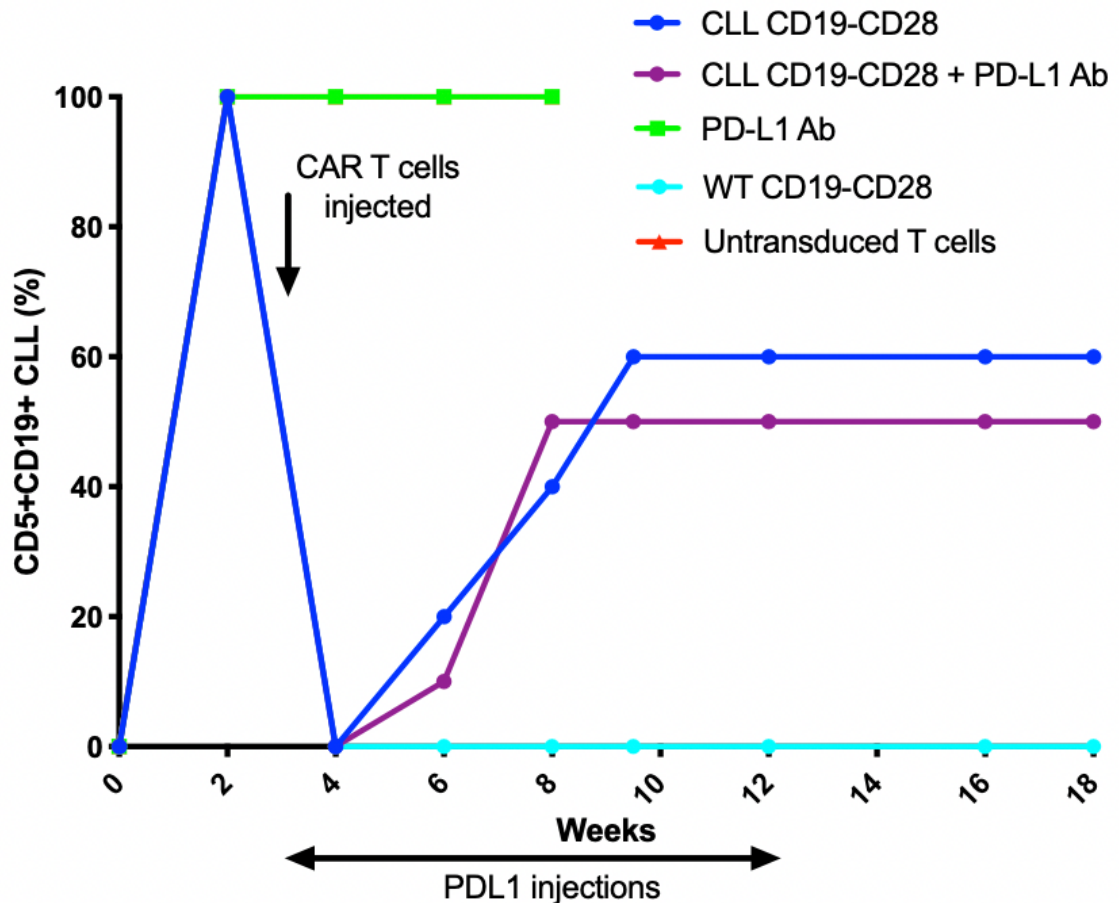


Figure 8.9: Percentage of mice in each treatment group with detectable CD5⁺CD19⁺ disease in the PB (>5%) measured by flow cytometry after AT of CLL in week 0 and injection of CAR T cells or untransduced T cells at week 3 with or without PD-L1 antibody IP.

At week 18, PB, spleen and BM were harvested and CD5⁺CD19⁺ in each organ shows their disease was cleared by the WT CAR ($P < 0.0001$ compared to α PD-L1 alone and untransduced T cell groups) (figure 8.10), although two mice did show very low level disease suggesting they had just started to relapse. This again demonstrates the very polar response in terms of the amount of disease found in mice treated with AT derived CAR (figures 8.10).

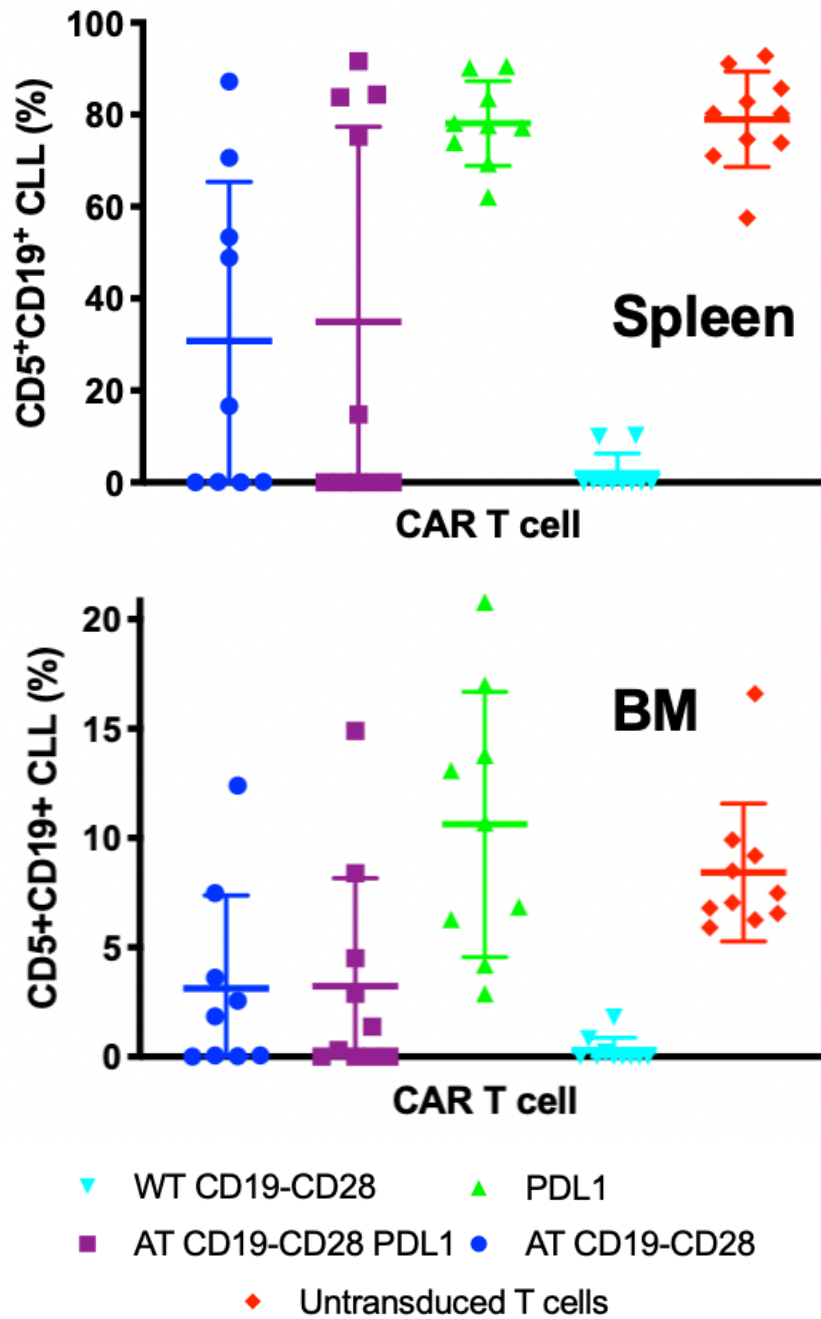


Figure 8.10: Percentage of DAPI⁻ viable, mononuclear cells from spleen (top) and BM (bottom) that are CD5⁺CD19⁺ after AT of CLL in week 0 and injection of CAR T cells or untransduced T cells at week 3 with or without PD-L1 antibody IP.

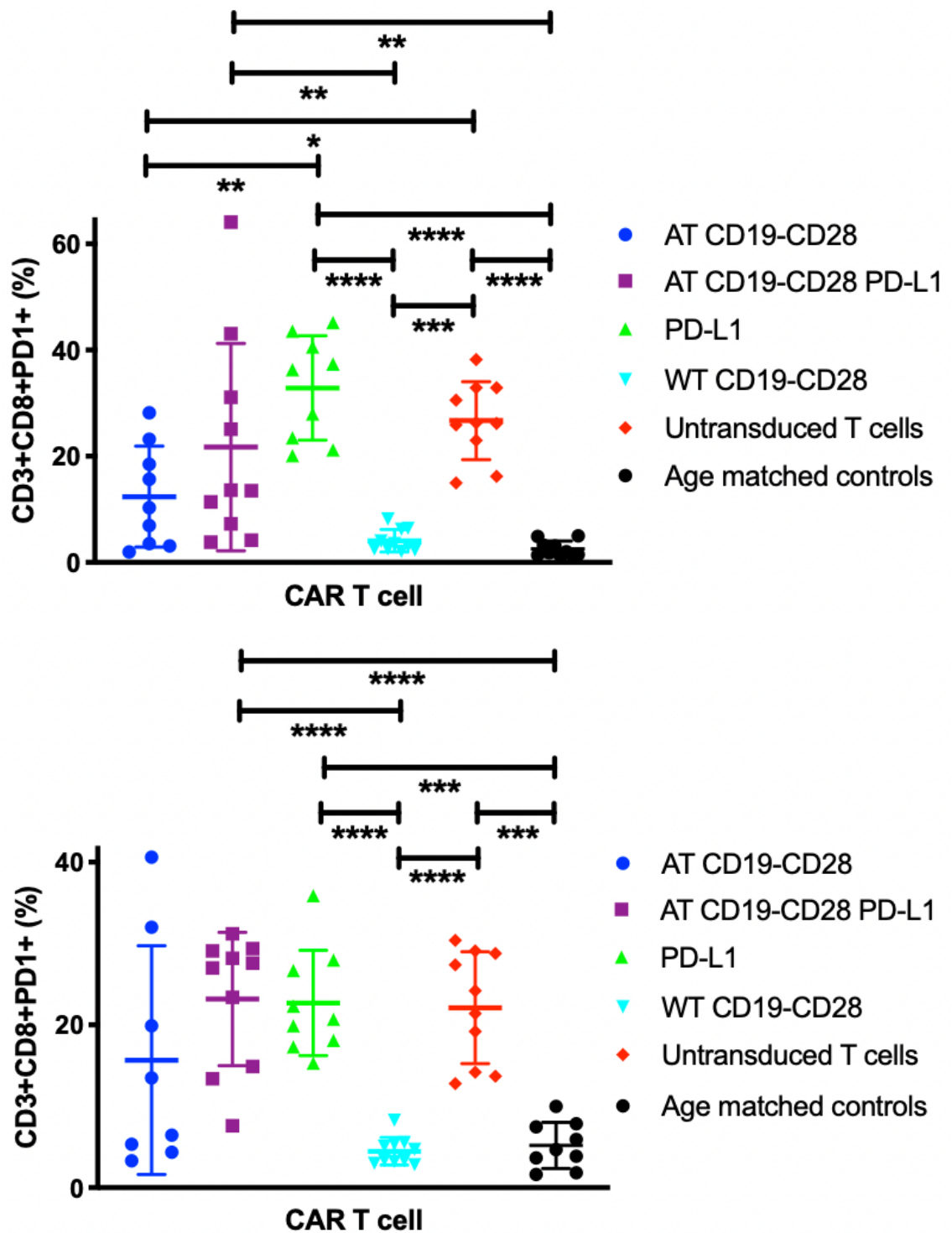


Figure 8.11/12: PD-1⁺ as a proportion of DAPI-, viable mononuclear CD3⁺ cells from spleens (figure 8.11/top) and BM (figure 8.12/bottom) after AT of CLL in week 0 and injection of CAR T cells or untransduced T cells at week 3 with or without PD-L1 antibody IP with significant differences.

CAR T cell expansion in all groups was greatest at D+7 and the majority of CAR⁺ cells were CD8⁺ (figure 8.13) and PD-1⁺ again in all groups. At this point all mice had no normal or CLL B cells in the PB but did have detectable Fab⁺ CAR T cells by flow in all CAR treatment groups. At this apparent point of maximum expansion, the percentage of fab⁺ cells in the PB was highly variable between mice, but there was again a trend that mice treated with AT derived CAR T cells had higher percentages of CAR T cells than mice treated with a WT CAR. However, this was not significantly different in CD3⁺Fab⁺ or either CD4⁺ or CD8⁺ separately. Certainly, in all the different CAR treatment groups, the majority of the CD3⁺Fab⁺ expansion was CD8⁺. At the same time point PD-1⁺ expression was significantly higher in AT compared to WT derived CD8⁺CAR/fab⁺ T cells (figure 8.14).

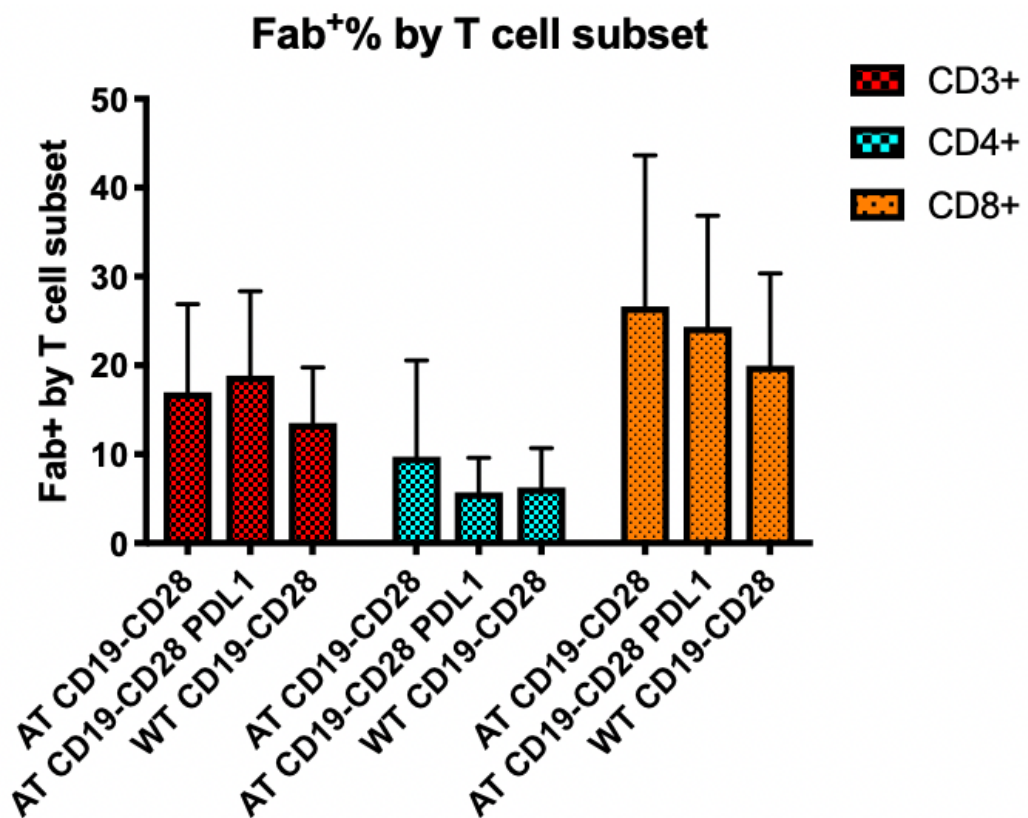


Figure 8.13: CAR⁺ T cells as a proportion of DAPI-, viable mononuclear CD3⁺/CD4⁺/CD8⁺ gated T cells at day 7 following injection of CAR T cells in the PB separated by CAR T cell treatment group.

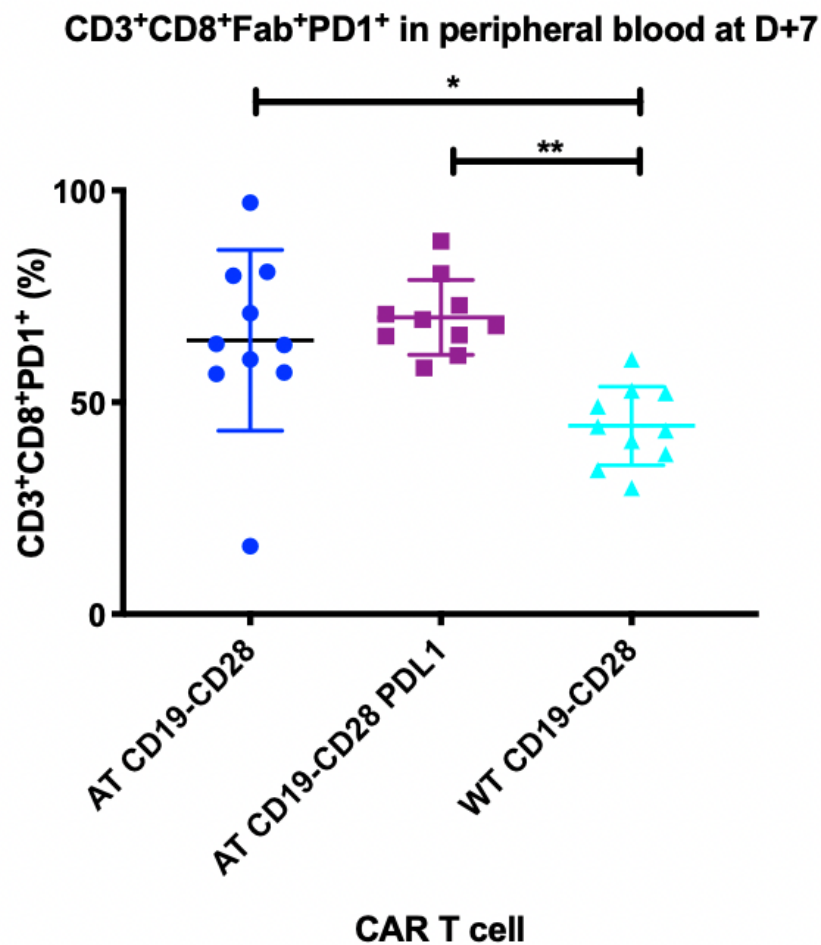


Figure 8.14: Percentage of cytotoxic CAR⁺ T cells (CD3⁺CD8⁺Fab⁺) DAPI-, viable mononuclear that are PD-1⁺ in PB at day 7 following injection of CAR T cells separated by CAR T treatment group showing significant differences.

At the time of the next bleed at D+21, the presence of the CAR⁺ cells were highly variable between groups. Figure 8.15 shows the progression of CD3⁺CAR⁺ cells in the PB for the 12 weeks in which one of the AT CD19-CD28 CAR groups was also administered the PD-L1 antibody. At both D+7 and D+21 there was a trend for mice treated with the WT CAR to have lower CAR⁺ percentages in the PB. This is an interesting observation, suggestive of the greater functional capacity of WT derived CAR T cells so with less need to proliferate rapidly (figure 8.15) since these mice remain in remission whilst the two groups treated with AT derived CAR T cells start to relapse.

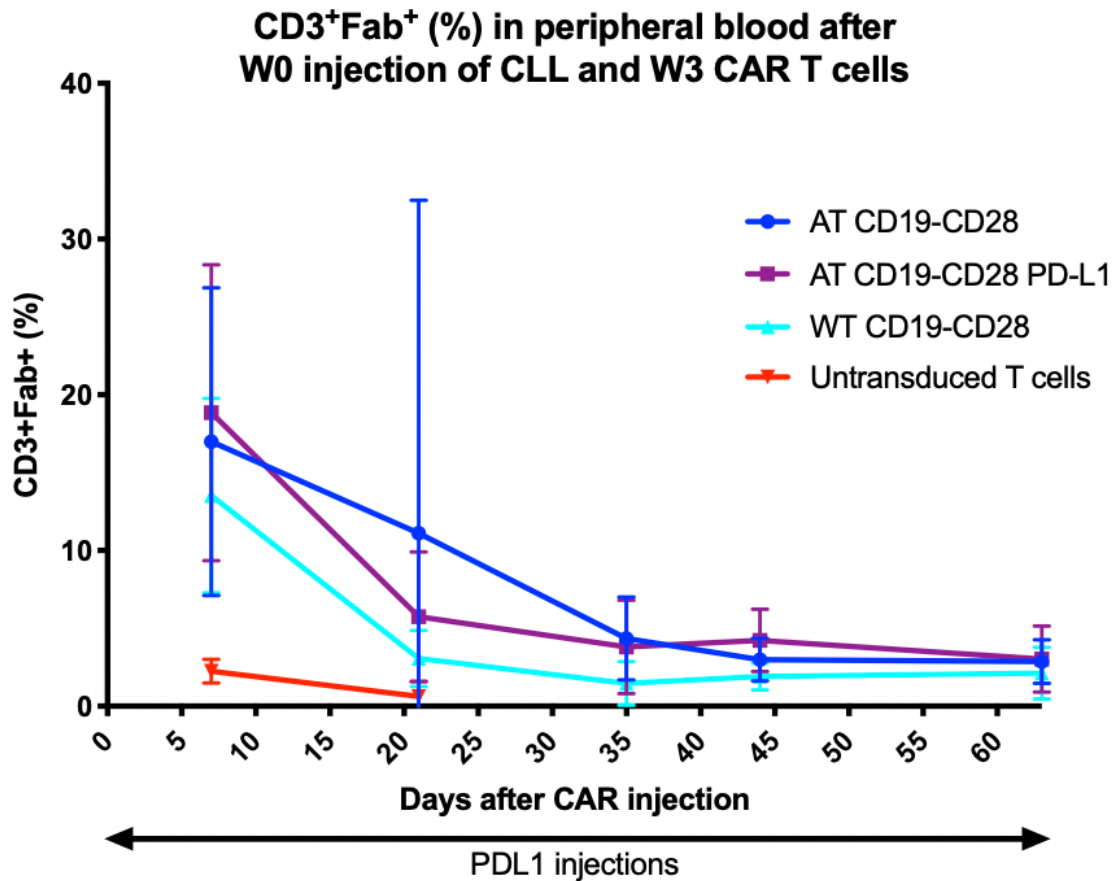


Figure 8.15: Percentage of DAPI-, viable mononuclear CD3⁺ T cells that are CAR⁺ (Fab⁺) in the PB days after CAR T cell injection separated by CAR treatment group or compared to untransduced T cells.

The dynamics of disease and CAR response are interesting to describe in the mice from D+21 and represent the some of the challenges of treating CLL. In all mice treated with the AT CD19-CD28 CAR ± αPD-L1, in the mice that relapse in the PB the blood test in which this is first identified, both a clonal B cell population and normal B cells are present. Prior to this, the responding mice all have B cell aplasia in the PB i.e. there are no CD19⁺ cells in the PB by flow. In all mice but one, once a CD5⁺CD19⁺ population >1% is identified in the PB, disease control is lost and they relapse. One mouse from the AT CAR ± αPD-L1 group, at week 16 has a PB CLL population of 2.3% with normal B cell population of 0.5%, which goes onto clear the PB, spleen and BM by week 18 at the end of the experiment. In all mice treated with an AT CD19-CD28 CAR, the disease status in the PB at the point the mouse is culled matches that in the spleen and BM i.e.

all mice with an ongoing PB CAR response at week 18, meaning no malignant or normal B cells also have the same response in the spleen and BM.

For the mice treated with a WT CD19-CD28 CAR there are some subtle differences. Until week 16, all of the mice have an ongoing CAR response, with no normal or malignant B cells in the PB by flow. At week 16 one mouse develops normal CD19⁺CD5⁻ B cells but with no clonal B cell population. By week 18 this mouse develops both normal and CLL B cell PB populations with concordant populations in its spleen and BM. A second mouse in this group also has low level PB CLL at week 18 again which is also found in the spleen and BM as it was culled at week 18. Taken together, these results say that in this model ongoing B cell aplasia is necessary and is indeed indicate of an ongoing CAR response, since the only mouse that had recurrence of their normal B cells first, went onto relapse. These mice are only bled every 1-2 weeks which is what is feasible in this experiment in terms of the project license. Perhaps if they were bled more often perhaps we would see mice first get recurrence of normal B cells prior to relapse of their CLL.

For both the AT and WT CAR T cells these data also demonstrate what is detectable in the PB by flow, in terms of both normal and CLL B cells, is matched by what is seen in the spleen and BM. Whilst many human trials have access to paired BM and PB samples, these data simple isn't available from splenic biopsies as it is not part of clinical practice to monitor human patients in this way. Given the previously stated two compartment disease that CLL is, it is interesting to correlate PB flow disease status with secondary organs since PB in a human is so easy to obtain. Clinically, these are important findings, because it suggests from PB flow if there is ongoing B cell aplasia there is ongoing CAR activity. More usefully, recurrence of PB B cells implies loss of CAR activity and inevitable relapse, which could warrant a therapeutic intervention. This is in contrast to what was recently reported using the same CD19-CD28 CAR in lymphoma in ZUMA-1 (182), in which there were many patients that lost their B cell aplasia which did not relapse. Perhaps though, the requirement for a persistent CAR is fundamentally different in CLL and ALL compared to lymphoma.

8.5 Cytokines

At the time points shown above in figure 8.15 plasma was obtained from the mice for cytokine analysis. The Mouse Th Cytokine Panel (BioLegend, San Diego CA) is a bead-based multiplex assay panel, using fluorescence-encoded beads selected to detect IFN- γ , TNF- α , IL2, IL6 and IL10, which are known to be important in CRS. Until recently, there has been no reported mouse models of CRS, as this toxicity was first described in detail in one of the first CAR T cell series reported in humans (151). Since then, Ruella et al. has described a SCID model injected with human MCL followed by CD19-41BB CAR T cells which become sick with signs of distress (reduced mobility, emaciation, hunched bodies and withdrawal) (279). Blood from these mice at D+4 show elevated levels of human cytokines including IL6, IFN- γ , TNF- α , IL2 and GM-CSF. An alternative model again used SCID mice but they were sub-lethally irradiated then injected with human cord blood CD34⁺ cells (280). Mice were injected with ALL followed by CAR T cells 5 or 7 weeks later. These humanized mice when treated with high leukaemia burden, developed high fevers and IL6. The syndrome was prevented by monocyte depletion or tocilizumab. Interestingly, tocilizumab didn't protect against lethal neurotoxicity, characterized by meningeal inflammation, which was abolished using the IL1 receptor antagonist anakinra. However, the author would argue an immunocompetent model of CRS or neurotoxicity would be much more clinically relevant as this model described cannot allow for the host immune response to modulate the T cell responses leading to CRS.

Unfortunately, after attempting to optimize the assay using samples collected later in the experiment, when testing the D+7 plasma, I was unable to demonstrate anything higher than negligible plasma cytokine levels. This is definitely due to technical issues, albeit a problem with bead capture or the quality/quantity of the samples. I have discussed in detail the differences between normal and CLL T cells, which have an exhausted phenotype but pseudo-exhausted cytokine profile (281). The comparison of cytokine results from WT versus AT derived CAR T cells at D+7, I believe would give a fascinating insight into the functional cytokine differences between a normal and an exhausted T cell, and whether this theory of pseudo-exhaustion is reflected

functionally in an appropriate preclinical model. In future work I will endeavour to make this assay work because I think it answers interesting questions about CLL T cells, as well as being a potential model to study interventions that treat these dramatic complications.

8.6 Discussion

This experiment confirms the findings from previous experiments that CAR T cells derived from AT/CLL T cells have a significantly worse performance than those derived from normal T cells in an immunocompetent syngeneic mouse model. The mice from which the CLL T cells were obtained, had CLL for 6 weeks before their spleens were harvested and T cells enriched to make CAR T cells, emphasizing how profound the impact exposure to CLL is on T cell function. In this experiment, impairment of CAR function is not reflected by initial efficacy, as all mice treated with a CAR respond at D+7 with no CLL or normal B cells, but the progressive relapse risk, which continues for the duration of the 18 week experiment. This is a fascinating observation that very much reflects the behaviour of CD19 CAR T cells in human CLL trials, and again shows the utility of the TCL1 mouse model in the investigation of CLL of potential therapeutic interventions in CLL.

Our group has previously demonstrated the importance of the PD-1/PD-L1 axis in the engraftment of CLL in this model, whilst in this experiment the use of the same α PD-L1 antibody and dosing after established engraftment of CLL had little disease activity as a standalone agent. This is perhaps not surprising, as the disease kinetics of CLL engrafting by intravenous injection into an immunocompetent mouse have to be vastly different to the established and rapidly progressing disease as in this experiment. Most importantly, the addition of the PD-L1 antibody commenced one day before AT/CLL CAR T cell injection for 12 weeks, did not prevent these mice relapsing after initially responding to the AT CAR. The pattern of rate of relapse post AT CAR without or without α PD-L1 antibody was the same. This demonstrates very different responses to a α PD-L1 which is effective in terms of establishment of CLL, but ineffective in treatment of established disease.

CAR expansion dynamics in the PB did not seem to be altered by the addition of α PD-L1, with peak CAR expansion in all groups was D+7 as in all previous experiments. Comparing the phenotype of the AT CAR T cells at peak expansion at D+7, the α PD-L1 antibody did not alter PD-1 expression of CAR+ cells compared to the group treated without α PD-L1 antibody. However, PD-1+ expression on CD8+CAR+ T cells was higher on AT CAR treated groups compared to WT CAR treated mice. Whilst the PD-1 expression of T cells obtained from AT mice is very much higher than WT mice, and this is again reflected at the end of the manufacturing process, it is interesting that the CAR T cells that expand in the mice also reflect this significant difference. Again, there was a trend for a higher proportion of CD3⁺/CD4⁺/CD8⁺ CAR⁺ T cells in the PB at D+7 to be CAR+ in the AT CAR treated group compared to WT CAR, which may reflect the relatively impaired CAR T cell function if derived from a CLL T cell source. Ultimately, mice treated with the AT CD19 CAR relapse, and this continues for the duration of the experiment, always with CD19+ disease. Ongoing CAR activity is always reflected by PB B cell aplasia, and PB flow always reflected what was ultimately found in the spleen and PB in terms of normal and CLL B cells. Taken together, whilst this α PD-L1 antibody did not have activity, the model is demonstrably useful to study the impact of immunotherapeutic agents on CAR efficacy and dynamics. There is preliminary evidence for the safety of this combination when used in lymphoma patients. Durvalumab has been used in combination with JCAR014 (CD19-41BB with 1:1 CD4:CD8 T cell product), and phase 1 data was presented at ASH (282). In this study, 15 patients were treated and 12 were evaluable for response, with an ORR of 50%. There was no new safety signal seen and CAR T cell expansion was detected in all patients.

For this thesis the α PD-L1 antibody was used first because it was available in the Gribben laboratory with safe dosing established in this model and has been shown to be effective in preventing CLL in this mouse model, but, there are many other commercially available murine checkpoint inhibitors which could be applied to this model in the same way, of particular interest would be a PD-1 inhibitor. There is increasing albeit preliminary evidence for this approach, at ASH 2018 the immunotherapy group at University of Pennsylvania presented their single centre

experience for their paediatric patients with ALL (283). Patients were given the PD-1 inhibitor pembrolizumab no sooner than 14 days after infusion for patients with early CAR T cell loss or a partial/no response in that time. Of the 14 patients treated, 3/6 treated for early B cell recovery re-established B cell aplasia for 5-15 months, 2 of which are ongoing. 4 patients started pembrolizumab for bulky extra-medullary disease with 2 CR and 2 PR seen. In one patient, significant CAR T cell proliferation was measured within days of starting pembrolizumab that correlated with a radiological response. In 4 other patients with poor initial BM response to CAR T cells no durable effect was seen. CRS symptoms and fever were seen in 3/14 patients within 2 days of starting pembrolizumab. However, there remains no evidence for this approach in CLL.

There are limitations due to technical challenges. I attempted to match CAR+ dose rather than T cell dose across groups, but this is not entirely possible since WT and AT CAR T cells have characteristically different phenotypes and T cell subsets. It is particularly difficult to match CD4+CAR+ cell doses, as in this model there is a strong skew to CD8+CAR+ after activation and transduction. Perhaps this explains the early response at D+7 in all CAR treated mice, but the lack of CD4+CAR+ cells in the AT CAR groups reduces the functional memory and persistence resulting in relapse.

In conclusion, CD19⁺ relapse post CAR T cells is determined by T cell fitness as WT CAR T cells can prevent relapse and can normalize PD-1⁺ expression. CAR T cells derived from CLL T cells are less able to prevent CD19⁺ relapse and this is not improved using concurrent α PD-L1, which also seems to have limited activity in treatment alone of AT TCL1 CLL. Further studies using CAR plus immunotherapy combinations are warranted to attempt to improve CAR T cell fitness.

9. In vivo modelling of CAR pre-treatment with BTK inhibitors

9.1 Introduction

The University of Pennsylvania Immunotherapy group were the first to report the impaired ex vivo expansion of CLL CAR T cells which was improved by the patients pre-treatment with ibrutinib (163), albeit in a very small number of patients. Prolonged ibrutinib treatment also decreased immunosuppressive checkpoint inhibitors such as PD-1, but did not alter memory phenotype. Given the major CAR lymphoma and ALL clinical trials did not allow concurrent use of chemotherapy or BCR inhibitors during CAR infusion or afterwards, the combination of CAR T cells with BTKi remains experimental.

Preclinical murine data supports the positive effect of concurrent ibrutinib on CAR function, in xenograft mouse models of mantle cell lymphoma (284), ALL and CLL (163) the addition of ibrutinib to CD19-41BB CAR T cells improved disease control. Since then, multiple groups have reported this effect in CLL patients, albeit in abstract form (214, 215). At ASH 2018, the Seattle group continued ibrutinib through leukapheresis, lymphodepletion and for a median of 21 days post JCAR14 (CD19-41BB with 1:1 CD4:CD8 T cell product). They demonstrated a higher ORR of 88% vs 56% compared to the CAR plus no ibrutinib group (215). Of note, although they noted no difference in the occurrence of mild CRS post CAR T cells, they saw a significantly reduced rate of severe CRS in the ibrutinib CAR treated group. Median follow-up of the ibrutinib CAR group is only 98 days so it is too soon for more detailed survival analysis. Also from the University of Pennsylvania group, Dr Saar Gill presented their data on the use of the standard CD19-41BB CAR with ibrutinib (214). Lymphodepletion was with the standard Flu/Cy conditioning regimen and this was a dose escalation study. This was a high-risk population as 11 of the 19 patients infused had del17p of *TP53*. 18 of the 19 patients had CRS which was mostly grade 1-2 and 5 patients had some degree of neurotoxicity. One patient died of a cardiac arrhythmia during severe neurotoxicity after resolution of CRS. The median follow-up for the 18 surviving patients was 18.5 months.

Examination of the bone marrow at 3 months post CAR T cells demonstrated morphological remission in 17 of these patients in particular, 15 of these patients' BM were MRD negative by flow cytometry. Both abstracts have identified a potential new safety concern, being cardiac death due to the addition of ibrutinib, which is well known to cause arrhythmias. Subsequently there have been recommendations that patients who have the combination of CAR T cells plus ibrutinib and have CRS or neurotoxicity, should have cardiac monitoring.

Acalabrutinib is a second generation BTKi, known to be very active in CLL but is currently only licensed in Europe in mantle cell lymphoma. This highly selective BTKi led to a 95% ORR in 61 patients with R/R CLL, including in patients with del(17p) although CR were limited (68). It is unclear if acalabrutinib will be positioned as an alternative to ibrutinib in both 1st line and relapsed CLL and this can only be resolved by the ongoing clinical trials. Despite the impressive clinical results seen with ibrutinib, most patients do not experience a CR and a subset develop resistance. This most commonly occurs due to mutations in BTK or PLC γ 2, emphasizing the importance of the BCR pathway to the action of ibrutinib in CLL (285). Ibrutinib also targets many other kinases, such as ITK and TEC that may account for its side effect profile (69). Therefore, the more selective BTK inhibition of acalabrutinib may be more potent and result in less toxicity. No reports have been provided of head to head studies of ibrutinib versus acalabrutinib in patients, so this suggestion of increased tolerability remains speculative, although interestingly in a cohort of 33 patients who were ibrutinib intolerant, 72% of the adverse events reported associated with ibrutinib intolerance did not recur with acalabrutinib. The two drugs have been compared using both the AT TCL1 and a CLL xenograft models, in which acalabrutinib showed increased BTK selectivity with anti-tumour efficacy equivalent to ibrutinib (70). Both drugs have established dosing in mouse models, with the drugs given continuously in their drinking water and have been used by our group. I therefore chose to investigate the pre-treatment of CAR T cells in the AT TCL1 mouse model using both BTKi ibrutinib and acalabrutinib. The use of acalabrutinib for this purpose is not described in the literature. Given the established importance of T cell subsets and function for CAR efficacy, it is interesting to note that in patients on clinical trials of ibrutinib and

acalabrutinib, it was ibrutinib that has a more prominent effect on effector/effector memory subsets which was not observed in acalabrutinib. Both drugs significantly reduced PD-1 and CTLA4 expression. Further, whilst with both drugs the numbers of Tregs were unchanged, the ratio of Tregs to CD4 was reduced with ibrutinib but not acalabrutinib, indicating there may be differences in the way these two drugs relieve their immunosuppressive microenvironment in CLL (286). Another project in our group has extensively examined the impact of ibrutinib versus acalabrutinib on T cell phenotype and function (120, 121).

9.2 Objectives

- Investigate the effect of treatment of AT TCL1 CLL with ibrutinib and acalabrutinib. Establish AT TCL1 in a litter of mice aged 3 months, leaving one group without AT as a control group. Of the mice treated with AT TCL1 leave one group untreated and treat the other two groups with either ibrutinib or acalabrutinib.
- Compare the progression of CLL in untreated AT TCL1 with mice treated with ibrutinib or acalabrutinib comparing the effect on the microenvironment of all groups, including WT controls.
- From these mice, apply the same optimized CD19-CD28 CAR manufacturing process to T cells obtained from WT mice without AT (WT CAR), AT mice without treatment (CLL CAR) and AT mice with CLL which had been treated with ibrutinib (ibrCAR) and acalabrutinib (acalaCAR), comparing the resulting CAR phenotype and ex vivo expansion.
- Compare the efficacy of WT CAR, CLL CAR, ibrCAR and acalaCAR in treating AT CLL in a second group of mice.

Not all the experiments planned for this chapter have been completed by the time of thesis submission at the end of my fellowship and thesis work forms the basis of planned future work.

9.3 Methods and Materials

This experiment has a complicated two-part format requiring two large sequential AT experiments running in parallel, with CAR manufacture on fresh T cells in the middle, summarized in figure 9.1. In part 1 forty-eight WT mice of 12 weeks of age were separated into 4 groups, separated by sex (numbers of males=females). Three groups, or thirty-six mice in total received AT of pooled B cell enriched (>95%) TCL1 splenocytes from fully leukaemic TC1 mice from the same background. The TCL1 used was pooled from thawed CLL vials our tissue bank and some fully leukaemic aged mice from our colony were used. All mice received the same pooled 29×10^6 TCL1 splenocytes by tail vein injection except the twelve mice in the WT group, which are a source of normal T cells and control group and therefore had no intervention and did not have CLL. All mice were then bled weekly and at week 2, when PB CLL was confirmed >10% in all mice, two groups were randomized to be treated with ibrutinib or acalabrutinib. This is given continuously via drinking water with the drug dissolved using a vehicle, 2-hydroxypropyl- β -cyclodextrin (HPBD) with both ibrutinib and acalabrutinib (Acerta) given at the same concentration (0.15mg/l). At week 5 all mice were culled for the second part of the experiment. Week 5 was chosen because prior AT experiments have shown that typically mice may need to be culled from week 6 due to progressive CLL due to humane previously defined endpoints.

This experiment was performed with Arantxa Romero-Toledo, a PhD student also working on the microenvironment in CLL in the Gribben laboratory. For both weekly PB bleeds and PB, spleen and BM assessment at the end of this part, samples and analysis were shared as she was undertaking different experimental questions with this material.

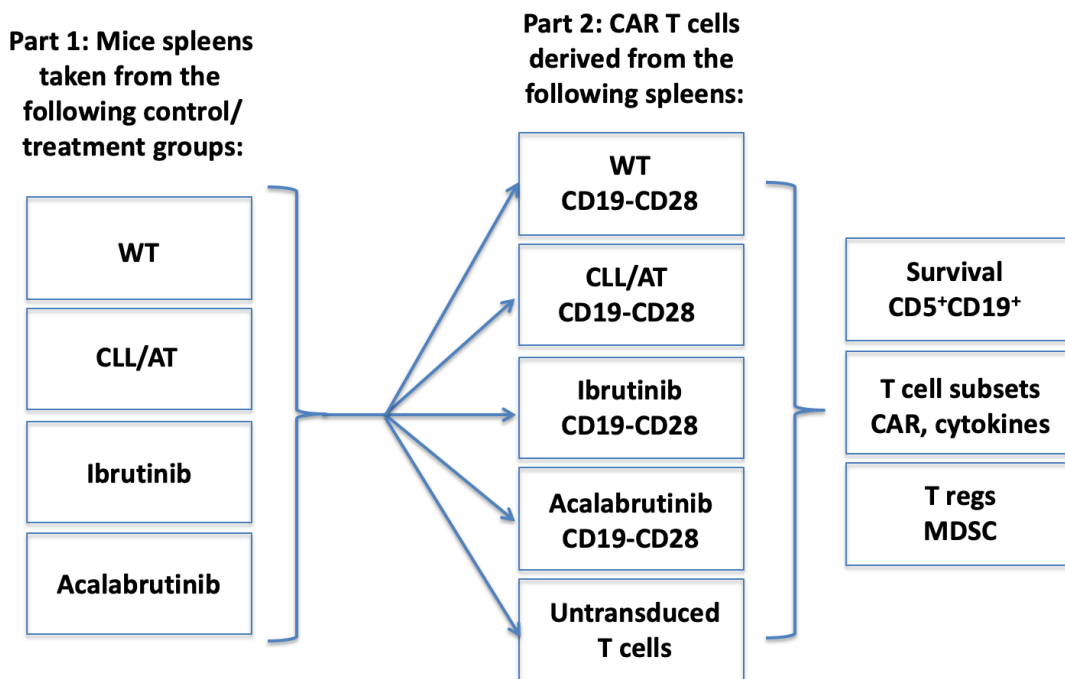


Figure 9.1: Two-part sequential AT experimental plan to investigate the effect of ibrutinib and acalabrutinib pre-treatment on CAR T cell function, with outcome measures on the right.

The AT for part 2 of this experiment was started at week 3 of part 1, so the CLL had time to engraft and mice become leukaemic before treatment with CAR T cells. Fifty WT mice aged 13 weeks were separated into 5 groups, with equal male and female mice. One group of 10 mice were bled prior to AT for baseline microenvironment assessment. Again, TCL1 pools were obtained from our tissue bank and fully leukaemic donors in our colony, the CLL was B cell enriched (>95%) and pooled and all fifty mice were injected with the same 23×10^6 TCL1 splenocytes. They were then bled at weeks 1 and 2 to confirm CLL engraftment, with lymphodepleting IP cyclophosphamide (100mg/kg) given one day before week 3 (D-1) as in previous CAR experiments. At week 3, which becomes CAR D0, mice were treated with WT CAR, CLL CAR, ibrCAR, acalaCAR or untransduced T cells, with equal cell doses within groups, but not between groups. They were then bled weekly, with the planned experiment end point when the majority of mice treated with ibrCAR and acalaCAR need to be culled due to progressive disease, but if possible not until week 18 as that was the duration of the experiment described in Chapter 8. Mice treated with untransduced T cells would be

culled as a group when the first mouse appeared sick with progressive CLL separately from the other groups.

9.4 Results

9.4.1 Ibrutinib and acalabrutinib treatment of AT CLL

In part 1 48 mice were bled weekly examine CLL load, T cell phenotype and other aspects of the microenvironment including MDSC, macrophages and Tregs (287). Week 0 of this part was AT of CLL and ibrutinib and acalabrutinib was commenced at week 2 with all mice culled at week 5. Figure 9.2 shows progression of PB CLL during this experiment, showing that whilst the CLL certainly responds to treatment, these mice still have very evident leukaemia at the end of this part in the PB. In AT TCL1 experiments of acalabrutinib vs. vehicle alone, acalabrutinib significant improves mouse survival (70), but for this experiment I deliberately chose the period of plateau of CLL response to cull the mice, hypothesizing this would be the time of maximum T cell effect. There was no significant difference between CLL load in the PB of acalabrutinib and ibrutinib treated mice.

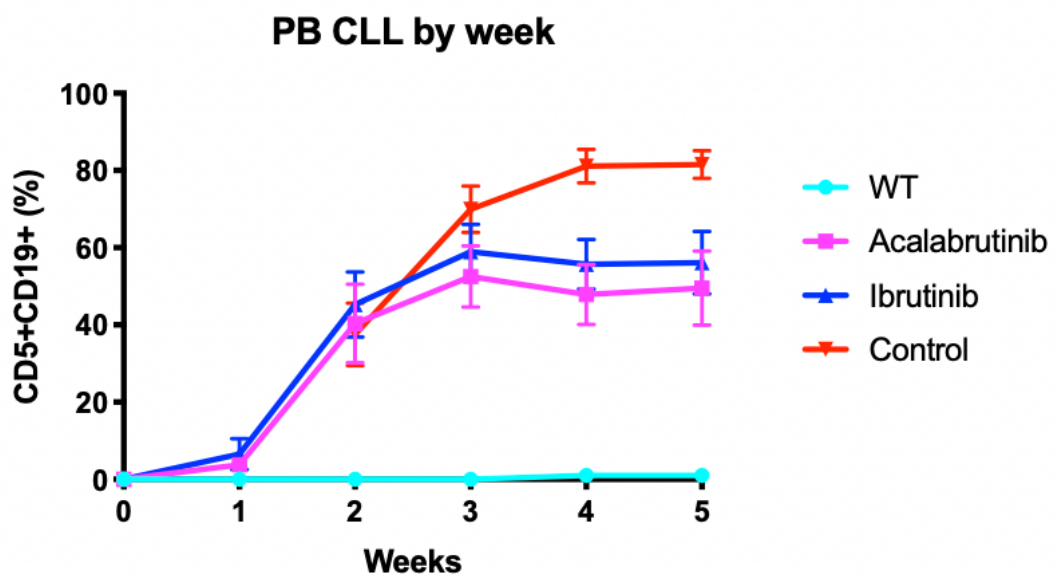


Figure 9.2: Percentage of DAPI-, viable mononuclear cells in PB that are CD5⁺CD19⁺ in weekly blood tests after commencing BTKi at week 2 in 48 mice.

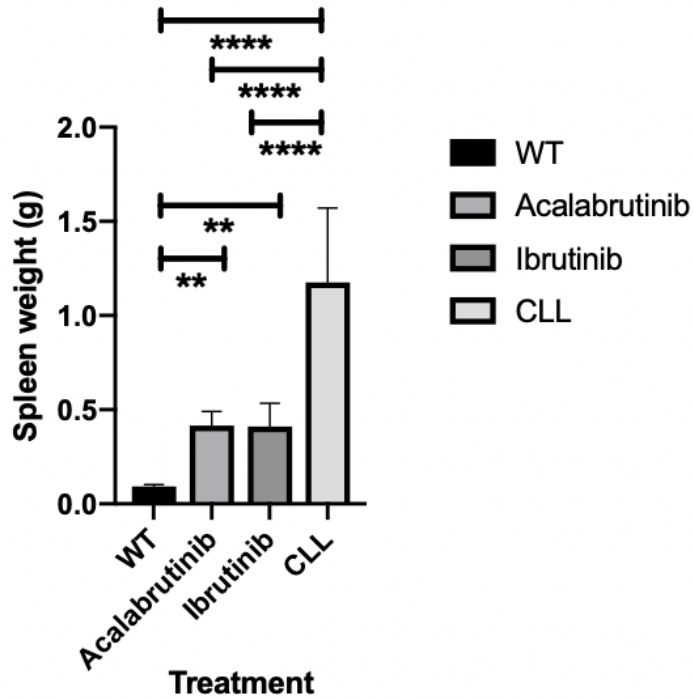


Figure 9.3: Differences in the spleen weight when culled at week 5 after AT of CLL at week 0 separated by BTKi treatment group in 48 mice.

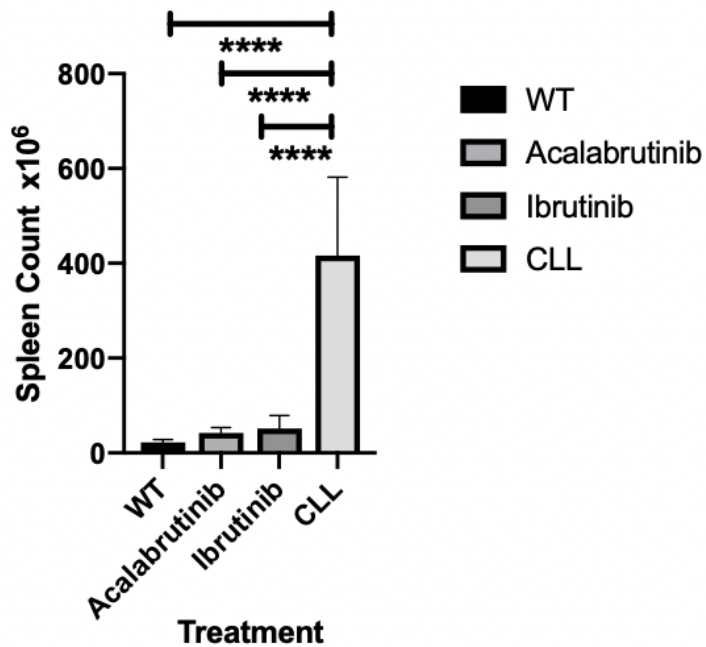


Figure 9.4: Differences in the total viable cell count of spleens of mice culled at week 5 after AT of CLL in each treatment group determined by an automated dual fluorescence (acridine orange/propidium iodide stain) haemocytometer (Logos Biosystems, South Korea) in 48 mice.

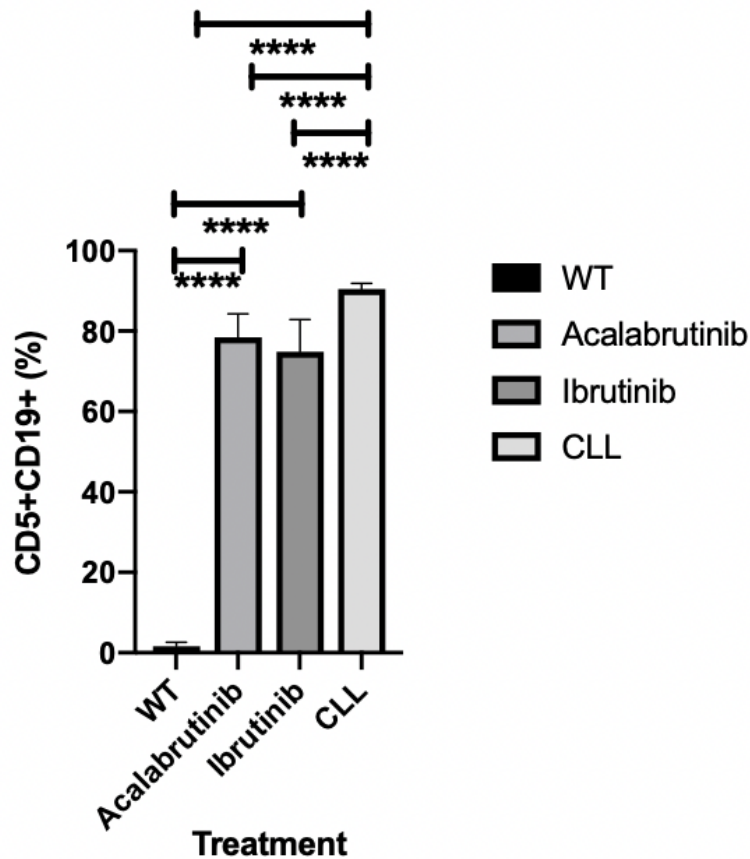


Figure 9.5: Percentage of DAPI-, viable mononuclear cells that are CD5⁺CD19⁺ in spleens when culled at week 5 after AT of CLL in each treatment group with significant differences in 48 mice.

As in previous experiments, spleen weight when culled reflects disease bulk of CLL at that time point (figure 9.3), as does total viable cell count of the spleen (figure 9.4). Acalabrutinib and ibrutinib significantly reduce spleen weight and total viable cell count compared to mice with untreated cell, but with no significant differences between the two BTKi performance by these measures. However, the CD5⁺CD19⁺% in the spleen of the BTKi treated mice remains very high, again not significantly different between ibrutinib and acalabrutinib, but both treatment groups were significantly lower than in a CLL spleen (figure 9.5). So whilst BTK inhibition results in much smaller spleens in these mice, they do contain considerable CLL load. However, in the PB there are significant differences between the two BTKi in terms of PD-1 expression, which is significantly reduced after treatment with acalabrutinib, but not ibrutinib (figure 9.6).

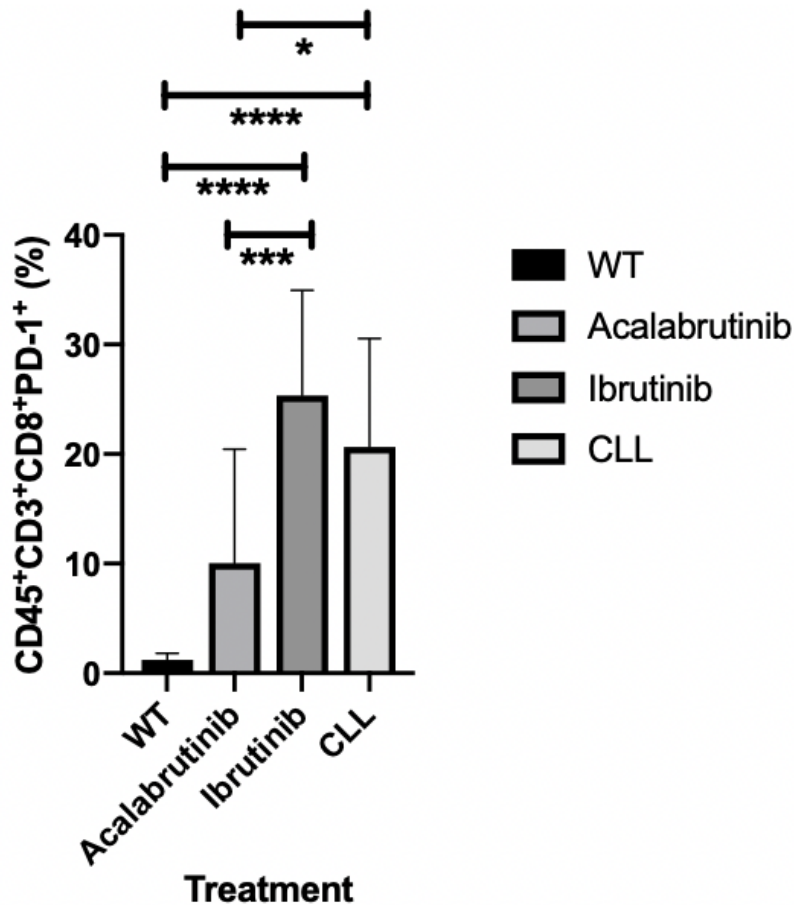


Figure 9.6: Percentage of cytotoxic T cells (CD3⁺CD8⁺) of DAPI-, viable mononuclear cells that have PD-1 expression in the PB at week 5, separated by treatment group showing significant differences (** $P < 0.01$, *** $P < 0.001$, **** $P < 0.0001$) in 48 mice.

9.4.2 CAR production and phenotype

CAR T cells were made for part 2, using pooled enriched T cells from the spleens of mice culled in part 1, separated by treatment group. The identical manufacturing process as previously described and optimized was applied to all T cells, and the retroviral supernatant used for transduction was pooled and split equally, so all groups of T cells were transduced with the same pooled and concentrated quantity of virus. Retroviral supernatant from the transfection of platinum-eco cells with MSGV-1D3-28Z-1.3mut (CD19-CD28) was made, concentrated with Retro-X and used fresh immediately prior to transduction.

Whilst the effect of CLL on T cell subsets has been described in previous chapters and in the literature, less is known about the effect of treatment with ibrutinib and acalabrutinib on T cell phenotype in this model. As there is evidence that subset selection for manufacture may impact on CAR efficacy it is important to describe the effect of ibrutinib and acalabrutinib pre-treatment on T cell subsets used for CAR manufacture. Table 9.1 shows the CD4/CD8% pre activation and post transduction in each of the pre-treatment groups. In this experiment, transduction seems to have the greatest effect on acalabrutinib and ibrutinib pre-treated CAR T cells, as there is reversal of their CD4/CD8 ratio not already established prior to transduction.

Treatment Group	Pre-activation (D0)		Post transduction (D4)	
	CD4 (%)	CD8 (%)	CD4 (%)	CD8 (%)
WT	44.8	58.4	47.4	48.5
CLL	24.8	72.3	10	62.7
Acalabrutinib	65.7	30.4	30.8	55.4
Ibrutinib	64.8	31.9	35.9	50.9

Table 9.1: Percentages of DAPI-, viable mononuclear splenocytes that were CD4⁺ and CD8⁺ subsets before (day 0) and after T cell activation and transduction (day 4) i.e. after CAR T manufacture separated by treatment group.

Overall, in this experiment the CD3⁺ T cells transduction efficiency was high in all groups. In the three groups of CAR T cells which had been exposed to CLL, there are again large differences in transduction efficiency noted between CD4 and CD8 subsets, which is not evident in WT mouse derived CAR T cells (figure 9.7). This appears to be partially reversed by both BTKi, but not fully.

Transduction efficiency by CAR T cell

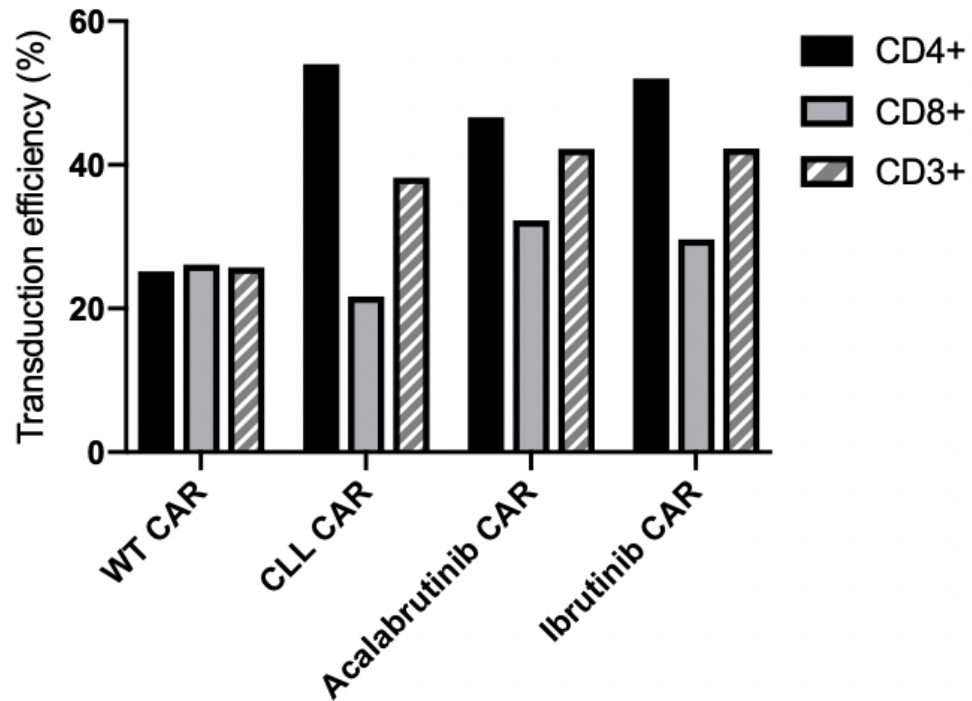


Figure 9.7: Percentage of cells in culture that are CAR⁺ (fab⁺) after activation and transduction i.e. transduction efficiency determined by cells that are DAPI-, viable, mononuclear and fab⁺ in CD3⁺/CD4⁺/CD8⁺ T cells separated by treatment group.

Again, there is a shift in CD3+CD8+ phenotypes which is exaggerated by the CAR manufacturing process, which can be partially reversed by ibrutinib and acalabrutinib pre-treatment. Table 9.2 shows CD3+CD8+ phenotype, pre-activation and post transduction, which again shows that CLL T cells disproportionately lose their naïve phenotype and shift to an effector phenotype post transduction and activation, whilst this effect is less marked with BTKi pre-treatment (table 9.2), which maintain more memory CD8+ T cells. After preparing single cell suspensions from the spleens of mice from part 1 for each pre-treatment group, around 20-30 x10⁶ T cells were enriched and then plated for 24 hours activation to be followed by CAR transduction.

	CD44 ⁻ CD62L ⁺	CD44 ⁺ CD62L ⁺	CD44 ⁺ CD62L ⁻
	Naïve (%)	Memory (%)	Effector (%)
WT pre	66.5	21.7	9.7
WT post	12.8	66.5	19.2
CLL pre	20.2	46.8	12.7
CLL post	0.095	49	50.7
Acalabrutinib pre	47.3	22.5	13.8
Acalabrutinib post	5.1	62.1	30.6
Ibrutinib pre	37.9	47.2	9.1
Ibrutinib post	4.7	59	33.0

Table 9.2: Percentages of DAPI-, viable mononuclear CD3⁺CD8⁺ splenocytes that naïve (CD44⁻CD62L⁺), memory (CD44⁺CD62L⁺) and effector (CD44⁺CD62L⁻) subsets pre (day 0) and post T cell activation and transduction (day 4) i.e. after CAR T manufacture separated by treatment group.

Remaining spleen and the bone marrow cell suspensions were prepared for freezing in cryovials as previously described for future work. Mice were each injected with between 5.5-6 x10⁶ CAR T cells, attempting to match the cell dose for each group in terms of viable CAR⁺ T cells, although this is not possible exactly because there are four groups with different transduction efficiencies. Table 9.3 shows the CAR⁺ cell dose given of between 1.3-2.3 x10⁶/mouse, which seemed optimum and feasible based on my previous experiments. However, matching for CD3⁺CAR⁺ cell dose leads to marked variability in CD4⁺/CD8⁺CAR⁺ cell doses. Of note, the only way to match the CAR⁺ cell dose for the CLL CAR mice, was to reduce the group size from 10 to 6, because of the significantly reduced ex vivo expansion of T cells in this group. This can be seen in table 9.3 by the total number of T cells post expansion and is significant, in that ibrutinib and acalabrutinib treated mice did not demonstrate impaired ex vivo expansion of their T cells when activated and transduced, as I have seen repeatedly in both Tg and AT CLL T cells, which is a bio-marker of CAR efficacy in patients (206). Again, as seen previously it is particularly challenging to match CD4⁺CAR⁺ cell dose because of markedly reduced

ex vivo expansion, but both ibrutinib and acalabrutinib reversed this effect. Overall, the expansion and resulting T cell subsets of CAR T cells with acalabrutinib and ibrutinib pre-treatment were very similar.

	T cells ($\times 10^6$)		CAR+ T cells ($\times 10^6$)		
	Total produced	T cells/mouse	CD3 ⁺ CAR ⁺	CD4 ⁺ CAR ⁺	CD8 ⁺ CAR ⁺
WT CAR	67.2	5.9	1.51	0.7	0.74
CLL CAR	32.7	5.5	1.32	0.19	0.47
Acalabrutinib CAR	59.5	5.95	2.34	1.22	0.99
Ibrutinib CAR	58.6	5.86	2.2	0.97	0.78

Table 9.3: Total number of T cells in culture determined by an automated dual fluorescence (acridine orange/propidium iodide stain) haemocytometer (Logos Biosystems, South Korea) by treatment group. Total number of T cells injected per mouse in each treatment group corrected by the percentage of CAR⁺ shown in figure 9.7 to give the number of CAR⁺ cells injected in each group by CD3⁺/CD4⁺/CD8⁺ subsets.

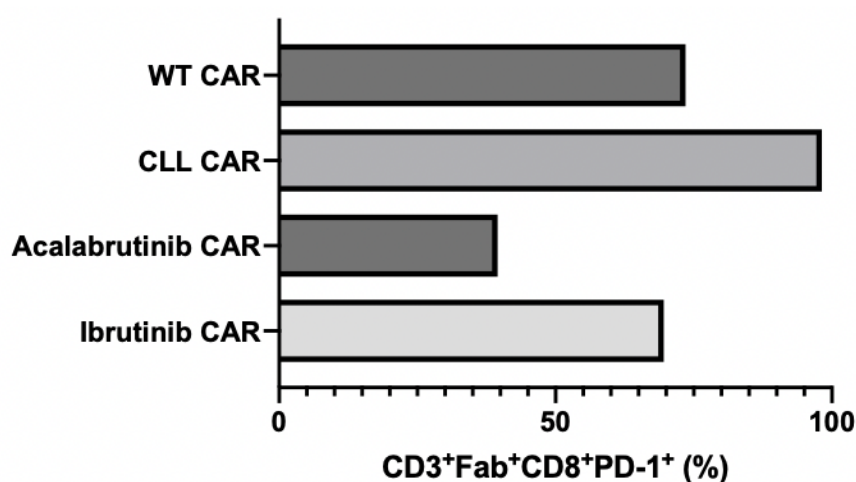


Figure 9.8: Percentage of cytotoxic CAR⁺ T splenocytes (CD3⁺CAR⁺CD8⁺) that have PD-1⁺ expression post activation and transduction under identical culture conditions separated by pre-treatment group. For each treatment group n=1 as CAR T cells were pooled and then split equally between the number of mice in that group.

PD-1⁺ expression is high on CLL T cells and CAR production increases PD-1⁺ in all groups as PD-1⁺ is also a marker of cell activation. It is difficult to interpret PD-1 expression immediately after completion of activation and transduction and compare this in if the CAR T cells came from mice with BTKi pre-treatment. It appears BTKi pre-treatment seem to reduce PD-1+ expression on the end CAR product (figure 9.8). However, when the T cells were taken out of culture they were pooled by group, so flow phenotyping was run once on each group before injecting into the mice. Figure 9.8 is therefore descriptive.

9.4.3 Efficacy of CAR T cells after pre-treatment with BTKi

In the second part of this experiment, a second large AT experiment required 50 mice to receive the same pooled CLL cells as previously described, with CLL engraftment being confirmed at weeks 1 and 2 in all mice. CAR T cells were injected after cyclophosphamide lymphodepletion one day before week 3 (D-1), after which mice had their first disease assessment at week 4 (D+7). All mice, except 3 mice from the ibrCAR group, had a complete response at D+7, with no normal or CLL B cells. The three ibrCAR treated mice lacking a complete response, had very low level CLL in the PB (<6%) with small but detectable normal CD19⁺ B cells (all <1%). This implies a failure of engraftment of the CAR T cells in these three mice, as opposed to early response and then disease progression. In these mice the drop in CLL is likely due to the preconditioning cyclophosphamide, which as I have seen in previous experiments does significantly reduce PB CLL after one week.

At week 4, early in the morning of CAR D+7, when the mice were checked prior to being transferred to the hot box to be warmed for pre-planned PB bleeds, all of the WT CAR treated mice looked sick and distressed, having been well the night before. There was no evidence of clinical distress in any of the other CAR treatment groups or the controls. The decision was therefore made to cull 8 of the 10 mice, as per our pre-defined end points in the project license. Two WT CAR mice in better condition were kept with mashed food to allow rapid rehydration and were clinically improved by the end of the day. Spleen, BM and PB were obtained for all culled mice, with

anticoagulated blood spun down and plasma frozen in -80°C for later analysis. Given previous experiments have clearly demonstrated peak CAR expansion at D+7, it was highly likely that the mice had some form of CRS or neurotoxicity. Perhaps CRS is more likely given the two surviving mice improved rapidly with rehydration. Unfortunately, planned cytokine analysis of the plasma has not yet been performed, but flow was performed on all D+7 PB samples to look for CAR expansion (figure 9.9). There are no significant differences between the percentage of CAR T cells in the PB in either CD4+ or CD8+ subsets considered separately, although there is a trend as I have shown before for CLL CD8+ CAR+ cells to represent a higher percentage of that subset at peak expansion. Whether this has any clinical meaning is unclear, as in all groups there is significant CAR⁺ T cell expansion at D+7.

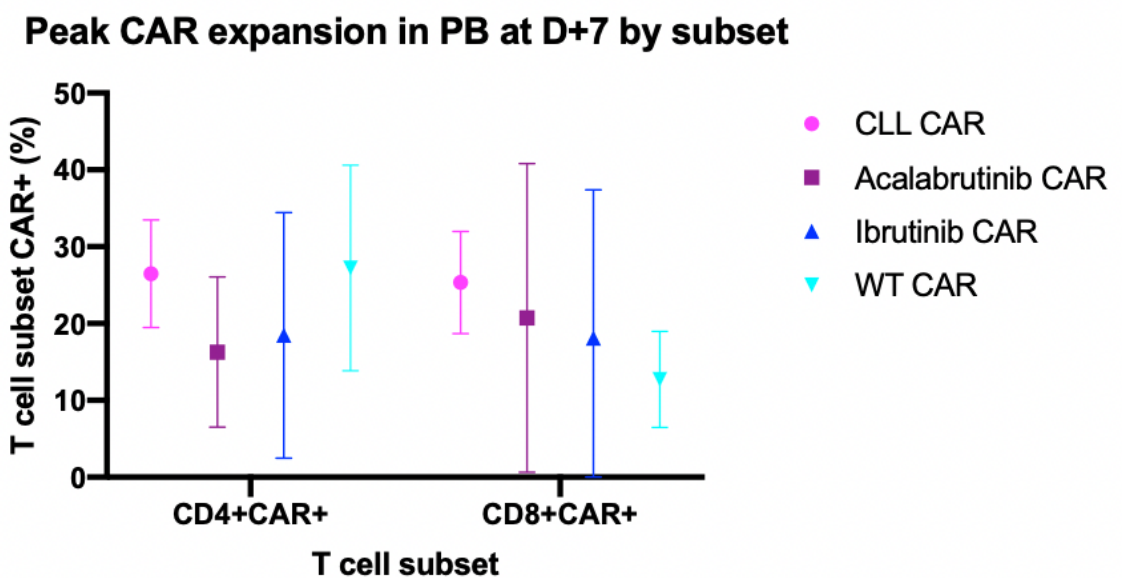


Figure 9.9: Percentage of DAPI⁻, viable mononuclear CD4⁺ or CD8⁺ that are CAR⁺ (fab⁺) in the PB at day 7 post CAR T injection separated by CAR pre-treatment group. No significant differences were seen on analysis by ANOVA.

Up till week 8, the mice were bled weekly and PB analysed for CAR T cells, T cell subsets, MDSC and macrophages. By week 8, some mice treated with cyclophosphamide and untransduced T cells appeared sick so all mice in the control group were culled separately. Since then all remaining mice have been bled every two weeks. However, as discussed above, the projected completion of this experiment will

end after the submission deadline for this thesis, so the complete analysis of this experiment is not possible at this point. Two ibrCAR treated mice that had not responded at D+7 demonstrated very slow progression, with a corresponding increase in the PB normal B cell population. They were pre-emptively culled at week 16 due to high PB CLL. All other mice currently seem to be in remission and look well with ongoing loss of normal and CLL B cells. Figure 9.10 shows the PB CLL results over the 20 weeks of follow-up to date. From weeks 8-10 there was a suggestion of low-level relapse amongst some mice treated with the CLL CAR, interestingly this reversed, which is perhaps a demonstration of the dynamic and ongoing tumour immunity CAR T cells have given the host.

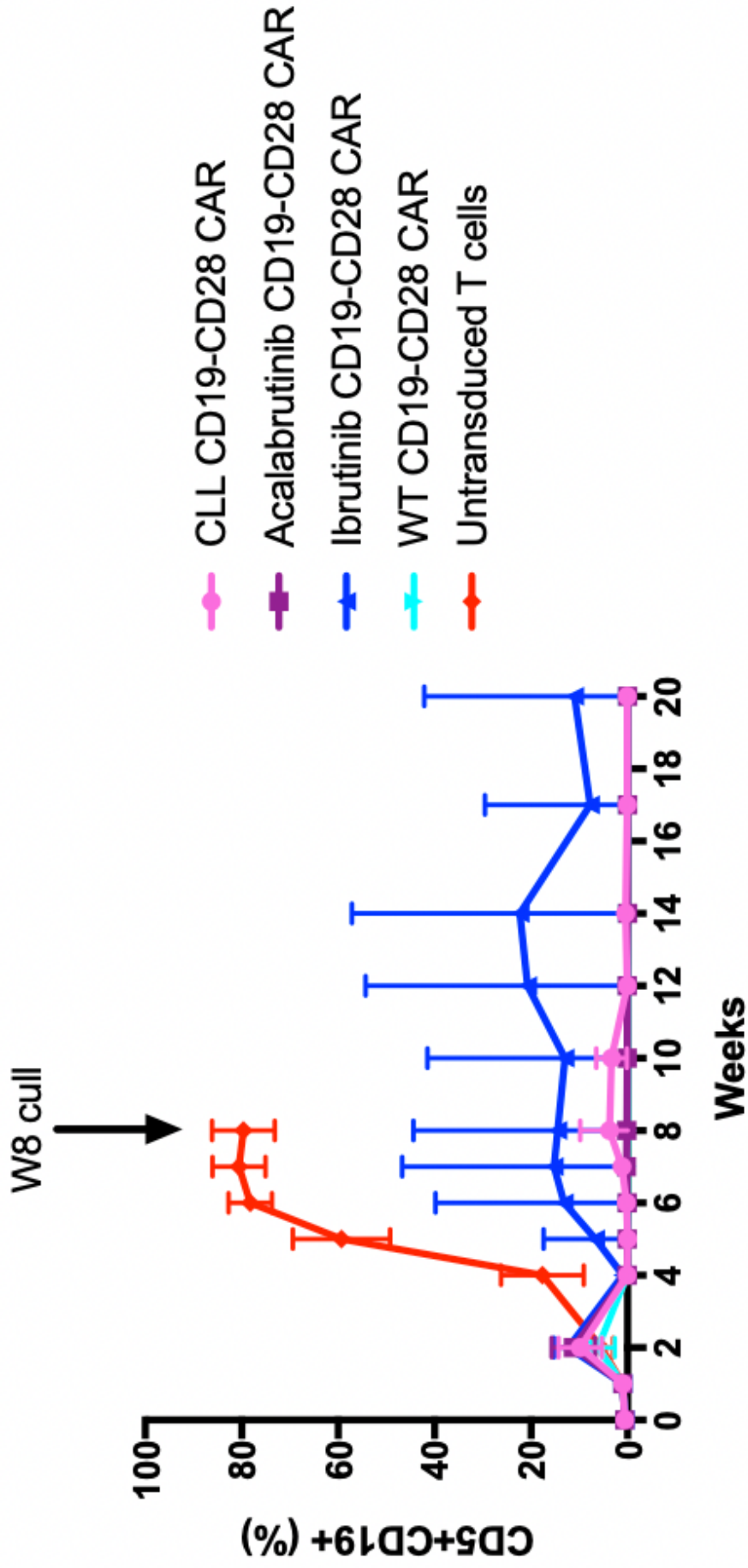


Figure 9.10. Progression of PB CD5⁺CD19⁺ by CAR T cell treatment group.

9.5 Discussion

Both ibrutinib and acalabrutinib have activity in the AT TCL1 model over a time limited experiment, as would be expected and has been previously demonstrated (70). At the point at which the effect of these BTKi in the PB had plateaued, mice treated with ibrutinib and acalabrutinib were culled and their T cells enriched from their spleens to make CAR T cells. Treatment with ibrutinib and acalabrutinib significantly reduces the spleen weight and total cell count of these spleens, although the cells that left remain highly infiltrated with CD5⁺CD19⁺ splenocytes. The same CAR T cell manufacturing process was then applied to these enriched T cells, as well as normal WT and fully leukaemic mice given the same CLL by AT, in age matched mice. There is resulting partial reversal of the CLL phenotype of BTKi pre-treated CAR T cells, despite there being high levels of CD5⁺CD19⁺ CLL evident in the spleens of these mice. This implies a direct T cell effect, that can partially correct measures such as ex vivo expansion, CD4:CD8 ratio, reduced disparity between CD4 and CD8 transduction efficiency, loss of naïve CD8⁺ T cells and an improved balance of memory to effector T cells reflected in the end CAR T cell phenotype. Certainly, acalabrutinib is a more specific BTKi than ibrutinib, with less off-target kinase effect (70). This experiment comprises two distinct but overlapping parts, with the second part meant to be a long-term survival experiment to model relapse risk after ibrutinib and acalabrutinib pre-treatment. The predefined endpoint of part 2 is the progression of disease in the majority of ibrutinib and acalabrutinib CAR pre-treated mice which has not yet been reached, therefore I cannot yet answer whether these resulting CAR T cell phenotypic changes are important for CAR T cell efficacy or perform a detailed comparison of the microenvironment in this model. However, preclinical studies have demonstrated that fixed combinations of CD4⁺ and CD8⁺ CAR T cells of varying naïve and memory phenotypes are more effective in xenograft ALL mouse models (208).

The ongoing second part of this experiment will address the issue of pre-treatment of CLL T cells in vivo with BTKi to improve CAR T cell efficacy by reversal of the CLL T cell phenotype. It will not address whether the addition of ibrutinib or acalabrutinib

alongside CAR T cells improve efficacy, although this model could be used to examine this question. In this model BTKi were only given in part 1, not in the second part with CAR T cells concurrently. Trials are underway in CLL which address whether a CD19-41BB CAR of fixed CD4: CD8 ratio (liso-cel) is effective in CLL, as well as studies investigating concurrent ibrutinib treatment, which have only been presented in abstract form for example at the recent International Conference on Malignant Lymphoma (ICML) in Lugano 2019 (288). In that study of 18 evaluable heavily pre-treated patients, 15 responded (Cri or PR) by iwCLL criteria (83%) including 11 patients (61%) who were MRD negative by IGHV sequencing, all of whom were alive at 1 year. Ibrutinib was scheduled from 2 weeks before leukapheresis to 3 months after CAR T cell infusion. From the work of these groups, two new toxicity signals have been identified. One patient died from a presumed ibrutinib induced arrhythmia during grade 2 CRS. However, although 14 patients developed CRS, all were grade 1-2. Despite the arrhythmia the author suggests that ibrutinib could perhaps make CAR T cells safer, due to a favourable cytokine response. This has been supported by preclinical data, Ruella et al. established a xenograft model of mantle cell lymphoma that can simulate CRS, demonstrating elevated serum levels of several human cytokines including IL6, IFN γ , TNF α , IL2 and GM-CSF. Mice xenografted the same mantle cell lymphoma and then treated with the same CAR with concurrent ibrutinib experienced longer overall survival, as well as significantly reduced cytokine levels (279). The use of acalabrutinib for this purpose remains novel, and would represent a logical step as most patients on CLL CAR studies have already been exposed to ibrutinib.

The unexpected finding at D+7 of the CAR experiment, was of the mice treated with the WT CAR becoming acutely unwell. I have not previously seen CRS in this model, but it is of course theoretically possible given these mice are immunocompetent. Other possibilities would include GVHD as the CAR T cells are syngeneic or perhaps infection. GVHD doesn't present acutely and resolve within 24 hours in mice, as it did in the two mice which were preserved from this group. Infection is always possible, but it seems unlikely an infection would only affect these two specific cages out of the many cages I was responsible for including for this experiment and my general colony mice. Again,

this experiment is ongoing and although I have samples frozen from D+7 to run cytokine analysis, I do not yet have these data to support my theory that AT transfer of TCL1 CLL can be used to model both CAR function and also demonstrate CRS, and that both ibrutinib and acalabrutinib pre-treatment reduce cytokines to safer levels. This would be an important and novel finding.

There are evident limitations to the interpretation of the efficacy part of this experiment, when compared to previous experiments. The TCL1 model and AT of TCL1 splenocytes are known to result in a heterogeneous phenotype of CLL. From my experience of having carried out AT of TCL1 many times, typically after AT of a reasonable cell dose, e.g. 20-30 $\times 10^6$ splenocytes, most mice in control groups, or treated with untransduced T cells would get sick and need to be culled before week 8. In part 2, the mice were injected with 23 $\times 10^6$ pooled splenocytes each, even after becoming fully leukaemic at week 6, the control mice treated with cyclophosphamide and untransduced T cells did not immediately show signs of ill health. This implies to me that the mice in part 2 have received a relatively indolent CLL pool, which is less useful in this situation as the purpose of part 2 is to model the progression or relapse risk post treatment with pre-treated CAR T cells. I have extensively investigated WT and CLL derived CAR T cells in previous chapters so they provide the positive and negative controls to this experiment to the groups of interest which are ibrCAR and acalaCAR. In Chapter 7, we saw by week 6 multiple mice treated with a CLL CAR relapsing, which has not been the case in this experiment. All of the CLL CAR treated mice in part of this experiment remain in remission, although late relapses are perfectly possible. For these reasons, the remaining mice are being monitored in a long-term survival experiment, so the detailed analysis of this experiment cannot yet be performed. There was certainly an engraftment issue of CAR T cells with 3 mice treated with the ibrCAR, which on reflection may simply represent technical issues with tail vein injections for those mice. This explains the appearance of the ibrCAR curve figure 9.9, which is due to CLL progression of the 3 mice which did not demonstrate CAR expansion at D+7, and at that point had both low level CLL and normal B cells.

10. Overall Discussion

Differential outcomes for CD19 CAR T cells between CLL and ALL illustrate unique challenges to overcome in different patient populations treated with the same investigational and licensed products. In ALL, initial remission rates are very high, but many patients will ultimately relapse (184). Conversely, CR rates in CLL are much lower, but can be remarkably durable (150, 151). Reasons for these differential outcomes receiving the same agents are both complex and poorly understood, and some of the strategies discussed may overcome these challenges.

The central hypothesis to then explore with this model, is that impaired T cell function explains the lower response rates seen in fully reported human clinical trials in CLL. The majority of pre-clinical testing of CAR T cells in general has been reported using xenograft models of human disease or cell lines into immunodeficient mice (208). Whilst this gives a good indicator of efficacy, it does not allow for complex modelling of the host immune response. In contrast to human T cells, which are readily transduced and expandable in the ex vivo setting, retroviral transduction of mouse T cells is compromised by poor gene transfer and inadequate subsequent T cell expansion and survival. My methods are derived from collaborations with the Sadelain laboratory at MSKCC, and I have optimized their methods to demonstrate rapid expansion of mouse T cells in culture using CD3/CD28 beads and mIL2 (145). Troubleshooting experiments particularly identified efficient transduction depends on concentrated viral supernatant produced using appropriate ecotropic packaging cells of low passage. In vitro experiments in Chapter 6 demonstrate the reduced cytotoxicity of the CD19-41BB compared to CD19-CD28 CAR T cells. When using these CAR T cells in an in vivo model in Chapter 7, CD19-41BB CAR T cells do not engraft and expand in the PB, or show efficacy like CD19-CD28 CAR T cells. A major difference in the construction between the two plasmids used is that CD19-41BB also has GFP, which CD19-CD28 does not, which may have relevance for the rejection of these CAR T cells. Certainly, this does not extrapolate to clinical practice in patients, where the most significant reported studies in CLL use CD19-41BB based CAR T cells (160, 161,

289). Recently there has been more limited evidence for efficacy of CD19-CD28 CAR T cell in CLL, although again low CR rates of 25% were demonstrated, but those patients achieving a CR had durable responses (290). Other reports have suggested the persistence of CD19-CD28 CAR T cells to be around 30 days (168, 291), in contrast to the sustained detection of CD19-41BB CAR T cells over 4 years after infusion (160). CD28 results in a more rapid expansion of CAR T cells and potentially faster tumour elimination in preclinical modelling (292). There is evidence CD19-41BB in certain CAR T cells ameliorates exhaustion (132), which presumably in CLL would be beneficial. Whether the limited engraftment of CD19-41BB I have seen is a species effect is unclear. Different co-stimulatory domains regulate specific metabolism pathways and impacts memory development in CAR T cells in vitro, with CD19-41BB leading to increased memory differentiation of CD8⁺ T cells and inducing mitochondrial biogenesis (177). CLL CD8⁺ T cells have reduced intracellular glucose transporter 1 (GLUT1) reserves, and have an altered mitochondrial metabolic profile resulting in impaired mitochondrial biogenesis upon stimulation (293). In a recent analysis of CD8⁺ CD19 CAR T cells prior to infusion in CLL patients, it was found that in patients with a subsequent CR, the infused CAR T cells have increased mitochondrial mass, compared to non-responders, which positively correlated with expansion and persistence of CAR T cells (294). Further, those patients with high mitochondrial mass correlated with CD27⁺ T cells that were negative for PD-1, TIM3 and LAG3 (294). Boosting mitochondrial biogenesis may therefore improve the efficacy of CAR T cells in CLL. Because production of CAR T cells requires both transduction of a CAR construct and ex vivo expansion, strategies could be designed as part of these processes to optimize metabolics to enhance CAR response.

Relatively, there remains a very small number of patients treated with these therapies and the reversal of the underlying T cell defects remains a promising strategy to help CAR T cells fulfil their potential in CLL. In Chapter 8, we see in a large in-vivo experiment where the key variable is the T cell source; mice given the same pooled leukaemia both initially fully respond to normal and CLL T cell derived CAR T cells, but mice treated with CLL T cell derived CAR T cells slowly relapse whereas mice treated with WT T cell derived CAR T cells do not. This is an exciting observation, as it focuses

the need for future research into optimizing T cell function prior to leukapheresis and researching strategies which can improve T cell function. This could be done in a number of ways. CLL clearly impacts T cell subsets in both humans and mouse models and progressive disease results in increased expression of exhaustion markers on T cells and a shift to a more terminally differentiated effector phenotype with loss of naïve T cells (94, 118). This may be significant when deriving CAR T cells from such an autologous T cell source. Since the source of CLL T cells in this model is CLL by adoptive transfer, it demonstrates that normal T cells only need exposure to CLL for a short period of time in vivo, in this case around 6 weeks, to significantly impair T cells enough to result in impaired CAR T cell function. This is fascinating, and emphasizes that it is the effect of the CLL on the T cells itself that is important, and perhaps not previous lymphocyte targeted chemotherapy such as the use of fludarabine which is often cited as an iatrogenic reason for impaired T cell function in CLL. The experiment also removes the confounding factor of age, as both normal T cells and CLL T cells are derived from the same aged matched litters, with the T cells of leukaemic mice being harvested around 6 weeks after AT.

In Chapter 8 the addition of the PD-L1 antibody did not impact on the relapse rate for mice receiving CAR T cells derived from CLL T cells. Further, as a treatment alone following engraftment of CLL it did not have activity, which at first appearance seems in conflict to previous reports from our group (96). However, this study showed that the same PD-L1 antibody prevents engraftment of CLL by AT in this model, so it should not be surprising that the kinetics of the disease preventing engraftment and its susceptibility to checkpoint inhibition differs from established and rapidly progressing disease. This model is ideal to study CAR plus novel immunotherapeutic approaches, and further work would combine CLL T cell derived CD19 CAR T cells with alternative or perhaps combinations of drugs including checkpoint inhibition. There are many alternative commercially available murine PD-1 inhibitors which could be tried either concurrently or as pre-treatment to optimize leukapheresis product by helping reverse the exhausted T cell phenotype.

An alternative strategy to improve CAR T cell function is to use the off-target T cell effects of BTK inhibitors to optimize T cell function or subsets, even in the context of a patient that has disease progression on ibrutinib. Given most patients with CLL have failed ibrutinib this also may be an exciting new indication for acalabrutinib. In Chapter 9 I describe a complex two-part experiment where mice are treated with ibrutinib and acalabrutinib as pre-treatment to optimize T cell phenotype and perhaps T cell function as a source of cells for CAR T cell manufacture. As the second part has been designed as a long-term relapse study it is not yet complete and the full efficacy data is not yet available. Future work will include detailed assessment of the microenvironment in mice treated with CAR T cells derived from mice with BTKi pre-treatment. In xenograft models of ALL, identifying subsets of T cells for manufacture confers superior efficacy, and it seems clear that both CD4⁺ and CD8⁺ CAR T cells are required (208). In the AT TCL1 model increasing CLL leads to a relative increase in CD8⁺ T cells (96), which is exaggerated when these T cells are enriched, activated and transduced to become CAR T cells. I have repeatedly demonstrated that when an optimized CAR manufacturing process is applied to both CLL and normal T cells, CLL CAR T cells skew to CD8 with lower transduction efficiencies and less ex vivo expansion. The proliferative capacity of T cells correlate with the anti-tumour activity of CAR T cells in CLL (206), and in this this experiment both ibrutinib and acalabrutinib pre-treatment restores ex vivo expansion compared to WT T cells. This may be important because CAR manufacture of CLL T cells is leading to a subset ratio that is less favourable for CAR T cell efficacy. This illustrates the importance of taking even established therapies back to preclinical modelling. Future work with this model should include a CAR T cell subset titration experiment, where different proportions of CD4 and CD8 CAR T cells are combined to treat AT TCL1 to see if increased efficacy can be demonstrated in a particular combination or ratio. To a degree this is already been explored with the clinical use of Liso-cel in the TRANSCEND studies, which use a CD19-41BB CAR in a 1:1 ratio of CD4: CD8 CAR T cells, with good preliminary efficacy results demonstrated in CLL (289).

In Chapters 7-9, when looking at the dynamics of CAR expansion, peak CAR⁺ T cells in the PB were always seen at D+7. Progressions were always CD19⁺, and mice with ongoing responses maintained their loss of normal CD19⁺ B cells. Going forwards, the type of progression in terms of CD19 detection is important for researching the implications of that progression. Mechanistic studies of relapsed tumours negative for CD19 after CAR T cells describe alternatively spliced isoforms lacking exons critical for CAR binding, including loss of epitopes recognized by the CAR or proteins involved in surface expression (295). In the pivotal CD19-41BB ELIANA study, 15 of 16 patients who progressed had ALL that lacked CD19 (184). Efforts in paediatric ALL have therefore been focused particularly on CAR design, for example bispecific CAR T cells, combining either CD22 or CD20 recognizing antibodies to the scFv of established CAR T cells. Many more adult patients with NHL have now been treated with licensed CD19 CAR T cells due to how much more common this disease is and preliminary abstract data from the ZUMA-1 study indicated of those patients which had relapsed biopsies 67% were CD19⁺ and 33% CD19⁻ (189, 190). In my current role at King's College Hospital our own cohort of 32 lymphoma patients treated with CD19 CAR T cells, 5 out of 6 patients with progression have been proven to be CD19⁺. This implies failure of CAR T cells to overcome the immunosuppressive microenvironment and future research should focus on how to overcome this. Phase 1 clinical trials combining CAR T cells with checkpoint inhibitors are already underway in the USA. Future exploratory work to study the phosphoproteomics of both enriched T cells collected at leukapheresis prior to transduction and CAR T cells themselves could identify relevant tyrosine kinases that may represent potential drug targets to enhance CAR T cell function.

There are of course limitations to these findings. The TCL1 mouse model is well established in the field of CLL research, particularly to model the T cell defects, on both a genetic and functional level (89). Given the long disease latency of the transgenic model, and that our group has fully characterized AT of TCL1 leukaemia into WT mice (118), AT TCL1 represents an extremely flexible and useful model in the investigation of potential therapeutic interventions in CLL. However, it may not fully represent the genetic complexity of CLL. TCL1 is highly expressed in U-CLL and this model resembles

an aggressive form of human U-CLL which has wild type *p53* (112). Therefore, this may mean the TCL1 model cannot be used to investigate *p53* resistance. Clearly, *TP53* mutations are clinically significant and are likely to be over-represented in CLL patients who need CAR T cells, for example in the phase I/II TRANSCEND of Liso-cel in relapsed refractory CLL, 60.9% of patients have a *TP53* mutation (289).

Further, it is already known that CLL is a two-compartment disease in which CLL cells are trafficked between peripheral vasculature and lymphoid tissues. Gene expression profiling studies of CLL in different compartments identified the lymph nodes as the predominant site of CLL activation and proliferation (109). In this model, all CAR T cells are derived from enriched spleen single cell suspensions, not the peripheral blood as would be the case in patients. There are known phenotypic and functional differences between T cells in these different compartments (110) and this may be reflected in CAR T cell function. Also, the cell dose given to the mice is relatively very large. The licensed cell dose of axi-cel is 1-2 $\times 10^6$ /kg CAR⁺ cells. Since a mouse typically weighs around 25g, and the mice in these experiments have typically been given 1-2 $\times 10^6$ CAR⁺ cells, this would be equivalent to 40 $\times 10^6$ CAR⁺ T cells. The significance of cell dose in clinical practice is not yet clear although it does seem that in the CLL CAR T cell studies much higher cell doses are required than in lymphoma. This could also be further investigated using this model.

Whilst the acquired T cell dysfunction that progresses with CLL is well described, it is unknown if the same T cell defects lead to the reduced efficacy seen in autologous CD19 CAR T cells in CLL. Specific T cell abnormalities include the impaired immunological synapse (88) and pseudo-exhausted T cell phenotype with impaired proliferation and cytotoxicity in CD8⁺ CLL T cells (94). Genetic and functional defects can be acquired by co-culture of previously healthy T cells with CLL cells, implicating a directly immunosuppressive effect by leukaemic B cells (87, 88). This is supported by these in vivo experiments, as the 'co-culture' of healthy T cells within WT mice become functionally impaired after the AT of TCL1 after as little as 6 weeks in terms of CAR T cell efficacy. In the future, a solution for avoiding the T cell dysfunction inherent in using autologous T cells from CLL patients could come from using alternative effector

cell sources. Allogeneic CD19 CAR T cell studies are in their infancy, one of the most significant having reported at ASH in 2018 (246). Such cells require two genetic manipulations, firstly a lentiviral transduction of CD19-41BB into healthy donor T cells followed by TALEN disruption of TRAC and CD52. Whilst such cells show efficacy in relapsed adult ALL, they are also very myelosuppressive and require the use of alemtuzumab for engraftment, which brings other clinical challenges such as viral reactivations and the need for rescue HSCT in some patients. An exciting alternative which avoids the use of alemtuzumab is the development of CAR NK cells derived from lentivirally transduced cord blood NK cells. The MDACC has open a phase 1 study for patients with relapsed or refractory CD19⁺ lymphoid malignancies, demonstrating CR in 6 out of 9 patients, 5 of whom had CLL or Richter's transformation (Rezvani, Personal Communication).

With two licensed CD19 CAR T cells covering DLBCL, tFL, PMBCL and ALL, with more indications likely to be approved soon such as for mantle cell lymphoma, the use of this form of cellular therapy is now fully embedded in the repertoire of treatments available for lymphoid malignancies. In lymphoma, CAR T cells have been used safely as part of consolidation D+2-3 post BEAM autologous stem cell transplant (296). The CD19 CAR most likely to be approved first for CLL is Liso-cel, which targets CD19 FMC63 as per the other two licensed products but uses a specific 1:1 CD4: CD8 ratio of CAR⁺ T cells. Combining CD19 CAR T cells with ibrutinib for either pre-treatment prior to leukapheresis or concurrently post infusion improves clinical responses, albeit in small numbers of patients treated (288, 289). The field is moving incredibly quickly, with advances in CAR design such as novel antigens, bispecific targeting and augmentation of the immune activating potential using CAR designs that combat the immunosuppressive microenvironment by secretion of cytokines or checkpoint blocking moieties. Alternative methods for gene editing such as CRISPR/Cas9 allows the CAR transgene to be targeted at a specific genetic locus, potentially could increase efficacy and reduce the risk of mutagenesis (297). This technology could also allow unwanted genes to be removed, such as inhibitory signals. Safety remains a key concern, as most CAR studies demonstrate significant CRS and ICANS with deaths reported from CAR related complications such as HLH and cerebral oedema. Suicide

switches have been incorporated into some novel CAR designs. Recently, the tyrosine kinase dasatinib has been shown to switch off phosphorylation in vitro and activity in xenografts using both CD19-CD28 and 41BB (298). They also demonstrated it could be used as an emergency drug to reduce mortality from CRS in a xenograft model of CRS, reducing mice mortality and cytokines typical of CRS such as IL6, IFN γ , IL2, GM-CSF and TNF α . This is an important finding because the use of safety switches in CAR design is likely permanent, whereas the effect of dasatinib was temporary and reversible, so could be used as a bridge during serious neurotoxicity for example without compromising the long term efficacy.

In CLL there is now certainly financial toxicity. Novel agents such as ibrutinib and venetoclax induce high response rates and are generally well tolerated, but their use as monotherapeutic agents are not curative. As a consequence, continuous therapy is required, leading to long-term remissions, but also high cost, toxicity, long-term compliance issues and increased risk of resistance. Indeed, for both drugs, resistance mechanisms have been described that lead to the bypass of the actions of these drugs (58, 285). Therefore, there is still scope for the use of CAR T cells in CLL, and the financial toxicity of the long-term treatment with expensive drugs, could be replaced by the use of a once only therapy like CAR T cells earlier in treatment algorithms. This would also potentially have the advantage of using autologous T cells which are less impaired. Further, an alternative strategy would be to offer patients with high risk genetic disease collection of their PBMC after responding to ibrutinib, at a time point when they are not heavily pre-treated and also likely to have optimized quality of T cell function.

There remain many areas of need. For example, in lymphoma there are now two licensed products that are being used in the NHS, broadly in line with the major trial criteria, but many potentially suitable patients fall out with the eligibility criteria due to the specific nature of the way these licensing studies were designed. One group is patients with primary and secondary CNS lymphoma, an area of huge clinical need but who were ineligible for prior studies due to concerns about potentially fatal neurotoxicity. Until recently, only one case report has been published demonstrating

the efficacy of CD19 CAR T cell directed therapy in a patient with simultaneous CNS and systemic involvement (299). This year, a case series of 8 patients was reported with early response assessments demonstrating activity within the CNS (300). The kinetics of responses were similar to those of systemic disease and high rates of neurotoxicity were not seen, suggesting CNS disease is not a risk factor for neurotoxicity. This is in line with recent reports suggesting CAR T cell mediated neurotoxicity is a CNS manifestation of an otherwise systemic inflammatory response involving blood brain barrier breakdown, endothelial and macrophage activation (280, 301). To reduce the anxiety of using cellular therapy for CNS disease has important implications for CAR T cells across oncology, because clearly many cancers invade the CNS, particularly in their end stage when patients are most in need of clinical trials. HIV is often an exclusion criterion for cellular therapy studies, but particularly with lymphoma given the increased incidence in this patient group, there is a real need for expansion of this treatment modality to this group of patients.

This type of cellular therapy as a platform in oncology has now arrived and is rapidly expanding. The momentum that has been generated behind CD19 CAR T cells is likely to accelerate to the translation of engineered cell therapies for not only blood and lymph node cancers but across solid tumour oncology and indeed in many other conditions of inflammatory, autoimmune and infective causes. The microenvironment is a challenge for the application of CAR T cells in solid tumours, which could be overcome using amphiphile ligands, when injected they traffic to lymph nodes and decorate the surface of antigen presenting cells, priming CAR T cells in the native lymph node microenvironment (302). Once these challenges of the microenvironment are overcome the opportunities for this cellular therapy in CLL are very broad.

10.2 Summary

The central hypothesis investigated in this thesis states the inefficiencies of CAR T cells in CLL are due to defects in T cell function. Whilst the TCL1 CLL mouse model is well established in the investigation of the CLL microenvironment, its use as a source of syngeneic T cells to model CAR T cell function is novel. I have described an optimized method for making retrovirally transduced murine CD19 CAR T cells from both normal and CLL T cells, which can be expanded ex vivo for downstream experiments. When applying this identical manufacturing process to both WT and CLL T cells, the latter exhibit reduced transduction efficiency and poorer ex vivo expansion. The CAR T cells that are made from CLL or normal T cells, exhibit markedly different phenotypes. Activation during ex vivo expansion skews most transduced T cells to CD8, but much more markedly so for CLL T cells, with a more marked loss of naive T cells. CLL T cells can be either primary transgenic TCL1 CLL T cells, or CLL T cell after AT of CLL, the latter demonstrating improved ex vivo expansion and viability making them a more feasible cell source for in vivo experiments. I have demonstrated AT of TCL1 CLL into immunocompetent mice is a viable model in which to study in vivo CAR T function and the host immune response. Syngeneic CD19-CD28 CAR T cells engraft in B6 WT mice when derived from both CLL and normal T cells, inducing both CAR⁺ T cell expansion in the PB of mice and also B cell aplasia. However, mice treated with CLL derived CAR T cells were liable to relapse with CD19⁺ disease, and the addition of a PD-L1 antibody did not improve this. Ongoing B cell aplasia seems necessary for an ongoing CAR response, although CAR T cells in the PB are generally undetectable after only two weeks even with an ongoing response. Low level MRD relapse detected by flow cytometry always resulted in florid relapse, which are useful observations in the clinical management of patients with CLL post CAR T cells.

There are limitations to the interpretations of these data. The CD19-41BB CAR showed some activity in vitro but no real activity in vivo, whilst the CD19-CD28 showed good efficacy. This is contrary to the clinical experience using CD19 CAR T cells in patients, where most trials opt for the persistent CD19-41BB CAR. Whilst both CAR plasmids have the same single chain variable fragment, the difference in performance is likely

related to the promoter and therefore the difference in in vivo activity demonstrated in this model between CD19-CD28 and CD19-41BB is not clinically relevant.

Whilst I made every effort to remove confounding variables from the in vivo experiments they still exist. For example, between groups I matched cell dose for the number of CAR⁺ T cells, but the differences I have described in transduction efficiency and subsets after ex vivo expansion means this inevitably results in differences in CAR⁺ phenotype between groups within the same experiment. Lower transduction efficiency in CAR T cells derived from CLL T cells means more CAR⁻ T cells are injected, the effect of which is unknown. Differences in PD-1 expression determined by flow cytometry, must be taken in a wider context using other techniques, to determine if they represent activation or exhaustion. Increased cytokine testing of PB samples after CAR T cell injection to characterise exhaustion would be particularly useful in this regard.

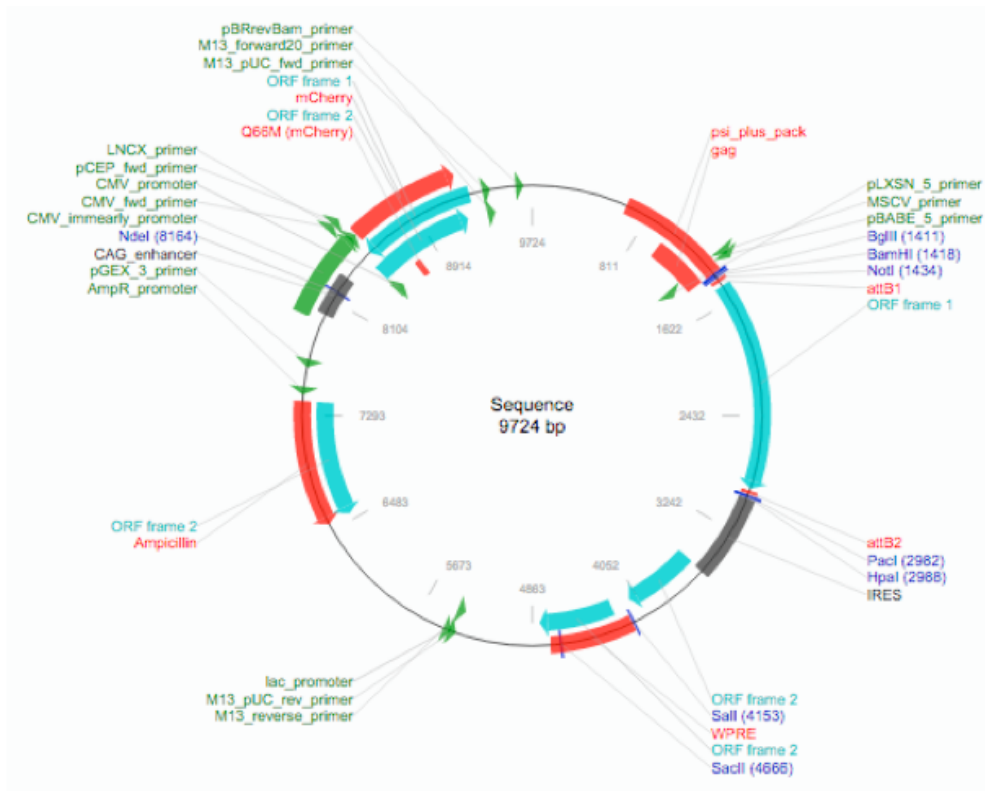
Future work can be multifaceted, my main focus would be to maintain the broad in vivo experimental design, but many other variables could be explored. Optimisation of ex vivo expansion, using novel methods of activating and expanding T cells could be investigated, for example using other cytokines or target cells which may lead to less T cell exhaustion. There are non viral methods for gene transfer such as electroporation and more novel methods of gene editing such as CRISPR and base editing which could be investigated. Rather than activating, transducing and expanding only CD3⁺ enriched T cells, it would be possible to make CAR T cells of defined subset ratios, be that CD4/CD8 or more complex subgroups of naïve, effector and memory T cells. This could be done using magnetic kit enrichment or cell sorting with flow cytometry. Rather than injecting a mixture of CAR⁺ and CAR⁻ T cells which is the same as what is done using the licensed CD19 CAR products, CAR⁺ T cells could be enriched at the end of manufacture and purified, to remove the unknown effect of CAR⁻ T cells. Further work could be done with this design titrating the cell dose to the minimum numbers of cells required to induce remission. This would be a useful step prior to another aim of future work, which would be to try alternative CAR and drug combinations. In subsequent experiments following completion of this thesis measuring plasma cytokines using

electrochemiluminescent sandwich immunoassay have been successful, and it would be important to measure changes in cytokines and correlate with the exhausted phenotype of CAR T cells in the PB after CAR T cell injection. Whilst CAR T cells plus cytotoxic chemotherapy options are not a likely way forward, there are many small molecule or kinase inhibitors which could be investigated. Some drugs of interest include the concurrent administration of CAR T cells plus the BTKi rather than pre-treatment using these drugs. Finally, drugs which have the potential to modify the cytokine profile post CAR T cell injection such as GM-CSF antibodies have demonstrated efficacy in an immunodeficient model of ALL (303) but would be of interest in this immunocompetent model.

In conclusion, in this thesis I have demonstrated that the underlying T cell dysfunction seen in CLL is important for CAR T cell function in both in vitro and immunocompetent in vivo modelling. AT of TCL1 CLL is an ideal model to study novel CAR plus immunotherapeutic strategies to improve CAR T cell function, which has broad relevance to improve this exciting new platform of immunotherapy.

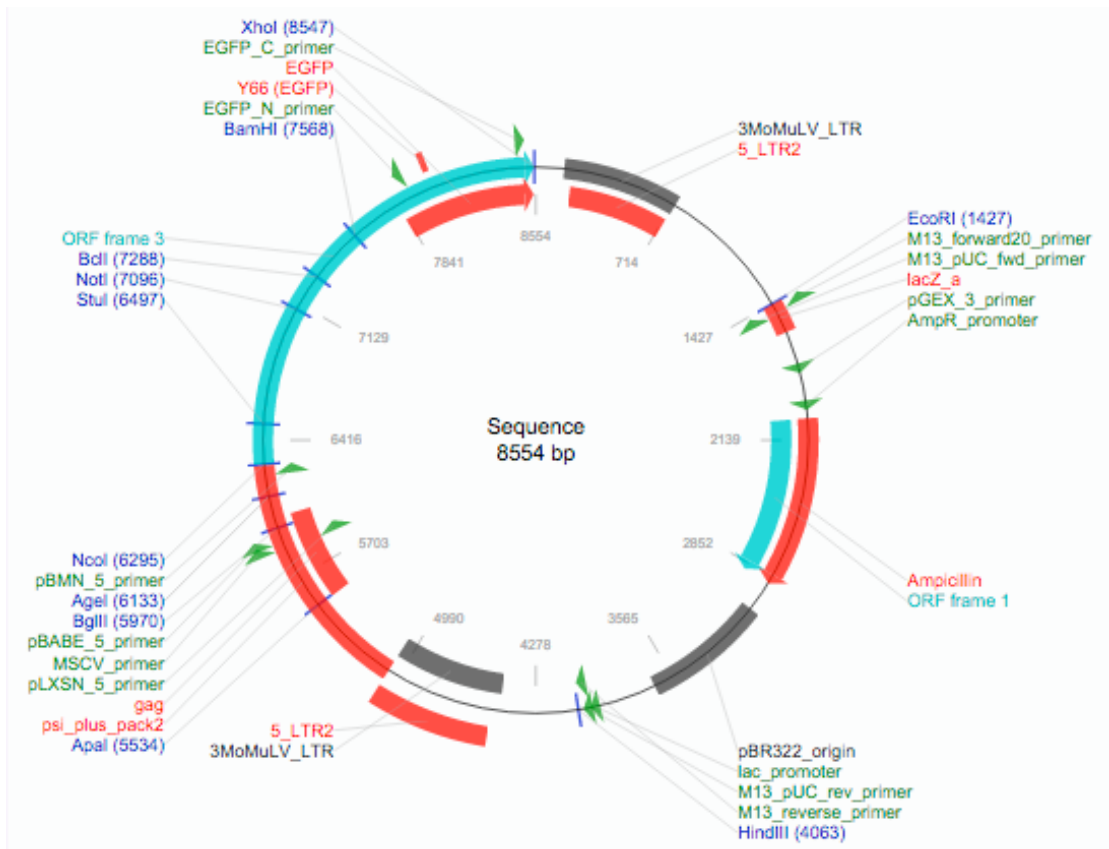
11. Appendix

Appendix 1

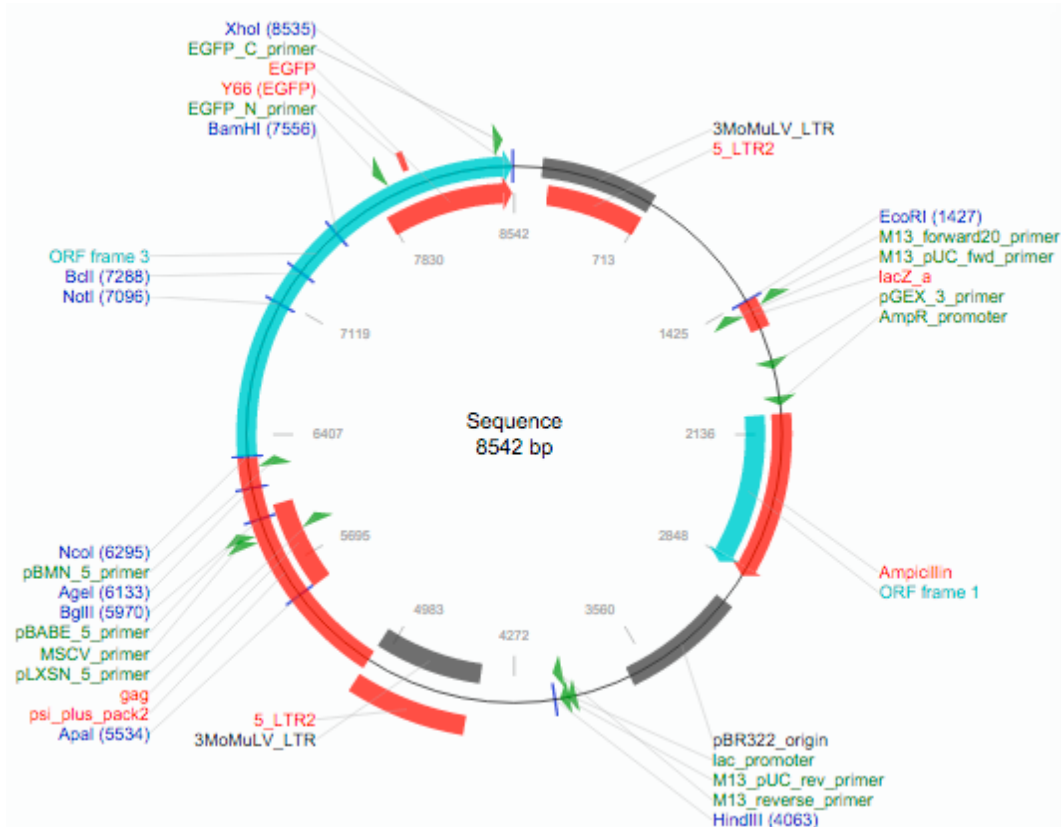


MDA CD19-1D3-28Z-mCherry

Appendix 2

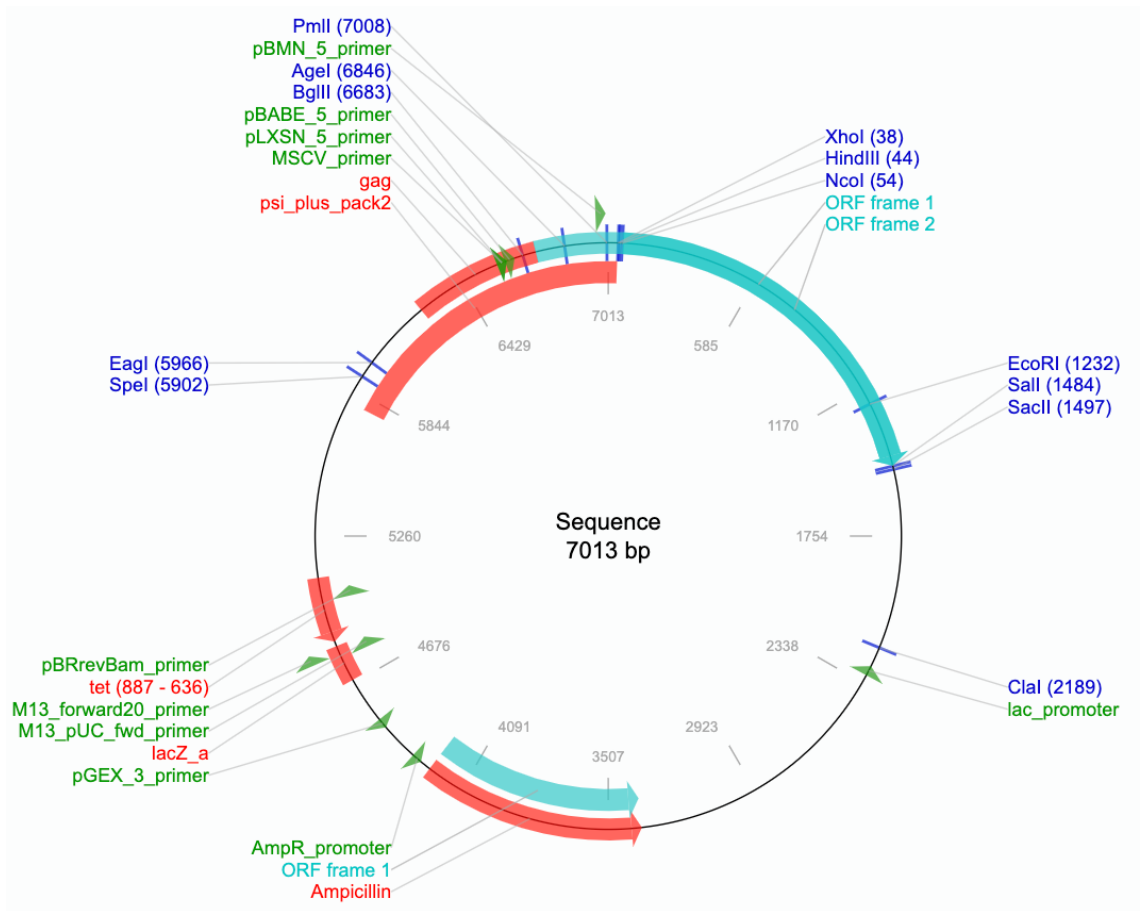


MSK CD19-1D3-41BBmZ-GFP



MSK CD19-1D3-28z-GFP

Appendix 3



NCI MSGV-1D3-28Z-1.3mut

12. References

1. Campo E, Muller-Hermelink H, Monserrat E, Ghia P, Harris N, Stein H. Chronic lymphocytic leukaemia/small lymphocytic lymphoma: WHO Classification of Tumours of Haematopoietic and Lymphoid Tissues. 4th ed. Lyon, France: IARC Press; 2017.
2. Hallek M, Cheson BD, Catovsky D, Caligaris-Cappio F, Dighiero G, Dohner H, et al. Guidelines for the diagnosis and treatment of chronic lymphocytic leukemia: a report from the International Workshop on Chronic Lymphocytic Leukemia updating the National Cancer Institute-Working Group 1996 guidelines. *Blood*. 2008;111(12):5446-56.
3. Moreau EJ, Matutes E, A'Hern RP, Morilla AM, Morilla RM, Owusu-Ankomah KA, et al. Improvement of the chronic lymphocytic leukemia scoring system with the monoclonal antibody SN8 (CD79b). *American journal of clinical pathology*. 1997;108(4):378-82.
4. Cancer Research UK: Chronic lymphocytic leukaemia incidence 2017 [Available from: <http://www.cancerresearchuk.org/health-professional/cancer-statistics/statistics-by-cancer-type/leukaemia-cll - heading-Zero>].
5. Rai KR, Sawitsky A, Cronkite EP, Chanana AD, Levy RN, Pasternack BS. Clinical staging of chronic lymphocytic leukemia. *Blood*. 1975;46(2):219-34.
6. Binet JL, Auquier A, Dighiero G, Chastang C, Piguët H, Goasguen J, et al. A new prognostic classification of chronic lymphocytic leukemia derived from a multivariate survival analysis. *Cancer*. 1981;48(1):198-206.
7. Hamblin TJ, Davis Z, Gardiner A, Oscier DG, Stevenson FK. Unmutated Ig V(H) genes are associated with a more aggressive form of chronic lymphocytic leukemia. *Blood*. 1999;94(6):1848-54.
8. Damle RN, Wasil T, Fais F, Ghiotto F, Valetto A, Allen SL, et al. Ig V gene mutation status and CD38 expression as novel prognostic indicators in chronic lymphocytic leukemia. *Blood*. 1999;94(6):1840-7.
9. Juliusson G, Gahrton G. Chromosome aberrations in B-cell chronic lymphocytic leukemia. Pathogenetic and clinical implications. *Cancer Genet Cytogenet*. 1990;45(2):143-60.
10. Dohner H, Stilgenbauer S, Benner A, Leupolt E, Krober A, Bullinger L, et al. Genomic aberrations and survival in chronic lymphocytic leukemia. *The New England journal of medicine*. 2000;343(26):1910-6.
11. Fischer K, Bahlo J, Fink AM, Goede V, Herling CD, Cramer P, et al. Long-term remissions after FCR chemoimmunotherapy in previously untreated patients with CLL: updated results of the CLL8 trial. *Blood*. 2016;127(2):208-15.
12. O'Brien S, Furman RR, Coutre S, Flinn IW, Burger JA, Blum K, et al. Single-agent ibrutinib in treatment-naïve and relapsed/refractory chronic lymphocytic leukemia: a 5-year experience. *Blood*. 2018;131(17):1910-9.
13. Lew T, Anderson MA, Tam C, Handunnetti S, Carney D, Wall D, et al. Long Term Outcomes of Venetoclax Therapy for Complex Karyotype Relapsed/Refractory CHronic Lymphocytic Leukemia. *Blood*. 2018;132:4431.
14. Parikh SA, Rabe KG, Kay NE, Call TG, Ding W, Schwager SM, et al. Chronic lymphocytic leukemia in young (<= 55 years) patients: a comprehensive analysis of prognostic factors and outcomes. *Haematologica*. 2014;99(1):140-7.

15. Calin GA, Dumitru CD, Shimizu M, Bichi R, Zupo S, Noch E, et al. Frequent deletions and down-regulation of micro- RNA genes miR15 and miR16 at 13q14 in chronic lymphocytic leukemia. *Proceedings of the National Academy of Sciences of the United States of America*. 2002;99(24):15524-9.
16. Balatti V, Bottoni A, Palamarchuk A, Alder H, Rassenti LZ, Kipps TJ, et al. NOTCH1 mutations in CLL associated with trisomy 12. *Blood*. 2012;119(2):329-31.
17. Stilgenbauer S, Liebisch P, James MR, Schroder M, Schlegelberger B, Fischer K, et al. Molecular cytogenetic delineation of a novel critical genomic region in chromosome bands 11q22.3-923.1 in lymphoproliferative disorders. *Proceedings of the National Academy of Sciences of the United States of America*. 1996;93(21):11837-41.
18. Landau DA, Carter SL, Stojanov P, McKenna A, Stevenson K, Lawrence MS, et al. Evolution and impact of subclonal mutations in chronic lymphocytic leukemia. *Cell*. 2013;152(4):714-26.
19. Puente XS, Pinyol M, Quesada V, Conde L, Ordonez GR, Villamor N, et al. Whole-genome sequencing identifies recurrent mutations in chronic lymphocytic leukaemia. *Nature*. 2011;475(7354):101-5.
20. Hallek M, Fischer K, Fingerle-Rowson G, Fink AM, Busch R, Mayer J, et al. Addition of rituximab to fludarabine and cyclophosphamide in patients with chronic lymphocytic leukaemia: a randomised, open-label, phase 3 trial. *Lancet*. 2010;376(9747):1164-74.
21. Landau DA, Tausch E, Taylor-Weiner AN, Stewart C, Reiter JG, Bahlo J, et al. Mutations driving CLL and their evolution in progression and relapse. *Nature*. 2015;526(7574):525-30.
22. Landau DA, Sun C, Rosebrock D, Herman SEM, Fein J, Sivina M, et al. The evolutionary landscape of chronic lymphocytic leukemia treated with ibrutinib targeted therapy. *Nature communications*. 2017;8(1):2185.
23. Dighiero G, Maloum K, Desablens B, Cazin B, Navarro M, Leblay R, et al. Chlorambucil in indolent chronic lymphocytic leukemia. *French Cooperative Group on Chronic Lymphocytic Leukemia. The New England journal of medicine*. 1998;338(21):1506-14.
24. Hoehstetter MA, Busch R, Eichhorst B, Buhler A, Winkler D, Eckart MJ, et al. Early, risk-adapted treatment with fludarabine in Binet stage A chronic lymphocytic leukemia patients: results of the CLL1 trial of the German CLL study group. *Leukemia*. 2017;31(12):2833-7.
25. Hallek M, Cheson BD, Catovsky D, Caligaris-Cappio F, Dighiero G, Dohner H, et al. iwCLL guidelines for diagnosis, indications for treatment, response assessment, and supportive management of CLL. *Blood*. 2018;131(25):2745-60.
26. Tam CS, O'Brien S, Wierda W, Kantarjian H, Wen S, Do KA, et al. Long-term results of the fludarabine, cyclophosphamide, and rituximab regimen as initial therapy of chronic lymphocytic leukemia. *Blood*. 2008;112(4):975-80.
27. Gribben JG. One step back but 2 steps forward. *Blood*. 2009;114(16):3359-60.
28. Balducci L, Extermann M. Management of cancer in the older person: a practical approach. *Oncologist*. 2000;5(3):224-37.
29. Benjamini O, Jain P, Trinh L, Qiao W, Strom SS, Lerner S, et al. Second cancers in patients with chronic lymphocytic leukemia who received frontline fludarabine,

cyclophosphamide and rituximab therapy: distribution and clinical outcomes. *Leukemia & lymphoma*. 2015;56(6):1643-50.

30. Eichhorst B, Fink AM, Bahlo J, Busch R, Kovacs G, Maurer C, et al. First-line chemoimmunotherapy with bendamustine and rituximab versus fludarabine, cyclophosphamide, and rituximab in patients with advanced chronic lymphocytic leukaemia (CLL10): an international, open-label, randomised, phase 3, non-inferiority trial. *The Lancet Oncology*. 2016;17(7):928-42.

31. Pavletic SZ, Khouri IF, Haagenon M, King RJ, Bierman PJ, Bishop MR, et al. Unrelated donor marrow transplantation for B-cell chronic lymphocytic leukemia after using myeloablative conditioning: results from the Center for International Blood and Marrow Transplant research. *Journal of clinical oncology : official journal of the American Society of Clinical Oncology*. 2005;23(24):5788-94.

32. Thompson PA, Tam CS, O'Brien SM, Wierda WG, Stingo F, Plunkett W, et al. Fludarabine, cyclophosphamide, and rituximab treatment achieves long-term disease-free survival in IGHV-mutated chronic lymphocytic leukemia. *Blood*. 2016;127(3):303-9.

33. Norris K, Hillmen P, Rawstron A, Hills R, Baird DM, Fegan CD, et al. Telomere length predicts for outcome to FCR chemotherapy in CLL. *Leukemia*. 2019.

34. Eichhorst BF, Busch R, Stilgenbauer S, Stauch M, Bergmann MA, Ritgen M, et al. First-line therapy with fludarabine compared with chlorambucil does not result in a major benefit for elderly patients with advanced chronic lymphocytic leukemia. *Blood*. 2009;114(16):3382-91.

35. Byrd JC, Flynn JM, Kipps TJ, Boxer M, Kolibaba KS, Carlile DJ, et al. Randomized phase 2 study of obinutuzumab monotherapy in symptomatic, previously untreated chronic lymphocytic leukemia. *Blood*. 2016;127(1):79-86.

36. Brown JR, O'Brien S, Kingsley CD, Eradat H, Pagel JM, Lymp J, et al. Obinutuzumab plus fludarabine/cyclophosphamide or bendamustine in the initial therapy of CLL patients: the phase 1b GALTON trial. *Blood*. 2015;125(18):2779-85.

37. Goede V, Fischer K, Busch R, Engelke A, Eichhorst B, Wendtner CM, et al. Obinutuzumab plus chlorambucil in patients with CLL and coexisting conditions. *The New England journal of medicine*. 2014;370(12):1101-10.

38. Fischer K, Al-Sawaf O, Bahlo J, Fink AM, Tandon M, Dixon M, et al. Venetoclax and Obinutuzumab in Patients with CLL and Coexisting Conditions. *The New England journal of medicine*. 2019;380(23):2225-36.

39. Dubovsky JA, Beckwith KA, Natarajan G, Woyach JA, Jaglowski S, Zhong Y, et al. Ibrutinib is an irreversible molecular inhibitor of ITK driving a Th1-selective pressure in T lymphocytes. *Blood*. 2013;122(15):2539-49.

40. Byrd JC, Furman RR, Coutre SE, Flinn IW, Burger JA, Blum KA, et al. Targeting BTK with ibrutinib in relapsed chronic lymphocytic leukemia. *The New England journal of medicine*. 2013;369(1):32-42.

41. Byrd JC, Brown JR, O'Brien S, Barrientos JC, Kay NE, Reddy NM, et al. Ibrutinib versus ofatumumab in previously treated chronic lymphoid leukemia. *The New England journal of medicine*. 2014;371(3):213-23.

42. Burger JA, Tedeschi A, Barr PM, Robak T, Owen C, Ghia P, et al. Ibrutinib as Initial Therapy for Patients with Chronic Lymphocytic Leukemia. *The New England journal of medicine*. 2015;373(25):2425-37.

43. Byrd JC, Hillmen P, O'Brien S, Barrientos JC, Reddy NM, Coutre S, et al. Long-term follow-up of the RESONATE phase 3 trial of ibrutinib vs ofatumumab. *Blood*. 2019;133(19):2031-42.
44. Woyach JA, Ruppert AS, Heerema NA, Zhao W, Booth AM, Ding W, et al. Ibrutinib Regimens versus Chemoimmunotherapy in Older Patients with Untreated CLL. *The New England journal of medicine*. 2018;379(26):2517-28.
45. Hoellenriegel J, Meadows SA, Sivina M, Wierda WG, Kantarjian H, Keating MJ, et al. The phosphoinositide 3^l-kinase delta inhibitor, CAL-101, inhibits B-cell receptor signaling and chemokine networks in chronic lymphocytic leukemia. *Blood*. 2011;118(13):3603-12.
46. Wu H, Wang W, Liu F, Weisberg EL, Tian B, Chen Y, et al. Discovery of a potent, covalent BTK inhibitor for B-cell lymphoma. *ACS Chem Biol*. 2014;9(5):1086-91.
47. Okkenhaug K, Bilancio A, Farjot G, Priddle H, Sancho S, Peskett E, et al. Impaired B and T cell antigen receptor signaling in p110delta PI 3-kinase mutant mice. *Science*. 2002;297(5583):1031-4.
48. Souers AJ, Levenson JD, Boghaert ER, Ackler SL, Catron ND, Chen J, et al. ABT-199, a potent and selective BCL-2 inhibitor, achieves antitumor activity while sparing platelets. *Nature medicine*. 2013;19(2):202-8.
49. Anderson MA, Deng J, Seymour JF, Tam C, Kim SY, Fein J, et al. The BCL2 selective inhibitor venetoclax induces rapid onset apoptosis of CLL cells in patients via a TP53-independent mechanism. *Blood*. 2016;127(25):3215-24.
50. Roberts AW, Davids MS, Pagel JM, Kahl BS, Puvvada SD, Gerecitano JF, et al. Targeting BCL2 with Venetoclax in Relapsed Chronic Lymphocytic Leukemia. *The New England journal of medicine*. 2016;374(4):311-22.
51. Stilgenbauer S, Eichhorst B, Schetelig J, Hillmen P, Seymour JF, Coutre S, et al. Venetoclax for Patients With Chronic Lymphocytic Leukemia With 17p Deletion: Results From the Full Population of a Phase II Pivotal Trial. *Journal of clinical oncology : official journal of the American Society of Clinical Oncology*. 2018;JCO2017766840.
52. Anderson MA, Tam C, Lew TE, Juneja S, Juneja M, Westerman D, et al. Clinicopathological features and outcomes of progression of CLL on the BCL2 inhibitor venetoclax. *Blood*. 2017;129(25):3362-70.
53. Eyre TA, Kirkwood AA, Gohill S, Follows G, Walewska R, Walter H, et al. Efficacy of venetoclax monotherapy in patients with relapsed chronic lymphocytic leukaemia in the post-BCR inhibitor setting: a UK wide analysis. *British journal of haematology*. 2019.
54. Mato AR, Thompson M, Allan JN, Brander DM, Pagel JM, Ujjani CS, et al. Real-world outcomes and management strategies for venetoclax-treated chronic lymphocytic leukemia patients in the United States. *Haematologica*. 2018;103(9):1511-7.
55. Seymour JF, Ma S, Brander DM, Choi MY, Barrientos J, Davids MS, et al. Venetoclax plus rituximab in relapsed or refractory chronic lymphocytic leukaemia: a phase 1b study. *The Lancet Oncology*. 2017;18(2):230-40.
56. Seymour JF, Kipps TJ, Eichhorst B, Hillmen P, D'Rozario J, Assouline S, et al. Venetoclax-Rituximab in Relapsed or Refractory Chronic Lymphocytic Leukemia. *The New England journal of medicine*. 2018;378(12):1107-20.

57. De Weerd DL, Hofland T, Dobber J, Dubois J, Eldering E, Mobasher M, et al. First Evidence of Restoration of T and NK Cell Compartment after Venetoclax Treatment. *Blood*. 2018;132:1860.
58. Blombery P, Anderson MA, Gong JN, Thijssen R, Birkinshaw RW, Thompson ER, et al. Acquisition of the recurrent Gly101Val mutation in BCL2 confers resistance to venetoclax in patients with progressive chronic lymphocytic leukemia. *Cancer discovery*. 2018.
59. Jain N, Keating M, Thompson P, Ferrajoli A, Burger J, Borthakur G, et al. Ibrutinib and Venetoclax for First-Line Treatment of CLL. *The New England journal of medicine*. 2019;380(22):2095-103.
60. Woyach JA. How I manage ibrutinib-refractory chronic lymphocytic leukemia. *Blood*. 2017;129(10):1270-4.
61. Jain P, Keating M, Wierda W, Estrov Z, Ferrajoli A, Jain N, et al. Outcomes of patients with chronic lymphocytic leukemia after discontinuing ibrutinib. *Blood*. 2015;125(13):2062-7.
62. Kolb HJ. Graft-versus-leukemia effects of transplantation and donor lymphocytes. *Blood*. 2008;112(12):4371-83.
63. Gribben JG, Zahrieh D, Stephans K, Bartlett-Pandite L, Alyea EP, Fisher DC, et al. Autologous and allogeneic stem cell transplantations for poor-risk chronic lymphocytic leukemia. *Blood*. 2005;106(13):4389-96.
64. van Gelder M, de Wreede LC, Bornhauser M, Niederwieser D, Karas M, Anderson NS, et al. Long-term survival of patients with CLL after allogeneic transplantation: a report from the European Society for Blood and Marrow Transplantation. *Bone marrow transplantation*. 2017;52(3):372-80.
65. Dreger P, Corradini P, Kimby E, Michallet M, Milligan D, Schetelig J, et al. Indications for allogeneic stem cell transplantation in chronic lymphocytic leukemia: the EBMT transplant consensus. *Leukemia*. 2007;21(1):12-7.
66. Gribben JG, Bosch F, Cymbalista F, Geisler CH, Ghia P, Hillmen P, et al. Optimising outcomes for patients with chronic lymphocytic leukaemia on ibrutinib therapy: European recommendations for clinical practice. *British journal of haematology*. 2018;180(5):666-79.
67. Kharfan-Dabaja MA, Reljic T, El-Asmar J, Nishihori T, Ayala E, Hamadani M, et al. Reduced-intensity or myeloablative allogeneic hematopoietic cell transplantation for mantle cell lymphoma: a systematic review. *Future Oncol*. 2016;12(22):2631-42.
68. Byrd JC, Harrington B, O'Brien S, Jones JA, Schuh A, Devereux S, et al. Acalabrutinib (ACP-196) in Relapsed Chronic Lymphocytic Leukemia. *The New England journal of medicine*. 2016;374(4):323-32.
69. Burger JA, Buggy JJ. Bruton tyrosine kinase inhibitor ibrutinib (PCI-32765). *Leukemia & lymphoma*. 2013;54(11):2385-91.
70. Herman SEM, Montraveta A, Niemann CU, Mora-Jensen H, Gulrajani M, Krantz F, et al. The Bruton Tyrosine Kinase (BTK) Inhibitor Acalabrutinib Demonstrates Potent On-Target Effects and Efficacy in Two Mouse Models of Chronic Lymphocytic Leukemia. *Clinical cancer research : an official journal of the American Association for Cancer Research*. 2017;23(11):2831-41.
71. Ramsay AG, Clear AJ, Fatah R, Gribben JG. Multiple inhibitory ligands induce impaired T-cell immunologic synapse function in chronic lymphocytic leukemia that

can be blocked with lenalidomide: establishing a reversible immune evasion mechanism in human cancer. *Blood*. 2012;120(7):1412-21.

72. Jain N, Basu S, Thompson PA, Ohanian M, Ferrajoli A, Pemmaraju N, et al. Nivolumab combined with ibrutinib for CLL and Richter transformation: A Phase II Trial. *Blood*. 2016;128(22):Abstract 59.

73. Younes A, Brody J, Carpio C, Lopez-Guillermo A, Ben-Yehuda D, Ferhanoglu B, et al. Safety and activity of ibrutinib in combination with nivolumab in patients with relapsed non-Hodgkin lymphoma or chronic lymphocytic leukaemia: a phase 1/2a study. *Lancet Haematol*. 2019.

74. Ding W, LaPlant BR, Call TG, Parikh SA, Leis JF, He R, et al. Pembrolizumab in patients with chronic lymphocytic leukemia with Richter's transformation and relapsed CLL. *Blood*. 2017.

75. Rogers KA, Huang Y, Dotson E, Lundberg J, Andritsos LA, Awan FT, et al. Use of PD-1 (PDCD1) inhibitors for the treatment of Richter syndrome: experience at a single academic centre. *British journal of haematology*. 2018.

76. Collins RJ, Verschuer LA, Harmon BV, Prentice RL, Pope JH, Kerr JF. Spontaneous programmed death (apoptosis) of B-chronic lymphocytic leukaemia cells following their culture in vitro. *British journal of haematology*. 1989;71(3):343-50.

77. Burger JA, Tsukada N, Burger M, Zvaifler NJ, Dell'Aquila M, Kipps TJ. Blood-derived nurse-like cells protect chronic lymphocytic leukemia B cells from spontaneous apoptosis through stromal cell-derived factor-1. *Blood*. 2000;96(8):2655-63.

78. Jia L, Clear A, Liu FT, Matthews J, Uddin N, McCarthy A, et al. Extracellular HMGB1 promotes differentiation of nurse-like cells in chronic lymphocytic leukemia. *Blood*. 2014;123(11):1709-19.

79. Kurtova AV, Tamayo AT, Ford RJ, Burger JA. Mantle cell lymphoma cells express high levels of CXCR4, CXCR5, and VLA-4 (CD49d): importance for interactions with the stromal microenvironment and specific targeting. *Blood*. 2009;113(19):4604-13.

80. Marquez ME, Hernandez-Uzategui O, Cornejo A, Vargas P, Da Costa O. Bone marrow stromal mesenchymal cells induce down regulation of CD20 expression on B-CLL: implications for rituximab resistance in CLL. *British journal of haematology*. 2015;169(2):211-8.

81. Burger JA, Burger M, Kipps TJ. Chronic lymphocytic leukemia B cells express functional CXCR4 chemokine receptors that mediate spontaneous migration beneath bone marrow stromal cells. *Blood*. 1999;94(11):3658-67.

82. Burkle A, Niedermeier M, Schmitt-Graff A, Wierda WG, Keating MJ, Burger JA. Overexpression of the CXCR5 chemokine receptor, and its ligand, CXCL13 in B-cell chronic lymphocytic leukemia. *Blood*. 2007;110(9):3316-25.

83. Bagnara D, Kaufman MS, Calissano C, Marsilio S, Patten PE, Simone R, et al. A novel adoptive transfer model of chronic lymphocytic leukemia suggests a key role for T lymphocytes in the disease. *Blood*. 2011;117(20):5463-72.

84. Pascutti MF, Jak M, Tromp JM, Derks IA, Remmerswaal EB, Thijssen R, et al. IL-21 and CD40L signals from autologous T cells can induce antigen-independent proliferation of CLL cells. *Blood*. 2013;122(17):3010-9.

85. Nunes C, Wong R, Mason M, Fegan C, Man S, Pepper C. Expansion of a CD8(+)/PD-1(+) replicative senescence phenotype in early stage CLL patients is associated with inverted CD4:CD8 ratios and disease progression. *Clinical cancer*

research : an official journal of the American Association for Cancer Research. 2012;18(3):678-87.

86. Brusa D, Serra S, Coscia M, Rossi D, D'Arena G, Laurenti L, et al. The PD-1/PD-L1 axis contributes to T-cell dysfunction in chronic lymphocytic leukemia. *Haematologica*. 2013;98(6):953-63.

87. Gorgun G, Holderried TA, Zahrieh D, Neuberg D, Gribben JG. Chronic lymphocytic leukemia cells induce changes in gene expression of CD4 and CD8 T cells. *The Journal of clinical investigation*. 2005;115(7):1797-805.

88. Ramsay AG, Johnson AJ, Lee AM, Gorgun G, Le Dieu R, Blum W, et al. Chronic lymphocytic leukemia T cells show impaired immunological synapse formation that can be reversed with an immunomodulating drug. *The Journal of clinical investigation*. 2008;118(7):2427-37.

89. Gorgun G, Ramsay AG, Holderried TA, Zahrieh D, Le Dieu R, Liu F, et al. E(mu)-TCL1 mice represent a model for immunotherapeutic reversal of chronic lymphocytic leukemia-induced T-cell dysfunction. *Proceedings of the National Academy of Sciences of the United States of America*. 2009;106(15):6250-5.

90. Barber DL, Wherry EJ, Masopust D, Zhu B, Allison JP, Sharpe AH, et al. Restoring function in exhausted CD8 T cells during chronic viral infection. *Nature*. 2006;439(7077):682-7.

91. Schlie K, Westerback A, DeVorkin L, Hughson LR, Brandon JM, MacPherson S, et al. Survival of effector CD8+ T cells during influenza infection is dependent on autophagy. *Journal of immunology*. 2015;194(9):4277-86.

92. Wherry EJ, Kurachi M. Molecular and cellular insights into T cell exhaustion. *Nature reviews Immunology*. 2015;15(8):486-99.

93. Greaves P, Gribben JG. The role of B7 family molecules in hematologic malignancy. *Blood*. 2013;121(5):734-44.

94. Riches JC, Davies JK, McClanahan F, Fatah R, Iqbal S, Agrawal S, et al. T cells from CLL patients exhibit features of T-cell exhaustion but retain capacity for cytokine production. *Blood*. 2013;121(9):1612-21.

95. Dühren-von Minden M, Ubelhart R, Schneider D, Wossning T, Bach MP, Buchner M, et al. Chronic lymphocytic leukaemia is driven by antigen-independent cell-autonomous signalling. *Nature*. 2012;489(7415):309-12.

96. McClanahan F, Hanna B, Miller S, Clear AJ, Lichter P, Gribben JG, et al. PD-L1 checkpoint blockade prevents immune dysfunction and leukemia development in a mouse model of chronic lymphocytic leukemia. *Blood*. 2015;126(2):203-11.

97. Speiser DE, Ho PC, Verdeil G. Regulatory circuits of T cell function in cancer. *Nature reviews Immunology*. 2016;16(10):599-611.

98. D'Arena G, D'Auria F, Simeon V, Laurenti L, Deaglio S, Mansueto G, et al. A shorter time to the first treatment may be predicted by the absolute number of regulatory T-cells in patients with Rai stage 0 chronic lymphocytic leukemia. *Am J Hematol*. 2012;87(6):628-31.

99. Weiss L, Melchardt T, Egle A, Grabmer C, Greil R, Tinhofer I. Regulatory T cells predict the time to initial treatment in early stage chronic lymphocytic leukemia. *Cancer*. 2011;117(10):2163-9.

100. Jitschin R, Braun M, Buttner M, Dettmer-Wilde K, Bricks J, Berger J, et al. CLL-cells induce IDOhi CD14+HLA-DRlo myeloid-derived suppressor cells that inhibit T-cell responses and promote TRegs. *Blood*. 2014;124(5):750-60.

101. Hanna BS, McClanahan F, Yazdanparast H, Zaborsky N, Kalter V, Rossner PM, et al. Depletion of CLL-associated patrolling monocytes and macrophages controls disease development and repairs immune dysfunction in vivo. *Leukemia*. 2016;30(3):570-9.
102. Kondo K, Shaim H, Thompson PA, Burger JA, Keating M, Estrov Z, et al. Ibrutinib modulates the immunosuppressive CLL microenvironment through STAT3-mediated suppression of regulatory B-cell function and inhibition of the PD-1/PD-L1 pathway. *Leukemia*. 2017.
103. Yin Q, Sivina M, Robins H, Yusko E, Vignali M, O'Brien S, et al. Ibrutinib Therapy Increases T Cell Repertoire Diversity in Patients with Chronic Lymphocytic Leukemia. *Journal of immunology*. 2017;198(4):1740-7.
104. Herman SE, Gordon AL, Wagner AJ, Heerema NA, Zhao W, Flynn JM, et al. Phosphatidylinositol 3-kinase-delta inhibitor CAL-101 shows promising preclinical activity in chronic lymphocytic leukemia by antagonizing intrinsic and extrinsic cellular survival signals. *Blood*. 2010;116(12):2078-88.
105. Collins RA, Oldham G, Francis PG, Craven N. Pathological changes following implantation of intramammary devices (IMD) and immunological mediator release by cells on recovered IMDs. *Res Vet Sci*. 1989;46(2):253-7.
106. van't Riet M, Burger JW, van Muiswinkel JM, Kazemier G, Schipperus MR, Bonjer HJ. Diagnosis and treatment of portal vein thrombosis following splenectomy. *Br J Surg*. 2000;87(9):1229-33.
107. Kellner J, Wierda W, Shpall E, Keating M, McNiece I. Isolation of a novel chronic lymphocytic leukemic (CLL) cell line and development of an in vivo mouse model of CLL. *Leukemia research*. 2016;40:54-9.
108. Stacchini A, Aragno M, Vallario A, Alfarano A, Circosta P, Gottardi D, et al. MEC1 and MEC2: two new cell lines derived from B-chronic lymphocytic leukaemia in prolymphocytoid transformation. *Leukemia research*. 1999;23(2):127-36.
109. Herishanu Y, Perez-Galan P, Liu D, Biancotto A, Pittaluga S, Vire B, et al. The lymph node microenvironment promotes B-cell receptor signaling, NF-kappaB activation, and tumor proliferation in chronic lymphocytic leukemia. *Blood*. 2011;117(2):563-74.
110. Pasikowska M, Walsby E, Apollonio B, Cuthill K, Phillips E, Coulter E, et al. Phenotype and immune function of lymph node and peripheral blood CLL cells are linked to transendothelial migration. *Blood*. 2016;128(4):563-73.
111. Bichi R, Shinton SA, Martin ES, Koval A, Calin GA, Cesari R, et al. Human chronic lymphocytic leukemia modeled in mouse by targeted TCL1 expression. *Proceedings of the National Academy of Sciences of the United States of America*. 2002;99(10):6955-60.
112. Johnson AJ, Lucas DM, Muthusamy N, Smith LL, Edwards RB, De Lay MD, et al. Characterization of the TCL-1 transgenic mouse as a preclinical drug development tool for human chronic lymphocytic leukemia. *Blood*. 2006;108(4):1334-8.
113. Hamblin TJ. The TCL1 mouse as a model for chronic lymphocytic leukemia. *Leukemia research*. 2010;34(2):135-6.
114. Simonetti G, Bertilaccio MT, Ghia P, Klein U. Mouse models in the study of chronic lymphocytic leukemia pathogenesis and therapy. *Blood*. 2014;124(7):1010-9.
115. Widhopf GF, 2nd, Cui B, Ghia EM, Chen L, Messer K, Shen Z, et al. ROR1 can interact with TCL1 and enhance leukemogenesis in Emu-TCL1 transgenic mice.

Proceedings of the National Academy of Sciences of the United States of America. 2014;111(2):793-8.

116. Liu J, Chen G, Feng L, Zhang W, Pelicano H, Wang F, et al. Loss of p53 and altered miR15-a/16-1short right arrowMCL-1 pathway in CLL: insights from TCL1-Tg;p53(-/-) mouse model and primary human leukemia cells. *Leukemia*. 2014;28(1):118-28.

117. Hofbauer JP, Heyder C, Denk U, Kocher T, Holler C, Trapin D, et al. Development of CLL in the TCL1 transgenic mouse model is associated with severe skewing of the T-cell compartment homologous to human CLL. *Leukemia*. 2011;25(9):1452-8.

118. McClanahan F, Riches JC, Miller S, Day WP, Kotsiou E, Neuberger D, et al. Mechanisms of PD-L1/PD-1-mediated CD8 T-cell dysfunction in the context of aging-related immune defects in the Emicro-TCL1 CLL mouse model. *Blood*. 2015;126(2):212-21.

119. Hanna BS, Roessner PM, Yazdanparast H, Colomer D, Campo E, Kugler S, et al. Control of chronic lymphocytic leukemia development by clonally-expanded CD8(+) T-cells that undergo functional exhaustion in secondary lymphoid tissues. *Leukemia*. 2018.

120. Schwarzbich M, Romero-Toledo A, Gribben J. Modulation of T-Cell Function and Immune Phenotype in the Microenvironment of Emu-TCL1 CLL Bearing Mice by Ibrutinib. *Blood*. 2018;132:3138.

121. Schwarzbich M, Romero-Toledo A, Frigault MJ, Gribben J. Modulation of T-cell Function in the Microenvironment of Emu-TCL1 ~CLL Bearing Mice By BTKi Appears Independent of ITK. *Blood*. 2018;132:3139.

122. Gu B, Ma H, Zhang X, Malaney P, Gallardo M, Liu J, et al. Combination Therapy with BTK Inhibitor Plus Anti-PD-1 Antibody Results in a Hyperprogressor Phenotype in a Mouse Model of CLL. *Blood*. 2018;132:Abstract 4416.

123. Sharpe C, Davis J, Mason K, Godfrey D, Uldrich A, Tam C, et al. More Than a BTK Inhibitor; Ibrutinib Impacts the Function of Cell Mediated Immunity. *Blood*. 2018;132:4417.

124. Hanna BS, Roessner PM, Scheffold A, Jebaraj BMC, Demerdash Y, Ozturk S, et al. PI3Kdelta inhibition modulates regulatory and effector T-cell differentiation and function in chronic lymphocytic leukemia. *Leukemia*. 2018.

125. Wierz M, Pierson S, Guyonnet L, Viry E, Lequeux A, Oudin A, et al. Dual PD1/LAG3 immune checkpoint blockade limits tumor development in a murine model of chronic lymphocytic leukemia. *Blood*. 2018;131(14):1617-21.

126. Zaborsky N, Gassner FJ, Hopner JP, Schubert M, Hebenstreit D, Stark R, et al. Exome sequencing of the TCL1 mouse model for CLL reveals genetic heterogeneity and dynamics during disease development. *Leukemia*. 2018.

127. Kloss CC, Condomines M, Cartellieri M, Bachmann M, Sadelain M. Combinatorial antigen recognition with balanced signaling promotes selective tumor eradication by engineered T cells. *Nature biotechnology*. 2013;31(1):71-5.

128. Gill S, Maus MV, Porter DL. Chimeric antigen receptor T cell therapy: 25years in the making. *Blood reviews*. 2016;30(3):157-67.

129. Tran E, Longo DL, Urba WJ. A Milestone for CAR T Cells. *The New England journal of medicine*. 2017.

130. Milone M, Younge BR, Wang J, Zhang S, Wong LJ. Mitochondrial disorder with OPA1 mutation lacking optic atrophy. *Mitochondrion*. 2009;9(4):279-81.

131. Maher J, Brentjens RJ, Gunset G, Riviere I, Sadelain M. Human T-lymphocyte cytotoxicity and proliferation directed by a single chimeric TCRzeta /CD28 receptor. *Nature biotechnology*. 2002;20(1):70-5.
132. Long AH, Haso WM, Shern JF, Wanhainen KM, Murgai M, Ingaramo M, et al. 4-1BB costimulation ameliorates T cell exhaustion induced by tonic signaling of chimeric antigen receptors. *Nature medicine*. 2015.
133. Enblad G, Karlsson H, Gammelgard G, Wenthe J, Lovgren T, Amini RM, et al. A Phase I/IIa Trial Using CD19-Targeted Third-Generation CAR T Cells for Lymphoma and Leukemia. *Clinical cancer research : an official journal of the American Association for Cancer Research*. 2018;24(24):6185-94.
134. Fesnak AD, June CH, Levine BL. Engineered T cells: the promise and challenges of cancer immunotherapy. *Nature reviews Cancer*. 2016;16(9):566-81.
135. Brentjens RJ, Latouche JB, Santos E, Marti F, Gong MC, Lyddane C, et al. Eradication of systemic B-cell tumors by genetically targeted human T lymphocytes co-stimulated by CD80 and interleukin-15. *Nature medicine*. 2003;9(3):279-86.
136. Singh H, Manuri PR, Olivares S, Dara N, Dawson MJ, Huls H, et al. Redirecting specificity of T-cell populations for CD19 using the Sleeping Beauty system. *Cancer research*. 2008;68(8):2961-71.
137. Hinrichs CS, Borman ZA, Gattinoni L, Yu Z, Burns WR, Huang J, et al. Human effector CD8+ T cells derived from naive rather than memory subsets possess superior traits for adoptive immunotherapy. *Blood*. 2011;117(3):808-14.
138. Berger C, Jensen MC, Lansdorp PM, Gough M, Elliott C, Riddell SR. Adoptive transfer of effector CD8+ T cells derived from central memory cells establishes persistent T cell memory in primates. *The Journal of clinical investigation*. 2008;118(1):294-305.
139. Gattinoni L, Lugli E, Ji Y, Pos Z, Paulos CM, Quigley MF, et al. A human memory T cell subset with stem cell-like properties. *Nature medicine*. 2011;17(10):1290-7.
140. Gill S, Tasian SK, Ruella M, Shestova O, Li Y, Porter DL, et al. Preclinical targeting of human acute myeloid leukemia and myeloablation using chimeric antigen receptor-modified T cells. *Blood*. 2014;123(15):2343-54.
141. Giordano Attianese GM, Marin V, Hoyos V, Savoldo B, Pizzitola I, Tettamanti S, et al. In vitro and in vivo model of a novel immunotherapy approach for chronic lymphocytic leukemia by anti-CD23 chimeric antigen receptor. *Blood*. 2011;117(18):4736-45.
142. Brentjens RJ, Santos E, Nikhamin Y, Yeh R, Matsushita M, La Perle K, et al. Genetically targeted T cells eradicate systemic acute lymphoblastic leukemia xenografts. *Clinical cancer research : an official journal of the American Association for Cancer Research*. 2007;13(18 Pt 1):5426-35.
143. Sommermeyer D, Hill T, Shamah SM, Salter AI, Chen Y, Mohler KM, et al. Fully human CD19-specific chimeric antigen receptors for T-cell therapy. *Leukemia*. 2017.
144. Kerkar SP, Sanchez-Perez L, Yang S, Borman ZA, Muranski P, Ji Y, et al. Genetic engineering of murine CD8+ and CD4+ T cells for preclinical adoptive immunotherapy studies. *Journal of immunotherapy*. 2011;34(4):343-52.
145. Davila ML, Kloss CC, Gunset G, Sadelain M. CD19 CAR-targeted T cells induce long-term remission and B Cell Aplasia in an immunocompetent mouse model of B cell acute lymphoblastic leukemia. *PloS one*. 2013;8(4):e61338.

146. Kochenderfer JN, Yu Z, Frasher D, Restifo NP, Rosenberg SA. Adoptive transfer of syngeneic T cells transduced with a chimeric antigen receptor that recognizes murine CD19 can eradicate lymphoma and normal B cells. *Blood*. 2010;116(19):3875-86.
147. Kochenderfer JN, Rosenberg SA. Treating B-cell cancer with T cells expressing anti-CD19 chimeric antigen receptors. *Nature reviews Clinical oncology*. 2013;10(5):267-76.
148. Kochenderfer JN, Wilson WH, Janik JE, Dudley ME, Stetler-Stevenson M, Feldman SA, et al. Eradication of B-lineage cells and regression of lymphoma in a patient treated with autologous T cells genetically engineered to recognize CD19. *Blood*. 2010;116(20):4099-102.
149. Kochenderfer JN, Feldman SA, Zhao Y, Xu H, Black MA, Morgan RA, et al. Construction and preclinical evaluation of an anti-CD19 chimeric antigen receptor. *Journal of immunotherapy*. 2009;32(7):689-702.
150. Porter DL, Levine BL, Kalos M, Bagg A, June CH. Chimeric antigen receptor-modified T cells in chronic lymphoid leukemia. *The New England journal of medicine*. 2011;365(8):725-33.
151. Kalos M, Levine BL, Porter DL, Katz S, Grupp SA, Bagg A, et al. T cells with chimeric antigen receptors have potent antitumor effects and can establish memory in patients with advanced leukemia. *Science translational medicine*. 2011;3(95):95ra73.
152. Grupp SA, Kalos M, Barrett D, Aplenc R, Porter DL, Rheingold SR, et al. Chimeric antigen receptor-modified T cells for acute lymphoid leukemia. *The New England journal of medicine*. 2013;368(16):1509-18.
153. Brentjens RJ, Riviere I, Park JH, Davila ML, Wang X, Stefanski J, et al. Safety and persistence of adoptively transferred autologous CD19-targeted T cells in patients with relapsed or chemotherapy refractory B-cell leukemias. *Blood*. 2011;118(18):4817-28.
154. Brentjens R, Yeh R, Bernal Y, Riviere I, Sadelain M. Treatment of chronic lymphocytic leukemia with genetically targeted autologous T cells: case report of an unforeseen adverse event in a phase I clinical trial. *Molecular therapy : the journal of the American Society of Gene Therapy*. 2010;18(4):666-8.
155. Lee DW, Santomasso BD, Locke FL, Ghobadi A, Turtle CJ, Brudno JN, et al. ASTCT Consensus Grading for Cytokine Release Syndrome and Neurologic Toxicity Associated with Immune Effector Cells. *Biology of blood and marrow transplantation : journal of the American Society for Blood and Marrow Transplantation*. 2019;25(4):625-38.
156. Park JH, Riviere I, Gonen M, Wang X, Senechal B, Curran KJ, et al. Long-Term Follow-up of CD19 CAR Therapy in Acute Lymphoblastic Leukemia. *The New England journal of medicine*. 2018;378(5):449-59.
157. Nellan A, McCully CML, Cruz Garcia R, Jayaprakash N, Widemann BC, Lee DW, et al. Improved CNS exposure to tocilizumab after cerebrospinal fluid compared to intravenous administration in rhesus macaques. *Blood*. 2018;132(6):662-6.
158. Locke F, Neelapu S, Bartlett N, Lekakis L, Jacobson C, Braunschweig I, et al. Preliminary Results of Prophylactic Tocilizumab after Azicabtagene-ciloleucel (axi-cel; KTE-019) Treatment for Patients with Refractory Aggressive Non-Hodgkin Lymphoma. *Blood*. 2017;130:Abstract 1547.

159. Santomasso BD, Park JH, Salloum D, Riviere I, Flynn J, Mead E, et al. Clinical and Biological Correlates of Neurotoxicity Associated with CAR T-cell Therapy in Patients with B-cell Acute Lymphoblastic Leukemia. *Cancer discovery*. 2018;8(8):958-71.
160. Porter DL, Hwang WT, Frey NV, Lacey SF, Shaw PA, Loren AW, et al. Chimeric antigen receptor T cells persist and induce sustained remissions in relapsed refractory chronic lymphocytic leukemia. *Science translational medicine*. 2015;7(303):303ra139.
161. Turtle CJ, Hay KA, Hanafi LA, Li D, Cherian S, Chen X, et al. Durable Molecular Remissions in Chronic Lymphocytic Leukemia Treated With CD19-Specific Chimeric Antigen Receptor-Modified T Cells After Failure of Ibrutinib. *Journal of clinical oncology : official journal of the American Society of Clinical Oncology*. 2017;35(26):3010-20.
162. Siddiqi T, Soumerai JD, Wierda W, Dubovsky J, Gillenwater HH, Gong L, et al. Rapid MRD- Responses in Patients with Relapsed/Refractory CLL Treated with Liso-Cel, a CD19-Directed CAR T-cell Product: Preliminary Results from TRANSCEND CLL 004, a Phase 1/2 Study Including Patients with High-Risk Disease Previously Treated with Ibrutinib. *Blood*. 2018;132:Abstract 300.
163. Fraietta JA, Beckwith KA, Patel PR, Ruella M, Zheng Z, Barrett DM, et al. Ibrutinib enhances chimeric antigen receptor T-cell engraftment and efficacy in leukemia. *Blood*. 2016;127(9):1117-27.
164. Kochenderfer JN, Dudley ME, Feldman SA, Wilson WH, Spaner DE, Maric I, et al. B-cell depletion and remissions of malignancy along with cytokine-associated toxicity in a clinical trial of anti-CD19 chimeric-antigen-receptor-transduced T cells. *Blood*. 2012;119(12):2709-20.
165. Maude SL, Frey N, Shaw PA, Aplenc R, Barrett DM, Bunin NJ, et al. Chimeric antigen receptor T cells for sustained remissions in leukemia. *The New England journal of medicine*. 2014;371(16):1507-17.
166. Davila ML, Riviere I, Wang X, Bartido S, Park J, Curran K, et al. Efficacy and toxicity management of 19-28z CAR T cell therapy in B cell acute lymphoblastic leukemia. *Science translational medicine*. 2014;6(224):224ra25.
167. Kochenderfer JN, Dudley ME, Kassim SH, Somerville RP, Carpenter RO, Stetler-Stevenson M, et al. Chemotherapy-refractory diffuse large B-cell lymphoma and indolent B-cell malignancies can be effectively treated with autologous T cells expressing an anti-CD19 chimeric antigen receptor. *Journal of clinical oncology : official journal of the American Society of Clinical Oncology*. 2015;33(6):540-9.
168. Lee DW, Kochenderfer JN, Stetler-Stevenson M, Cui YK, Delbrook C, Feldman SA, et al. T cells expressing CD19 chimeric antigen receptors for acute lymphoblastic leukaemia in children and young adults: a phase 1 dose-escalation trial. *Lancet*. 2015;385(9967):517-28.
169. Grupp S, Laetsh T, Buechner J, Bittencourt H, Maude SL, Verneris MR, et al. Analysis of a global registration trial of the efficacy and safety of CTL019 in paediatric and young adults with relapsed/refractory acute lymphoblastic leukaemia. *Blood*. 2016;128(22):Abstract 221.
170. Schuster SJ, Svoboda J, Nasta S, Chong EA, Winchell N, Landsburg DJ, et al. Treatment with chimeric antigen receptor modified T cells directed against CD19 (CTL019) resulted in durable remissions in patients with relapsed or refractor DLBCL of germinal centre and non-germinal center origin, "double hit" DLBCL and transformed follicular lymphoma to DLBCL. *Blood*. 2016;128(22):Abstract 3026.

171. Neelapu SS, Locke FL, Bartlett N, Lekakis L, Miklos D, Jacobson C, et al. KTE-C19 (anti-CD19 CAR T cells) induces complete remissions in patients with refractory DLBCL: Results from Pivotal Phase 2 ZUMA-1. *Blood*. 2016;128(22):Abstract LBA-6.
172. Locke FL, Neelapu SS, Bartlett N, Siddiqi T, Jacobson C, Westin J, et al. A Phase 2 multicenter trial of KTE-019 (anti-CD19 CAR T cells) in patients with chemorefractory primary mediastinal B-cell lymphoma and transformed follicular lymphoma: Interim results from ZUMA-1. *Blood*. 2016;128(22):Abstract 998.
173. Turtle CJ, Hanafi LA, Li D, Chaney C, Heimfeld S, Riddell SR, et al. CD19 CAR T-cells are highly effective in Ibrutinib-refractory CLL. *Blood*. 2016;128(22):Abstract 56.
174. Turtle CJ, Hanafi LA, Berger C, Gooley TA, Cherian S, Hudecek M, et al. CD19 CAR-T cells of defined CD4+:CD8+ composition in adult B cell ALL patients. *The Journal of clinical investigation*. 2016;126(6):2123-38.
175. Turtle CJ, Hanafi LA, Berger C, Hudecek M, Pender B, Robinson E, et al. Immunotherapy of non-Hodgkin's lymphoma with a defined ratio of CD8+ and CD4+ CD19-specific chimeric antigen receptor-modified T cells. *Science translational medicine*. 2016;8(355):355ra116.
176. Sadelain M, Riviere I, Riddell S. Therapeutic T cell engineering. *Nature*. 2017;545(7655):423-31.
177. Kawalekar OU, O'Connor RS, Fraietta JA, Guo L, McGettigan SE, Posey AD, Jr., et al. Distinct Signaling of Coreceptors Regulates Specific Metabolism Pathways and Impacts Memory Development in CAR T Cells. *Immunity*. 2016;44(2):380-90.
178. Maude SL, Teachey DT, Porter DL, Grupp SA. CD19-targeted chimeric antigen receptor T-cell therapy for acute lymphoblastic leukemia. *Blood*. 2015;125(26):4017-23.
179. Fraietta JA, Lacey SF, Wilcox NS, Bedoya F, Chen F, Orlando E, et al. Biomarkers of response to anti-CD19 CAR T-cell therapy in patients with CLL. *Blood*. 2016;128(22):Abstract 57.
180. Schuster SJ, Svoboda J, Chong EA, Nasta SD, Mato AR, Anak O, et al. Chimeric Antigen Receptor T Cells in Refractory B-Cell Lymphomas. *The New England journal of medicine*. 2017.
181. Neelapu SS, Locke FL, Bartlett NL, Lekakis LJ, Miklos DB, Jacobson CA, et al. Axicabtagene Ciloleucel CAR T-Cell Therapy in Refractory Large B-Cell Lymphoma. *The New England journal of medicine*. 2017.
182. Locke FL, Ghobadi A, Jacobson CA, Miklos DB, Lekakis LJ, Oluwole OO, et al. Long-term safety and activity of axicabtagene ciloleucel in refractory large B-cell lymphoma (ZUMA-1): a single-arm, multicentre, phase 1-2 trial. *The Lancet Oncology*. 2018.
183. Crump M, Neelapu SS, Farooq U, Van Den Neste E, Kuruvilla J, Westin J, et al. Outcomes in refractory diffuse large B-cell lymphoma: results from the international SCHOLAR-1 study. *Blood*. 2017;130(16):1800-8.
184. Maude SL, Laetsch TW, Buechner J, Rives S, Boyer M, Bittencourt H, et al. Tisagenlecleucel in Children and Young Adults with B-Cell Lymphoblastic Leukemia. *The New England journal of medicine*. 2018;378(5):439-48.
185. Schuster SJ, Bishop MR, Tam CS, Waller EK, Borchmann P, McGuirk JP, et al. Tisagenlecleucel in Adult Relapsed or Refractory Diffuse Large B-Cell Lymphoma. *The New England journal of medicine*. 2019;380(1):45-56.

186. Neelapu BC, Ghobadi A, Jacobson C, Miklos D, Lekakis L, Oluwole OO, et al. 2-Year Follow-Up and High-Risk Subset Analysis of ZUMA-1, the Pivotal Study of Axicabtagene Ciloleucel (Axi-Cel) in Patients with Refractory Large B Cell Lymphoma. *Blood*. 2018;132:Abstract 2967.
187. Sotillo E, Barrett DM, Black KL, Bagashev A, Oldridge D, Wu G, et al. Convergence of Acquired Mutations and Alternative Splicing of CD19 Enables Resistance to CART-19 Immunotherapy. *Cancer discovery*. 2015;5(12):1282-95.
188. Evans AG, Rothberg PG, Burack WR, Huntington SF, Porter DL, Friedberg JW, et al. Evolution to plasmablastic lymphoma evades CD19-directed chimeric antigen receptor T cells. *British journal of haematology*. 2015.
189. Neelapu S, Locke FL, Bartlett N, Lekakis L, Miklos D, Jacobsen E, et al. Long-term follow-up ZUMA-1: A pivotal trial of axicabtagene ciloleucel (KTE-019) in patients with refractory aggressive NHL. *Blood*. 2017;130:Oral 578.
190. Galon J, Rossi J, Turcan S, Danan C, Locke F, Neelapu S, et al. Characterization of anti-CD19 chimeric antigen receptor (CAR) T cell-mediated tumour microenvironment immune gene profile in a multicenter trial (ZUMA-1) with axicabtagene ciloleucel. *Journal of clinical oncology : official journal of the American Society of Clinical Oncology*. 2017;35:Abstract 3025.
191. Gardner R, Wu D, Cherian S, Fang M, Hanafi LA, Finney O, et al. Acquisition of a CD19-negative myeloid phenotype allows immune escape of MLL-rearranged B-ALL from CD19 CAR-T-cell therapy. *Blood*. 2016;127(20):2406-10.
192. Hay KA, Gauthier J, Hirayama AV, Voutsinas JM, Wu Q, Li D, et al. Factors associated with durable EFS in adult B-cell ALL patients achieving MRD-negative CR after CD19 CAR-T cells. *Blood*. 2019.
193. Ruella M, Xu J, Barrett DM, Fraietta JA, Reich TJ, Ambrose DE, et al. Induction of resistance to chimeric antigen receptor T cell therapy by transduction of a single leukemic B cell. *Nature medicine*. 2018;24(10):1499-503.
194. Haso W, Lee DW, Shah NN, Stetler-Stevenson M, Yuan CM, Pastan IH, et al. Anti-CD22-chimeric antigen receptors targeting B-cell precursor acute lymphoblastic leukemia. *Blood*. 2013;121(7):1165-74.
195. Shah N, Stetler-Stevenson M, Yuan C, Shalabi H, Yates B, Delbrook C, et al. Minimal residual disease negative complete remissions following anti-CD22 chimeric antigen receptor in children and young adults with relapsed/refractory acute lymphoblastic leukaemia. *Blood*. 2016;128(22):Abstract 650.
196. Gardner R, Annesley C, Finney O, Summers C, Lambie A, Rivers J, et al. Early Clinical Experience of CD19 x CD22 Dual Specific CAR T Cells for Enhanced Anti-Leukemic Targeting of Acute Lymphoblastic Leukaemia. *Blood*. 2018;132:Abstract 278.
197. Schultz L, Davis K, Baggott C, Chaudry C, Marcy A, Mavroukakis S, et al. Phase 1 Study of CD19/CD22 Bispecific CAR Therapy in Children and Young Adults with B Cell Acute Lymphoblastic Leukemia (ALL). *Blood*. 2018;132:Abstract 898.
198. Amrolia P, Wynn R, Hough R, Vora A, Bonney D, Veys P, et al. Simultaneous Targeting of CD19 and CD22: Phase I Study of AUTO3, a Bicistronic CAR T-cell Therapy, in Pediatric Patients with R/R B-Cell Acute Lymphoblastic Leukemia: Amelia Study. *Blood*. 2018;132:Abstract 279.
199. Shah N, Zhu F, Taylor C, Schneider D, Krueger W, Worden A, et al. A Phase 1 Study with Point-of-Care Manufacturing of Dual Targeted, Tandem Anti-CD19, Anti-

CD20 CAR Modified T-Cells for Relapsed, Refractory, Non-Hodgkin Lymphoma. *Blood*. 2018;132:Abstract 4193.

200. Ruella M, Barrett DM, Kenderian SS, Shestova O, Hofmann TJ, Perazzelli J, et al. Dual CD19 and CD123 targeting prevents antigen-loss relapses after CD19-directed immunotherapies. *The Journal of clinical investigation*. 2016;126(10):3814-26.

201. Daneshmanesh AH, Mikaelsson E, Jeddi-Tehrani M, Bayat AA, Ghods R, Ostadkarampour M, et al. Ror1, a cell surface receptor tyrosine kinase is expressed in chronic lymphocytic leukemia and may serve as a putative target for therapy. *International journal of cancer Journal international du cancer*. 2008;123(5):1190-5.

202. Hudecek M, Schmitt TM, Baskar S, Lupo-Stanghellini MT, Nishida T, Yamamoto TN, et al. The B-cell tumor-associated antigen ROR1 can be targeted with T cells modified to express a ROR1-specific chimeric antigen receptor. *Blood*. 2010;116(22):4532-41.

203. Cui B, Ghia EM, Chen L, Rassenti LZ, DeBoever C, Widhopf GF, 2nd, et al. High-level ROR1 associates with accelerated disease progression in chronic lymphocytic leukemia. *Blood*. 2016;128(25):2931-40.

204. Deniger DC, Yu J, Huls MH, Figliola MJ, Mi T, Maiti SN, et al. Sleeping Beauty Transposition of Chimeric Antigen Receptors Targeting Receptor Tyrosine Kinase-Like Orphan Receptor-1 (ROR1) into Diverse Memory T-Cell Populations. *PLoS one*. 2015;10(6):e0128151.

205. Scarfo I, Ormhoj M, Frigault MJ, Castano AP, Lorrey S, Bouffard AA, et al. Anti-CD37 chimeric antigen receptor T cells are active against B- and T-cell lymphomas. *Blood*. 2018;132(14):1495-506.

206. Fraietta JA, Lacey SF, Orlando EJ, Pruteanu-Malinici I, Gohil M, Lundh S, et al. Determinants of response and resistance to CD19 chimeric antigen receptor (CAR) T cell therapy of chronic lymphocytic leukemia. *Nature medicine*. 2018;24(5):563-71.

207. Hirayama AV, Gauthier J, Hay KA, Voutsinas JM, Wu Q, Gooley T, et al. The response to lymphodepletion impacts PFS in patients with aggressive non-Hodgkin lymphoma treated with CD19 CAR T cells. *Blood*. 2019;133(17):1876-87.

208. Sommermeyer D, Hudecek M, Kosasih PL, Gogishvili T, Maloney DG, Turtle CJ, et al. Chimeric antigen receptor-modified T cells derived from defined CD8 and CD4 subsets confer superior antitumor reactivity in vivo. *Leukemia*. 2015.

209. Rossi J, Paczkowski P, Shen YW, Morse K, Flynn B, Kaiser A, et al. Preinfusion polyfunctional anti-CD19 chimeric antigen receptor T cells are associated with clinical outcomes in NHL. *Blood*. 2018;132(8):804-14.

210. Klebanoff CA, Scott CD, Leonard AJ, Yamamoto TN, Cruz AC, Ouyang C, et al. Memory T cell-driven differentiation of naive cells impairs adoptive immunotherapy. *The Journal of clinical investigation*. 2016;126(1):318-34.

211. Sabatino M, Hu J, Sommariva M, Gautam S, Fellowes V, Hocker JD, et al. Generation of clinical-grade CD19-specific CAR-modified CD8+ memory stem cells for the treatment of human B-cell malignancies. *Blood*. 2016.

212. Niemann CU, Herman SE, Maric I, Gomez-Rodriguez J, Biancotto A, Chang BY, et al. Disruption of in vivo Chronic Lymphocytic Leukemia Tumor-Microenvironment Interactions by Ibrutinib--Findings from an Investigator-Initiated Phase II Study. *Clinical cancer research : an official journal of the American Association for Cancer Research*. 2016;22(7):1572-82.

213. Sagiv-Barfi I, Kohrt HE, Czerwinski DK, Ng PP, Chang BY, Levy R. Therapeutic antitumor immunity by checkpoint blockade is enhanced by ibrutinib, an inhibitor of both BTK and ITK. *Proceedings of the National Academy of Sciences of the United States of America*. 2015;112(9):E966-72.
214. Gill S, Vides V, Frey N, Metzger S, O'Brien M, Hexner E, et al. Prospective Clinical Trial of Anti-CD19 CAR T Cells in Combination with Ibrutinib for the Treatment of Chronic Lymphocytic Leukaemia Shows a High Response Rate. *Blood*. 2018;132:298.
215. Gauthier J, Hirayama A, Hay KA, Li D, Lymp J, Sheih A, et al. Comparison of Efficacy and Toxicity of CD19-Specific Chimeric Antigen Receptor T-Cells Alone or in Combination with Ibrutinib for Relapsed and/or Refractory CLL. *Blood*. 2018;132:299.
216. Ryan CE, Sahaf B, Logan AC, O'Brien S, Byrd JC, Hillmen P, et al. Ibrutinib efficacy and tolerability in patients with relapsed chronic lymphocytic leukemia following allogeneic HCT. *Blood*. 2016;128(25):2899-908.
217. Kantarjian H, Stein A, Gokbuget N, Fielding AK, Schuh AC, Ribera JM, et al. Blinatumomab versus Chemotherapy for Advanced Acute Lymphoblastic Leukemia. *The New England journal of medicine*. 2017;376(9):836-47.
218. Viardot A, Goebeler ME, Hess G, Neumann S, Pfreundschuh M, Adrian N, et al. Phase 2 study of the bispecific T-cell engager (BiTE) antibody blinatumomab in relapsed/refractory diffuse large B-cell lymphoma. *Blood*. 2016;127(11):1410-6.
219. Robinson HR, Qi J, Cook EM, Nichols C, Dadashian EL, Underbayev C, et al. A CD19/CD3 bispecific antibody for effective immunotherapy of chronic lymphocytic leukemia in the ibrutinib era. *Blood*. 2018;132(5):521-32.
220. Durr C, Hanna BS, Schulz A, Lucas F, Zucknick M, Benner A, et al. Tumor necrosis factor receptor signaling is a driver of chronic lymphocytic leukemia that can be therapeutically targeted by the flavonoid wogonin. *Haematologica*. 2018;103(4):688-97.
221. Garfall AL, Maus MV, Hwang WT, Lacey SF, Mahnke YD, Melenhorst JJ, et al. Chimeric Antigen Receptor T Cells against CD19 for Multiple Myeloma. *The New England journal of medicine*. 2015;373(11):1040-7.
222. Hajek R, Okubote SA, Svachova H. Myeloma stem cell concepts, heterogeneity and plasticity of multiple myeloma. *British journal of haematology*. 2013;163(5):551-64.
223. Tai YT, Mayes PA, Acharya C, Zhong MY, Cea M, Cagnetta A, et al. Novel anti-B-cell maturation antigen antibody-drug conjugate (GSK2857916) selectively induces killing of multiple myeloma. *Blood*. 2014;123(20):3128-38.
224. Cohen AD, Garfall AL, Stadtmauer EA, Melenhorst JJ, Lacey SF, Lancaster E, et al. B cell maturation antigen-specific CAR T cells are clinically active in multiple myeloma. *The Journal of clinical investigation*. 2019;130.
225. Mailankody S, Htut M, Lee K, Bensinger W, Devries T, Piasecki J, et al. JCARH125, Anti-BCMA CAR T-cell Therapy for Relapsed/Refractory Multiple Myeloma: Initial Proof of Concept Results from a Phase 1/2 Multicenter Study (EVOLVE). *Blood*. 2018;132:Abstract 957.
226. Ansell SM, Lesokhin AM, Borrello I, Halwani A, Scott EC, Gutierrez M, et al. PD-1 blockade with nivolumab in relapsed or refractory Hodgkin's lymphoma. *The New England journal of medicine*. 2015;372(4):311-9.

227. Ramos CA, Ballard B, Zhang H, Dakhova O, Gee AP, Mei Z, et al. Clinical and immunological responses after CD30-specific chimeric antigen receptor-redirected lymphocytes. *The Journal of clinical investigation*. 2017;127(9):3462-71.
228. Wang CM, Wu ZQ, Wang Y, Guo YL, Dai HR, Wang XH, et al. Autologous T Cells Expressing CD30 Chimeric Antigen Receptors for Relapsed or Refractory Hodgkin Lymphoma: An Open-Label Phase I Trial. *Clinical cancer research : an official journal of the American Association for Cancer Research*. 2017;23(5):1156-66.
229. Ramos C, Bilgi M, Gerken C, Dakhova O, Mei Z, Grilley B, et al. CD30-Chimeric Antigen Receptor T cells for Hodgkin Lymphoma (HL). *Blood*. 2018;132:Abstract 680.
230. Wang D, Xiao Y, Wang N, Huang L, Zhang Y, Zhang T, et al. Anti-CD30 Chimeric Antigen Receptor T cell Therapy for CD30+ Relapsed/Refractory Hodgkin Lymphoma and Anaplastic Large Cell Lymphoma Patients. *Blood*. 2018;132:Abstract 1660.
231. Grover N, Park S, Ivanova A, Eldridge P, McKay K, Cheng C, et al. Clinical Responses to CAR CD30 T cells in Patients with CD30+ Lymphomas Relapsed Multiple Treatments Including Brentuximab Vedotin. *Blood*. 2018;132:Abstract 681.
232. Laszlo GS, Harrington KH, Gudgeon CJ, Beddoe ME, Fitzgibbon MP, Ries RE, et al. Expression and functional characterization of CD33 transcript variants in human acute myeloid leukemia. *Oncotarget*. 2016;7(28):43281-94.
233. Taussig DC, Pearce DJ, Simpson C, Rohatiner AZ, Lister TA, Kelly G, et al. Hematopoietic stem cells express multiple myeloid markers: implications for the origin and targeted therapy of acute myeloid leukemia. *Blood*. 2005;106(13):4086-92.
234. Mardiros A, Dos Santos C, McDonald T, Brown CE, Wang X, Budde LE, et al. T cells expressing CD123-specific chimeric antigen receptors exhibit specific cytolytic effector functions and antitumor effects against human acute myeloid leukemia. *Blood*. 2013;122(18):3138-48.
235. Bakker AB, van den Oudenrijn S, Bakker AQ, Feller N, van Meijer M, Bia JA, et al. C-type lectin-like molecule-1: a novel myeloid cell surface marker associated with acute myeloid leukemia. *Cancer research*. 2004;64(22):8443-50.
236. Wang J, Chen S, Xiao W, Li W, Wang L, Yang S, et al. CAR-T cells targeting CLL-1 as an approach to treat acute myeloid leukemia. *Journal of hematology & oncology*. 2018;11(1):7.
237. Liu F, Cao Y, Pinz KG, Ma Y, Wada M, Chen K, et al. First-in-Human CLL1-CD33 Compound CAR T cell Therapy Induces Complete Remission in Patients with Refractory Acute Myeloid Leukaemia: Update on Phase 1 Clinical Trial. *Blood*. 2018;132:Abstract 901.
238. Campana D, van Dongen JJ, Mehta A, Coustan-Smith E, Wolvers-Tettero IL, Ganeshaguru K, et al. Stages of T-cell receptor protein expression in T-cell acute lymphoblastic leukemia. *Blood*. 1991;77(7):1546-54.
239. Mamonkin M, Rouce RH, Tashiro H, Brenner MK. A T-cell-directed chimeric antigen receptor for the selective treatment of T-cell malignancies. *Blood*. 2015;126(8):983-92.
240. Chen KH, Wada M, Pinz KG, Liu H, Lin KW, Jares A, et al. Preclinical targeting of aggressive T-cell malignancies using anti-CD5 chimeric antigen receptor. *Leukemia*. 2017;31(10):2151-60.
241. Went P, Agostinelli C, Gallamini A, Piccaluga PP, Ascani S, Sabbatini E, et al. Marker expression in peripheral T-cell lymphoma: a proposed clinical-pathologic

prognostic score. *Journal of clinical oncology : official journal of the American Society of Clinical Oncology*. 2006;24(16):2472-9.

242. Sims JE, Tunnacliffe A, Smith WJ, Rabbitts TH. Complexity of human T-cell antigen receptor beta-chain constant- and variable-region genes. *Nature*. 1984;312(5994):541-5.

243. Maciocia PM, Wawrzyniecka PA, Philip B, Ricciardelli I, Akarca AU, Onuoha SC, et al. Targeting the T cell receptor beta-chain constant region for immunotherapy of T cell malignancies. *Nature medicine*. 2017;23(12):1416-23.

244. Juillerat A, Pessereau C, Dubois G, Guyot V, Marechal A, Valton J, et al. Optimized tuning of TALEN specificity using non-conventional RVDs. *Sci Rep*. 2015;5:8150.

245. Qasim W, Zhan H, Samarasinghe S, Adams S, Amrolia P, Stafford S, et al. Molecular remission of infant B-ALL after infusion of universal TALEN gene-edited CAR T cells. *Science translational medicine*. 2017;9(374).

246. Benjamin R, Graham C, Yallop D, Jozwik A, Ciocarlie O, Jain N, et al. Preliminary Data on Safety, Cellular Kinetics and Anti-Leukemic Activity of UCART19, an Allogeneic Anti-CD19 CAR T-Cell Product, in a Pool of Adult and Pediatric Patients with High-Risk CD19+ Relapsed/Refractory B-Cell Acute Lymphoblastic Leukemia. *Blood*. 2018;132:Abstract 896.

247. Georgiadis C, Preece R, Nickolay L, Etuk A, Petrova A, Ladon D, et al. Long Terminal Repeat CRISPR-CAR-Coupled "Universal" T Cells Mediate Potent Anti-leukemic Effects. *Molecular therapy : the journal of the American Society of Gene Therapy*. 2018;26(5):1215-27.

248. Brudno JN, Somerville RP, Shi V, Rose JJ, Halverson DC, Fowler DH, et al. Allogeneic T Cells That Express an Anti-CD19 Chimeric Antigen Receptor Induce Remissions of B-Cell Malignancies That Progress After Allogeneic Hematopoietic Stem-Cell Transplantation Without Causing Graft-Versus-Host Disease. *Journal of clinical oncology : official journal of the American Society of Clinical Oncology*. 2016;34(10):1112-21.

249. Chong EA, Melenhorst JJ, Lacey SF, Ambrose DE, Gonzalez V, Levine BL, et al. PD-1 blockade modulates chimeric antigen receptor (CAR)-modified T cells: refueling the CAR. *Blood*. 2017;129(8):1039-41.

250. Cherkassky L, Morello A, Villena-Vargas J, Feng Y, Dimitrov DS, Jones DR, et al. Human CAR T cells with cell-intrinsic PD-1 checkpoint blockade resist tumor-mediated inhibition. *The Journal of clinical investigation*. 2016;126(8):3130-44.

251. Jacobson C, Locke F, Miklos D, Herrera A, Westin J, Lee J, et al. End of Phase 1 Results from Zuma-6: Axicabtagene-Ciloleucel (Axi-Cel) in Combination with Atezilizumab for the Treatment of Patients with Refractory Disease Large B Cell Lymphoma. *Blood*. 2018;132:4192.

252. Bernabei L, Garfall A, Melenhorst J, Lacey S, Stadtmauer E, Vogl D, et al. PD-1 Inhibitor Combinations As Salvage Therapy for Relapsed/Refractory Multiple Myeloma Patients Progressing after BCMA-Directed CAR T cells. *Blood*. 2018;132:Abstract 1973.

253. Liu X, Zhang Y, Cheng C, Cheng AW, Zhang X, Li N, et al. CRISPR-Cas9-mediated multiplex gene editing in CAR-T cells. *Cell research*. 2017;27(1):154-7.

254. Wasmeier C, Hume AN, Bolasco G, Seabra MC. Melanosomes at a glance. *Journal of cell science*. 2008;121(Pt 24):3995-9.

255. Rubio V, Stuge TB, Singh N, Betts MR, Weber JS, Roederer M, et al. Ex vivo identification, isolation and analysis of tumor-cytolytic T cells. *Nature medicine*. 2003;9(11):1377-82.
256. Combadiere B, Freedman M, Chen L, Shores EW, Love P, Lenardo MJ. Qualitative and quantitative contributions of the T cell receptor zeta chain to mature T cell apoptosis. *The Journal of experimental medicine*. 1996;183(5):2109-17.
257. Lee J, Sadelain M, Brentjens R. Retroviral transduction of murine primary T lymphocytes. *Methods in molecular biology*. 2009;506:83-96.
258. Zheng Z, Chinnasamy N, Morgan RA. Protein L: a novel reagent for the detection of chimeric antigen receptor (CAR) expression by flow cytometry. *Journal of translational medicine*. 2012;10:29.
259. Hoffmann JM, Schubert ML, Wang L, Huckelhoven A, Sellner L, Stock S, et al. Differences in Expansion Potential of Naive Chimeric Antigen Receptor T Cells from Healthy Donors and Untreated Chronic Lymphocytic Leukemia Patients. *Frontiers in immunology*. 2017;8:1956.
260. Magalhaes I, Kalland I, Kochenderfer JN, Osterborg A, Uhlin M, Mattsson J. CD19 Chimeric Antigen Receptor T Cells From Patients With Chronic Lymphocytic Leukemia Display an Elevated IFN-gamma Production Profile. *Journal of immunotherapy*. 2018;41(2):73-83.
261. Steeber DA, Green NE, Sato S, Tedder TF. Lymphocyte migration in L-selectin-deficient mice. Altered subset migration and aging of the immune system. *Journal of immunology*. 1996;157(3):1096-106.
262. Lee WT, Vitetta ES. The differential expression of homing and adhesion molecules on virgin and memory T cells in the mouse. *Cell Immunol*. 1991;132(1):215-22.
263. Ernst DN, Weigle WO, Noonan DJ, McQuitty DN, Hobbs MV. The age-associated increase in IFN-gamma synthesis by mouse CD8+ T cells correlates with shifts in the frequencies of cell subsets defined by membrane CD44, CD45RB, 3G11, and MEL-14 expression. *Journal of immunology*. 1993;151(2):575-87.
264. Nastoupil L, Jain M, Spiegel JH, Ghobadi A, Lin Y, Dahiya S, et al. Axicabtagene Ciloleucel (Axi-cel) CD19 Chimeric Antigen Receptor (CAR) T-Cell Therapy for Relapse/Refractory Large B-Cell Lymphoma: Real World Experience. *Blood*. 2018;132:Abstract 91.
265. Tumeh PC, Harview CL, Yearley JH, Shintaku IP, Taylor EJ, Robert L, et al. PD-1 blockade induces responses by inhibiting adaptive immune resistance. *Nature*. 2014;515(7528):568-71.
266. Cherkassky L, Morello A, Villena-Vargas J, Feng Y, Dimitrov DS, Jones DR, et al. Human CAR T cells with cell-intrinsic PD-1 checkpoint blockade resist tumor-mediated inhibition. *The Journal of clinical investigation*. 2016.
267. John LB, Devaud C, Duong CP, Yong CS, Beavis PA, Haynes NM, et al. Anti-PD-1 antibody therapy potently enhances the eradication of established tumors by gene-modified T cells. *Clinical cancer research : an official journal of the American Association for Cancer Research*. 2013;19(20):5636-46.
268. Amarnath S, Mangus CW, Wang JC, Wei F, He A, Kapoor V, et al. The PDL1-PD1 axis converts human TH1 cells into regulatory T cells. *Science translational medicine*. 2011;3(111):111ra20.

269. Green MR, Monti S, Rodig SJ, Juszczynski P, Currie T, O'Donnell E, et al. Integrative analysis reveals selective 9p24.1 amplification, increased PD-1 ligand expression, and further induction via JAK2 in nodular sclerosing Hodgkin lymphoma and primary mediastinal large B-cell lymphoma. *Blood*. 2010;116(17):3268-77.
270. Green MR, Rodig S, Juszczynski P, Ouyang J, Sinha P, O'Donnell E, et al. Constitutive AP-1 activity and EBV infection induce PD-L1 in Hodgkin lymphomas and posttransplant lymphoproliferative disorders: implications for targeted therapy. *Clinical cancer research : an official journal of the American Association for Cancer Research*. 2012;18(6):1611-8.
271. Chen R, Zinzani PL, Fanale MA, Armand P, Johnson NA, Brice P, et al. Phase II Study of the Efficacy and Safety of Pembrolizumab for Relapsed/Refractory Classic Hodgkin Lymphoma. 2017;35(19):2125-32.
272. Armand P, Chen YB, Redd RA, Joyce RM, Bsai J, Jeter E, et al. PD-1 Blockade with Pembrolizumab for Classical Hodgkin Lymphoma after Autologous Stem Cell Transplantation. *Blood*. 2019.
273. Haverkos BM, Abbott D, Hamadani M, Armand P, Flowers ME, Merryman R, et al. PD-1 blockade for relapsed lymphoma post-allogeneic hematopoietic cell transplant: high response rate but frequent GVHD. *Blood*. 2017;130(2):221-8.
274. Ahearne MJ, Bhuller K, Hew R, Ibrahim H, Naresh K, Wagner SD. Expression of PD-1 (CD279) and FoxP3 in diffuse large B-cell lymphoma. *Virchows Archiv : an international journal of pathology*. 2014;465(3):351-8.
275. Kiyasu J, Miyoshi H, Hirata A, Arakawa F, Ichikawa A, Niino D, et al. Expression of programmed cell death ligand 1 is associated with poor overall survival in patients with diffuse large B-cell lymphoma. *Blood*. 2015;126(19):2193-201.
276. Andorsky DJ, Yamada RE, Said J, Pinkus GS, Betting DJ, Timmerman JM. Programmed death ligand 1 is expressed by non-hodgkin lymphomas and inhibits the activity of tumor-associated T cells. *Clinical cancer research : an official journal of the American Association for Cancer Research*. 2011;17(13):4232-44.
277. Lesokhin AM, Ansell SM, Armand P, Scott EC, Halwani A, Gutierrez M, et al. Nivolumab in Patients With Relapsed or Refractory Hematologic Malignancy: Preliminary Results of a Phase Ib Study. *Journal of clinical oncology : official journal of the American Society of Clinical Oncology*. 2016;34(23):2698-704.
278. Armand P, Nagler A, Weller EA, Devine SM, Avigan DE, Chen YB, et al. Disabling immune tolerance by programmed death-1 blockade with pidilizumab after autologous hematopoietic stem-cell transplantation for diffuse large B-cell lymphoma: results of an international phase II trial. *Journal of clinical oncology : official journal of the American Society of Clinical Oncology*. 2013;31(33):4199-206.
279. Ruella M, Kenderian SS, Shestova O, Klichinsky M, Melenhorst JJ, Wasik MA, et al. Kinase inhibitor ibrutinib to prevent cytokine-release syndrome after anti-CD19 chimeric antigen receptor T cells for B-cell neoplasms. *Leukemia*. 2017;31(1):246-8.
280. Norelli M, Camisa B, Barbiera G, Falcone L, Purevdorj A, Genua M, et al. Monocyte-derived IL-1 and IL-6 are differentially required for cytokine-release syndrome and neurotoxicity due to CAR T cells. *Nature medicine*. 2018;24(6):739-48.
281. Zenz T. Exhausting T cells in CLL. *Blood*. 2013;121(9):1485-6.
282. Hirayama A, Gauthier J, Hay KA, Sheih A, Cherian S, Chen X, et al. Efficacy and Toxicity of JCAR014 in Combination with Durvalumab for the Treatment of Patients

with Relapsed/Refractory Aggressive B-cell Non-Hodgkin Lymphoma. *Blood*. 2018;132:Abstract 1680.

283. Li A, Hucks G, Dinofia A, Teachey D, Baniewicz D, Callahan C, et al. Checkpoint Inhibitors Augment CD19-Directed Chimeric Antigen Receptor (CAR) T cells Therapy in Relapsed B-cell Acute Lymphoblastic Leukemia. *Blood*. 2018;132:556.

284. Ruella M, Kenderian SS, Shestova O, Fraietta JA, Qayyum S, Zhang Q, et al. The Addition of the BTK Inhibitor Ibrutinib to Anti-CD19 Chimeric Antigen Receptor T Cells (CART19) Improves Responses against Mantle Cell Lymphoma. *Clinical cancer research : an official journal of the American Association for Cancer Research*. 2016;22(11):2684-96.

285. Woyach JA, Furman RR, Liu TM, Ozer HG, Zapatka M, Ruppert AS, et al. Resistance mechanisms for the Bruton's tyrosine kinase inhibitor ibrutinib. *The New England journal of medicine*. 2014;370(24):2286-94.

286. Long M, Beckwith K, Do P, Mundy BL, Gordon A, Lehman AM, et al. Ibrutinib treatment improves T cell number and function in CLL patients. *The Journal of clinical investigation*. 2017;127(8):3052-64.

287. Romero-Toledo A, Schwarzbich M, Sanderson RN, Gribben J. Monocytic But Not Granulocytic MDSC Increase with Ibrutinib but not Acalabrutinib Treatment in Eu-TCL1 Mice with CLL, Suggesting a Role for ITK Inhibition in Monocytic MDSC. *HemaSphere*. 2019;3:514.

288. Gauthier J, Hirayama A, Hay KA, Lymp J, Sheih A, Purushe J, et al. Durable Responses after CD19-Targeted CAR-T Cell Immunotherapy with Concurrent Ibrutinib for CLL after Ibrutinib Failure. *Hematological Oncology*. 2019;2019:Abstract 120.

289. Siddiqi T, Dorritie K, Soumerai JD, Dubovsky J, Gillenwater HH, Gong L, et al. TRANSCEND CLL 004: Minimal Residual Disease Negative Responses After Lisocabtagene Maraleucel (Liso-cel) in Patients with Relapsed/Refractory Chronic Lymphocytic Leukemia or Small Lymphocytic Lymphoma. *HemaSphere*. 2019;3:6-7.

290. Geyer MB, Riviere I, Senechal B, Wang X, Wang Y, Purdon TJ, et al. Safety and tolerability of conditioning chemotherapy followed by CD19-targeted CAR T cells for relapsed/refractory CLL. *JCI Insight*. 2019;5.

291. Brentjens RJ, Davila ML, Riviere I, Park J, Wang X, Cowell LG, et al. CD19-targeted T cells rapidly induce molecular remissions in adults with chemotherapy-refractory acute lymphoblastic leukemia. *Science translational medicine*. 2013;5(177):177ra38.

292. Zhao Z, Condomines M, van der Stegen SJC, Perna F, Kloss CC, Gunset G, et al. Structural Design of Engineered Costimulation Determines Tumor Rejection Kinetics and Persistence of CAR T Cells. *Cancer cell*. 2015;28(4):415-28.

293. Siska PJ, van der Windt GJ, Kishton RJ, Cohen S, Eisner W, Maclver NJ, et al. Suppression of Glut1 and Glucose Metabolism by Decreased Akt/mTORC1 Signaling Drives T Cell Impairment in B Cell Leukemia. *Journal of immunology*. 2016;197(6):2532-40.

294. van Bruggen JAC, Martens AWJ, Fraietta JA, Hofland T, Tonino SH, Eldering E, et al. Chronic lymphocytic leukemia cells impair mitochondrial fitness in CD8(+) T cells and impede CAR T-cell efficacy. *Blood*. 2019;134(1):44-58.

295. Schultz L, Mackall C. Driving CAR T cell translation forward. *Science translational medicine*. 2019;11(481).

296. Sauter CS, Senechal B, Riviere I, Ni A, Bernal Y, Wang X, et al. CD19 CAR T Cells Following Autologous Transplantation in Poor Risk Relapsed and Refractory B cell non-Hodgkin Lymphoma. *Blood*. 2019.
297. Eyquem J, Mansilla-Soto J, Giavridis T, van der Stegen SJ, Hamieh M, Cunanan KM, et al. Targeting a CAR to the TRAC locus with CRISPR/Cas9 enhances tumour rejection. *Nature*. 2017;543(7643):113-7.
298. Mestermann K, Giavridis T, Weber J, Rydzek J, Frenz S, Nerreter T, et al. The tyrosine kinase inhibitor dasatinib acts as a pharmacologic on/off switch for CAR T cells. *Science translational medicine*. 2019;11(499).
299. Abramson JS, McGree B, Noyes S, Plummer S, Wong C, Chen YB, et al. Anti-CD19 CAR T Cells in CNS Diffuse Large-B-Cell Lymphoma. *The New England journal of medicine*. 2017;377(8):783-4.
300. Frigault MJ, Dietrich J, Martinez-Lage M, Leick M, Choi BD, DeFilipp Z, et al. Tisagenlecleucel CAR-T Cell Therapy in Secondary CNS Lymphoma. *Blood*. 2019.
301. Giavridis T, van der Stegen SJC, Eyquem J, Hamieh M, Piersigilli A, Sadelain M. CAR T cell-induced cytokine release syndrome is mediated by macrophages and abated by IL-1 blockade. *Nature medicine*. 2018;24(6):731-8.
302. Ma L, Dichwalkar T, Chang JYH, Cossette B, Garafola D, Zhang AQ, et al. Enhanced CAR-T cell activity against solid tumors by vaccine boosting through the chimeric receptor. *Science*. 2019;365(6449):162-8.
303. Sterner RM, Sakemura R, Cox MJ, Yang N, Khadka RH, Forsman CL, et al. GM-CSF inhibition reduces cytokine release syndrome and neuroinflammation but enhances CAR-T cell function in xenografts. *Blood*. 2019;133(7):697-709.